Process Intensification in Syngas Production and Cleaning

Abdulaziz Hemmali Mohamed

B. Sc. M. Phil. (Chem. Eng.)

A thesis submitted to Newcastle University,

United Kingdom in partial fulfilment of the requirements for the

degree of Doctor of Philosophy (PhD)

School of Chemical Engineering and Advanced Materials

Faculty of Science, Agriculture and Engineering

June - 2013

Author's Declaration

This thesis is submitted in fulfilment of the requirements for the degree of Doctor of Philosophy at Newcastle University, Newcastle upon Tyne, United Kingdom. I hereby declare that all studies and work described within this thesis are my own work and that, to the best of my knowledge and belief, it contains no material previously published or written by another person nor material which has been submitted for a degree or any other qualification at the above or any other University or Institute, except where due acknowledgement has been made in the text. All work was carried out at the School of Chemical Engineering and Advanced Materials (CEAM) under the supervision of Professor G. Akay between January 2007 and December 2012.

Neither the author nor Newcastle University accepts any liability for the contents of this document.

Preface

Back in January 2007, I have commenced my studies for the degree of Doctor of Philosophy (PhD) in the School of Chemical Engineering and Advanced Materials (CEAM), at Newcastle University, United Kingdom under the supervision of Professor G. Akay. For the completion of this study, 3-3.5 years were required. During this period, extensive research and experimental work have been carried out. Initially, I thought that these tasks are easy, clear and straight forward to achieve; nevertheless, they are tedious and time consuming; *it is always more*. Therefore, personally speaking; I think that these tasks require patience, understating, flexibility and keenness to have them running through so the 'ball can get rolling'. In fact, one should have patience and be inspired since, according to Rohn, E. J.: ''the worst days of those who enjoy what they do, are better than the best days of those who don't''.

In this study, a novel downdraft intensive 50 kWe air-blown auto-thermal gasifier was used for the gasification of refinery sludge (petroleum industry waste) which indicating that refinery sludge could be gasified. As a result, gasification is a viable option for the utilization of refinery sludge as ever increasing environmental awareness and legislation demand that refinery sludge should be treated at source by localized small scale treatment facilities (gasification) operating near the feedstock source. The work/research has also focused on developing an intensified syngas cleaning techniques for different applications as a secondary measure to remove tars from syngas. These methods resulted in over 97% model tar reduction or/and removal efficiency which is sufficient for power generation applications of syngas. It is concluded that, in order to reduce and/or refrain particularly from the environmental pollution, it should be encouraged that refinery sludge is converted to syngas by applying appropriate conversion techniques such as downdraft gasification instead of directly combustion or landfill.

The work/research has resulted in one patent, three archival journal papers and several national and international conference presentations. Hence the results obtained from this work can provide information that can be benefit to academia or industry, although it may still require further consideration from both technical and economical viewpoints.

Dedication

I would like to dedicate this work to the **soul of my dear Father**, who passed away on 11th of January 1984. It was always his dream that I become a doctor. This work is for you **my dear mother** for everything you do. You brought me up, made sacrifice, care, prayers and supplication for me and you taught me the right from the wrong. You did the hardest job in the world. And that's why I would like to say a very, very big thank you. This is the fruit of your labour.

I also dedicate this work to **my dear wife** for her support and sacrifice throughout this long and difficult journey. To **my beautiful daughters**; Mawada and Rahma. To **my lovely sons**; Omar, Ahmed, Sofian and little El-Hammale. Thank you all and may Allah bless all of you. I could not have this done without you, I love you too much.

Finally, I would like to dedicate this work to the **souls of 17th February, 2011** Libyan Revolution Martyrs who scarified their precious lives for the sake of real democracy, better future for our beloved country Libya, social justice, freedom and better quality of life for all Libyans.

Acknowledgements

Time has passed so quickly since I have started my PhD. It was a rich experience full of joy and pain at the same time. But, finally I could reach the end line of this lengthy and difficult journey. There were many people along the way who stood beside me and without their support and faith in me, I could not make it. These words are just for them to express my gratitude and appreciation for their help.

First of all, I would like to thank Allah almighty for the strength, inspiration, guidance and encouragement through out this lengthy and difficult journey. In fact, many experiences and knowledge have been gained.

Further, I want to thank my research supervisor Professor Galip Akay for his years of guidance, generous advice, as well as undaunted patience and understanding throughout this work. Time after time, his strong grasp and in-depth knowledge of the subject has helped me in the struggle for my own understanding. On the personal side, his kind words and thoughtfulness have seen me through a lot of difficult times. His endeavour and encouragement is very invaluable and will always be remembered. It has been a great privilege and an honour for me to work with such an inspirational and expert inventor who has been credited with several EU and US patents in different disciplines so far.

I am indebted to my dear mother for her prayers and supplication she made for me, to my dear wife, to my beautiful daughters; Mawada and Rahma and to my lovely sons; Omar, Ahmed, Sofian and little El-Hammale for their love, encouragement, understanding, support and simply for being the best reasons in the world to go home at the end of the day.

Moreover, I would like to express my highest and never-ending gratitude to my mother-in-law, my sisters, my brothers, my sisters-in-law, my brothers-in-law and all my family for their unconditional love, encouragement and confidence in my ability.

I would also like to acknowledge the continuous care and valuable financial support from my sponsor; Libyan Cultural Bureau in London on behalf of the

Abstract

Process Intensification in Syngas Production and Cleaning

A. H. Mohamed

The aim of this work was to develop an intensified syngas cleaning system for different applications of the cleaned gas. The main target of syngas cleaning is the destruction of tars although the removal of heavy metals is also important. The syngas cleaning strategies include water scrubbing followed by further cleaning and moisture reduction, low temperature capture of tars and destruction of tars at high temperatures preferably at the gasifier exit temperature. In the present study, initially a novel downdraft intensive 50kWe air-blown auto-thermal gasifier was used for the gasification of refinery sludge indicating that refinery sludge could be gasified with low levels of tar as a result of catalytic tar cracking during gasification since refinery sludge initially contained large amounts of catalytic rare earth elements. It contained tar and particulate matter of less than 90 ± 6.0 mg/Nm^3 and calorific value of 3.71 ± 0.4 MJ/Nm^3 (wet gas), which is sufficient for power generation using an internal combustion engine (ICE). Gas composition, tar content and heat content of the produced gas were determined. Results were compared with those obtained with wood chips (reference feedstock).

In the development of intensified syngas cleaning systems, we used a model syngas (carbon dioxide) and model tar (crude oil). A new/novel, multi-functional tar removal rig was designed and fabricated. It can be used as a water scrubber or for tar removal under electric field in the absence or presence of biphilic (both hydrophilic to adsorb water and lipophilic to adsorb tars) adsorbents in the form of functionalized PolyHIPE Polymers (PHPs). These PHPs were produced, functionalized and characterized using environmental scanning electron microscopy (ESEM) and surface area analysis (SAA) and then used in the form of packed bed for the adsorption of model tars from model syngas. According to the literature, using the syngas in a power production application, the tar concentration in syngas needs to be less than 100 mg/Nm^3 which requires particle and tars reduction efficiencies of 90 % for a satisfactory operation of an Internal Composition Engine (ICE) using syngas produced in a downdraft gasifier.

Maximum tar removal efficiencies under the prevailing process conditions were: water scrubbing 45.9 ± 4.5 %; adsorption by the sulphonated PolyHIPE Polymers (s-PHP) 61.8 ± 2.5 %; high voltage application with conductive electrodes 97.5 ± 1.5 % at 25kV; and the combination of s-PHP with electric field resulted in 96.7 ± 1.9 % % tar removal efficiency. The advantage of high voltage gas cleaning is that it can be used at high temperatures and that no other material is used as adsorbent which requires regeneration once they are saturated with tar, etc.

Finally, another electrical method was designed to crack the model tars using plasma induced catalytic conversion. The results indicate that hydrocarbon profile of crude oil in the model syngas shifted towards low carbon number.

Publications/Patent and Conferences for this work/research

Publications

1. **Mohamed, A. H.**, Calkan, O. and Akay, G. 'Intensified gasification of refinery sludge for power production' International Workshop on Process Intensification, Tokyo Institute of Technology O-okayama Campus, Tokyo Japan, October 15-18, 2008.

2. Akay, G., Jordan, C. A. and **Mohamed, A. H.** 'Syngas cleaning with nano-structured micro-porous ion exchange polymers in biomass gasification using a novel downdraft gasifier', Journal of Energy Chemistry 2013, vol. 22, Issue (3) :426-435.

3. Akay, G., Jordan, C. A., **Mohamed, A. H.** and Zhang, K. 'Process intensification in syngas cleaning for Syngas-to-Biofuel/Bioammonia conversion and power generation', in preparation.

Patent

Akay, G., Al-Harrasi, W. S. S., El-Naggar, A. A., Chiremba, E., **Mohamed, A. H.** and Zhang, K. World Patent Application, PCT/GB2013/050125. 2013

Conferences

1. The 8th European Gasification Conference (Gasification–Effective Carbon) 10-12th September 2007 Antwerp, Belgium **(Attendance)**.

2. Hydrogen and fuel cells: for a low carbon future Conference, Gallery Suite, NEC, Birmingham, UK. 2nd April 2008 **(Poster Presentation)**.

3. 1st Academic Symposium of Libyan Students-Universities of UK, University of Nottingham, 12th June 2008 Nottingham UK **(Oral Presentation)**.

4. 2nd Academic Symposium of Libyan Students-Universities of UK, University of Bradford 20th June 2009 Bradford UK **(Oral Presentation)**.

5. Akay, G., Bull, S., Al-Harrasi, W. S. S., Burke, D. R., Elizalde, F. J. H., El-Nagger, A. A., Fleming, S., Hasan, H., Jordan, A. C., Kazak, C., **Mohamed, A. H.**, Mohamed, R. and Tham, M. (2010) 'Development of Biomass Based Energy Technologies and Intensified Integrated BioRefineries' **(Poster Presentation)**

Table of Contents

List of Figures

List of Tables

Nomenclature (Unit of Measurement, Abbreviations and Symbols)

Units of Measurement

kV	Kilovolt
kWe	Kilowatt of electrical energy
Nm^3	Normal cubic metre
Vol %	Percentage by volume
W	Watt
wt %	Percentage by weight

Abbreviations

AC	Alternative Current
API	American Petroleum Institute
CEAM	Chemical Engineering and Advanced Materials
CIE	Completely Insulated Electrode
CFB	Circulating Fluidized Bed
CPI	Chemical and Process Industry
CV	Calorific Value
Db	Dry basis
DBD	Dielectric Barrier Discharge
DC	Direct Current
ECD	Electron Capture Detector
EDX	Energy Dispersive X-ray Analysis
ER	Equivalence Ratio
ESEM	Environmental Scanning Electron Microscopy
ESP	Electrostatic Precipitator
FID	Flame Ionisation Detector
FPD	Flame Photometric Detector
GC	Gas Chromatography
GCV	Gross Caloric Value
HHV	High heating value

HIPE	High internal phase emulsion
HPAHs	Heavy Poly Aromatic Hydrocarbons
ICE	Internal Combustion Engine
ICI	Imperial Chemical Industries
LAH	Light Aromatic Hydrocarbons
LHV	Low Heating Value
LPAHs	Light Poly Aromatic Hydrocarbons
LPG	Liquefied Petroleum Gas
MHV	Medium Heating Value
MSW	Municipal Solid Waste
NPD	Nitrogen-Phosphorous Detector
PAHs	Polyaromatic Hydrocarbons
PIE	Partially Insulated Electrode
PHP	PolyHIPE Polymer
PI	Process Intensification
PID	Photo Ionization Detector
PIM	Process Intensification and Miniaturization
PM	Process Miniaturization
SEM	Scanning Electron Microscopy
SEM-EDX	Scanning Electron Microscopy-Energy Dispersive X-ray
Syngas	Synthesis Gas
TCD	Thermal Conductivity Detector
TEM	Transmission Electron Microscope
TPI	Tilted Plate Interceptor
VOC	Volatile Organic Compound
WESP	Wet Electrostatic Precipitator

Symbols

C_{in}	Inlet Tar Concentration, g/Nm^3
C_{out}	Outlet Tar Concentration, g/Nm^3
X	Tar reduction efficiency, %

Chapter One
Introduction

Chapter One

General Introduction

1.1. Background

High rate of development of petroleum products processing has resulted in the generation of enormous amounts of waste including refinery sludge. Such waste causes a serious risk to the environmental quality on the mother earth and its populations. In addition, it *does* place a huge strain on the petroleum industry worldwide; such a problem cannot be ignored.

Refinery sludge in particular is an important problem all over the world because of its harmful impact on the environment. Refinery sludge is a complex mixture of hydrocarbons together with clay, sand, inorganic matter, heavy metals and water. It contains a large amount of combustibles with high heating value. The severity of petroleum sludge problem depends on the nature of the crude oil, the processing capacity, the downstream capacities and the design of the effluent treatment plant. Sludge usually accumulates in refineries because of pumps and desalter failures, oil draining from tanks and operation units, periodic cleaning of storage tanks and pipeline ruptures (Kuriakose and Manjooran, 2001). Treatment of sludge is; therefore, important and of great significance element for oil refineries.

So far, techniques that have been employed in petroleum sludge treatment have included sludge disposal in lagoon/pit, incineration, land farming and secure landfill. Although these techniques have been successful; however, they still have been a major challenge to the petroleum industry worldwide. They generally demonstrate an environmental barrier. For instance, treatment of oily sludge through incineration suffers from the escape of some products of incomplete combustion. In addition, ashes produced from incineration contain heavy metals and; therefore, require some kind of environmental-friendly disposal. Likewise, land farming method causes contamination to ground water and soil. In addition, although in secure landfill method, the environmental issues are mitigated, this method requires special arrangement. In order to meet the ever increasing environmental awareness and legislations by which petroleum sludge is no longer landfilled, it becomes more and more essential to develop better techniques to efficiently deal with such sludges.

Development of a technology for conversion of waste feedstock into energy has the potential to address a number of economic, environmental, societal and resource issues. A path for the conversion of waste into energy should be economical; otherwise, fees required for waste disposal management become a credit against the cost of the produced energy. Furthermore, conversion of waste into energy has the environmental advantage of decreasing the number of future landfill sites needed with a contaminant decrease in the associated air and water pollution issues (Wallman et al., 1998).

Several thermochemical conversion technologies (combustion, pyrolysis and gasification) can be utilized for the production of energy from biomass and/or biomass waste. The end products for each of these processes vary and also different energy and matter recovery systems can be used according to the market or requirements. However, gasification in which solid organic matter is converted into a syngas is considered as the most appropriate option as it offers higher efficiencies as compared to combustion or pyrolysis (Bridgwater, 2003). In addition, gasification is central to the development of any sustainable biomass and/or biomass waste based energy and feedstock technologies. Also, syngas mixture produced via gasification can be used in internal combustion engines (ICEs), gas turbines, fuel cells and for hydrocarbon synthesis (Bain, 2004).

Gasification is a viable option for the utilization of oil sludge as ever increasing environmental awareness and legislation demand that oily sludge should be treated at source, as it is no longer acceptable for it to be sent to landfill in lagoons, etc. Gasification is a thermochemical conversion of solid organic material into a combustible gas by partial oxidation at temperatures greater than 500 ^{o}C (Higman and van der Burgt, 2008). The gasifying agent can be air, O_2 or steam. Gas produced is known as product gas, producer gas or syngas. It consists mainly of H_2, CO, CH_4 and CO_2; depending on the gasifying agent used, the dry basis heating value varies from 4-18 MJ Nm^{-3}. If air is used, the syngas is diluted with N_2 and a dry basis heating value between 4-7 MJ Nm^{-3} is obtained (McKendry, 2002a; McKendry, 2002c). Biomass and/or biomass waste into energy conversion efficiencies obtained can be further enhanced through the use of combined cycles to generate electricity. Furthermore, it has been shown that refinery sludge is not only useful for power generation, but also a good source of valuable chemicals which are recovered from

the ash produced from the refinery sludge gasification (Hall, 1981; Akay *et al.*, 2005). However, syngas produced from most biomass and/or biomass wastes usually contains varying amounts of tars and particulate matters. The applications of the syngas are purification level dependent, so these contaminants need to be removed via gas cleaning up equipment prior to its use for any application. Gas cleaning is important to prevent erosion, corrosion and environmental problems (Bridgwater and Maniatis, 2004; Smith and Shantha, 2007). The presence of tars in the fuel gas is one of the main technical barriers in the biomass and/or biomass waste gasification development and has been the main concern for many researchers. These tars can cause several problems, such as cracking in the pores of filters, forming coke and plugging the filters and condensing in the cold spots and plugging the lines, resulting in serious operational interruptions. Moreover, these tars are dangerous because of their carcinogenic character and they contain significant amounts of energy which should be transferred to the fuel gas as H_2, CO, CH_4, etc. In addition, high concentration of tars can damage or lead to unacceptable levels of maintenance for engines and turbines (Corella *et al.*, 1998).

Tars are defined as a generic term comprising all organic compounds present in the producer gas excluding gaseous hydrocarbons (C_1-C_6) and benzene (Neeft, 2002). Different classifications of tars are found in the literature (Milne *et al.*, 1998; Maniatis and Beenackers, 2000; Padban, 2001; van Paasen *et al.*, 2002; Devi *et al.*, 2005). In general, these classifications are based on: properties of the tar components and the application of producer gas.

Tar removal/conversion for the purpose of syngas cleaning has been a subject of several investigations (Milne *et al.*, 1998; Maniatis and Beenackers, 2000; Padban, 2001; van Paasen *et al.*, 2002; Devi *et al.*, 2003; Devi *et al.*, 2005; Anis and Zainal, 2011). The main target of syngas cleaning is the destruction of tars although the removal of heavy metals is also important. Tar removal methods can be categorized in two types; a primary method in which the treatment is carried out inside the gasifier itself and a secondary method in which the cleaning or conditioning takes place after the gasifier (downstream of the gasifier). Primary methods are of three types: (a) optimization of operating conditions; (b) modification of the gasifier design and (c) addition of catalysts and/or additives in the fuel bed. Secondary methods are characterized by syngas cleaning system and the type of secondary method used is

mainly set in accordance to the end application of the syngas and to the main types of contaminants present. Tar removal technologies are classified as physical or chemical. In physical removal systems, gas cleaning systems generally in use are wet scrubbers, gas cyclone separators, baffle filters, fabric filters and electrostatic precipitators by which particulates as small as 5 μm can be removed. Chemical conversion of tars is carried out by thermal or catalytic means. Catalysts used in this method are as those used in the primary treatment (Nair et al., 2003). Syngas cleaning strategies include water scrubbing followed by further cleaning and moisture reduction, low temperature capture of tars and destruction of tars at high temperatures preferably at the gasifier exit temperature.

According to the literature, using the syngas in a power production application, tar concentration in syngas needs to be less than 100 mg/Nm^3 which requires particle and tars reduction efficiencies of 90 % which are required for a satisfactory operation of ICEs using syngas produced in a downdraft gasifier (Devi *et al.*, 2003; Anis and Zainal, 2011).

1.2. Process Intensification and Miniaturisation (PIM)

Reduction in the processing volume without compressing the process output in terms of magnitude and quality, use of high pressures and temperatures and significant enhancement in mass and heat transfer rates are all aspects of an intensified process. This design philosophy is known as process intensification (PI). The concepts of PI were originally pioneered in the 1970s by Colin Ramshaw and his co-workers at Imperial Chemical Industries (ICI), where PI was defined as a "reduction in plant size by at least a factor of 100".

In the beginning, the development of PI was mainly driven by cost saving, given that a sustainable part of plant cost is associated with piping, support structures and other mechanical or civil engineering items (Stankiewicz and Moulijn, 2004; Akay *et al.*, 2005; Akay, 2006). PI is then applied throughout the chemical and process industry (CPI) to reduce investment and operating costs of chemical plants to increase profitability and mitigate greenhouse gas emissions. The toolbox that's process-intensifying equipment (hardware) and process intensifying methods (software) for PI is schematically shown in Figure (1.1).

By integrating PI with another design approach known as Process Miniaturization (PM) which is commonly applied in chemical and biological areas, the scope of the original PI can be expanded and the importance of miniaturization in intensification can be emphasized. Integration of Process Intensification and Miniaturization (PIM) not only creates a synergy in achieving the main design objectives, but also delivers other benefits which according to Akay and others (Akay *et al.*, 2005; Akay, 2006) are:
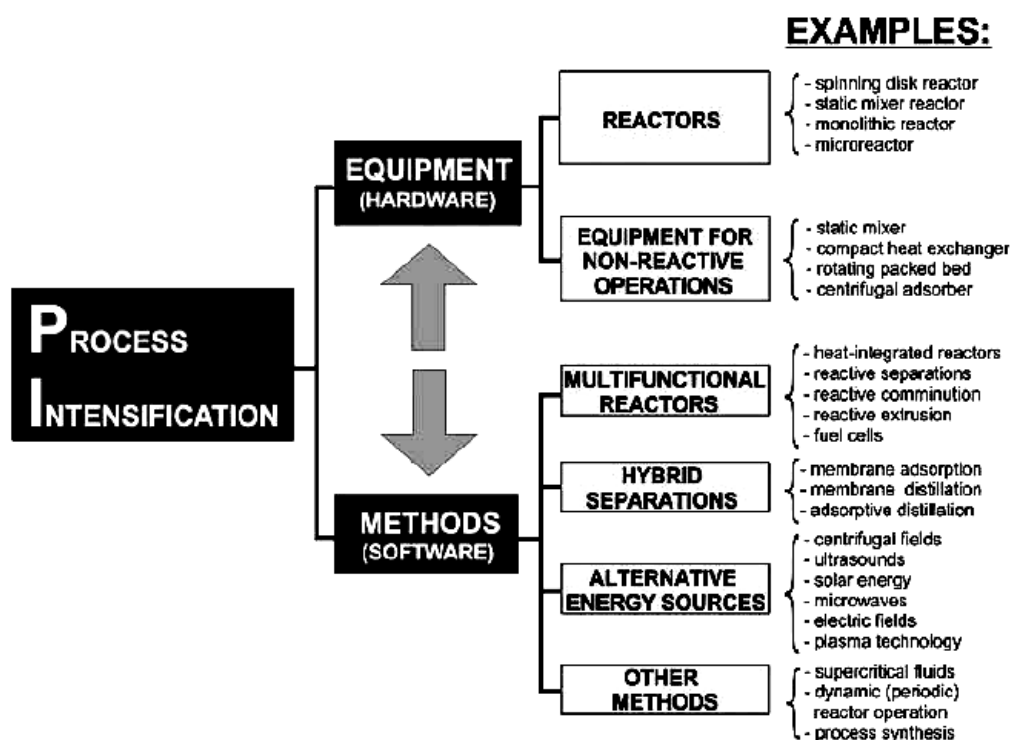
Figure (1.1): Process intensification toolbox (Stankiewicz and Moulijn, 2004).

* Novel products which in turn provide novel intensified processes;
* Inherent safety due to reduced reactor volume;
* At least ten fold decrease in process equipment volume;
* Eliminating of parasitic steps and unwanted by-products; thus, eliminating some downstream processing operations;
* A sustainable (energy, capital and operating cost reduction and environmentally friendly) process;
* Plant mobility, responsiveness and security; and finally
* A platform for other technologies.

Recently, a PIM Centre at Newcastle University, UK, has been established. The main objective of this Centre was to deliver the aspects of an intensified chemical process through the reduction of reactor volume, use of high pressures and temperatures, significant enhancement of mass and heat transfer, attain higher efficiencies of operation, lower costs, reduced plant foot print and reduction in volume of hazardous materials (Akay *et al.*, 2005; Akay, 2006).

The integrated small-scale gasifier-ICE system is one of several emerging energy technologies in which PIM has become an essential tool in the development of high efficiency power production from low heating value feedstocks. The intensified throated downdraft gasifier developed by Dogru and Akay (Dogru and Akay, 2006) is a small scale (< 5 MW) autothermal gasification system. In this gasifier in which temperatures greater than 1100 ^{o}C are generated for the conversion of biomass and/or biomass waste to syngas, PIM has been achieved by reducing reactor volume; thus, providing a reduction in specific capital investment by a factor of 2.5. According to Akay (2006), intensified distributed production plants consisting of intensified unit operations can deliver low specific capital and operating costs in addition to short start up and shutdown times.

In this study, gasification of refinery sludge will be investigated using a novel fixed bed throated downdraft intensive 50 kWe air- blown auto-thermal gasifier. In addition, as syngas quality is central to most applications of syngas, including ICE operation, we will develop intensified syngas cleaning systems for different applications of the cleaned gas. The main target of syngas cleaning is the destruction of tars although the removal of heavy metals is also important. Traditionally, the syngas cleaning strategies include water scrubbing followed by further cleaning and moisture reduction, low temperature capture of tars and destruction of tars at high temperatures preferably at the gasifier exit temperature. On the basis of these findings we will evaluate the measures for the reduction and/or elimination of these contaminants in the syngas.

1.3. Objectives of the Thesis

Initially, several batches of wood chips as a reference will be gasified. Wood chips are used as a reference due to the ease in handling, relative consistency and availability.

Part of this work/research is to use PIM to utilize briquetted refinery sludge to produce and clean syngas throughout gasification for power generation via an ICE. To achieve this goal, a small scale gasification system, which employs a novel fixed bed throated downdraft intensive 50 kWe air-blown auto-thermal reactor and gas clean-up trains consisting of cyclone, water scrubber and filter box, will be used.

Next, in the development of an intensified syngas cleaning system to achieve more efficient and safer gas cleanup and treatment technologies, PIM design philosophy will be applied as the basis to design, construct and test two novel/new different setup systems namely, small (plasma reactor) and pilot (electric field enhanced tar removal equipment) scale intensified syngas cleaning systems for tar reduction or/and removal. In the demonstration of both techniques, a model tar and a model syngas under laboratory conditions will be used. As model tar, fresh crude oil (supplied by BP Amoco) and as model syngas, pure carbon dioxide (supplied by BOC) will be employed.

Different types of post-functionalized PolyHIPE Polymers (PHPs), plasma at different power intensities and combination of plasma at different power intensities with a packed bed of sulphonated PolyHIPE Polymer (s-PHP) particles will be investigated via the small scale intensified syngas cleaning system (intensify the separation of model tar from model syngas and the efficiency of removal). These polymers will be produced, functionalized and characterized using environmental scanning electron microscopy (ESEM) and surface area analysis (SAA). In addition, more experiments will be carried out using the pilot scale intensified syngas cleaning system in different profiled central high voltage electrode is either completely (totally) insulated electrode (CIE) when it is used with water spray, or it is partially isolated electrode (PIE) when no conductive material is present in the gas stream or in the fixed bed. In all cases, the inlet and outlet gas composition will be monitored using gas chromatography (GC).

1.4. Thesis Layout

This thesis covers the work undertaken over the last five and half years. The thesis has been organized into five chapters. It first provides a survey of the relevant literature and background information relevant to this study (Chapter one). Chapter two represents a summary of crude oil refinery and processing. Moreover, sources of sludges in refineries are briefly represented and the importance of refinery sludge treatment and disposal methods such as lagoon/pit, incineration land farming and secure landfill in petroleum industry are discussed. Also, biomass and/or biomass waste conversion technologies such as combustion, pyrolysis and gasification are summarized. History of gasification, details of gasification process, specification of feed materials along with the effect of main operating conditions on syngas production such as temperature, gasifying agent, equivalence ratio, residence time, as well as the required pretreatment processes and different types of gasifiers are reviewed, focusing on the fixed bed throated downdraft gasifier as it is the type that has been utilized in this work. Finally, a review of the main contaminants in syngas from biomass and/or biomass waste gasification, contaminants removal technologies which broadly can be divided into two approaches; cleaning or conditioning that takes place after the gasifier (secondary methods), and treatments inside the gasifier (primary methods) and possible end use routes for the producer clean gas are the other topics covered in this chapter.

In chapter three, details of the methodology, experimental setup, procedure, equipment description, chemicals used for PolyHIPE Polymers (PHPs) production (which have been used in the form of a packed bed for the adsorption of model tar from model syngas), modification and analysis ESEM and SAA are all described. Also, the gasification experimental system, that consists of a down draft gasifier (50 kWe output), water scrubber, filter box, gas suction fan and a pilot burner, is covered in this chapter. Design, fabrication and use of a new/novel multi-functional model tar reduction and/or removal of tar from syngas rig as a water scrubber, combined water scrubbing and electric field at different intensities and/or electric field at different intensities in the absence and presence of a packed bed of sulphonated PolyHIPE Polymer (s-PHP) are also discussed in this chapter.

In chapter four, the gasification/co-gasification experiments, in which wood chips and 70% wt/wt refinery sludge blending with 30% wt/wt sawdust were used as the feedstock, are detailed. Also, the development of intensified syngas cleaning systems, namely, small and pilot scale to achieve more efficient and safer gas cleanup technologies via PIM design philosophy, has been presented. In this chapter, the effect of various types of Poly HIPE Polymers (PHPs), the effect of plasma at different power intensities and the effect of combination of plasma at different power intensities with a packed bed of s-PHP on model tar reduction and/or removal efficiency are covered. Moreover, in the pilot scale (electric field enhanced tar removal equipment) intensified system, experiments were carried out in two different profiled electrode configurations: completely insulated electrode (CIE) or a partially insulated electrode (PIE) are briefly represented in this chapter.

In chapter five, the conclusions arising from this study along with the outstanding issues that require further investigation and evaluation are given.

Chapter Two
Literature Review

Chapter Two

Literature Review

2.1. Introduction

This chapter reviews the literature relevant to this study. Firstly, in this chapter, a summary of crude oil refinery and processing is shown. Moreover, sources of sludges in refineries are briefly represented and the importance of refinery sludge treatment and disposal methods such as lagoon/pit, incineration land farming and secure landfill in petroleum industry are discussed. Also, biomass and/or biomass waste conversion technologies such as combustion, pyrolysis and gasification are summarized. History of gasification, details of gasification process, specification of feed materials along with the effect of main operating conditions such as temperature, gasifying agent, equivalence ratio, residence time as well as the required pretreatment processes and types of gasifiers are reviewed, focusing on the fixed bed throated downdraft gasifier as it is the type that has been utilized in this work. Finally, a review of the main contaminants in syngas from biomass and/or biomass waste gasification, contaminants reduction and/or elimination technologies which broadly can be divided into two approaches; cleaning or conditioning that takes place after the gasifier (secondary methods), and treatments inside the gasifier (primary methods) and possible end use routes for the producer gas are the other topics covered in this chapter.

2.2. Crude Oil Refinery and Processing

Petroleum is a complex mixture of organic liquids called crude oil and natural gas, which occurs naturally underground and was formed millions of years ago. Crude oil varies from oilfield to another in colour and composition, from a pale yellow low viscous liquid to heavy black 'treacle' consistencies.

Crude oil and natural gas are extracted from underground, on land or under the oceans, by sinking an oil well and are then transported by pipeline and/or ship to refineries where their components are processed into refined products. Crude oil and natural gas are of little use in their raw state; their value lies in what is created from them: fuels, lubricating oils, waxes, asphalt, petrochemicals and pipeline quality natural gas.

An oil refinery or petroleum refinery is an industrial process plant where crude oil is processed and refined into more useful petroleum products, such as liquefied petroleum gas (LPG), naphtha, gasoline, kerosene, diesel fuel, asphalt base and heating oil. Historically, the first oil refinery in the world was built in 1851 at Bathgate, Scotland, by the Scottish chemist James Young. Figure (2.1) illustrates a flowchart of a refinery process.
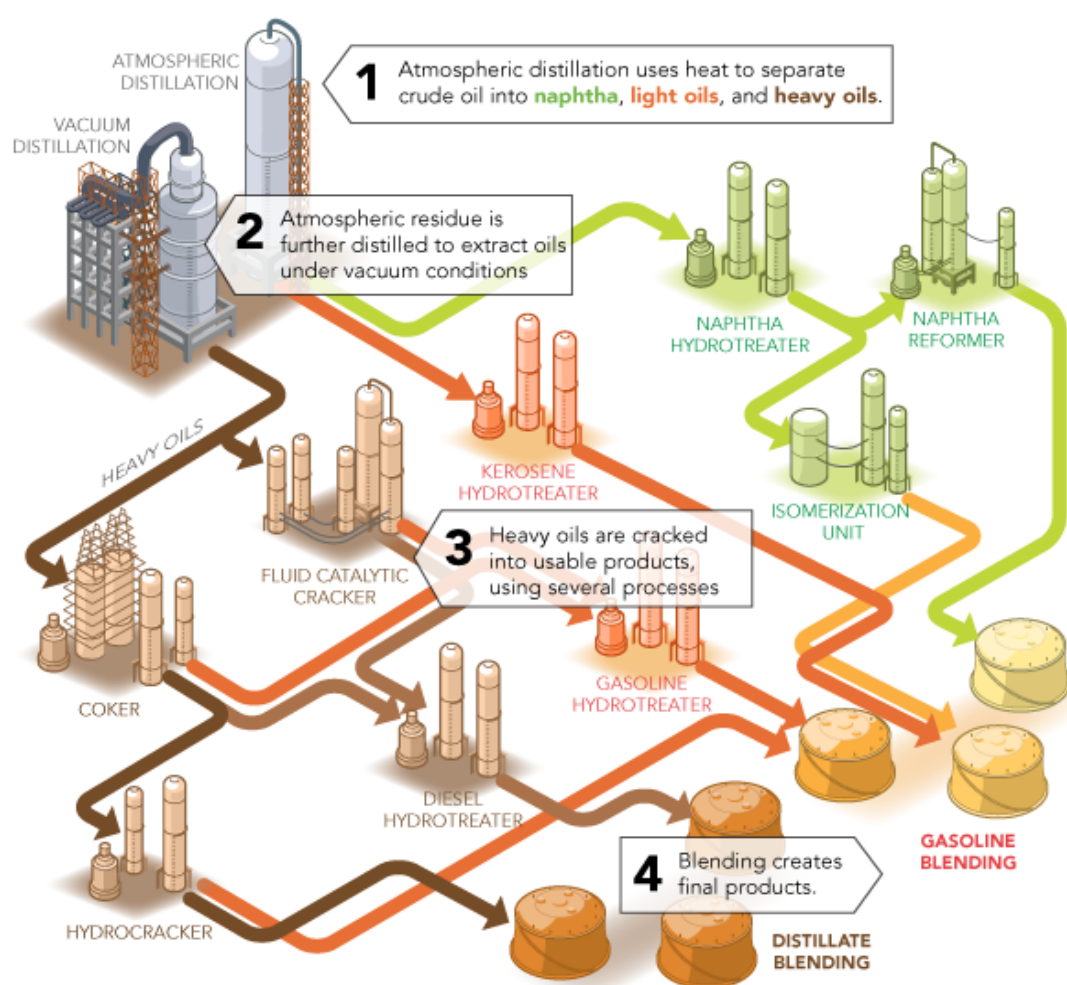
Figure (2.1): Flowchart of a refinery process.

http://www.cieng.com/a-11-156-Industries-Refining.aspx

Generally, refinery operations include: fuel production; by-product processing; ancillary operations and waste management (Alshammari et al., 2008). In a petroleum refining process, hydrocarbons of varying molecular masses are separated into fractions through distillation (fractionation). In this process, crude oil from its

storage tank is preheated and fractionated in the crude distillation unit. Through a chemical conversion, hydrocarbons are converted into product(s) while impurities are separated out. A lower grade crude oil may require a more complex refining process to remove impurities. Atmospheric distillation, vacuum distillation, reforming, cracking (catalytic cracking, fluid catalytic cracking, hydrocracking and thermal cracking), alkylation, isomerisation, polymerization, hydrotreating and sulphur plants, sulphur recovery plants, delayed coking and blending, etc. are among the processes involved in refineries (Bakr, 2010).

2.2.1. Sources of Sludges in Refineries

Air, water and land can all be affected by refinery operations, since out of a refinery process; both hazardous and non-hazardous solid wastes can be produced. Such wastes include sludge, spent process catalyst, filter clay and incinerator ash (Bakr, 2010). Refineries should be aware of their responsibility to the community and employ a variety of processes to safeguard the environment. The main sludges generated are oily sludge, bio sludge and chemical sludge. Sources of such sludges generation in refineries are schematically shown in Figure (2.2).
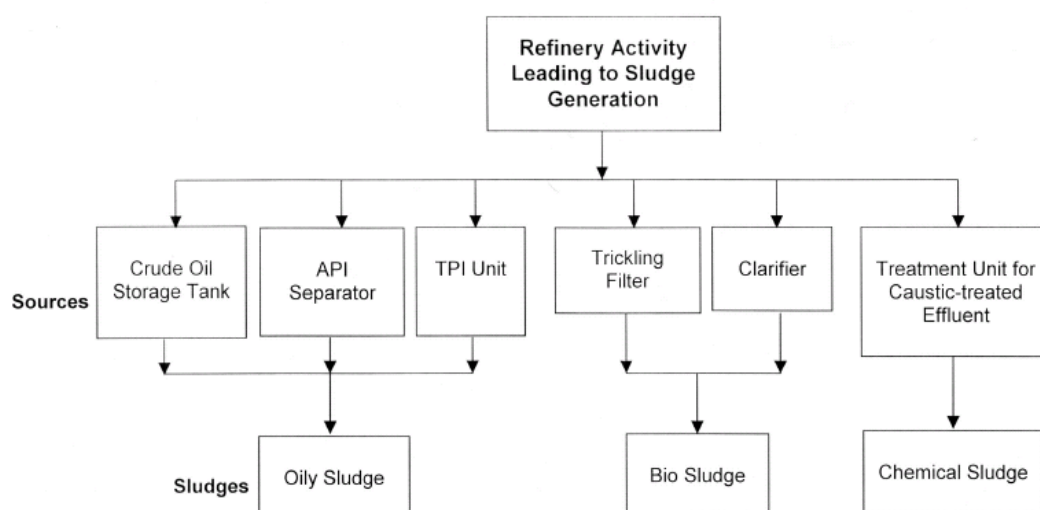
Figure (2.2): Sources of sludges in refineries (Bakr, 2010).

Presence of oily sludge in a refinery can be as a result of pumps and desalter failures, periodic cleaning of storage tanks, oil draining from tanks and operation units and also as a result of pipeline ruptures (Kuriakose and Manjooran, 2001). It can also

be generated while treating wastewater in an American Petroleum Institute (API) separator and Tilted Plate Interceptor (TPI) unit of effluent treatment plants. Biological sludge can be generated during biological treatment of wastewater from trickling filter and clarifier unit. Finally, chemical sludge is generated during the treatment of caustic treated effluent with ferric chloride and polyelectrolyte. In this study, only oily sludge will be further considered, other sludges will not be. In accordance to: nature of crude oil, processing capacity, downstream capacities and design of the effluent treatment plant, etc., the amount of sludge generated is determined (Kuriakose and Manjooran, 2001). Due to rapid expansion of petroleum processing operations; generation of waste has rather been enormous by which a serious threat to environmental quality on the mother earth and its inhabitants is caused. By looking at what is remaining from the natural resources; one should exploit such resources efficiently in a way that even waste is considered as a beneficial matter (Alshammari et al., 2008). In a survey by Kuriakose & Manjooran (Kuriakose and Manjooran, 2001) it was shown that oily sludge contains approximately 25% water, 5% inorganic sediments such as sand, clay, scales, etc., and the rest 70% hydrocarbons. Table (2.1) shows the characteristics of a purified refinery sludge (hydrocarbon fraction), while the weight percentages of the metal elements found in the ash following burning are shown in Table (2.2).

Table (2.1): Characteristics of a purified refinery sludge (hydrocarbon fraction) (Kuriakose and Manjooran, 2001).

Physical properties	Value
Density at 15°C (kg/m^3)	957.3
Pour point ($^{\circ}$C)	42
Wax (%wt)	6
Asphaltenes (%wt)	7.8
Acidity (mg KOH/g)	4.30
Flash Point ($^{\circ}$C)	> 200
Kinematic viscosity at 100 $^{\circ}$C (cS)	30.33
Total sulphur (% wt)	3.43
Ash content (% wt)	4.8

Table (2.2): The weight percent of the different metal elements in the ash (Kuriakose and Manjooran, 2001).

Element	Weight percentage (wt %)
Iron (Fe)	23.49
Aluminium (Al)	10.57
Calcium (Ca)	1.64
Sodium (Na)	0.57
Potassium (K)	0.46
Nickel (Ni)	0.12
Vanadium (V)	0.23
Magnesium (Mg)	0.65
Zinc (Zn)	0.21
Titanium (Ti)	0.53
Manganese (Mn)	0.10

2.2.2. Treatment and Disposal of Oily Sludges

Available treatment and disposal methods for refinery sludges are discussed in this section. They include: sludge disposal in lagoon/pit, incineration, land farming and secure landfill of oily sludge. Storing an oily sludge in a lagoon has been commonly used. A lagoon is made with bricks and cement. Although lagoons are used to store an oily sludge, they; however, do not provide a long term and an environmentally friendly solution to ultimately dispose of an oily sludge (Einawawy Amins et al., 1987). In incineration, air in excess amounts is used to achieve complete combustion of waste by which a significant reduction in the amount of waste is secured. Combustion time, temperature and turbulence are important factors in the incineration process. Although it has been used in few developed countries, due to some reasons it has not found a wide application (Patel Naranbhai and Sing, 1999). These reasons include: incomplete combustion by which environmental pollution, by stack emissions, is caused. Also, it requires landfill facilities for the final disposal of ashes which contain heavy metals and require to be disposed of in an environmentally friendly manner. In land farming, as the name implies, waste in certain amounts is landfilled followed by the application of fertilizer and regular planting of crops. Mainly, it depends on the natural in-situ biological decomposition of hydrocarbons by

the vast and varied population of microflorain natural soils associated with photo-degradation. Both structure of the soil and humus content can influence the process of hydrocarbon decomposition as they influence oil and water retention, type and population of microflora and the rate of oxygen transfer. This method requires further investigations prior to any large scale applications in the following environmental issues: the presence of oily odour during initial spreading, groundwater pollution due to migration of leachate contaminated with hydrocarbons, phenols and heavy metals and health problems associated with the contact of oily sludge. The last treatment process for refinery sludges is the secure landfill techniques. In this process, waste is isolated by thick layers of impermeable clay and synthetic liner to avoid contamination of air and ground water.

Recently, treatment and disposal of refinery sludge have become a problem of increasing urgency in industrialized societies. Certain methods of treatment and disposal of refinery sludge *do* exist, but they are not entirely satisfactory. Therefore, it is important to develop a technology for adequate treatment of refinery sludge in order to reduce the environmental problem and costs of treatment. It can be assumed that gasification is a suitable technology because it reduces waste volume, removes toxic organic compounds and fixes heavy metals in the resultant solid instead of landfill and/or incineration option. The gasification process converts any carbon containing material into a combustible gas composed primarily of carbon monoxide, hydrogen and methane, which can be used as a fuel to generate electricity and heat, and a little amount of these gases, can be used to dry wet refinery sludge. Typical raw materials used in gasification are coal, biomass, agricultural wastes, sewage sludge, and petroleum based materials. Gasification also adds value to low or negative feedstocks by converting them to marketable fuels and useful products.

2.3. Fundamentals of Biomass Gasification

Biomass can be defined as any organic material of a plant origin. The contribution of biomass to the world's energy supply has been estimated at 10 to 14 % (Peter, 2002). The European Union leaders also set a binding overall goal of 20% for renewable energy sources by 2020 compared to the present 6.5 % (Yang et al., 2007).

Biomass gasification represents some interesting advantages that could be key points for its integration to the energy production grid. Traditionally, crude oil is the raw material of choice for power or electricity generation. Unfortunately, oil possesses problems that must be addressed in order to sustain the same energy consumption required for both developed and developing countries. Also, crude oil is linked to a lot of serious problems which is mainly associated with our life. Two of these most serious problems faced nowadays due to the continuous dependence on the fossil fuel as a main source for energy are global warming and environmental pollution. This is of course because of its pollutants emission. Furthermore, the combustion of fossil fuel usually produces greenhouse gas (carbon dioxide) and toxic gases, such as SO_2, NO_x and other pollutants which take part directly in causing the global warming (Klass, 1998; Ni *et al.*, 2006).

Mostly important, oil is not a renewable source of energy. If its rate of consumption continues as it is today, it is expected, optimistically, that the global reserves will last for no longer than another 100 years (Klass, 1998). On the other hand, biomass gasification can overcome this setback with ease. The constant generation of organic material makes it a renewable source capable of satisfying global energy demands without difficulties (Akay, 2006; Peterson, 2010).

Together with the regional independence that it possesses, biomass gasification has another advantage. The technology produces a tangible material fuel that can be easily stored and manipulated. The produced gas could be used together with a fuel cell or it could be converted to a liquid fuel that can be processed later for further improvements. The types and characteristics of the processed fuel depend on the medium that is used to gasify the solid feedstock. It is expected that the biomass gasification technologies may play an important role in meeting the set goals for renewable energies. This is because of the higher efficiencies that may be produced by gasification compared to other technologies such as combustion. Biomass can be converted to energy carriers by biochemical or thermochemical processes.

2.3.1. Biomass Conversion Technologies

The conversion of biomass into useful forms of energy can be carried out via biochemical and thermochemical processes as illustrated in Figure (2.3).
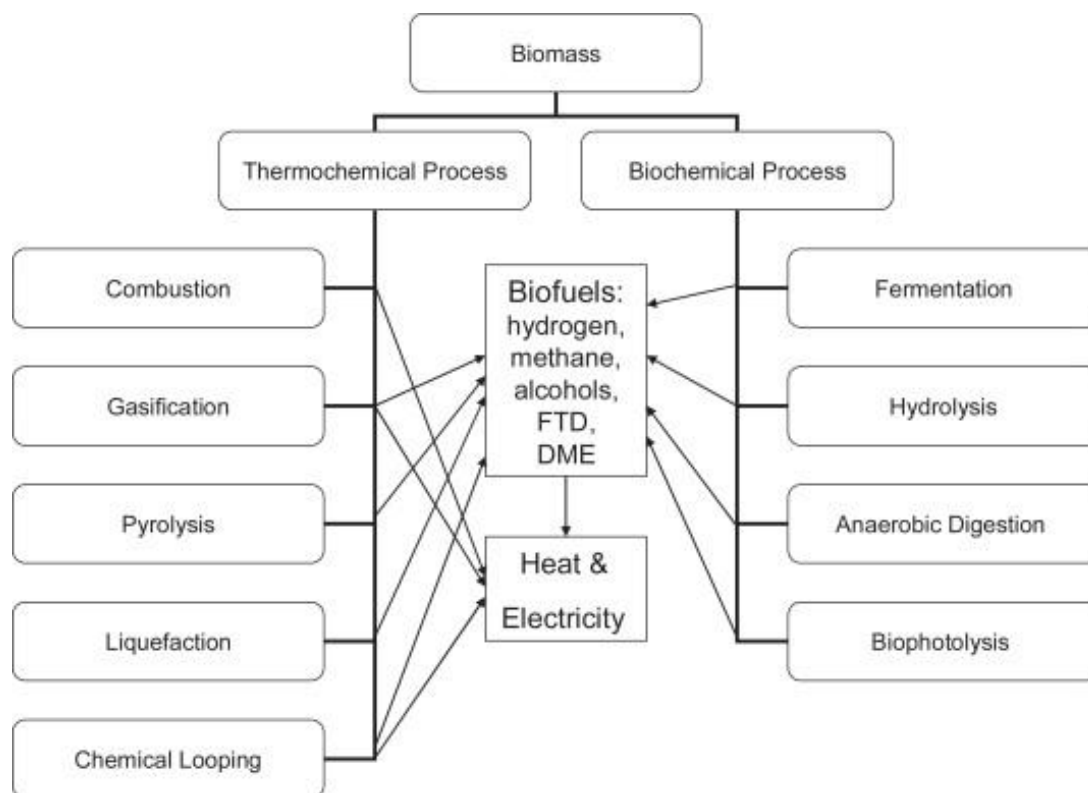
Figure (2.3): Biomass conversion processes, products and applications.

2.3.1.1. Biochemical Biomass Conversion Processes

Biochemical conversion gives single or specific products such as biofuels and is a slow process, typically taking hours, days, weeks (anaerobic fermentation and farm digestion) or years (landfill gas by digestion) for reactions to be completed. Reviewing such a process is a huge topic and may further widen the scope of the study and will not be discussed further. However, biomass conversion via the thermochemical processes in general, and the biomass gasification in particular, will be discussed in this chapter.

2.3.1.2. Thermochemical Biomass Conversion Processes

Thermal conversion gives multiple and often complex products, with catalysts often used to improve the product quality, and this usually takes place in very short reaction times of typically seconds or minutes. Thermochemical conversion processes change the chemical structure of the biomass by means of heat. These conversion processes are used for both volume reduction and energy recovery. Depending on the process and its conditions, the end product may have varying percentages of solid (charcoal), liquid (oils and tars) or gaseous (combustible gas) products. The main difference in the thermochemical conversion processes is their air (oxygen) requirements. Main thermal biomass conversion technologies are: combustion (stoichiometric or excess air/oxygen); pyrolysis (no oxygen) and gasification (substoichiometric air/oxygen).

The end products for each of these processes vary and also different energy and matter recovery systems can be used according to the market or requirements (Bridgwater, 1994). Figure (2.4) shows these processes and conversion routes.
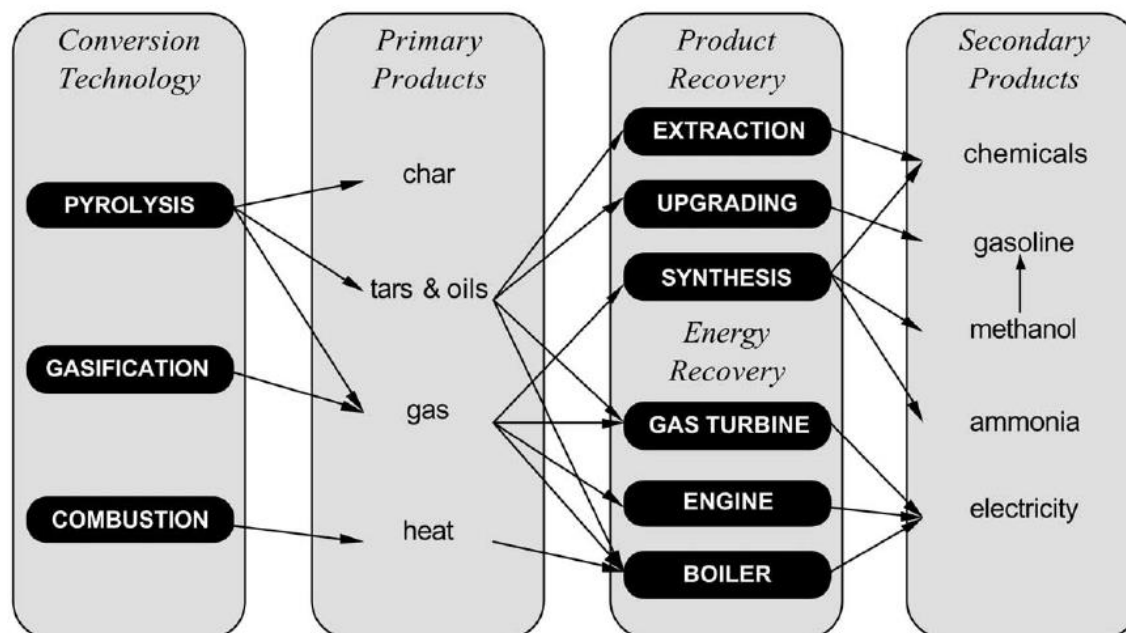
Figure (2.4): Thermochemical conversion processes and products (Bridgwater, 1994).

2.3.1.2.1. Combustion

Combustion is an exothermic reaction between a substance (the fuel) and a gas (the oxidizer), usually O_2, to release heat. Combustion of biomass fuels proceeds by two alternative pathways. In the first pathway, which operates at higher temperatures, pyrolysis or thermal decomposition of the biomass provides a mixture of combustible gases. These gases mix with air to fuel the flaming combustion that could rapidly spread in the gas phase. In the second pathway, which dominates at lower temperatures, pyrolysis gives mainly carbonaceous char and a gas mixture containing combustible gases, water and carbon dioxide that is not very flammable. Oxidation of the resulting active char then provides glowing or smouldering combustion (Shafizadeh, 1981).

Although theoretically stoichiometric oxygen is demanded because of the inconsistencies in solid fuels, excess air should be supplied to combustion systems. Excess air promotes mixing and turbulence but it decreases the combustion temperature. In low temperature combustion, emissions of odorous and toxic gases may occur (Tchobanoglous et al., 1993). Furthermore, incomplete combustion can result in excessive emissions of particulate matter, fly ash, metal oxides and partially oxidized derivatives, some of which are toxic. Therefore, the amount of oxygen fed to the system can be used to control the combustion temperature. The heat released by combustion can be used directly or transformed to produce more valuable energy product or electricity through energy recovery units.

Although combustion is an old and well established technology, there are still studies being published about modelling, efficiency and energy analysis and combustion characteristics of different bio fuels (Williams *et al.*, 2001; San José Alonso *et al.*, 2006).

2.3.1.2.2. Pyrolysis

Pyrolysis is the thermal decomposition of biomass in the absence of oxygen with the objective to obtain as much liquid fuel as possible. As discussed above and in the work of Shafizadeh (Shafizadeh, 1981), pyrolysis is always the first step in gasification and combustion processes. In combustion, it is followed by total oxidation where as in gasification; pyrolysis is followed by partial oxidation of the

primary product. The three major output fractions from a pyrolysis process are: a combustible gas; a liquid fraction (tars and oils) and a char consisting of almost pure carbon plus inert material originally present in the feedstock (Belgiorno et al., 2003).

Depending on the operating conditions, pyrolysis process can be divided into three subclasses, which are: conventional pyrolysis, fast pyrolysis and flash pyrolysis (Demirbas, 2004). The range of main operating parameters for these processes were summarized by Maschio and others (Maschio et al., 1992) and are given in Table (2.3).

Table (2.3): Main operating parameters for conventional, fast and flash pyrolysis (Maschio et al., 1992).

Pyrolysis subclasses → Operating parameters ↓	Conventional Pyrolysis	Fast Pyrolysis	Flash Pyrolysis
Pyrolysis Temp. (K)	550 – 950	850 – 1250	1050 – 1300
Heating Rate (K s^{-1})	0.1 – 1	10 – 200	> 1000
Particle Size (mm)	5 – 50	< 1	< 0.2
Solid Residence Time (s)	450 – 550	0.5 – 10	< 0.5

The process can be adjusted to favour any of the end products stated above with a 95.5 % fuel-to-feed efficiency (Ayhan, 2001). The products from the pyrolysis of different solid materials studied by different authors. Küçük and Demirbaş have summarized them as shown in Table (2.4).

Table (2.4): The yield and composition of different solid materials (Küçük and Demirbaş, 1997).

Yield and Composition → Solid Material ↓	T (K)	(wt %)			(vol %)				
		Char	Liquid	Gas	CO_2	CO	O_2	HC	Others
Wood chips	754	39.30	48.34	12.33	21.5	19.6	5.4	53.5	-
Fir bark	755	41.6	48.90	8.20	-	-	-	-	-
Newspaper	1089	30.11	44.07	25.82	22.9	30.1	1.3	21.5	24.2
Refuse	755	24.71	61.08	12.33	44.77	33.5	-	15.91	5.56

Pyrolysis's potential to contribute to the energy supply is huge and the process also has considerable environmental benefits. However, there are still problems to overcome with the process and use of produced oil due to its poor thermal stability and corrosivity (McKendry, 2002b). Another disadvantage is the high costs due to the early stages in development (Kaltschmitt and Dinkelbach, 1997). The number of publications made in this area also reflects the growing interest in the field and high potential of overcoming these problems in future (Solantausta *et al.*, 1993; Frederick *et al.*, 1994; Raveendran and Ganesh, 1996; Bridgwater, 1999; Bridgwater *et al.*, 1999; Meier and Faix, 1999; Bridgwater and Peacocke, 2000; Yaman, 2004; Kersten *et al.*, 2005).

2.3.1.2.3. Gasification

Gasification is a thermochemical process in which partial oxidation of organic matter at high temperatures results in a mixture of products, mainly consisting of a gaseous fuel that can be utilized for energy-dependant applications. The gas generated is more usable than the organic feedstock material (used for the gasification process) for generation of heat and power (Priyadarsan et al., 2005). Various oxidizing agents can be utilized for gasification; air, oxygen, steam or a mixture of these gases. For economical reasons, air remains the most commonly utilized oxidizing agent.

The producer gases released from gasification generally contain CO (18-20%), H_2 (18-20%), CH_4 (1-2%), H_2O (11-12%) and N_2. With excess air, combustion produces CO_2 and H_2O, but in sub-stoichiometric conditions, products such as CO and H_2 can be enhanced (Quaak *et al.*, 1999). Gasification of biomass can generate gases with calorific value in the order of 3.9 to 11.8 MJ/m^3 using air, and from 11.8 to 27.5 MJ/m^3 with the use of oxygen. With a greater degree of control leading to higher production of methane and other light hydrocarbons, the value can reach 27.5 to 39.3 MJ/m^3. The values mentioned for air and oxygen-induced gasification correspond to approximately 20-50% of the energy content of natural gases and biogas on volume basis (Reed and Das, 1998).

2.3.2. History of Gasification

The technology of gasification is not new as its basic principle has been known since the late 18th century (Overend, 1979). It goes back to 1792 involving some experiments by means of pyrolysis on coal. This work was supported by some patents targeting gas production (syngas) for power generation (Rezaiyan and Cheremisinoff, 2005; Peterson, 2010).

In the 19th century, in England, the United States and Canada producer gas (town gas) was produced. Initially, this gas with its cleaner flame than that generated from coal or candles, was used for cooking. Later, due to low production cost, it was also used for lighting of houses and streets. With the economic prosperity at the end of the century, town gas started to be introduced as heating fuel for residences (Klass, 1998; Rezaiyan and Cheremisinoff, 2005; Higman and van der Burgt, 2008; Peterson, 2010).

In the next century, countries like Germany searched for an independence from oil fuels and promoted research in gasification technology (Schilling et al., 1981). But, it was during the Second World War that Europe was forced to use and develop more air-blown gasifiers for the production of the energy demanded in the cities (Rezaiyan and Cheremisinoff, 2005). Roughly, during this time a million air-blown gasifiers were constructed (Klass, 1998) and the use of cars powered with syngas peaked (Higman and van der Burgt, 2008). Later, once the war has come to an end and oil was introduced to the energy market at cheap prices, use of gasification for power generation has been reduced (Rezaiyan and Cheremisinoff, 2005). Reduction in the use of gasification was also due to some difficulties in storing large amounts of gas under pressurized conditions (Higman and van der Burgt, 2008). Instead, the gasifiers were used mainly to produce synthetic gases for the chemical industry in developed countries (Rezaiyan and Cheremisinoff, 2005). However, in developing countries, the use of gasifiers began to increase (Peterson, 2010). The technology introduced ways to provide cheap and convenient energy where oil and natural gas could not be spent.

Currently, the search for renewable technologies is giving a new light to gasification. The use of biomass together with a gasifier is proving to be an excellent path for the generation of clean and sustainable energy (Akay et al., 2007; Calkan,

2007; Sunggyu et al., 2007). The renewed interest in gasification is also creating new companies and open source societies where the know-how is shared so that it could speed up the development of localized energy generators (Reed, 2009; Peterson, 2010). These companies are focussing on the use of biomass as an alternative fuel for the generation of energy in places located outside the power grid, such as farms and small localities.

2.3.3. Gasification Process

The gasification process is not simple. Gasification of a particle of biomass and/or biomass waste takes place in four steps Figure (2.5) (Bridgwater, 2003).

1. Drying to evaporate moisture,
2. Pyrolysis to give gas, vaporized tars or oils and a solid char residue,
3. Gasification or partial oxidation of the solid char, pyrolysis tars and pyrolysis gases, and
4. Reduction

In the first step, the fuel particle dries, with moisture in the particle being evaporated.

$$C + H_2O_{(l)} \xrightarrow{\text{Heat}} C + H_2O_{(g)} \qquad \Delta H_{298K} = +385 - 646 \text{ kJ kg}^{-1}$$

Thermal conversion processes require low moisture content feedstock (typically < 50%). Fuels with higher moisture content can also be used in thermal conversion processes but the overall energy balance for the conversion process can be adversely compacted (McKendry, 2002a). According to McKendry (2002a) the biomass moisture content should be below 10–15% before gasification. High moisture content reduces the temperatures in the oxidation zones as it acts as a heat-sink requiring energy to evaporate it from the feed. Low temperature in the oxidation zone can lead to incomplete cracking of tars formed in the pyrolysis zone. However, there is some conflicting information in the literature about the required moisture content for gasification processes. Reed (1981) states that starting with dry gasification, the gas heating value increases with increasing moisture input including chemically bound water and air blast humidity as well as moisture content of the feed, and makes a peak between 30 and 40% total moisture input. Theoretically, there is no lower limit for the moisture content as lower moisture content would lead to lower tar contamination in the producer gas.

23

In the second step the fuel particle will then pyrolyse and gases and vapours are released which consist mainly of hydrocarbons, water vapour and other light gases such as CO, CO_2 and H_2. This is accompanied by a large decrease in mass and volume. Both endothermic and exothermic reactions occur, and physical and thermodynamic properties vary continuously.

Solid fuel $\longrightarrow$ Gas + Tar + Water + Char

C_xH_yO + heat $\longrightarrow$ $H_2O + CO_2 + H_2 + CO + CH_4 + C_2H_6 + CH_2O + ... + $ tar + char
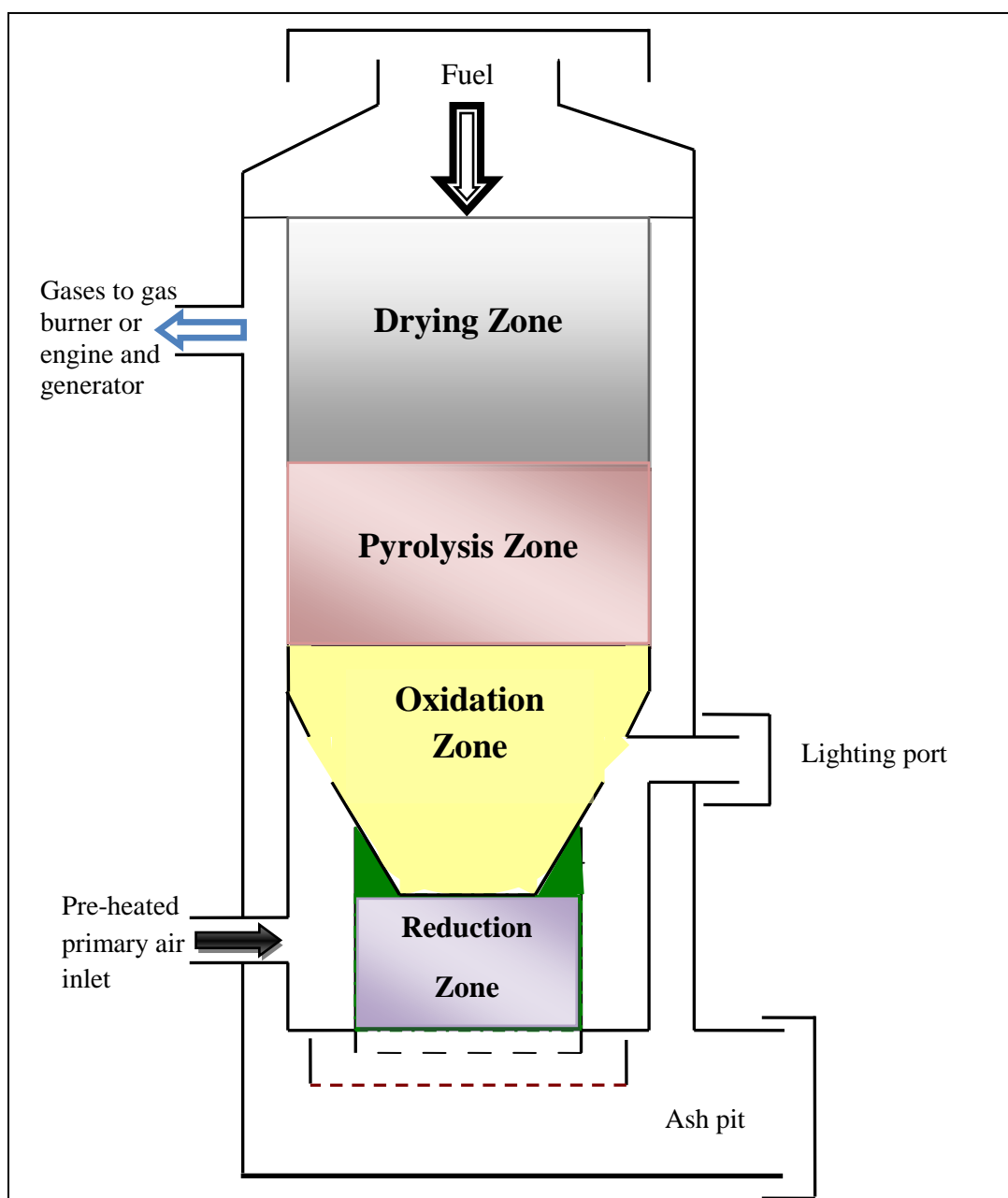
Figure (2.5): Reaction zones in a throated downdraft gasifier.

The relative yields of the gaseous, liquid and solid products are a function of the pyrolysis reaction conditions such as: reaction temperature, particle heating rate, fuel moisture content, particle size, composition of the ambient atmosphere, pressure and vapour residence time, see Table (2.5) below.

Table (2.5): Influence of reaction conditions on relative yields of pyrolysis products (Earp, 1988; McKendry, 2002c).

Relative yields → Reaction condition ↓	Yield of			
	Gas	Low MW Liquids	High MW Liquids	Char
Reaction temperature	Increases	Increases	Decreases	Decreases
Particle heating rate	Decreases	Increases	Increases	Decreases
Feed moisture content	Decreases	Decreases	Decreases	Increases
Vapour residence time	Increases	Increases	Decreases	Decreases
Fuel size	Increases	Decreases	Decreases	Increases
Pressure	–	Decreases	Decreases	Increases

In the gasification stage, all the pyrolysis products undergo a series of reduction and oxidation reactions to produce the final product gas containing mainly H_2, CO, CO_2, CH_4 and H_2O. The main reactions involved in the gasification process with enthalpy changes accompanying the reaction are reproduced from the work of Belyaev and co-workers (Belyaev *et al.*, 2003) and Dogru (Dogru, 2000) as outlined below:

(a) Gasification with oxygen or air (Partial Oxidation)

$$C + \tfrac{1}{2}\,O_2 \longrightarrow CO \qquad\qquad \Delta H_{298K} = -111 \text{ kJ mol}^{-1}$$

(b) Combustion with oxygen (Complete Oxidation)

$$C + O_2 \longrightarrow CO_2 \qquad\qquad \Delta H_{298K} = -399 \text{ kJ mol}^{-1}$$

(c) Gasification with steam (Water Gas Reaction)

$$C + H_2O \longleftrightarrow CO + H_2 \qquad\qquad \Delta H_{298K} = +131 \text{ kJ mol}^{-1}$$

(d) Gasification with CO (Boudouard Reaction)

$$C + CO_2 \longrightarrow 2CO \qquad \Delta H_{298K} = + 172.5 \text{ kJ mol}^{-1}$$

(e) Gasification with hydrogen (Methane Formation)

$$C + 2H_2 \longleftrightarrow CH_4 \qquad \Delta H_{298K} = - 75 \text{ kJ mol}^{-1}$$

$$CO + 3H_2 \longleftrightarrow CH_4 + H_2O \qquad \Delta H_{298K} = - 206 \text{ kJ mol}^{-1}$$

(f) Water-Gas Shift Reaction

$$CO + H_2O \longleftrightarrow CO_2 + H_2 \qquad \Delta H_{298K} = - 42 \text{ kJ mol}^{-1}$$

(g) Methanation (Methane Reforming Reaction)

$$CH_4 + H_2O \longleftrightarrow CO + 3H_2 \qquad \Delta H_{298K} = 165 \text{ kJ mol}^{-1}$$

The most important gasification reactions are (c), (d) and (f). According to Dogru (2000) these three reactions are sufficient to describe the gasification process.

In the final zone (reduction) as in the drying and pyrolysis zones, the thermal energy required for the reactions is provided by the exothermic reactions in the oxidation zone (Reed and Das, 1998). The concentration of oxygen in this zone is insufficient for oxidation and a series of reduction reactions occur. Here, some of the unreacted char from the oxidation zone is converted into non-condensable gases and water vapour by reaction with the volatiles from the pyrolysis zone and gases from the oxidation zone. These reactions increase the percentage of H_2, CO, CH_4 and other incondensable gases in the syngas mixture.

2.3.4. Feed Materials Specifications

The feed material is an important factor in the design, operation and performance of a gasifier system. There is a wide range of feed characteristics that influence the gasification process of which the most important are generally considered to be fuel shape, moisture content, ash content, volatile matter, heating value and absolute and bulk density.

2.3.4.1. Fuel Shape

According to Hernandez and others, (2010) and Luo and co-workers, (2010) the size of the fuel particle has a direct influence on the rate of biomass heating and solid-gas interaction since it controls the rate of reactant and product diffusion between the particle and its surroundings. Fuel shape was originally defined by observation that is whether the material appeared to be of a specific shape; for example, a sphere or a cube, or by consideration of its geometry, that is its length, depth, breadth ratio. The effect of particle size on the rate of gasification is highlighted by the work of Erlich et al. (2006) who conducted experiments on the pyrolysis of sugar cane bagasse at atmospheric pressure. They reported that the initial loss of mass during pyrolysis occurred at a higher temperature for 12 mm diameter bagasse pellets compared to 6 mm diameter pellets confirming that the rate of gasification was faster with smaller particle size. Investigations by the same researchers using wood chips also showed that a loss in mass occurred at a higher temperature for the larger pellets than that for the smaller pellets. They also found that the larger the pellet, the slower the rate of gasification. Fuel particle size; therefore, exerts significant control over the gasification process.

2.3.4.2. Moisture content

The moisture content limit for gasifier fuels is dependent on the reactor geometry. The upper limit acceptable for a downdraft reactor is generally considered to be around 40% dry basis (Bridgwater et al., 1986), as the water acts a 'heat-sink' requiring energy to evaporate it from the feed, and it also takes part in predominantly endothermic reactions such as the water gas reaction (see section 2.3.3.). There is theoretically no lower limit on the moisture content and it would be feasible and may in fact be desirable to gasify a feed with as low moisture content as possible to reduce the tar level in the product gas.

2.3.4.3. Ash Content (high mineral matter)

There are constraints on the maximum level and type of ash content of fuels to be gasified. The gasification of high ash fuels can lead to great operational challenges. High ash content fuel gasification requires much greater attention in the ash removal. These problems can be reduced or avoided by the use of low ash fuels such as most woods or in the design of the reactor by the use of reactor-bed stirring,

continuous charcoal removal and/or specialized methods of ash removal such as rotating grates or screws. The oxidation temperature is often above the melting point of the biomass ash, which leads to clinkering/slogging problems and subsequent blockages. Clinkering is a problem especially with biomass fuels having more than 5% ash content (McKendry, 2002a).

2.3.4.4. Volatile Matter

The volatile matter content of biomass is the incondensable organic portion of the biomass which is devolatilized during pyrolysis and determines the amount of tar which will be produced during gasification. The greater the percentage content of volatile matter, the higher the tar production.

2.3.4.5. Fixed Carbon Content

The fixed carbon content is the quantity of material remaining after the release of volatiles and excludes the ash and the moisture content. The volatile matter and fixed carbon content provide a measure of the ease with which biomass can be ignited and subsequently gasified (McKendry, 2002a).

2.3.4.6. Absolute and Bulk Density

Bulk density is the mass of powdered, granulated or shredded solid material per unit volume; so unlike absolute density, it takes the space between the particles into account. The absolute and bulk densities of biomass are of great importance in process design in biomass gasification. Biomass with a high bulk density requires less reactor space for a given refuelling time. Of particular importance is the observation that insufficient flow under gravity can be obtained with low bulk density biomass fuels which results in a reduced calorific value product gas and burning char in the reduction zone (Dogru et al., 2002a). Since a gas of stable calorific value is required for efficient operation of internal combustion engines, establishing the absolute and bulk density is critical in formulating process design in biomass gasification. Low bulk density fuels can be compressed into uniformly sized pieces known as briquettes which allow for the optimal operation of the gasifier (Calkan, 2007).

2.3.4.7. Heating Values

The high heating value (HHV) is the total energy content released when a fuel undergoes combustion, including the latent heat contained in the water vapour. Therefore, the HHV represents the maximum amount of energy potentially recoverable from a biomass source (McKendry, 2002c). Whereas the low heating value (LHV) is the energy content released from combustion of fuel and excludes the heat of water vaporization and the moisture content of the fuel (Suarez *et al.*, 2000). It is an important thermal property of biomass for the design and evaluation of gasification systems as it represents the realistic amount of energy which can be provided by a given type of biomass.

2.3.5. Influence of Operating Conditions on the Gasification Process

Generally, among the factors that are with an effect on gasification are: operating conditions, oxidizing agents and the equivalence ratio (Souza-Santos, 2004).

2.3.5.1. Operating Conditions

Residence times, rate of fuel delivery, temperature and gas-solid contact are all essential operational conditions to reach the equilibrium state (Reed, 1981; Souza-Santos, 2004). In addition, pressure in the reactor/gasifier is also important as higher pressure may result in a reduction in the equilibrium concentration of both CO_2 and H_2. However, with higher pressures, equilibrium concentration of both CO and CH_4 are decreased. Typically, at low temperature production of CH_4, H_2 and CO_2 are improved.

2.3.5.2. Oxidizing Agents

The main gasifying agent is usually air but oxygen/steam gasification and hydrogenation are also used. The use of air as the gasifying agent is common because of the ease in handling, economical benefits and availability; but the main disadvantage is the nitrogen content which dilutes the producer gas and reduces the calorific value or the heating value of the gas. By varying the gasifying agent and the process operating conditions, the composition and as a result the calorific value of the product gas from biomass and/or biomass waste gasification can be varied (Lucas *et al.*, 2004; Hanaoka *et al.*, 2005). The three types of product gas have different

calorific values (CV) as it can be seen from Table (2.6) (McKendry, 2002a; McKendry, 2002c):

Table (2.6): Types of syngas produced in gasification.

Syngas Type	Heating Value (MJ m$^{-3}_n$)	Gasifying Agent
Low heating value gas (LHV)	4-6	Air
Medium heating value gas (MHV)	12-18	O_2 or Steam
High heating value gas (HHV)	40	H_2

The characteristics of air and steam gasification are studied and reported by Lucas and co-workers (Lucas et al., 2004). Table (2.7) which is adapted from the work of Bridgwater (Bridgwater, 1995) shows the difference in gas composition when a downdraft gasifier system is operated by oxygen or air as the gasifying agent. As it can be seen from Table (2.7), the difference in the HHV is caused by the prevention of nitrogen dilution and the increased ratio of hydrogen and carbon monoxide when oxygen is fed to the system.

Table (2.7): Variation of gas composition and quality with different gasifying agents

Gas composition and quality → Gasifying agent ↓	Gas Composition (vol % dry)					HHV (MJ/m^3)	Gas Quality	
	H_2	CO	CO_2	CH_4	N_2		Tars	Dust
Downdraft-Air blown	17	21	13	1	48	5.7	Good	Fair
Downdraft-Oxygen blown	32	48	15	2	3	10.4	Good	Good

The main advantage of gasification is the utilization of the energy from the biomass as a combustible gas. In practice, gasification can convert 60 % to 90 % of the energy in the biomass into energy in the syngas, which can be burned to produce industrial or residential heat, to run engines for mechanical or electrical power or to make synthetic fuels (Reed and Das, 1998).

2.3.5.3. The Equivalence Ratio

The quantity of oxygen used in gasification relative to the quantity of biomass determines the operating temperature in the oxidation zone and as a consequence it is the prevailing temperature in the remaining zones. It is; therefore, the principal operating parameter which influences the heating value of the syngas produced. The quantity of oxygen used is expressed as the equivalence ratio (ER) which is defined as a measure of the ratio of actual air used to the stoichiometric amount of air required for combustion (Reed and Das, 1998).

$$ER = \frac{Actual\ amount\ of\ air\ used}{Stoichiometric\ amount\ of\ air\ required\ for\ combustion}$$

Typically, the optimum ER for biomass gasification is approximately 0.25; therefore, low values of ER are indicative of pyrolysis and high values of ER are indicative of combustion (Reed and Das, 1998). Zhao and co-workers (2009), investigating the impact of the ER, showed that during the gasification of rice husk in an entrained flow gasifier as the ER increased from 0.22 to 0.25 the yield of CO and H_2 decreased rapidly and that of CO_2 increased. This was due to the increase in the concentration of O_2 in the gasifier leading to an increase in the combustion reactions. Therefore, the higher the ER, the lower the heating value of the syngas. However, lower values of ER can also result in high tar concentrations in the syngas.

2.3.6. Pre-treatment of Fuel for Gasification

Pre-treatment of biomass feedstock is generally the first step in gasification. Pre-treatment stage may involve several steps regarding the quality and quantity of the feedstock. During this stage, the physical characteristics of the biomass may be modified in respect of the requirements dictated by the gasification process. The main steps in pre-treatment may include drying and densification.

Drying is a unit operation used to control the moisture content limit of the biomass and/or biomass waste so that the problems associated with moisture level in fuels can be avoided. Several technologies are available for the drying of fuels. A rotary dryer consisting of a horizontally inclined rotating cylinder is used in the plants. Material is fed at one end and discharged at the other. In this rotary dryer, hot

gases move through the cylinder in direct contact with the material against the direction of material flow. The cylinder is also equipped with flights, which lift the material and shower it down through the hot gas stream. The exhaust of the engine is used as the source of hot gas in the system (Calkan, 2007). A picture and a cross section schematic of a rotary dryer can be seen in Figure (2.6). During the course of this study the drying was achieved indoors at laboratory-ambient conditions.

Figure (2.6): Picture and cross section schematic of the dryer (Calkan, 2007).

Densification is a unit operation used to increase the density of the biomass so that the problems associated with small particle size fuels can be avoided. Several technologies are available for the densification of fuels like: cubing, briquetting and pelleting (Tchobanoglous et al., 1993). A simplified schematic diagrams of a briquetter, a cubing and a pelleting machines can be seen in Figures (2.7–9); respectively representing the principles of briquetters and cubing or pelleting machines. A complete densification unit requires a shredder, a conveyor and a moisture control system.
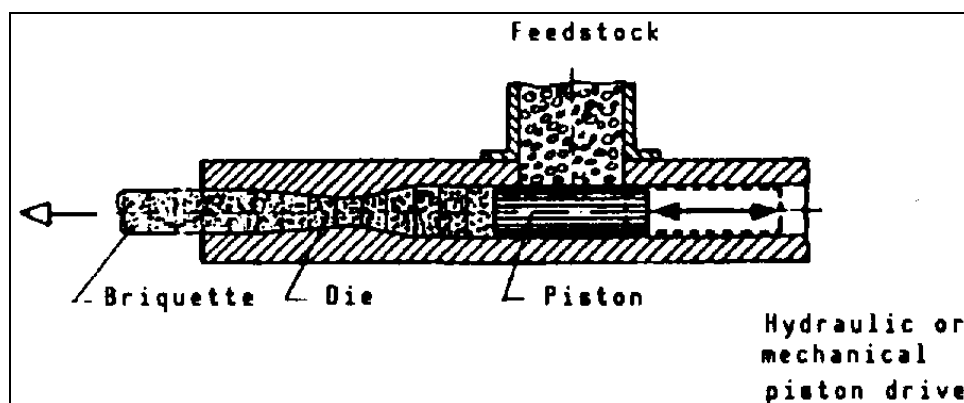
Figure (2.7): Hydraulic or mechanical piston drive for a briquetter machine
(Tchobanoglous et al., 1993).

For gasification processes, the most important criteria for the selection of densification equipment are the required shape and size of the material after the process. Unit capacity (ton/h) and energy requirements are other important factors. Cubing and pelleting machines operate in similar principle and both tend to produce densified fuels with small diameters, where briquetters can produce densified materials within a high range of diameter.
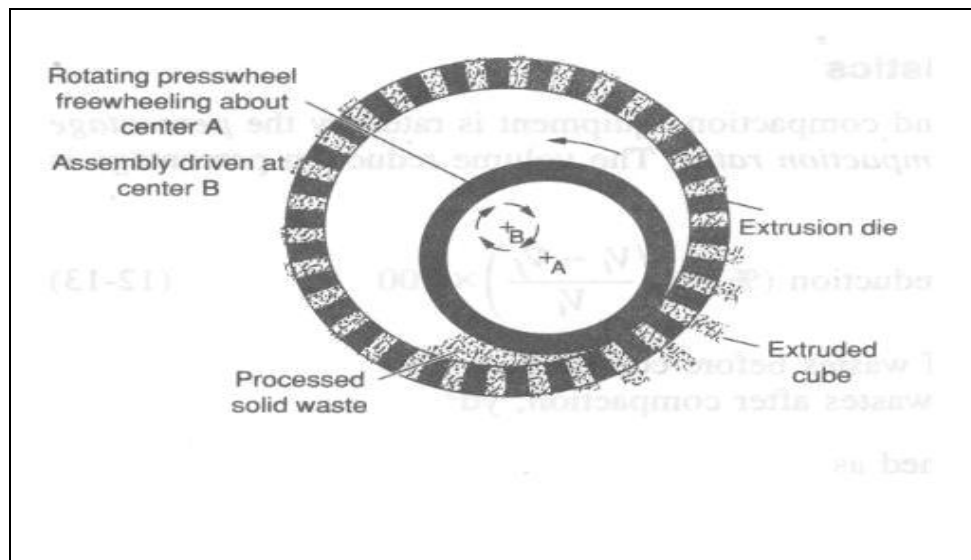
Figure (2.8): Cross section of extrusion dies used in typical cubing or pelleting machine (Tchobanoglous et al., 1993).
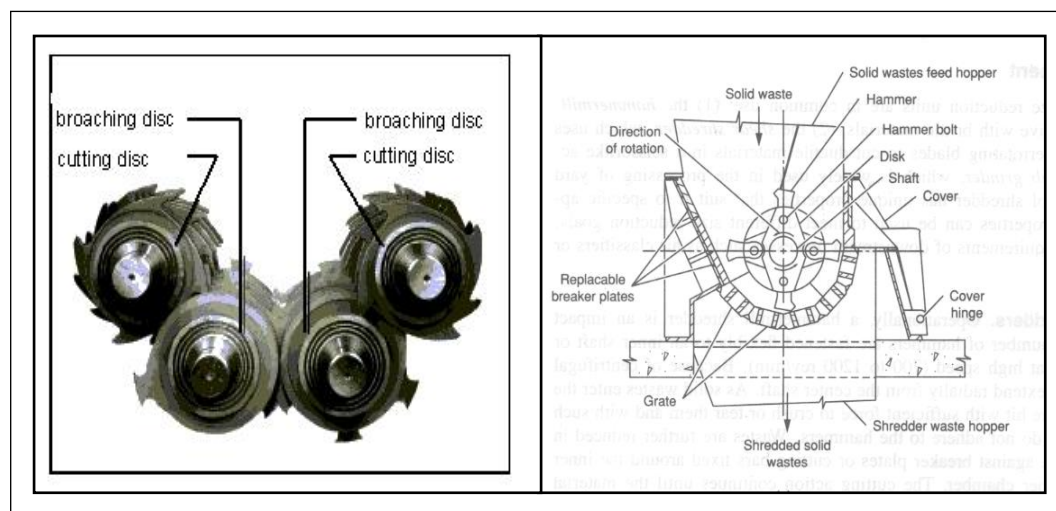
Figure (2.9): Cutting blades of a shear shredder (left) and cross section of hammermill shredders (right) (Tchobanoglous et al., 1993).

2.3.7. Types of Gasifiers

Many different types of reactors have been developed to gasify different feedstock materials. There are two main types of gasifiers, which are lean phase (fluidized bed reactor) and dense phase (fixed bed reactors). Gasifiers are classified by `density factor`, that is the ratio of the volume of biomass present in the reactor under normal operating conditions to the total reactor volume (Dogru, 2000).

2.3.7.1. Lean Phase Gasifiers

Lean phase reactors tend to be homogenous with no distinct reaction zones and drying, pyrolysis, oxidation and reduction take place in the same region around each particle. Typical values for the density factor are in the range of 0.05 to 0.2 for lean phase systems (Maniatis, 1986; Jordan, 2002). There are several types of lean phase reactors for biomass gasification, but the two main configurations which are in use are: circulating fluidized bed and the bubbling bed (McKendry, 2002c; Bridgwater, 2003). Generally, a uniform temperature distribution (700 – 1000 ^{o}C) is achieved throughout the gasifier volume by introducing the gasifying agent to a bed of fine grained materials (usually sand) and ensuring the intimate mixing of the hot bed material with the hot combustion gas and the biomass feed.

2.3.7.1.1. Fluidized Bed Gasifiers

Fluidized bed gasifiers have been a later development. This design provides a uniform contact temperature between gases and solids (Reed, 1981). A fluidized bed gasifier uses a bed of heating media such as sand for thermal process to occur. The bed is heated at desired temperature and feedstock is inserted to it. The heating media bed and biomass are maintained in a suspended stage as the name indicates.

The major operational problem experienced with fluidized bed gasifiers is the potential for the slagging of the bed material due to the ash content of the biomass. The produced gas contains impurities such as particulates, tar, nitrogen compound, sulphur compounds and alkali compounds (McKendry, 2002a). The desired end use determines the design of the downstream gas clean up train, which may be technically challenging and economically demanding. Fluidized bed gasifiers are quite commonly used for larger power applications (Quaak et al., 1999).

2.3.7.2. Dense Phase Gasifiers

Dense phase reactors have well defined reaction zones and density factor ranging from 0.3 to 0.6 (Jordan, 2002) and have been the traditional process used for gasification, operated at temperatures around 1000 $^{\circ}$C (McKendry, 2002c). Fixed bed gasifiers are named according to the direction of air flow in the reactor as updraft, crossdraft and downdraft. According to Hasler and Nussbaumer (1999), fixed bed gasifiers have a capacity range from 100 up to 5000 kW which is in agreement with the comment made by Wen (1999). Simplified schematic representation of these three types of reactors and discrete reaction zones can be seen in Figure (2.10).

| Updraft gasifier | Crossdraft | Downdraft |
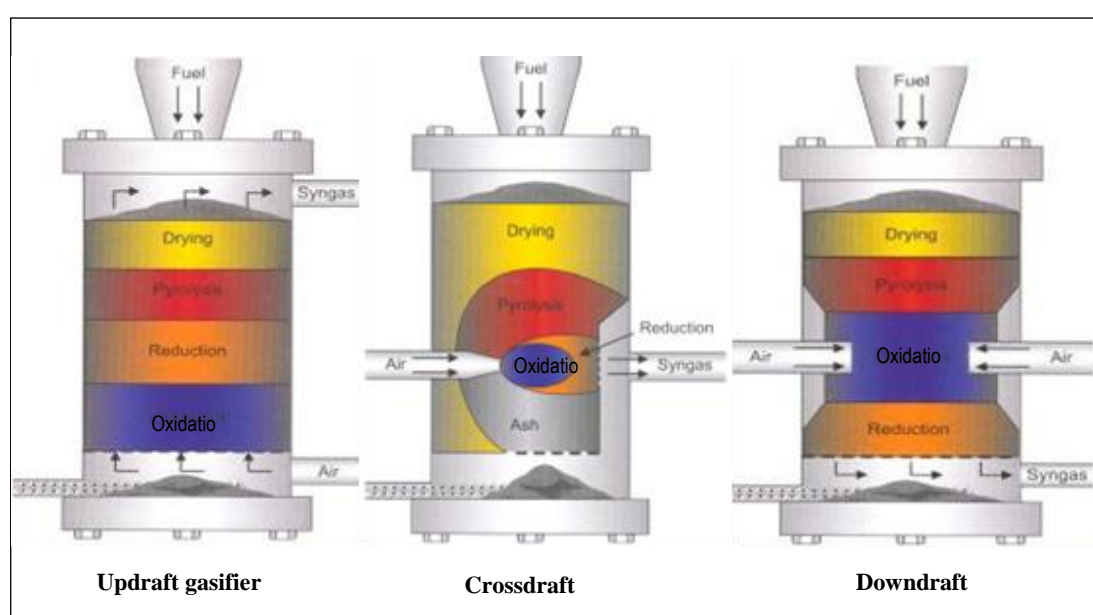
Figure (2.10): Schematic of updraft, crossdraft and downdraft gasifiers.

2.3.7.2.1. Updraft Gasifiers

Upward gasifier refers to a counter flow gasifier where biomass fuel moves downward while the producer gas moves upward. Updraft gasifiers are sometimes called counter current gasifiers because of the counter flow between the fuel and the hot gas. The temperature profile with the height of such a reactor can be seen in Figure (2.11).

Gases follow a natural upward movement as the increasing temperature reduces their density. Updraft gasifier can be designed to work under a natural or forced draft. With this configuration, the air or oxidizing agent entering gets in contact with the chars creating the combustion zone. The gases coming out of the combustion

zone have to pass through the layer of chars above them created by the heat of the combustion zone. Here CO_2 and H_2O are reduced into CO and H_2 (refer to section 2.3.3.). The reduced gases still contain enough energy to pyrolyse the descending biomass along a temperature range of 200 to 500 °C; thus, creating the chars that feed the combustion zone.
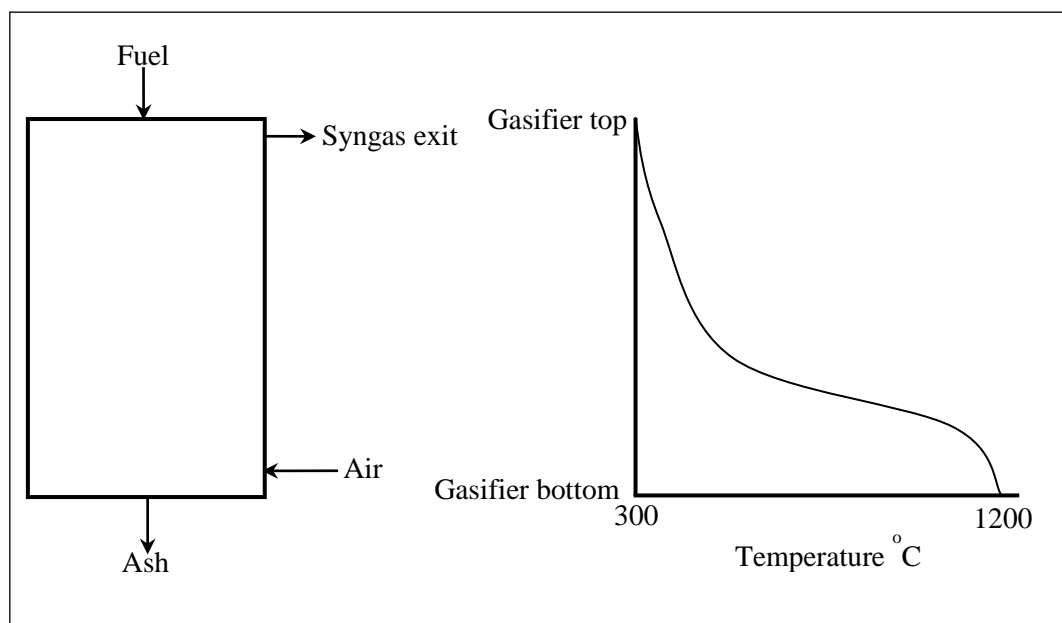
Figure (2.11): Schematic of an updraft gasifier with the temperature profile.

Here CO_2 and H_2O are reduced into CO and H_2 (refer to section 2.3.3.). The reduced gases still contain enough energy to pyrolyse the descending biomass along a temperature range of 200 to 500 °C; thus, creating the chars that feed the combustion zone. In a reaction chain, pyrolysis gases also have sufficient temperature to dry the wet biomass entering above them. However, during pyrolysis, chemicals, tars and oils are released and become part of the producer gases. This drawback restrains the application of the updraft gasifier, because these products released from pyrolysis would be detrimental in a heat engine; however, it could be used for heating applications. Another major drawback in an updraft gasifier is the high temperature at the grate melting ashes and leading to slagging (Reed, 1981).

2.3.7.2.2. Cross-draft Gasifiers

Cross-draft in design is similar to downdraft; instead of air or oxygen entering parallel to the fuel movement, the entry is by the side, usually at the same height of the outlet. The outlet is situated on the side of the gasifier (Goswami, 1986). Just like

any other gasifier, in crossdraft gasifiers the fuel is fed from the top and moves downward. The air enters the reactor from the side and leaves the reactor from the same height level. Because of this design, the temperature in the oxidation zone goes up to 2000 ^{o}C. The produced gas leaves the reactor at a temperature of 800 – 900 ^{o}C. The overall energy efficiency is low due to this high producer gas temperature at the reactor exit. The gas also contains a lot of tar and dust. The temperature profile with the height of such a reactor can be seen in Figure (2.12).
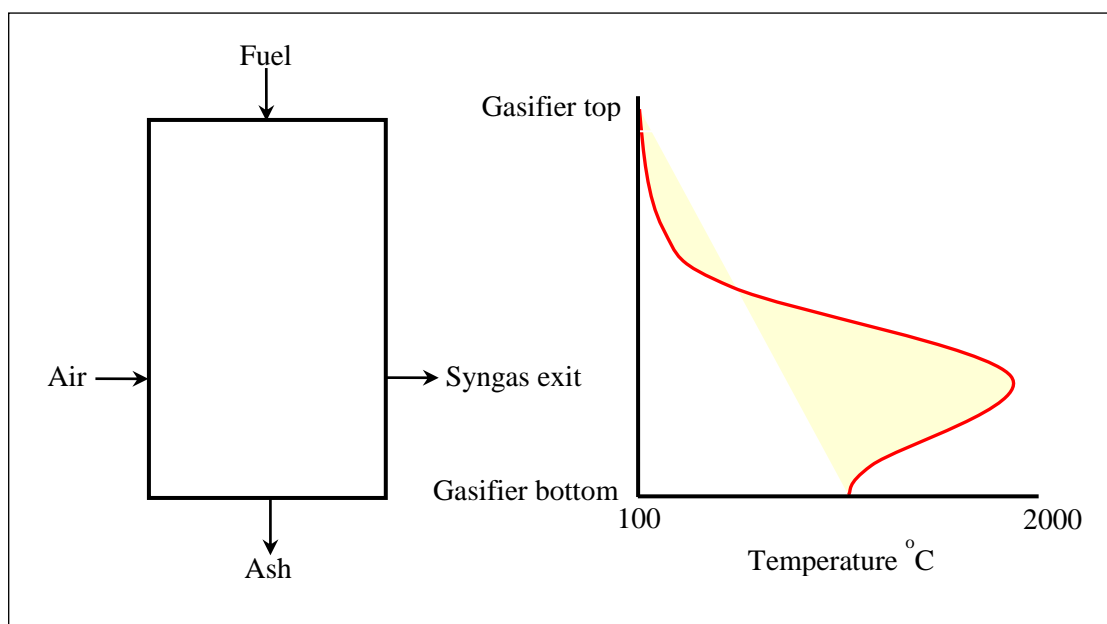
Figure (2.12): Schematic of a crossdraft gasifier with the temperature profile.

2.3.7.2.3. Downdraft Gasifiers

The downdraft is a co-current flow; thus, the biomass and air flow both follow a downward movement. In this system, air first enters the combustion zone and then passes downwards through the reduction zone that made of charcoal bed. Above the combustion zone, despite the fact air or gases are going down, heat from the combustion zone enhances pyrolysis of biomass feed. The oils and vapours formed due to pyrolysis have to pass through the charcoal bed below and this leads to "flame stabilization". This phenomenon occurs due to the cracking of the oil vapour, maintaining temperature around 800 – 1000 °C. Therefore, as temperature rises, the endothermic reactions are favoured from the cracking of oil vapours; and as temperature decreases, release of vapour decreases, enhancing the exothermic reactions. Due to this combination of reactions, the temperature is maintained constant. When the gases are cracked, they become simpler gases leading to reduction

in oils and tars; as much as 90% reduction in the value obtained in an updraft gasifier is observed. Some designs add a paddle to mix material in the combustion zone, avoiding preferential flow where tar could pass without getting cracked (Souza-Santos, 2004). Implemented with filters, these gases can be used in fuel spark and diesel engines (Reed, 1981). The temperature profile with the height of such a reactor can be seen in Figure (2.13).
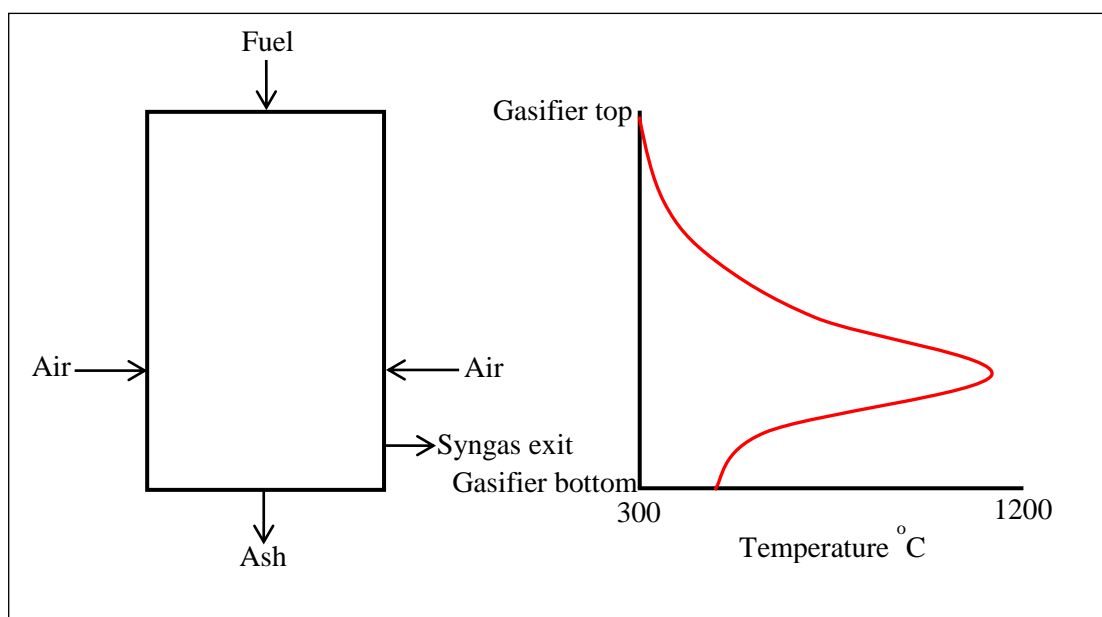
Figure (2.13): Schematic of a downdraft gasifier with the temperature profile.

2.3.7.2.3.1. Throated Downdraft Gasifiers

The name 'throated' is derived from a constriction, the throat (or alternatively the choke plate) near the base of the reactor, into the vicinity of which the oxidant/gasifying agent is injected. In downdraft gasifiers, both air and fuel move downwards. Hot gas which is produced in the pyrolysis zone, contaminated by heavy hydrocarbons passes through the oxidation zone which is normally at elevated temperature (around $1200^{\circ}C$). The hot char in the gasification zone enables the burning and cracking of tars into lighter and combustible gases and a cleaner gas is produced. This is one of the most important features of downdraft gasifiers as all the pyrolysis products are forced to pass through oxidation and reduction zones to produce a cleaner gas. As shown in Figure (2.5), the throated downdraft gasifier has four distinct reaction zones, which are drying, pyrolysis, oxidation and reduction zones from top to bottom.

38

In the drying zone, the fuel descends into the gasifier and moisture is removed using the heat generated in the zones below by evaporation. The rate of drying depends on the surface area of the fuel, the temperature difference between the feed and the hot gases, the re-circulation velocity and relative humidity of these gases as well as the internal diffusivity of moisture within the fuel. The moisture content of the feed is limited to approximately 40% dry basis (Bridgwater *et al.*, 1986). The average temperature in this zone is between 70 and 200 $^{\circ}$C.

In the pyrolysis zone, the particle decomposes; devolatilization occurs on its surface releasing the volatile components as combustible and non-combustible gases, tars and water vapour. Depending on the chemical composition of the fuel, the release of volatiles begins at temperatures as low as 200 $^{\circ}$C (Gani and Naruse, 2007). In the pyrolysis zone of a downdraft gasifier, 80 to 90 % of the original mass is converted to a complex liquid fraction composed of water, tars and oils and a gaseous phase including CO, CO_2, H_2 and hydrocarbons, leaving 5 to 20 % highly reactive charcoal (Reed *et al.*, 1983). The pyrolysis product distribution and composition depend on many factors such as temperature, heating rate, particle size of the fuel and solid residence time, etc. The energy required for pyrolysis to take place is supplied by the released heat in the oxidation zone. In an air-blown downdraft gasifier, the typical temperature range in the pyrolysis zone is 350-500 $^{\circ}$C (Dogru *et al.*, 2002a).

In the oxidation zone, the reactions that take place in this zone are highly exothermic and result in a sharp rise in temperature within the reactor which generates the thermal energy needed to initiate and sustain pyrolysis (Kinoshita *et al.*, 1997) and also to dry the fuel in the drying zone. The temperature in this zone is up to 1200 $^{\circ}$C.

In the reduction zone, often referred to as gasification zone, the char is converted to the produced gas by reaction with the hot gases from the upper zones. The gases are reduced to form a greater proportion of H_2, CO and CH_4,

2.3.8. Contaminants in the Producer Gas

In the gasification/pyrolysis process, with exception of generating useful products, many byproducts such as fly ash, NOx, SO2 and tar are also formed. Generally, byproducts can cause erosion and corrosion on metals. Belgiorno and co-workers (Belgiorno et al., 2003) reported the types of contaminants contained in the producer gas and the potential problems that can be generated as shown in Table (2.8).

Table (2.8): Contaminant presence in the gas and relative problems (Belgiorno et al., 2003)

Contaminant	Presence	Problems
Tars	It is bituminous oil constituted by a complex mixture of oxygenated hydrocarbons existing in vapour phase in the producer gas, it is difficult to remove by simple condensation	Clog filters and valves and produce metallic corrosion
Particulates	Derive from ash, condensing compounds and bed material for the fluidized bed reactor	Cause erosion of metallic components and environmental pollution
Alkali metals	Alkali metals compounds, specially sodium and potassium, exist in vapour phase	Alkali metals cause high-temperature corrosion of metal, because of the stripping off of their protective oxide layer
Fuel-bound nitrogen	Cause potential emissions problems by forming NO_x during combustion	NO_x pollution
Sulfur and chlorine	Usually sulfur and chlorine contents of biomass and waste are not considered to be a problem	Could cause dangerous pollutants and acid corrosion of metals

2.3.8.1. Tars

The major contaminant contained in a gasifier syngas are tars. These compounds are a complex mixture of more than 10,000 organic compounds and are produced during pyrolysis in a series of complex reactions (Morf, 2001). As a result of their complex nature, many definitions of tar have been reported. It is usually

influenced by the gas quality specifications required for a particular end-use application and how the tar is collected and analyzed. One of the definitions of tar was reported by Milne and co-workers and Li and Suzuki (Milne *et al.*, 1998; Li and Suzuki, 2009) as follows: The organics produced under thermal or partial-oxidation regimes (gasification) of any organic material are called "tar" and are generally assumed to be largely aromatic including benzene. The yield and composition of tar produced during biomass gasification are dependent on several process parameters, including gasifier type, biomass composition (including the presence or absence of catalytically active substances), moisture content and size of the biomass particles as well as operating conditions such as pressure, peak temperature and residence time (Morf, 2001; van Paasen and Kiel, 2004). Figure (2.14) shows the typical composition of the biomass tars.
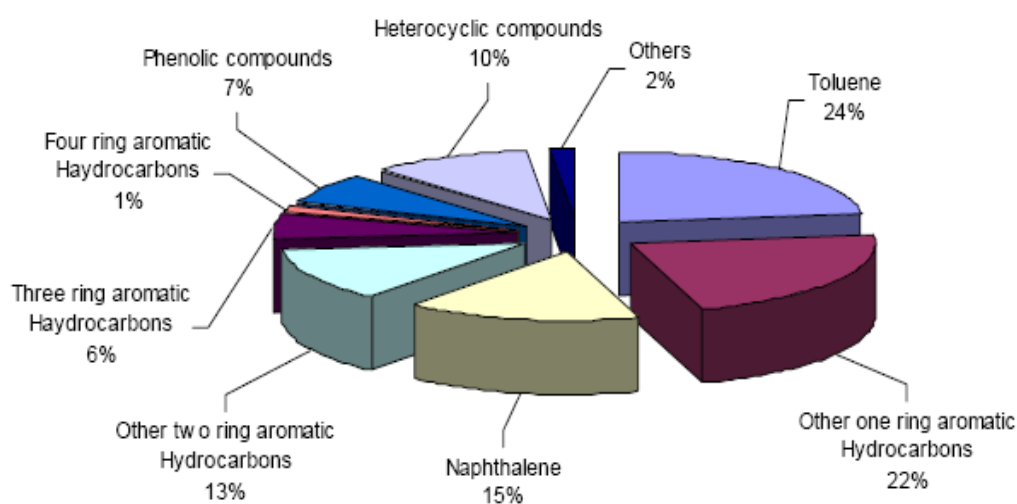
Figure (2.14): Typical composition of biomass tars (wt %) (Coll et al., 2001).

As it was mentioned in Table (2.8), tar derived from biomass gasification or pyrolysis will be condensed as temperature is lower than its dew point, then block and foul process equipment like fuel lines, filters, engines and turbines. It was reported that tar content in the syngas from an air-blown circulating fluidized bed (CFB) biomass gasifier was about 10 g/m^3 (Anis and Zainal, 2011). For other types of gasifiers, tar content varied from about 0.5 to 100 g/m^3 (Devi et al., 2003). However, most applications of product gases require low tar content, of the order of 0.05 g/m^3 or less. Figure (2.15) shows the tar covered induced draft fan of a downdraft gasifier.

Moreover, tars contain approximately 10 % of the total biomass HHV which is lost to the syngas if not converted to H_2, CO and CH_4 (Fermeglia *et al.*, 2005). Most syngas applications; therefore, require the removal of some or all of the tars before the gas can be used (Li and Suzuki, 2009) but degradation of tars is preferred rather than capture in order to enhance the syngas heating value. The reduction and/or removal of tar from the syngas is; therefore, one of the major technical barriers to be overcome in the development of biomass gasification for the use of syngas for efficient and economic generation of power (Han and Kim, 2008).
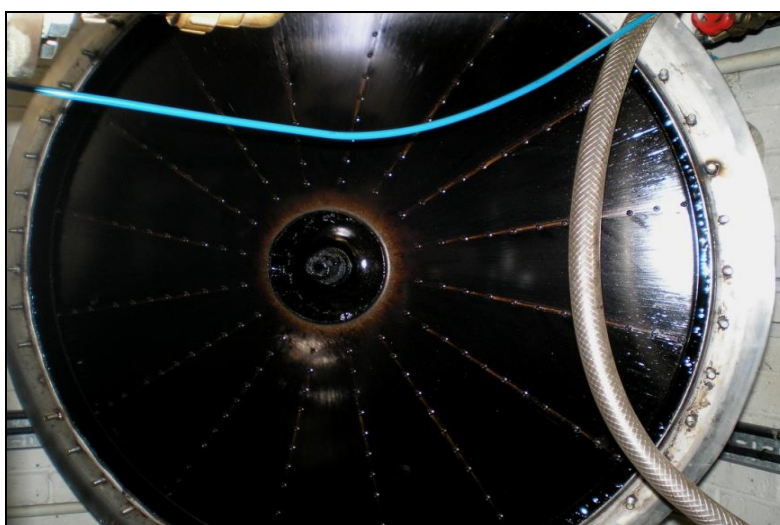
Figure (2.15): Tar depositions on the induced draft fan of a downdraft gasifier (Jordan, 2010).

Tar Classification

Different classifications for tars are found in literature (Milne *et al.*, 1998; Maniatis and Beenackers, 2000; Padban, 2001; van Paasen *et al.*, 2002; Devi *et al.*, 2005). In general, these classifications are based on: properties of the tar components and the aim of the producer gas application. The tar components can be segregated and classified into five classes based on their chemical, condensation and solubility behaviour, as given in Table (2.9).

In this classification system, the potential for condensation of a given composition of tars is determined by calculating the tar dew point which is defined as the temperature at which the real total partial pressure of tar equals the saturation pressure of tar (Rabou et al., 2009). When the temperature of a downstream syngas system falls below the thermodynamic dew point, tar can condense out of the syngas

and deposits are formed. The tar dew point is; therefore, a major consideration for commercialization of biomass gasification systems.

Table (2.9): Classification of tars (Milne *et al.*, 1998; Maniatis and Beenackers, 2000; Padban, 2001; van Paasen *et al.*, 2002; Devi *et al.*, 2005).

Tar Class	Class name	Tar components	Representative compounds
Class 1	GC-Undetectable Tars	The heaviest tars, cannot be detected by GC	Very heavy, 7-membered and higher ring compounds
Class 2	Heterocyclic aromatics	Tars containing hetero atomic; highly water-soluble compounds	Pyridine, phenol, cresols, quinoline, soquinoline, dibenzophenol
Class 3	Light Aromatic Hydrocarbons (LAH)	Aromatic components. Light hydrocarbons with single ring. Important from the point view of tar reaction pathways, do not pose a problem on condensability and solubility	Toluene, ethylbenzene, xylenes, styrene
Class 4	Light Poly Aromatic Hydrocarbons (LPAHs)	Two and three rings compounds; condense at low temperature even at very low concentration	Indene, naphthalene, methylnaphthalene, biphenyl, acenaphthalene, fluorine, phenanthrene, anthracene
Class 5	Heavy Poly Aromatic Hydrocarbons (HPAHs)	Larger than three-rings, condense at high temperatures at low concentrations	Fluoranthene, pyrene, chrysene, perylene

The relationship between the tar dew point and the tar classes as categorized by van Paasen and Kiel, (2004) is illustrated in Figure (2.16).
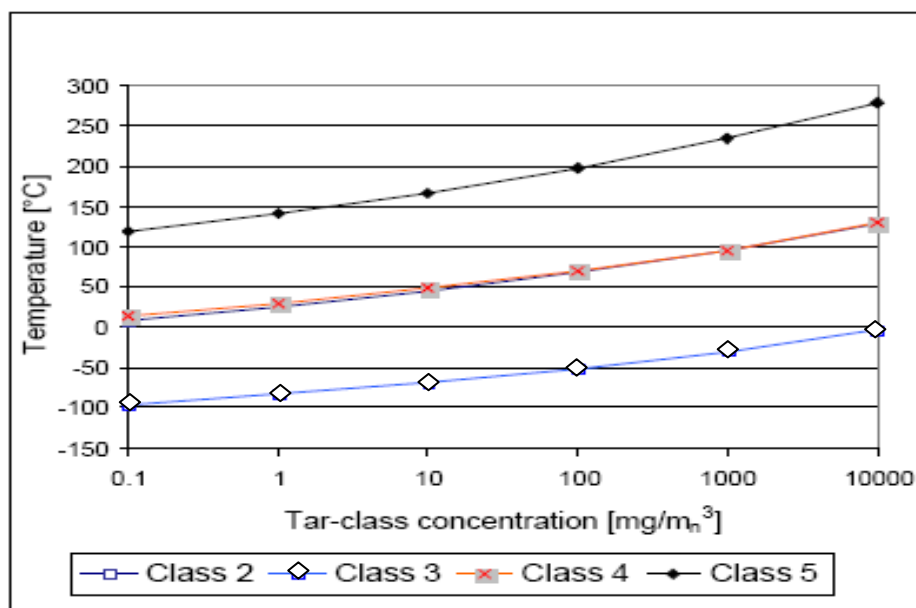
Figure (2.16): Relationship between the tar dew point and the concentration of the different tar classes (van Paasen and Kiel, 2004).

As can be seen in Figure (2.16), even at concentrations of approximately 0.1 mg m_n^{-3} Class 5 tars have a tar dew point of 120 ^{o}C which exceeds the dew point at which condensation of concentrations in excess of 1000 mg m_n^{-3} of Class 2, 3 and 4 would occur. It can also be seen that even at concentrations as high as 10 000 mg m_n^{-3} condensations of Class 3 tars do not occur. After syngas water scrubbing systems, the gas temperature is typically less than 80°C which means, therefore, that any Class 5 Polyaromatic Hydrocarbons (PAHs) present will condense on cool surfaces resulting in fouling of power production systems.

2.3.8.2. Inorganic Impurities and Particulates

In addition to organic (tars), producer gas contains an inorganic impurities and particulates such as H_2S, HCl, NH_3 and alkali metals which are also detrimental to electrical generators and to the environment. These are listed below:

- Particulate matter such as fly ash, fine particulates consisting of sorbent and un-burnt hydrocarbons, entrained biomass bed material and entrained solid inorganic impurities which were initially contained in the biomass feedstock;
- Heavy metals especially volatiles such as mercury and cadmium which are

present in the biomass feedstock;

– Acid gases which are produced from sulphur, nitrogen, chlorine, fluorine, phosphorous and other non-metals in the feedstock;

– Ammonia which is produced mainly from nitrogenous materials, and

– Alkali and alkali earth metals and ash forming elements which are an extremely important group of contaminants in syngas as they exert significant influence on fuel bed behaviour and on the ultimate composition and distribution of the products of gasification.

It can be seen; therefore, that the volatilization of these elements and the associated anions as well as their behaviour in the fuel bed is of tremendous concern to biomass-fuelled power generation systems as:

1. When released alkali and alkali earth metals can condense on downstream prime movers by various mechanisms including Brownian diffusion, thermophoresis and gravity settling eventually resulting in high temperature corrosion;

2. These species influence the behaviour of the biomass material during thermochemical conversion. Some act as catalysts and control the rate of degradation and yield of char in pyrolysis (Fahmi et al., 2007) whereas others undergo transformation which can result in the formation of low melting eutectics which can cause sintering and slagging within the biomass feedstock. Ultimately, immobilization of the fuel bed can lead to reduced efficiency of conversion of fuel to syngas and can have an impact on the final heating value of the gas (Wei et al., 2005), and

3. Alkali and alkali earth metals and ash forming elements can cause erosion of piping and turbine blades as a result of the repeated impact of particulates on these surfaces (Sonwane et al., 2006).

Both alkali and alkali earth metals retained in char during pyrolysis are important catalysts for the gasification of char. They reduce the gasification temperature and; therefore, increase the overall gasification process efficiency and process economy. Furthermore, it is believed that they also act as catalysts for the steam reforming of volatiles in the syngas (Keown et al., 2005).

2.3.9. Gas Cleaning Technologies for Removal of Contaminants from Syngas

Minimizing the occurrence and concentration of contaminants such as tars, particulates, alkali metals, acid gases and alkaline gases, the removal of tars is the most critical to economically viable operation of small scale gasifier systems (McKendry, 2002a). Gas clean-up has; therefore, been identified as one of the major technical challenges to the implementation of gasifier fuelled internal combustion engines and gas turbines (Bridgwater, 2003). Generally, tar removal technologies can be divided into two fundamental approaches depending on the location where tar is removed; either in the gasifier itself (known as primary method) or outside the gasifier (known as secondary method) (Devi et al., 2003).

2.3.9.1. Primary Methods – In situ Removal of Contaminants

Primary methods consider the measures needed to be taken in order to prevent tar formation and tar conversion in the gasifier itself. Considerations should be given on the proper selection of the operating conditions, the use of proper bed additives or catalysts in the gasifier itself and a proper gasifier design. Figure (2.17) represents the ideal primary method concept which eliminates the need for secondary treatments.
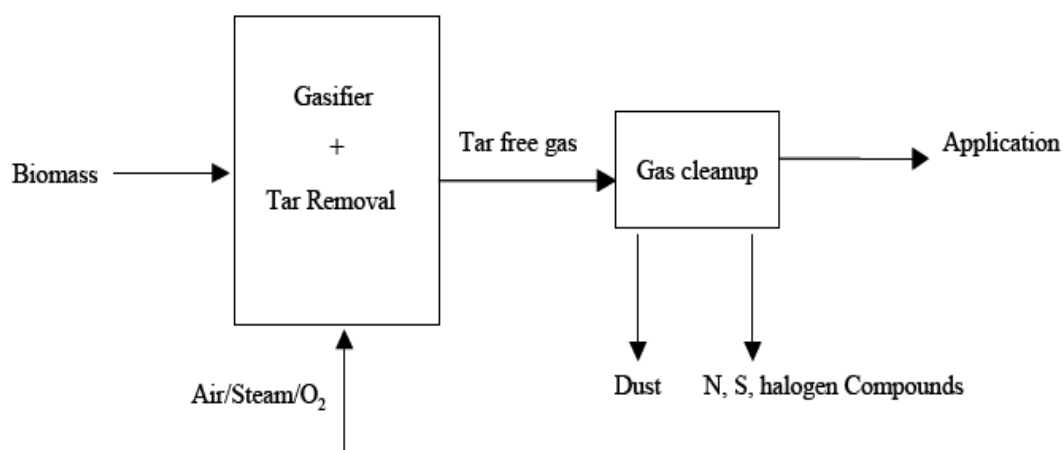
Figure (2.17): Tar reduction concept by primary methods (Devi et al., 2003).

Bergman and others (Bergman et al., 2002) stated that although measures inside the gasifier (primary methods) may be fundamentally more ideal, they have not yet resulted in satisfactorily solutions. Some of the primary measures *do* result in low tar emissions, but suffer from disadvantages related to; for instance, limits in feedstock flexibility and scale-up, the production of waste streams, a decrease in cold gas efficiency, complex gasifier constructions and/or a narrow operating window. The

primary methods are not yet fully understood and are yet to be applied commercially as quoted by (Devi *et al.*, 2003). Although primary measures can reduce the tar content considerably, it is foreseen that complete removal is not feasible without applying secondary measures, see Figure (2.18).
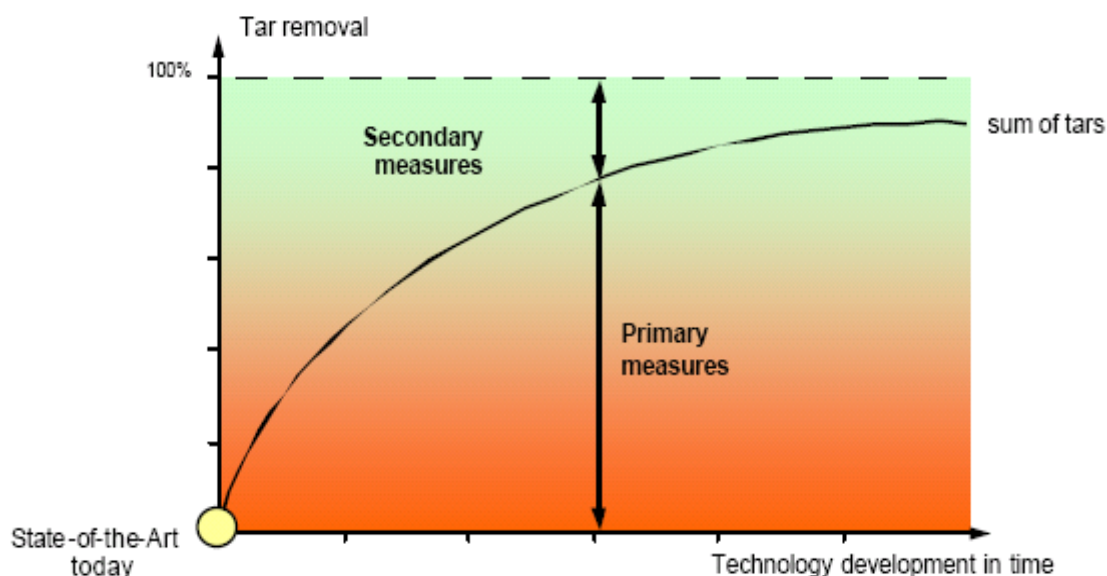
Figure (2.18): Illustration of the need of primary and secondary measures versus technology development in time (Bergman *et al.*, 2002).

2.3.9.1.1. Catalytic Tar Destruction

Catalytic systems are comprised of the same substances used as in-bed additives in primary systems but instead are located in fixed bed reactors downstream of the gasifier. The mechanism and reaction mechanisms are not well known but high levels of tar elimination has been reported by many authors via this method (Caballero *et al.*, 1997; Pérez *et al.*, 1997; Aznar *et al.*, 1998; Caballero *et al.*, 2000; Wang *et al.*, 2000). In most of these studies, nickel catalysts were used. The operation temperature for catalytic tar crackers vary from 700 – 900 ^{o}C. The most important variables affecting the tar conversion are temperature of the catalytic bed, space time or space velocity, catalyst particle size and gas atmosphere composition (Aznar et al., 1998). Another important variable in catalytic tar removal system is the lifetime of the catalysts.

Deactivation of the catalysts could be due to three main causes for gasification processes, which are, particulates or dust, sulphur and coke formation mainly from tars (Caballero et al., 2000). Catalytic tar crackers not only eliminate tars

47

but also modify the gas composition, heating value of the gas, gas yield and thermal efficiency of the gasification process (Aznar et al., 1998).

2.3.9.1.2. Thermal Tar Destruction

Tar destruction can also be done thermally without the presence of any catalyst. However, operation at higher temperature of 1200 ℃ and above is required. For efficient destruction, the minimum required temperature is not clearly described but it is dependent on type of tars formed. For example, oxygenated tars from updraft gasifier are treated at 900 ℃ while the refractory tars from high temperature reactors need to be treated at temperatures of 1200 ℃ and above. Thermal cracking for large scale gasifier is less attractive due to the difficulties in achieving complete thermal cracking, operational problems and high cost.

The technique has also been tested on tar destruction in pyrolysis or gasification of organic wastes. The application in systems designed for waste reduction is more economical compared to the one that uses clean biomass since energy by-products are produced along with the elimination of waste. Neeft et al. (1999a) reviewed several processes applied in disposal of organic waste systems.

In tar thermal decomposition using electric arc plasmas, plasmas are created by heating gases in the discharge arc between two electrodes. Due to electric discharge and the temperature increase in the arc, parts of the gases are ionized and followed by reactions. A review on tests of several plasma arc reactors was discussed by Neeft et al. (1999a). It is not likely feasible for applications in big-scale biomass gasification systems due to high cost of electricity and a large gas volumes to be treated. Further discussion on plasma technology is done in Section (2.3.9.3)

2.3.9.2. Secondary Methods – Removal of Contaminants Downstream of the Gasifier

Secondary methods are characterized by syngas cleaning systems which are located downstream of the gasifier. The type of secondary method used is determined primarily by the end use application of the syngas and the main types of contaminants present. These technologies are classified as physical or chemical. In physical removal systems, the most common gas cleaning systems are wet scrubbers, gas cyclone separators, baffle filters, fabric filters and electrostatic precipitators, consequently particulates as small as 5 μm can be removed from the syngas. Any mineral matter and tar adsorbed onto particulates may be removed by physical systems; however, chemical removal systems are the main route by which adsorption of alkali metals is achieved (Turn *et al.*, 2000). Chemical conversion of tars is carried out by thermal or catalytic means with the latter being the same catalysts used in primary treatment (Nair et al., 2003). The concept of secondary methods is given in Figure (2.19).
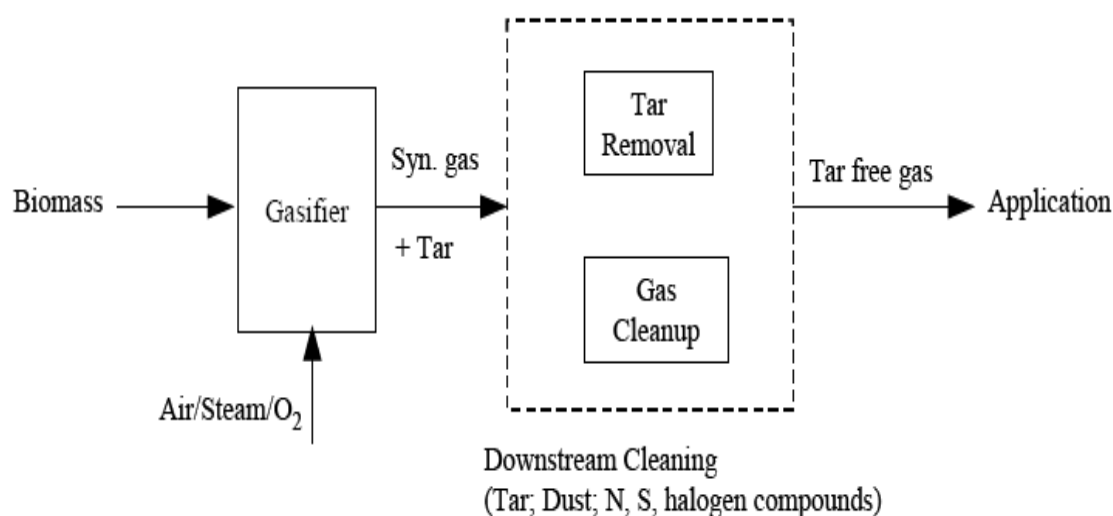
Figure (2.19): Tar reduction concept by secondary methods (Devi et al., 2003)

2.3.9.2.1. Electrostatic Precipitators

Electrostatic precipitators (ESP) are very commonly used in industry to produce exceptionally clean gas. The principle is to use non-uniform, high-voltage fields to apply large electrical charges to particles moving through the field to charge particles and make them move toward an oppositely charged collection surface, where

they accumulate. This collection surface may be washed continuously to remove these particles. The simplified schematic diagram of an ESP is shown in Figure (2.20).

Wetted-wall precipitators (sometimes called wet precipitators) are often used to collect mist and/or solid material that are moderately sticky. These ESPs are effective for all drop and particle sizes (Reed and Das, 1998). The power consumed by the ESP is very low and the pressure drop is also very low, at considerably less than 1 in of water. The main disadvantage; however, is the safety measures associated with high voltage and the unforeseen power failures to stop the operation (Reed and Das, 1998)
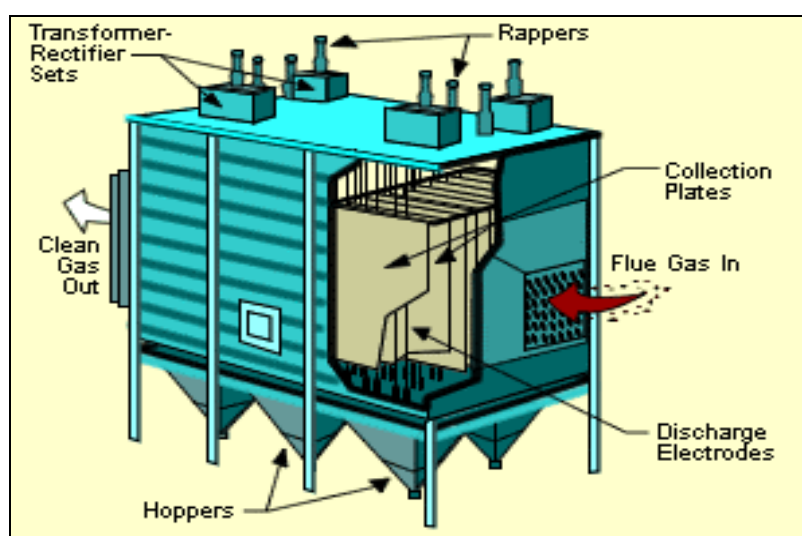
Figure (2.20): Simplified schematic diagram of a conventional ESP.

2.3.9.2.2. Filters

Filters are a very effective and simple way of removing solid matter from the gas stream. The filtering media can be a cloth or a porous medium as well as biomass (Dogru *et al.*, 2002a). The main advantages of using biomass as the filtering media may be the low pressure drops and the possibility of reuse as a fuel in the gasification process when the collection efficiency drops.

2.3.9.2.3. Cyclone Separators

Cyclones are simple and inexpensive dust and droplet separators which are widely used in gasifier systems. The gas stream enters the cyclone tangentially and creates a weak vortex of spinning gas in the cyclone body. Large diameter particles move toward the cyclone body wall and then settle into the hopper of the cyclone. The

cleaned gas turns and exits the cyclone, see Figure (2.21). A cyclone separator enhances the settling rate of the impurities in the gas stream by many times due to the rotary motion of the gas. A cyclone separator is simply a gravitational separator with a centrifugal force component.
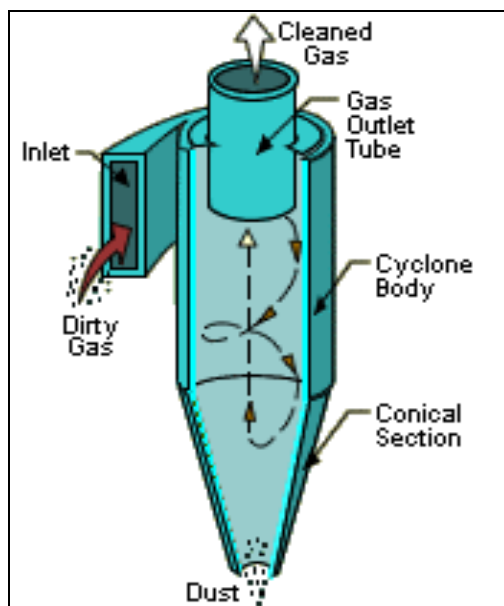
Figure (2.21): Cross section of a conventional cyclone.

2.3.9.2.4. Wet Scrubbers

Wet scrubbers are widely used to cool the gas streams and to remove the precipitating tars, oils and solid particulates. There is a wide range of wet scrubbers varying primarily in the method of liquid contacting. The most common types are spray towers, packed bed scrubbers, plate scrubbers, impingement scrubbers, baffle scrubbers and Venturi scrubbers. The design and construction of wet scrubbers can be found in the literature (Kaupp and Goss, 1984; Perry *et al.*, 1997). In a typical spray tower, most of the tar is condensed by contact with water sprays. In addition to cooling the gas and condensing tar, water washes the condensed tar droplets from the gas together with particles. Wet scrubbing is usually part of the gas cleaning train for product gas being fed to an ICE as the temperature of this gas must be kept as low as possible (40-50°C) to achieve acceptable efficiencies. All wet scrubbers produce a liquid stream, which usually requires further treatment prior to disposal (Calkan, 2007). The performance of some available gas clean up equipment for reduction of particulates and tars can be seen in Table (2.10) and Figure (2.22).

Table (2.10): Reduction of particles and tars in various producer gas cleaning equipment (Hasler and Nussbaumer, 1999).

Particle and tar reduction → Cleaning system ↓	Temperature (^{o}C)	Particle reduction (%)	Tar reduction (%)
Sand bed filter	10 – 20	70 – 99	50 – 97
Wash tower	50 – 60	60 – 98	10 – 25
Venturi scrubber	-	-	50 – 90
WESP*	40 – 50	>99	0 – 60
Fabric filter	130	70 – 95	0 – 50
Rotational separator	130	85 – 90	30 – 70
Catalytic tar cracker	900	-	>95

* Wet Electrostatic Precipitators
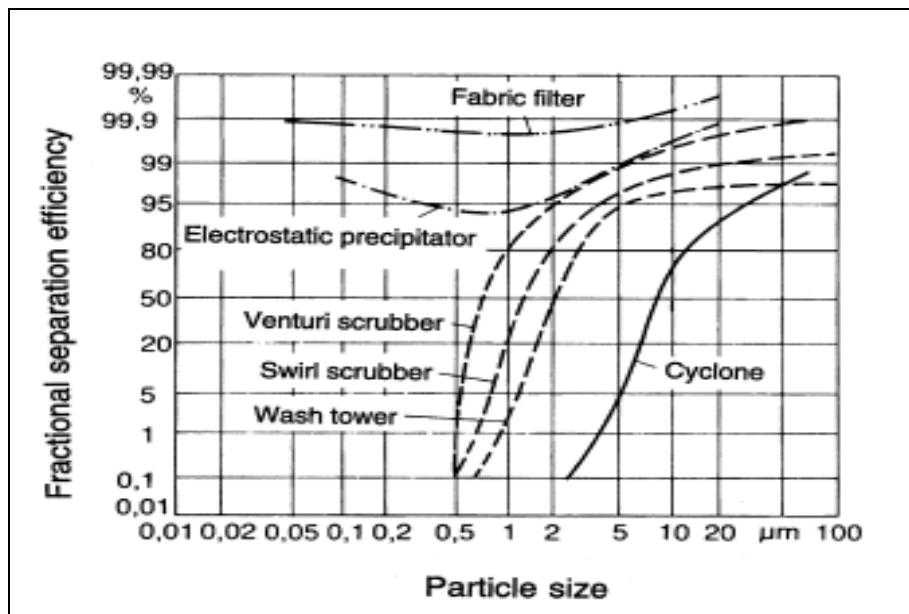
Figure (2.22): Particle collection efficiencies of conventional gas cleaning systems (Hasler and Nussbaumer, 1999).

2.3.9.3. Plasma Technology

Plasmas are found everywhere in the universe; 99% of the matter in the observable cosmos is in the plasma state (Graham, 2001). Plasma can be defined as the fourth state of matter after solid, liquid and gas as introduced by Langmuir in 1928.

2.3.9.3.1. What is Plasma?

As quoted by (Whitehead, 2007), plasma is a partially or completely ionized gas containing electrons, ions, excited and ground state atoms and/ or molecules, reactive free radicals and photons. Plasmas can be categorized based on the operating pressure; low pressure or atmospheric pressure. Plasmas can also be described by its degree of equilibrium. High pressure or thermal plasmas all have species (electrons, ions, atoms and molecules) at a thermal equilibrium; they can be described by a single temperature. Atmospheric pressure or non-thermal plasmas are those with high temperature electrons compared to the temperature of ions, atoms and molecules. A high degree of disequilibrium exists in non-thermal plasma; the electrons have a very high energy (temperature of tens of thousands of degrees Kelvin), the ions are less energetic, and the residual gas atoms and molecules are close to room temperature. Lately, most of the studies have been centred on the application of non-thermal, atmospheric pressure plasmas.

Plasmas can be created by applying an electrical field created by a high voltage alternating current (AC), a direct current (DC) discharge (continuous or pulsed), and a microwave or radiofrequency field to a gas. In the field, electrons are stripped from some or all of the gas atoms or molecules; the electrons then gain energy. These energetic electrons then collide with the atoms and molecules in the gas, producing more ions and excited states. Electrons can also cause the molecules to split apart producing reactive fragments or free radicals. However, not all the molecules are dissociated. Even though the study on gas discharges began as early as 1808 by Sir Humpry Davy, Sir William Crookes was the first one to produce and recognize plasmas in 1839. He heated a solid to very high temperatures, melted it, vaporized it to a gas and then broke the gas into electrons and ions.

Plasmas have two main characteristics, temperatures and energy densities which are very important for practical applications. The temperatures and energy densities produced by plasma are greater than those produced by ordinary chemical mechanisms. In other words, plasma performances are not possible in any other methods. In fact, plasmas can provide an efficient increase in processing methods and in comparison to more conventional processes they may often reduce the impact on the environment (Fridman, 2004).

2.3.9.3.2. Plasma in Pollution Abatement

Low-temperature, non-equilibrium plasmas are among the emerging technologies used in treating low volatile organic compound (VOC) emissions and other industrial exhausts. Amongst the wide range of emission products effectively treated using the plasma processes are aliphatic hydrocarbons, chlorofluorocarbons, methyl cyanide, phosgene, formaldehyde, sulphur and organophosphorus compounds, and sulphur and nitrogen oxides.

As quoted by (Pemen *et al.*, 2007), in a non-thermal plasma, molecules will be dissociated by high energy electrons of 6 ~ 10 eV (Van Veldhuizen, 2000), resulting in the creation of a favourable reactive environment, regardless of the gas temperature. Therefore, conversion of tars is possible for a system with low temperature gas. This is another added advantage when compared to catalytic cracking which is possible at 800 °C and thermal cracking at a temperature of >1000 °C. Even though non-thermal plasma produces a host of species and reactive radicals, it does not have selectivity towards the desired process. Consequently, in many cases, the radicals are not efficiently utilized, leading to high energy consumption as discussed previously. In order to overcome this problem, the studies on a combination of plasma and catalyst have been actively pursued to find an alternative in reducing the energy consumption (Wang *et al.*, 2004; Nozaki *et al.*, 2004a; Nozaki *et al.*, 2004b; Pemen *et al.*, 2007).

Nair et al. (2003; 2004; 2005) discussed in detail the corona plasma system for tar removal in biomass gasification. The studies were done using pulsed corona plasma system and, streamer corona generation by an AC/DC power source. Results demonstrated that the chemical efficiencies of both pulsed corona system and AC/DC system were about the same.

Pemen et al. (2007) studied the application and synergistic effect of both plasma and catalyst on removal of tars from gas produced by biomass gasification. Tar removal process was enhanced by a combination of streamer corona plasma and a monolith, made of cordierite, having 400 cpsi. A cordierite monolith was chosen as a catalyst due to its low pressure drop and its easiness to be incorporated into a non-thermal plasma reactor. The result demonstrated the decrease in energy requirement at the temperature of 300 °C. Thus, the system has a potential for lowering the operating temperature of the process, and for enhancing tar removal processes.

2.3.9.4. Tar Removal from Syngas using Sulphonated PolyHIPE Polymer (PHP)

2.3.9.4.1. Overview on PolyHIPE Polymer (PHP)

Polymer is derived from the Greek, *poly* means many and *meros* means parts (Katz, 1998). There are several polymerization techniques including emulsion polymerization. Lissant and Mayhan in 1970s described a high internal phase emulsion (HIPE) polymerization technique using an organic phase as the continuous phase to develop microcellular polymeric foam (Hoisington et al., 1997). In 1985, polyHIPE polymers (PHPs) were first patented by Barby and Haq (Hoisington *et al.*, 1997; Deleuze *et al.*, 2002; Benson, 2003; Zhang and Cooper, 2005). In HIPE emulsions, the internal phase (aqueous) consists of water and a polymerization initiator such as potassium persulphate/peroxide, represents at least 74 vol. % of the emulsion volume, the continuous phase (organic) consists of a monomer such as styrene or acrylates, crosslinker components such as divinylbenzene (DVB) and a surfactant to stabilize the emulsion such as sorbitan monooleate (span80) (Hainey *et al.*, 1991; Aronson and Petko, 1993; Bhumgara, 1995; Hoisington *et al.*, 1997; Tai *et al.*, 2001; Deleuze *et al.*, 2002; Sergienko *et al.*, 2002; Cameron, 2005; Krajnc *et al.*, 2005; Zhang and Cooper, 2005; Haibach *et al.*, 2006; Menner *et al.*, 2006; Livshin and Silverstein, 2008; Ergenekon *et al.*, 2011). In polymerization, a crosslinker is used in an effort to enhance the physical/structural stability of the produced polymer by tying together its backbones and also to prevent them not to separate to the larger intermolecular distances favoured for side-chain crystallization (Livshin and Silverstein, 2008). Alternatively, other monomers such as methacrylate, isobornyl acrylate, butyl acrylate, 4-vinylbenzyl chloride, 4-nitrophenyl acrylate, 2-ethylhexyl

acrylate and 2, 4, 6-trichlorophenyl acrylate have also been in use (Cameron, 2005; Menner *et al.*, 2006).

Preparation of PHPs has been described in a number of studies. While depending on the features of the desired PHP; procedures of synthesis of different PHPs through a polymerization route may vary as demonstrated in the literature reviewed (Hainey *et al.*, 1991; Bhumgara, 1995; Walsh *et al.*, 1996; Hoisington *et al.*, 1997; Sotiropoulos *et al.*, 1998; Brown *et al.*, 1999; Akay *et al.*, 2004; Barbetta *et al.*, 2005; Bokhari *et al.*, 2005; Cameron, 2005; Krajnc *et al.*, 2005; Haibach *et al.*, 2006; Menner *et al.*, 2006). However, it appears that in all cases polymerization process principle remains the same and follows a two-stage process but with various compositions in accord to the application. In the first stage, an emulsion is created from an oil phase that contains a monomer mixture of styrene linked with DVB, and a dispersed phase which is made up from distilled water, a polymerization initiator such as potassium persulphate and a surfactant like span 80. This emulsion is afterwards rapidly stirred for a preset period of time depending on the desired PHP pore size. The longer the mixing time, the smaller the pore size of the PHP would be. A schematic representation of polymerization process is illustrated in Figure (2.23).
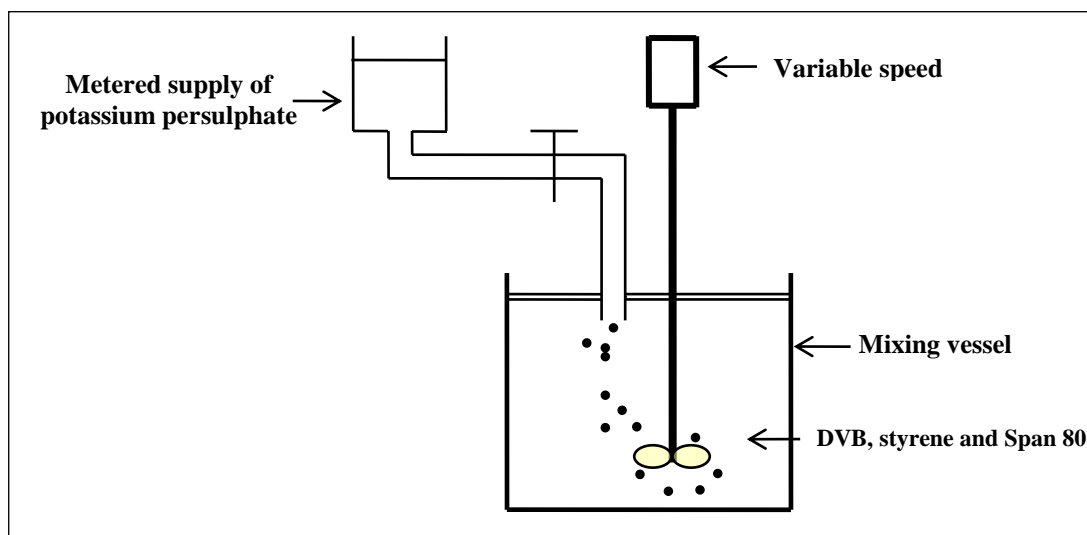
Figure (2.23): Illustration of PolyHIPE Polymer (PHP) production process.

In addition, with respect to final production application, a third stage that involves product post-functionalization may also be required. Produced solid PHP can be of the close/open- cell type and the internal aqueous phase is trapped within the cellular structure but can be readily and quickly removed (Hainey et al., 1991).

56

PolyHIPE are also known as aphrons, biliquid foams, hydrocarbon gels, gel emulsions and high internal phase ratio emulsions (HIPRE) (Aronson and Petko, 1993).

Following polymerization, drying of the obtained PHPs is necessary so as to remove any residual water (Hoisington et al., 1997). In addition to that; depending on the application of the produced PHPs, further processing, e.g. sulphonation at different levels may also be required to modify their surface characteristics (hydrophobicity / hydrophilicity) (Al-Malack and Anderson, 1997). Once synthesized, a styrene-DVB PHP is with a hydrophobic character and it; therefore, prefers to absorb tar-based liquids. In order to modify this character, PHPs which comprise hydrocarbon residues (Haq, 1985) are sulphonated so as to become a hydrophilic (acidic) material instead (Bhumgara, 1995; Wakeman *et al.*, 1998; Shen *et al.*, 2003). Complete (100 %) sulphonation cannot be achieved (Wakeman et al., 1998) due to polymer internal stresses due to polymer swelling by which inability of the sulphonating agent to effectively penetrate into the polymer to be sulphonated (Akay et al., 2005). The higher the temperature of sulphonation, the higher the degree of sulphonation and the shorter the time required to attain that degree of sulphonation. Although, current sulphonation techniques might be powerful and; therefore, have found a wide range of applications; however, they reportedly suffer from some drawbacks. Among of these are:

– Production of hazardous waste; that's the spent acid (dilute sulphuric acid) which requires a special disposal procedure; otherwise, it can be dangerous (Akay et al., 2005);

– Side reactions, particularly at elevated temperatures (Roth, 1957);

– Though sulphonation is a very rapid reaction; nevertheless, it is highly exothermic and *does* require some sort of cooling to avoid occurrence of side reaction(s) (Gopichandran, 2003);

– Necessity for precise control and difficulty to scale up (Roth, 1957);

– Use of excessive amounts of sulphonating agents, perhaps due to low solubility of product in the reaction environment (Ergenekon et al., 2011), and

– Long processing time is required (Ergenekon et al., 2011).

PHPs produced in accordance to the aforementioned procedure are characterized with:

– Light weight, open cellular microstructure, very high degree of porosity (up to 97%), interconnectivity, homogenous morphology and low bulk density (less than 0.15 g/m^3 (Sergienko et al., 2002).

– Good mechanical properties (Bhumgara, 1995; Hoisington *et al.*, 1997; Benson, 2003; Krajnc *et al.*, 2005; Haibach *et al.*, 2006; Menner *et al.*, 2006; Livshin and Silverstein, 2008);

– Accessibility, controllability of the pores and interconnected structures (0.5 < pore size < 5000 μm) and flexibility of production and chemical modification of their walls (Akay et al., 2005).

The internal structure of a PHP can be viewed by a scanning electron microscopy (SEM). Out of an SEM investigation, PHP pores are in the range of (5-100) μm (Zhang and Cooper, 2005). PHP pores are connected via pore throats; see Figure (2.24) (Menner et al., 2006). PHPs have average area of 5 m^2/g (Hainey *et al.*, 1991; Haibach *et al.*, 2006). It should also be mentioned that concentrations of both potassium persulphate in the aqueous phase (Williams et al., 1990) and DVB in the organic phase (Benson, 2003) are with adverse effect on the pore size of the produced polymer.
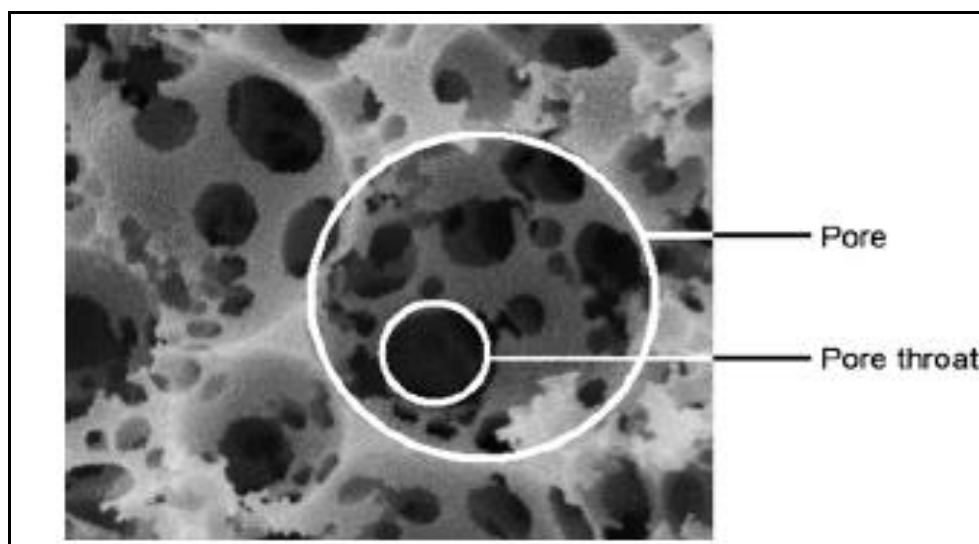
Figure (2.24): Definition of pore and pore throat (Menner et al., 2006).

Taking into account these features of PHPs, they have found several applications including: filtration process (Hainey *et al.*, 1991; Akay *et al.*, 1995;

Bhumgara, 1995; Kučera and Jančář, 1998; Akay *et al.*, 2005; Krajnc *et al.*, 2005; Zhang and Cooper, 2005; Haibach *et al.*, 2006), support for heterogenic catalytic reactions (Zhang and Cooper, 2005; Haibach *et al.*, 2006), tissue engineering applications (Hoisington *et al.*, 1997; Busby *et al.*, 2001; Busby *et al.*, 2002; Akay *et al.*, 2005; Barbetta *et al.*, 2005; Zhang and Cooper, 2005; Haibach *et al.*, 2006; Menner *et al.*, 2006; Burke *et al.*, 2010; Ergenekon *et al.*, 2011), ion exchange module systems (Hoisington *et al.*, 1997; Kučera and Jančář, 1998; Wakeman *et al.*, 1998; Benson, 2003; Naim *et al.*, 2004; Menner *et al.*, 2006; Ergenekon *et al.*, 2011), monolithic polymer supports for catalysis applications (Sergienko *et al.*, 2002; Menner *et al.*, 2006), removal of arsenic from contaminated water sources (Katsoyiannis and Zouboulis, 2002), production of nickel electrodeposits (Sotiropoulos *et al.*, 1998; Brown *et al.*, 1999), cleaning materials (Hoisington et al., 1997), medical applications, e.g., absorbent for body fluids (Haq, 1985; Hainey *et al.*, 1991; Hoisington *et al.*, 1997) and to enhance osteoblast growth and differentiation in vitro (Bokhari et al., 2005) and help growth of human stem cell-derived neurons (Hainey *et al.*, 1991; Hayman *et al.*, 2005), immobilization of pseudomonas syringe for the degradation of phenol (Erhan et al., 2004) and they are even used in aerospace industry as well (Hoisington et al., 1997), etc.

2.3.10. End Uses for Producer Gas

Gas clean up or downstream processing depends on the end use of the producer gas as different applications for power generation impose different quantities of contamination. Generally, tar content in the producer gas depends on the type of gasifier. It was reported that tar content in the syngas from an air-blown circulating fluidized bed (CFB) biomass gasifier was about 10 g/m^3. For other types of gasifiers, tar content varied from about 0.5 to 100 g/m^3 (Lopamudra *et al.*, 2003; van Paasen and Kiel, 2004; Ayhan, 2005).

Internal combustion gas engines are more tolerant with contaminants than gas turbines. For instance, it is possible to have tar content up to 50–100 mg/Nm^3 for an ICE and less than 5mg/Nm^3 for gas turbines (Milne et al., 1998). Typical values of the main components as well as the particulate and tar contents in the raw producer gas from fixed and fluidized bed gasifiers are tabulated in Table (2.11)

Table (2.11): The gas quality requirement for power generation (Hasler and Nussbaumer, 1999).

Contaminant	Unit	IC engine	Gas turbine
Particles	mg/Nm^3	<50	<30
Particles size	µm	<10	<5
Tar	mg/Nm^3	<100	Not Indicated
Alkali metals	mg/Nm^3	n.i	0.24

If the producer gas is to be used for heat production, downstream processing can be totally omitted (Reed and Das, 1998). In the case of ICE applications, the gas should not only be cleaned, but also cooled to increase its volumetric efficiency. Figure (2.25), below summarizes the range of fuel, electricity and chemical products that can be derived from the product gas (Bridgwater, 2003).
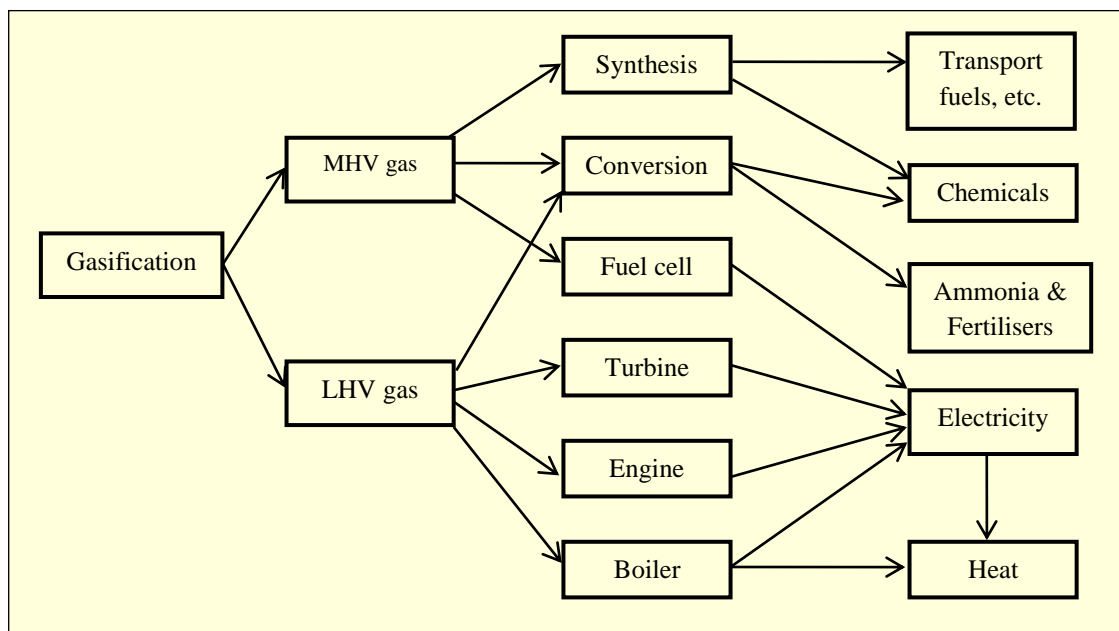
Figure (2.25): Applications for gas from biomass gasification (Bridgwater, 2003).

Chapter Three

Experimental Work

Chapter Three

Experimental Work

3.1. Introduction

In this Chapter, details of the experimental setup and procedures, operating conditions and parameters, analytical techniques and the chemicals and other resources used are presented and described. Analytical techniques used include: ultimate analysis, proximate analysis, moisture content, gallenkamp autobomb calorimeter, gas chromatography (GC), environmental scanning electron microscopy (ESEM) with energy dispersive x-ray analysis (EDX) and surface area analysis (SAA). The experimental work in this thesis was carried out in three stages: polymer preparation, gasification and co-gasification experiments and the development of an intensified syngas cleaning systems experiments.

Part of this work was devoted to the preparation of several batches of hydrophobic PolyHIPE Polymers (PHPs). These PHPs were then sliced into 4 mm thick discs. In order to turn these hydrophobic PHPs into hydrophilic ones, a sulphonation procedure was followed. Having sulphonated them, PHPs were ready to be used as packed bed for the adsorption of model tar from model tar/syngas mixture. In this work in the small scale intensified syngas cleaning system as would be explained later in section 3.5.2., we also have used other PHPs namely, silica containing styrene PolyHIPE Polymers (PHP-B30), crosslinked styrene-vinyl silane high internal phase emulsion co-polymer (PHP-S30), and crosslinked silica filled styrene-vinyl silane high internal phase emulsion co-polymer (PHP-S30B10). These PHPs were not prepared during this work; they were prepared by other PhD student Hasan (Hasan, 2012).

Next, some gasification and co-gasification experiments of wood chips and blending of oil sludge and sawdust using a novel downdraft intensive 50kWe air-blown auto-thermal gasifier were performed. Out of the results obtained from these experiments, comparisons were made between wood chips and oil sludge−sawdust mixture in terms of their syngas composition, heating value and tar level.

Finally, in the development of intensified syngas cleaning systems to achieve more efficient and safer gas cleanup and treatment technologies, PIM design philosophy has been applied as the basis to design, construct and test two different novel/new setup systems, small and pilot scale intensified syngas cleaning systems. In the demonstration of both technique, a model tar (fresh crude oil) and a model syngas (pure carbon dioxide) under laboratory conditions were used. Out of the results obtained from these experiments, comparisons were made in terms of tar reduction efficiency and concentration. A synopsis of the sequence of the experimental programme is schematically shown in Figure (3.1).
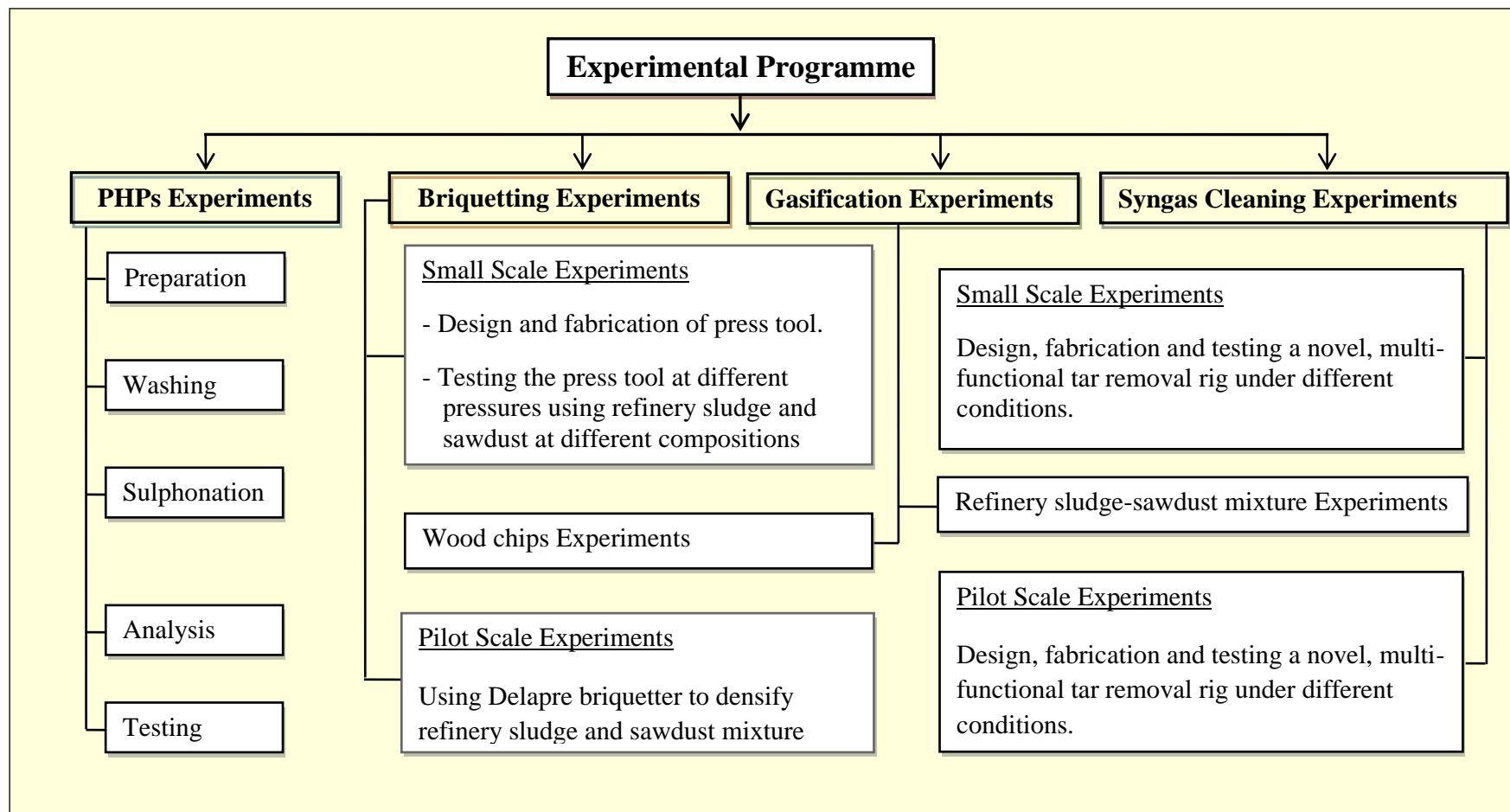
Figure (3.1): A synopsis of the sequence of the experimental programme

3.2. Materials

The materials and chemicals used in this study are tabulated in Table (3.1) according to their supplier and application.

Table (3.1): Materials and chemicals used in this study and their applications

Material/Chemical	Supplier	Application
Wood chips	Biofuels Corporation plc.	Gasifier fuel
Oil Sludge	Willacy Oil Services Ltd	Gasifier fuel
Sawdust	Biofuels Corporation plc.	Gasifier fuel
Crude Oil	BP-field in the North Sea	Model tar
Carbon dioxide	BOC	Model syngas
Divinyl benzene (crosslinkere)	Sigma-Aldrich, UK (Gillingham-Dorset, UK)	Polymer Preparation / Continuous phase
Styrene (monomer)	Sigma-Aldrich, UK (Gillingham-Dorset, UK)	Polymer Preparation / Continuous phase
Sorbitan monooleate (span 80) (surfactant)	Sigma-Aldrich (Gillingham-Dorset, UK)	Polymer Preparation / Continuous phase
Potassium persulphate (polymerization initiator)	Sigma-Aldrich, UK (Gillingham-Dorset, UK)	Polymer Preparation / Aqueous phase
98% concentrated Sulphuric acid	Sigma-Aldrich, UK (Gillingham-Dorset, UK)	Polymer Preparation / Aqueous phase and Polymer sulphonation
Double distilled water	Newcastle University Laboratory	Polymer Preparation / Aqueous phase.

3.3. PolyHIPE Polymers (PHPs) for Syngas Cleaning

3.3.1. Preparation of PolyHIPE Polymers (PHPs)

PHP was used for the collection and removal of model tars from model syngas. The preparation of PHP polymers has been described by several workers elsewhere (Hainey *et al.*, 1991; Walsh *et al.*, 1996; Hoisington *et al.*, 1997; Akay, 1998; Wakeman *et al.*, 1998; Brown *et al.*, 1999; Deleuze *et al.*, 2002; Sergienko *et al.*, 2002; Akay *et al.*, 2005; Barbetta *et al.*, 2005; Cameron, 2005; Krajnc *et al.*, 2005; Zhang and Cooper, 2005; Haibach *et al.*, 2006; Menner *et al.*, 2006; Livshin and

Silverstein, 2008; Ergenekon *et al.*, 2011). Polymers produced via these procedures can be described with: microporous structure, well controlled internal architecture, pore and interconnect sizes and their distributions (Akay, 2005). PHP is a highly porous material that is prepared through a high internal phase emulsion (HIPE) polymerization route of the monomeric continuous phase. The development of a PHP polymer involves three stages; these are HIPE formation, polymerization of this emulsion and then, according to the final application, finally post-functionalization, respectively. Sulphonated PolyHIPE Polymer (s-PHP) used in this work was prepared in-house in Newcastle University laboratory. In this study in line with procedures described by Akay and co-workers (Akay, 1998; Akay *et al.*, 2004; Akay *et al.*, 2005), PHP polymer was prepared by mixing the oil phase (25 ml) which consisted of styrene as a monomer, Divinyl benzene (DVB) as a cross linker and sorbitan monooleate (span 80) as a surfactant; and the aqueous phase (225 ml) which comprised double distilled water, potassium persulphate as the aqueous phase initiator and concentrated sulphuric acid (98%). 100 ml of continuous phase and 1l of aqueous phase were prepared using the reagents listed below.

1. Sulphonated PolyHIPE Polymer (s-PHP)

Continuous / Polymerisable Oil Phase:

Styrene (monomer) = 76 %;

Divinyl benzene (crosslinking agent) = 10 %; and

Sorbitan monooleate (Span 80, surfactant) = 14 %

Dispersed /Aqueous Phase:

Concentrated sulphuric acid (as nano-structuring agent) = 5 wt%;

Potassium persulphate (polymerisation initiator) = 1 wt%; and

Double distilled water = 94%

Nevertheless, other PHPs namely, silica containing styrene poly high internal phase emulsion polymer (PHP-B30), crosslinked styrene vinyl silane high internal phase emulsion co-polymer (PHP-S30) and crosslinked, silica filled styrene - vinyl silane high internal phase emulsion co-polymer (PHP-S30B10) used in this work were prepared in another work by Hasan (Hasan, 2012). Details of preparations are not given in this study. In brief, the recipes of continuous/polymerisable oil phases and dispersed/aqueous phases used in the preparation of these PHPs were:

2. Silica containing styrene PolyHIPE Polymer (PHP-B30)

Continuous / Polymerisable Oil Phase:

Styrene (monomer) = 67 %;

Divinyl benzene (crosslinking agent) = 20 %;

Sorbitan monooleate (Span 80, surfactant) = 12 %; and

Lauroyl peroxide (polymerization initiator) = 1 %

Dispersed / Aqueous Phase:

Bindzil CC30 (coated silica content 30 wt %)

3. Crosslinked Styrene - Vinyl Silane High Internal Phase Emulsion Co-polymer: (PHP-S30)

Continuous / Polymerisable Oil Phase:

Styrene (monomer) = 38 %;

VTMS (vinyl trimethoxy silane, co-monomer) = 30 %;

Divinyl benzene (crosslinking agent) = 20 %; and

Sorbitan monooleate (Span 80, surfactant) =12 %

Dispersed /Aqueous Phase:

Distilled water with 1 % Potassium persulphate

4. Crosslinked, Silica Filled Styrene - Vinyl Silane High Internal Phase Emulsion Co-polymer: (PHP-S30B10)

Continuous / Polymerisable Oil Phase:

Styrene (monomer) = 38 %;

VTMS (vinyl trimethoxy silane, co-monomer) = 30 %;

Divinyl benzene (crosslinking agent) = 20 %; and

Sorbitan monooleate (Span 80, surfactant) = 12 %

Dispersed /Aqueous Phase:

Bindzil CC30 diluted with double distilled water to obtain 10 % silica with 1% Potassium persulphate.

PHP Emulsion Preparation

The detailed procedure for preparing PHP was as follow: 25 ml (10 vol. % of the total emulsion) of continuous phase were poured into a stainless steel mixing vessel (internal diameter 12 cm), and 225 ml (90 vol. % of the total emulsion) of aqueous phase were then dosed drop-wise continuously to the vessel by using peristaltic pump for exactly 5 minutes with constant stirring to break up large droplets. Mixing was facilitated by a 9 cm diameter double blade impeller in which the two blades are positioned 1cm apart at right angles to each other. The base of the impeller was positioned 1cm above the bottom of the vessel. Rotational speed of the impeller was kept constant at 300 rpm. The impeller was started at the same time as dosing the aqueous phase into the mixing vessel. Stirring of both phases was continued for another minute after dosing all the aqueous phase (225 ml) into the mixing vessel. Polymerization factors such as temperature of emulsification and mixing speed and duration are decisive with regards to cell structure and pore size of the produced PHP. Control of pore size and structure of a produced PHP has been described in previous works of Akay and others (Akay et al., 1995; Akay et al., 2004). Once the emulsion has been prepared, it was poured into 50 ml plastic tubes (26 mm diameter) through an outlet situated at the bottom of the vessel. To ensure the wasted emulsion is minimal, having no emulsion is collected from the bottom of the vessel, the vessel was taken apart to recover any trapped emulsion within the vessel and on the impellers. The plastic containers were then placed in the oven overnight at 60oC to allow polymerization to occur. A simplified schematic diagram of the experimental setup used to produce PHPs is given in Figure (3.2). After polymerization of the HIPE, the solid PHP cylinders were removed from the plastic containers and sliced with care with a bandsaw into 4 mm thick discs. Picture of the setup, the impeller and the mixing vessel are given in Appendix A.

3.3.2. Washing and Drying of PolyHIPE Polymers (PHPs)

Any residues of chemicals such as surfactants and initiators as well as the excess sulphuric acid, which may have remained in the pores and interconnects of the produced PHPs, have to be washed. The 4 mm thick discs were then washed in a beaker with a magnetic stirrer for 30 min with deionized water, the discs were rinsed and the process of washing and rinsing was repeated twice. On completion, the discs

were air dried overnight in a fume cupboard. Dryness was determined qualitatively by visual inspection of the tissue surface on which the discs had been placed. Once washed and dried, the dried discs were then sulphonated.
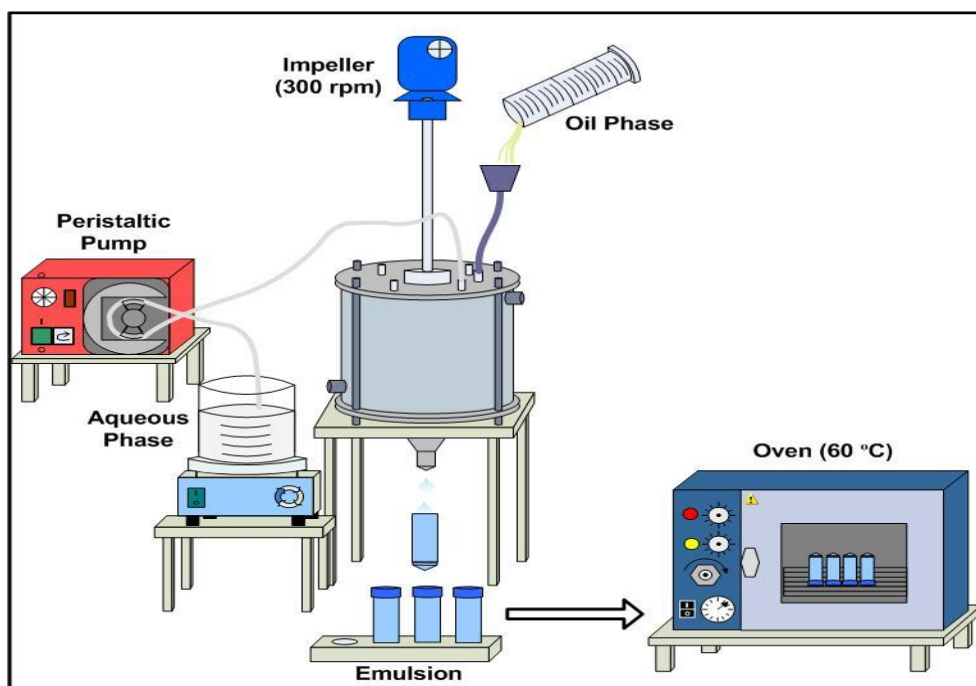
Figure (3.2): A simplified schematic diagram of the experimental setup used to produce PolyHIPE Polymers (PHPs) (Ndlovu, 2008).

3.3.3. Sulphonation of PolyHIPE Polymers (s-PHPs)

Sulphonation process was carried out according to the procedure described by Akay and co-workers (Akay et al., 2005). PHP discs were soaked in concentrated sulphuric acid (98 %) for 2.5 h without stirring at laboratory temperature to increase the absorptive capacity. During this time the contents were agitated periodically to ensure that both surfaces of the discs remained in contact with the acid. After soaking, the discs were removed from the acid and microwaved at 180 ^{o}C for 5 x 30 s periods with four alternating 1 min cooling periods. They were inverted after the third heating interval so as to reduce the occurrence of uneven heating. On cooling, the discs were washed in deionized water for 2 h in a 500 ml beaker with stirring with a magnetic bar. During this process, used distilled water was disposed of in a specified container and replaced by a fresh one every 30 min. Finally, Sulphonated PHP discs were rinsed and left to dry in a fume cupboard overnight. Once dried, the discs were then ready to be used in gas cleaning. Figure (3.3) illustrates the differences in size and colour of

69

the Sulphonated PHP discs as compared to the prepared un-Sulphonated PHP. The increased diameter of the Sulphonated PHP discs is a result of swelling due to water absorption. The method is graphically shown in Figure (3.4).
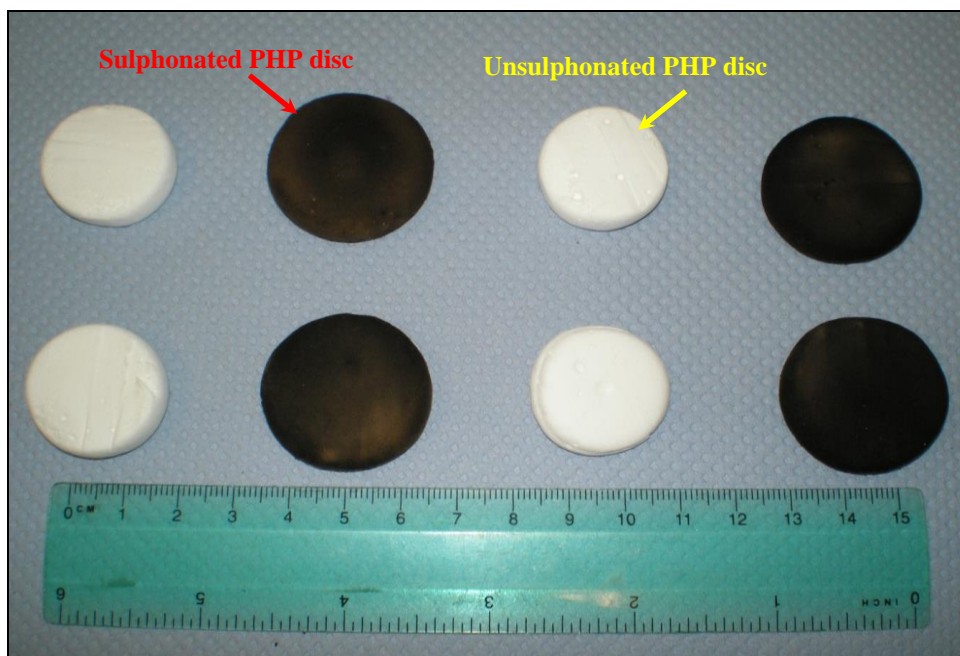
Figure (3.3): Comparison of unsulphonated PolyHIPE Polymer (PHP) and Sulphonated PolyHIPE Polymer (s-PHP) discs.
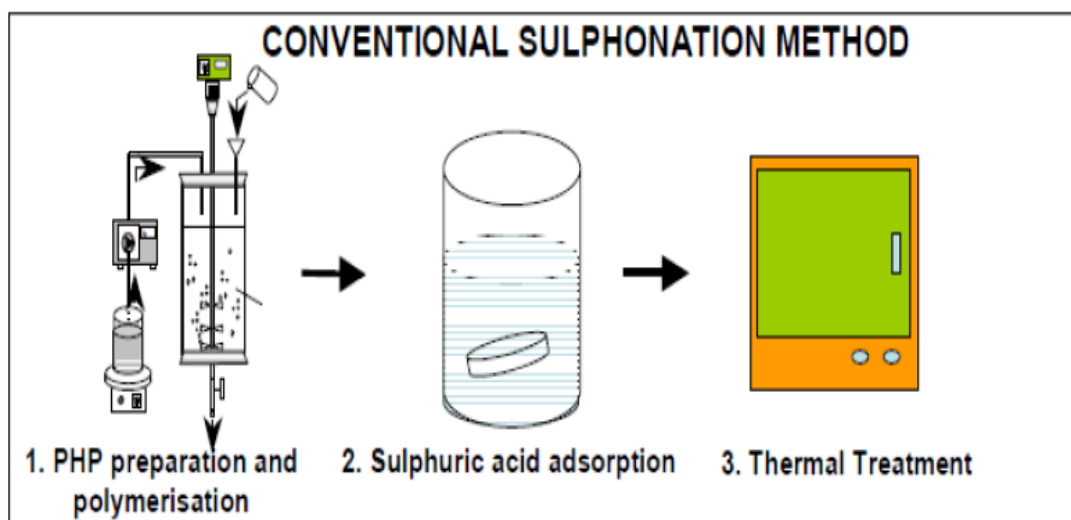
Figure (3.4): The Conventional PolyHIPE Sulphonation method

3.4. Gasification Experiment

Two types of feedstock (wood chips and oil sludge-sawdust mixture) were tested in an intensified autothermal 50 kWe throated downdraft gasifier at Newcastle University in which air was used as the oxidation agent. Proximate and ultimate analyses of both materials were carried out.

Wood chips were supplied by Biofuels Corporation plc. whereas, the refinery sludge was supplied by Willacy Oil Services Ltd sealed in polypropylene bags for use in this study. The oil sludge was already free from any valuable hydrocarbons as it was treated on site to recover oil and also to minimize the amount of waste. The refinery sludge had to be briquetted before gasification. Because of its "soft-solid" like behaviour, refinery sludge was adsorbed on a carrier (sawdust) and then briquetted. The sawdust was supplied by Biofuels Corporation plc. The delivered sawdust was in powdered form in polypropylene bags. The types of feedstock were air dried indoors at laboratory-ambient conditions.

3.4.1. Feedstock Properties

One of the requirements for gasification of biomass and/or biomass waste fuels is that the fuel has a gross calorific value greater than 11 MJ kg^{-1} (Dogru, 2000). The main parameters used to determine the gross heating value of biomass and/or biomass waste feedstock are the proximate and ultimate analysis (Dogru et al., 2002a).

3.4.2. Feedstock Briquetting

Prior to gasification, biomass and/or biomass waste fuels were densified either to form briquettes or pellets.

3.4.2.1. Small Scale Briquetting

Small scale briquetting experiments were carried out to produce uniform briquettes. In order to mix the oil sludge and sawdust, a 4.2 litre capacity kitchen mixer, Kenwood chef 800W as seen in Appendix B, was used. Several compositions of oil sludge and sawdust were tested (50, 70 and 90 wt. % of oil sludge). A sample that is densified enough was then used in large scale briquetting experiments. Other samples; however, were excluded. To press this mix to the desired shape, it was first contained in a special press tool. This press tool was designed and fabricated from

stainless steel in the CEAM workshop, Newcastle University, and had the dimensions of 25 mm diameter and 60 mm length as seen in Appendix C. This press tool was then attached to a press machine, as given in Appendix D, at Herschel Building, Newcastle University, at room temperature. Having run this press machine at different pressures, it was found that a pressure of 9 Tons is the suitable pressure to produce a briquette that does not fracture. This pressure was employed in all large scale briquetting experiments. The diameter of produced briquettes is 52 mm and the length is around 29 mm.

3.4.2.2. Large Scale Briquetting

The recipe that gave densified briquettes in small scale briquetting experiments was then employed in large scale briquetting experiments. In these experiments, a cement mixer (Minimix 130), as seen in Appendix E, was used prior to using the briquetter machine, 100 kg/h supplied by Por Ecomec SRL, Figure (3.5). The briquetter had 30/50 kg/h capacity with adjustable pressure hydraulic press.

Figure (3.5): 100 kg/h capacity briquetter supplied by Por Ecomec SRL.

The material to be briquetted was fed to the system from the top. There is a rotating, cross shaped blade at the bottom of the main cylindrical container which pushes the material into a hole at the base. Once the material was pushed into the hole

it was then forced to a cylindrical cavity by the side ram. A second ram squeezes the waste material into shape and the finished briquettes were produced. The ideal moisture content of the feed for briquetting was reported to be no more than 20 % in the manual provided by the supplier. This data seems well in line with the gasifier requirements.

3.4.3. Experimental Setup

A schematic diagram and the dimensions of the experimental pilot-scale throated downdraft gasifier used in the studies are presented in Figure (3.6). The design parameters and design methodology of the gasifier was studied by Dogru and Akay,2004 (Dogru and Akay, 2004).
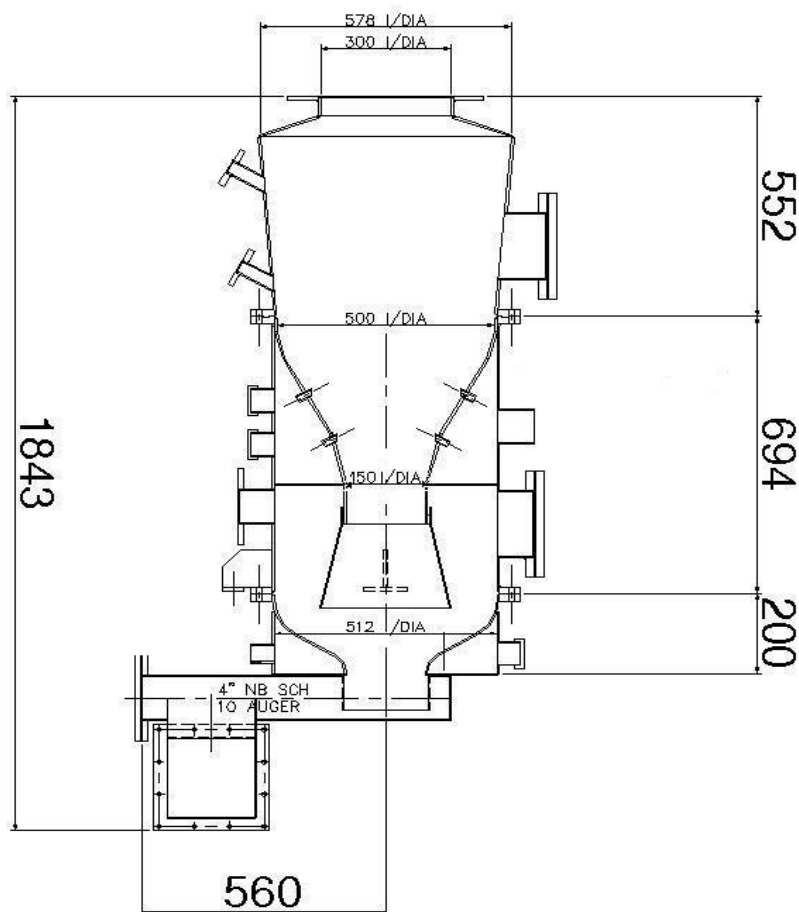
Figure (3.6): Schematic diagram of the pilot-scale downdraft gasifier and its dimensions (All dimensions are in mm).

The complete assembled setup of an intensified autothermal air-blown 50 kWe throated downdraft gasifier is shown in Figure (3.7) using air as the gasifying agent. The system consists of an Imbert type reactor with a throat near the base, an air

73

blower, a gas clean up system consisting of two cyclones, a water scrubber and an ash collector. The reactor is a double wall conical vessel with a height of 2 m and an internal throat diameter of 100 mm.
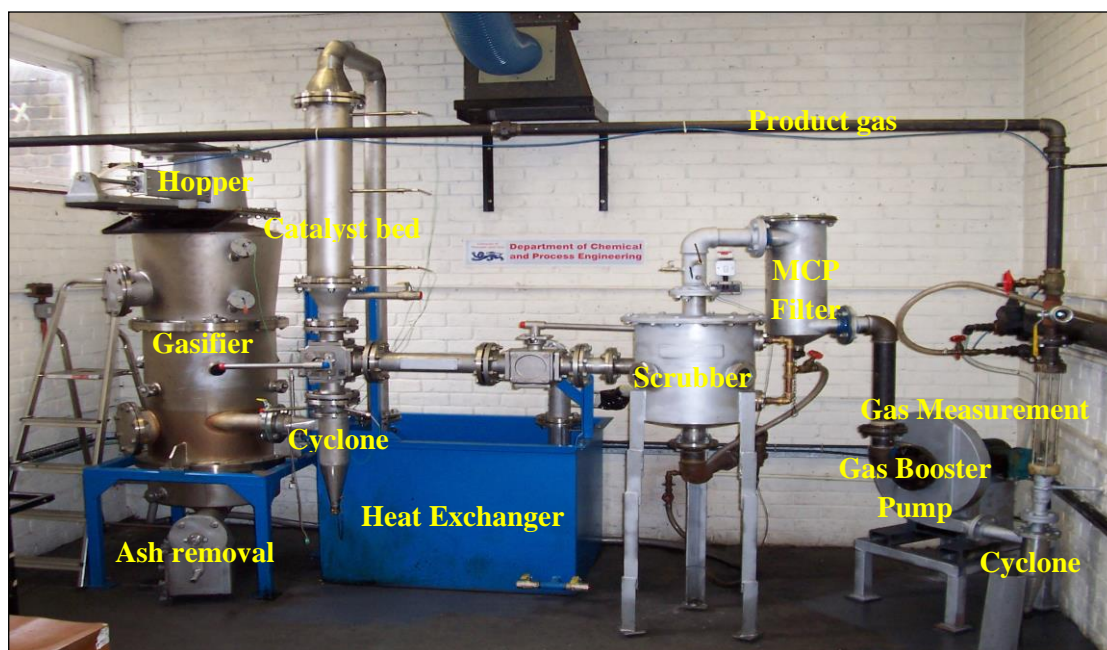
Figure (3.7): Photograph of 50 kWe Newcastle University gasifier system.

The gasifier is a conical shaped vessel in which all the components except the throat are constructed of 10 mm thick stainless steel. The throat; however, is made of high temperature stainless steel which ensures that the oxidation zone (throat zone) is able to withstand the extreme temperatures (up to 1200°C) which occur in this area. The suction effect of the gas booster fan pulls air into the gasifier through the main air valve and into a circular chamber which surrounds the throat and partially encloses the reduction zone. The suction fan was a single stage gas booster supplied by Fans and Blowers Ltd. The air then flows into the oxidation zone through a plane of air nozzles. Heat loss is further reduced by a purpose made fibreglass lagging which covers the outer shell. A schematic of the gasifier, the associated gas clean-up system, induced draft fan and flue gas stack is illustrated in Figure (3.8).
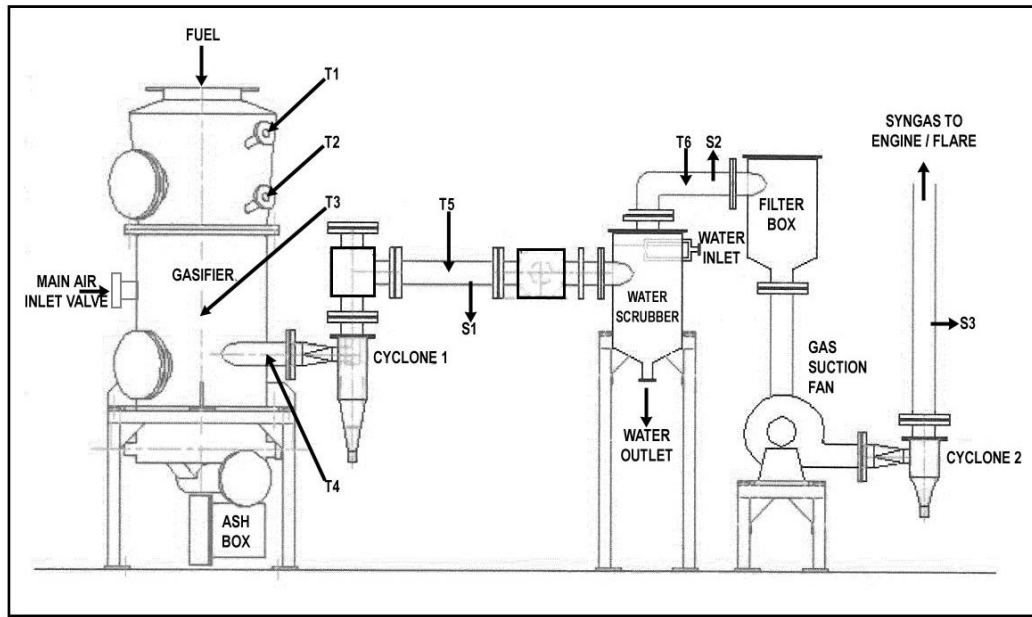
Figure (3.8): Schematic of 50 kWe Newcastle University gasifier system.

The principle stages in the gasification are drying, pyrolysis, oxidation and reduction, the operating temperatures in the gasifier are summarized in Table (3.2).

Table (3.2): Operating temperatures in the gasifier

Zones in the gasifier	Temperature (^{o}C)
Drying Zone	70 – 200
Pyrolysis Zone	350 – 500
Oxidation Zone	900 – 1200
Reduction Zone	700 – 900

The temperature in each of the four reaction zones in the gasifier was monitored at 10 second intervals using type K shielded thermocouples, labelled T1–T4 in Figure (3.8). These thermocouples were located in the centre of the reactor to minimize the localized effects from fuel flow along the wall of the reactor. Two additional thermocouples T5 and T6 measured syngas temperatures at the outlet of cyclone 1 and the water scrubber, respectively. The specific locations of the thermocouples are listed in Table (3.3).

Table (3.3): Location of thermocouples in the gasifier

Thermocouple	Position from top of Gasifier (mm)	Reaction Zone
T1	82	Drying
T2	98	Pyrolysis
T3	113	Throat
T4	133	Reduction

The data generated by these thermocouples was processed using the Pico Log® data acquisition system which produced real time temperature profiles of the gasifier system during operation. From the temperature measurements, it was possible to estimate the general location of the four main reaction zones in the gasifier. The typical temperature profile of this throated downdraft gasifier is illustrated in Figure (3.9).
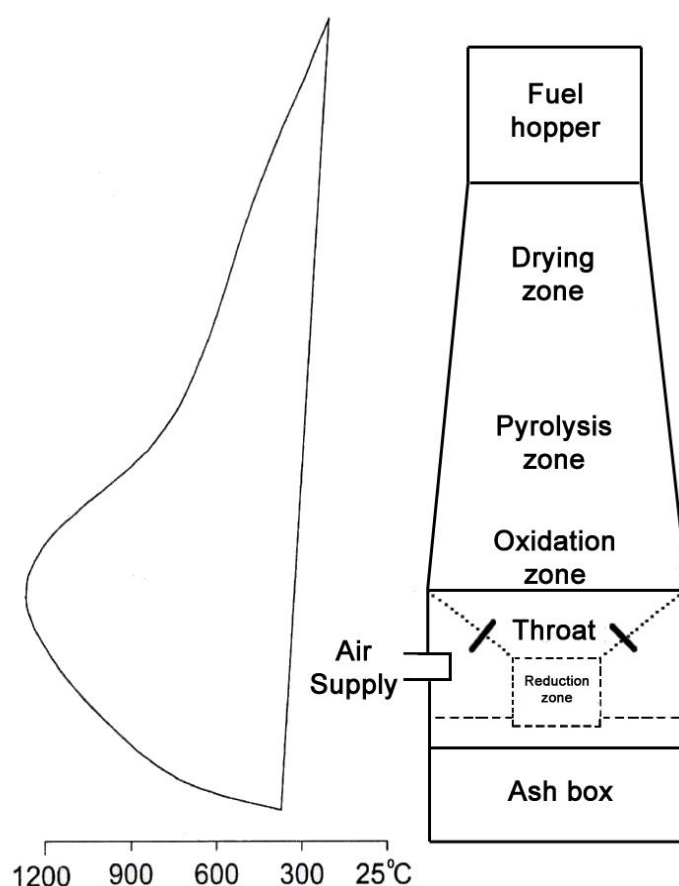
Figure (3.9): Schematic of the reaction zones and temperature profile of a throated downdraft gasifier (Dogru, 2000).

3.4.4. Gas Clean Up System
3.4.4.1. Water Scrubber

The product gas was cleaned by a V-tex vortex scrubber which is shown in detail in Figure (3.10). In the scrubber, the soluble inorganic compounds and some organic compounds in the gas were removed by the scrubbing action of the high-pressure water jet. The high pressure of the water through the narrow orifice in the scrubber creates a jet of tiny water droplets. The increased surface area for gas/liquid contact significantly increased the rate of mass transfer of water soluble compounds between the two phases. Furthermore, the rapid cooling caused deposition of high boiling tars removing these from the product gas. The scrubbed gas then left the V-tex scrubber through a hole in the ceiling of the scrubber vessel.
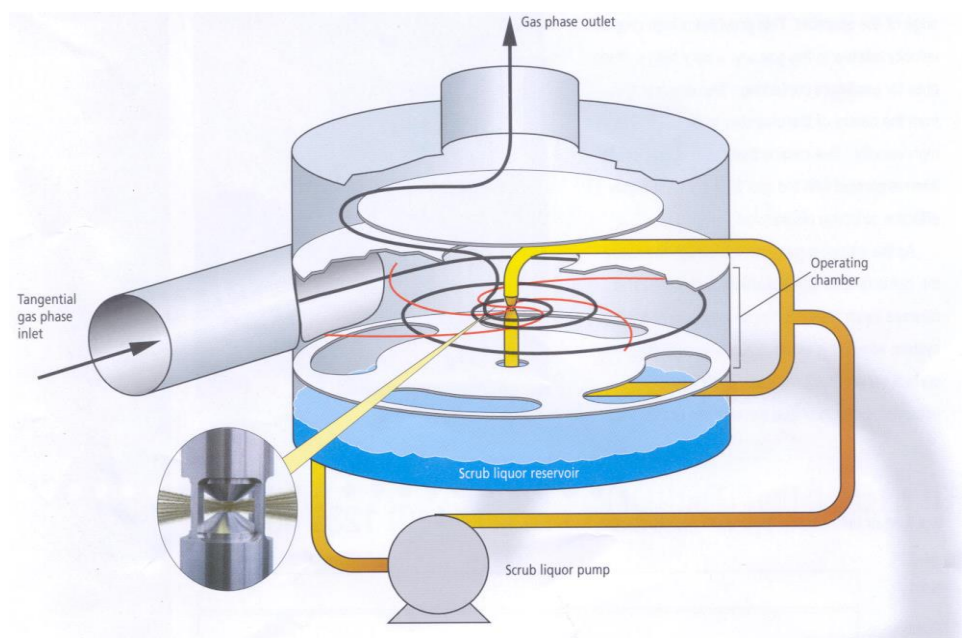
Figure (3.10): Schematic of the vortex scrubber (Dogru, 2000).

3.4.4.2. Filter Box

After the initial cooling and cleaning in the scrubber, the product gas passed through a vertical box filter, Figures (3.7−8). The diameter and the height of the box filter were 21 and 50 cm, respectively. A bucket was placed in the box filter with a mesh at the bottom for gas. The bucket was tightly fitted inside the box filter to avoid channeling of the gas from the sides without filtration. The height of the bucket was 30 cm. The box filter is mainly used for filtration of remaining tars and impurities (fly ash, particulates and condensate). The filter box has two layers. Wood chips and

charcoal were chosen as the filter medium so that the contaminated filter can be recycled as fuel in the subsequent use of the gasifier. To prevent excessive pressure drop over the box filter, the wood chips and charcoal were thoroughly sieved to remove any fines before they were placed in the filter trays. In the filter box, the charcoal tray occupies the lower tray, while the dry wood chips are on the upper tray. After each run, the box filter medium was refreshed and the used filtering media (wood chips) was fed to the gasifier.

3.4.4.3. Cyclones

Both cyclones, Figures (3.7−8), employed in the gasifier setup were designed and constructed by Morecroft Engineering, UK. A cyclone works on the principle of creating a high-speed spiral gas flow. The spiral motion exerts a centrifugal force on the particles and the inertia of the larger particles forces them to the outside walls of the cyclone, from where they fall to the bottom where they were collected. The conical section at the base of the cyclone gradually decreases the diameter of the spinning gas stream resulting in a more efficient removal of the smaller particles. The overall efficiency is related to the velocity of the gas flow and the diameter of the cyclone, the smaller the diameter, the more efficient the particle removal.

3.4.5. Gas Measurement

The flow of product gas from the gasifier was measured by a Platon GMT metal tube flow meter as shown in Figure (3.7) which was supplied by Roxspur Measurement and Control Ltd UK. The rotameter is magnetically coupled VA meter requiring no external power. Within the tapered flow tube, fluid flow lifts the metering element, which contains a magnet. The external pointer follows the magnetic field and indicates flow against a scale. The rotameter was located downstream of the gas clean up system so as to minimize the risk of damage from contaminants in the product gas. The rotameter measured in the flow range 1-120 m^3/h at atmospheric temperature and pressure (ATP, 15°C and 760 mmHg). The gas flow rate was regulated by a gate valve positioned immediately after the rotameter.

3.4.6. Experimental Procedure

The following procedures were performed during the experiments. In each experimental run, a batch of fuel of known weight was loaded into the gasifier. The

height of the feedstock was measured so as to determine the rate of feedstock consumption after gasification. The induced draft fan was then switched on and the gasification process started by manually lighting the air inlet ports with a butane torch. Air, the gasifying agent, was sucked into the gasifier through the main air inlet valve and into the chamber surrounding the throat by the induced draft fan at a controlled flow rate. From there, the air then flowed into the oxidation zone through a set of 8 air nozzles distributed symmetrically in two planes. Heat loss from this high temperature zone was limited by the double chamber around the throat area.

The syngas generated in the gasifier was extracted from the reactor by the suction effect of the induced draft fan. As the solid fuel was converted to syngas, this caused the remaining fuel to move through the reactor under gravity. The ash and residues of char produced were emptied into the ash box manually by turning the ash box handles at fixed intervals during gasification. Tar, particulates and other entrained aerosols were removed from the syngas stream by the gas clean up system which consists of cyclone 1, the scrubber tank, the filtration media in the filter box and cyclone 2, Figures (3.7–8). The syngas was then flared in the flare stack. The flow rate of the syngas generated was measured using a Platon GMT stainless steel flow meter and readings were taken manually at 5 minute intervals. A number of potential hazards are associated with the operation of a gasifier. The hazards associated with the operation of a gasifier can be considered as either a toxic or an explosion/fire hazard (see Appendix F).

3.4.7. Syngas Sampling and Analysis

Syngas composition was determined from samples collected from a constant flow of gas from sampling point S3, (Figure (3.7)); to an online Agilent 6890 gas chromatograph (GC). The GC was equipped with a six port gas sampling valve, a six port column isolation valve with an adjustable restrictor; the schematic diagram of the valve system and a thermal conductivity detector (TCD) can be seen in Figure (3.11). Before each gasification run, the GC was calibrated using a standard gas mix (15 mol% H_2, 10 mol% CO_2, 3 mol% C_2H_4, 3 mol% C_2H_6, 2 mol% O_2, 49 mol% N_2, 3 mol% CH_4, 15 mol% CO).
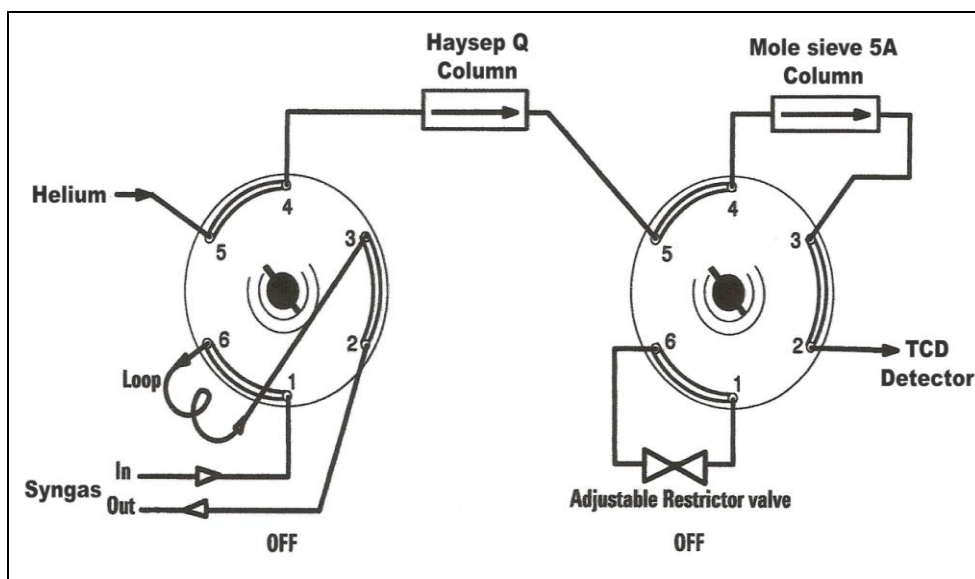
Figure (3.11): Agilent 6890N GC column and gas sampling valve flow configuration.

3.4.8. Tar Sampling

The quantity of tar and particulates carried over in the product gas after gas clean up was determined using a U-tube apparatus. The apparatus was connected to a sampling valve on the gas line via flexible PVC tubing. The tubing was kept as short as possible so as to minimize the possibility of heavy tar deposition during sampling; Figure (3.12) illustrates the U-tube sampling arrangement.
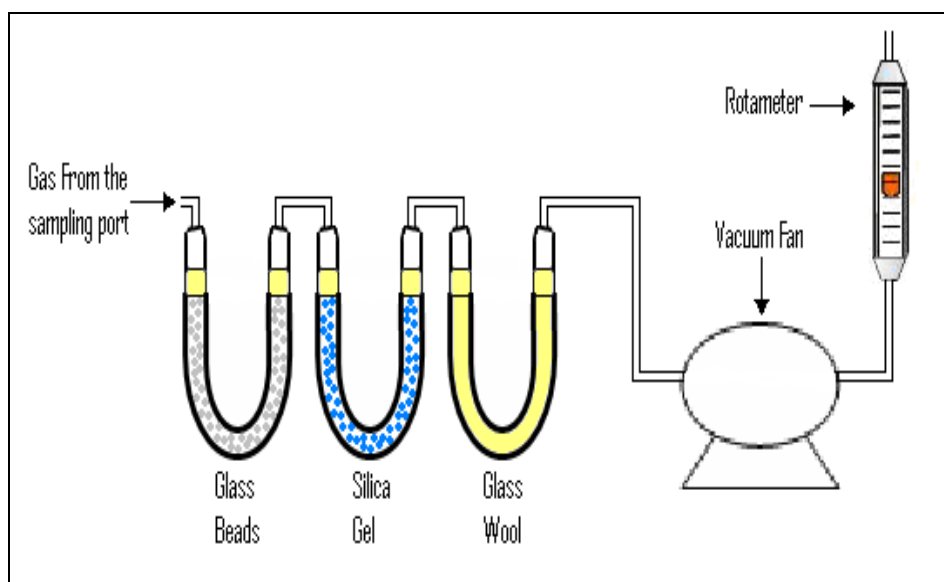
Figure (3.12): U-tube arrangement for tar sampling.

The U-tubes were placed in series in a cold water container for trapping tar and moisture. The first U-tube contained glass beads to provide a large surface area,

which were retained in the tube by glass wool, tar and particulate deposition, occurred on these beads. The second tube contained silica gel which absorbed the condensate in the product gas and the third tube enclosed glass wool or the final filtration of the gas.

Prior to sample collection, the U-tubes were oven dried at 105°C overnight; they were then weighed to an accuracy of 0.01g and kept in a dessicator to prevent any condensation of moisture in the tubes. After sampling for 5 minutes at a flow rate of 3.0 litre/min, the tubes were capped, allowed to equilibrate to room temperature, towel dried, weighed immediately and then heated at 105 ^{o}C to constant weight. The weight after drying was recorded. The increase in weight after sampling was recorded as this represents the quantity of tar, particulates and condensate trapped in the U-tubes whereas the reduction in weight after drying was recorded as the quantity of condensate alone. Therefore, the quantity of tar, particulates and condensate carried over in the product gas could be calculated.

3.5. An Intensified Syngas Cleaning Systems Experiments

In the development of an intensified syngas cleaning system to achieve more efficient and safer gas cleanup and treatment technologies, PIM design philosophy has been applied as the basis to design, construct and test two different new/novel set-up systems namely, small (plasma reactor) and pilot (electric field enhanced tar removal equipment) scale intensified syngas cleaning systems. In the demonstration of both techniques, a model tar and a model syngas under laboratory conditions were used. As a model tar, fresh crude oil (supplied by BP Amoco) and as a model syngas, pure carbon dioxide (supplied by BOC) were employed. Relevant physical properties of the crude oil used are given in Table (3.4).

Table (3.4): Physical properties of BP-Amoco fresh crude oil (Noor, 2006).

Property	Value/colour
Specific gravity	0.80
Dynamic viscosity, cP at 25 ^{º}C	153
Colour	Dark brown to black

In the small (plasma reactor) scale intensified syngas cleaning system experiments, effectiveness of different types of porous PolyHIPE Polymers (PHPs),

namely, sulphonated PolyHIPE Polymers (s-PHP), silica containing styrene PolyHIPE Polymers (PHP-B30), crosslinked styrene-vinyl silane high internal phase emulsion co-polymer (PHP-S30), and crosslinked silica filled styrene-vinyl silane high internal phase emulsion co-polymer (PHP-S30B10) on tar reduction or/and removal were carried out. The PHPs used in this work/research were prepared 'in-house', in Newcastle University laboratory, by the methods explained in section 3.3.1. These PHPs were differing in composition as a result of which they have different physical and chemical properties. The effect of plasma tar cleaning at different power intensities (40 - 50 W) in the presence and absence of a packed bed of s-PHP particles were also studied.

Next, in order to carry out the pilot scale (electric field enhanced tar removal equipment) intensified syngas cleaning system experiments on tar reduction or/and removal on tar reduction efficiency. The experiments were carried out in different profiled high voltage electrode was either completely (totally) insulated electrode (CIE) when it was used with water spray, or it was partially isolated electrode (PIE) when no conductive material was present in the gas stream or in the fixed bed. Using the CIE configuration, the equipment was tested under the following processing conditions:

1. Creating a planar water spray either at the bottom or top or indeed both sprays could be used.
2. Combined water scrubbing and electric field at different intensities, and
3. An electric field at different intensities in the absence and presence of a packed bed of s-PHP particles.

At the same time as, with the PIE configuration the equipment was performed under an electric field at different intensities in the absence and presence of a packed bed of s-PHP particles.

3.5.1. Reference Experiment

As reference, a dry run was performed. Due to the temperature reduction in the cleaning equipment (from 40 °C down to 20 °C), some model tar condensation occurs in the syngas cleaning equipment. Therefore, this reference gas cleaning efficiency was evaluated by running the experiment without any tar removal facility (i.e., dry run).

3.5.2. Small Scale Intensified Syngas Cleaning System Experiments

Initially, the experimental set-up used for small (plasma reactor) scale intensified syngas cleaning system is shown in Figure (3.13) below.

Key:
01 = Pressurised CO_2 Cylinder (Model syngas)
02 = Crude oil vessel (Model
03 = Plasma reactor
04 = Cold traps
05 = Gas Chromatography (GC)
06 = Digital temperature controller
07 = Thermocouple (TC-1)
08 = Gas sample before treatment (SP1)
09 = Gas sample after treatment (SP2)
SP = Sample Point
MFC = Mass Flow Controller
V = Valve

Pure CO_2 (Model syngas)
Model tar/syngas mixture before treatment
Model tar/syngas mixture after treatment

Figure (3.13): Flow diagram of the small (plasma reactor) scale intensified syngas cleaning system.

The used system essentially consisted of pressurised pure carbon dioxide (CO_2) cylinder (01), crude oil stainless steel vessel (02); the internal dimensions of this vessel are as follow: height and internal diameter are 335 mm and 204 mm respectively. Schematic and picture of this unit (crude oil vessel) is given in Appendix G. The vessel (02) is insulated with ceramic fibre insulation to minimise heat loss during heating up. For the purpose of heating the oil (model tar), the vessel is equipped with an electrical coil controlled using a digital temperature controller (06) and K-type thermocouple TC-1 (07) and TC-2 to measure and monitor the crude oil and model tar/syngas mixture temperatures respectively. During the experiments, it was always necessary to ensure that crude oil level is always above the electrical coil

to avoid the heating system damage. The plasma reactor (03) which is further illustrated in section 3.5.1.1., consist of two cylindrical tubes made from quartz tube (can be used in different modes, test the performance of different types of porous PHPs particles, effectiveness of the plasma tar cleaning at different power intensities and combined plasma at different power intensities with a packed bed of s-PHP particles). Set of U-tubes (04) placed in sequence in an ice water container, for trapping tar and moisture at ambient temperature. The first U-tube contained glass beads, to provide a large surface area for gas condensation, which are retained in the tube by glass wool, tar and particulate deposition, occurred on these beads. The second U-tube contained silica gel to absorb the condensate in the produced gas and the third U-tube enclosed glass wool for the final filtration of the gas. The outlet from these U-tubes was fume cupboarded. The gas (model syngas) flow was controlled using a volume flow meter (MFC-1) supplied by Platon, flow bits, UK, and the inlet and outlet model tar/syngas mixture composition were monitored using an off-line Agilent 6890N Gas Chromatography (05). Pictorial representation of the assembled experimental rig of small (plasma reactor) scale intensified syngas cleaning system is given in Appendix H.

3.5.2.1. Reactor Design

The design of the plasma reactor is a simple glass tube of 30 mm inner diameter and 300 mm length. It consisted of two glass tubes one inside the other made from quartz tube. The outer glass tube has 28 mm inner diameter and 300 mm length. The inner tube has 18 mm outer diameter. Hence, the gap between the two tubes is 5 mm. The gas inlet is introduced through a side arm capped with a GL 18 cap. The gas outlet is from the top end of the glass tube. Schematic illustration and pictorial representation of the plasma reactor is shown in Figures (3.14) and (3.15) below.
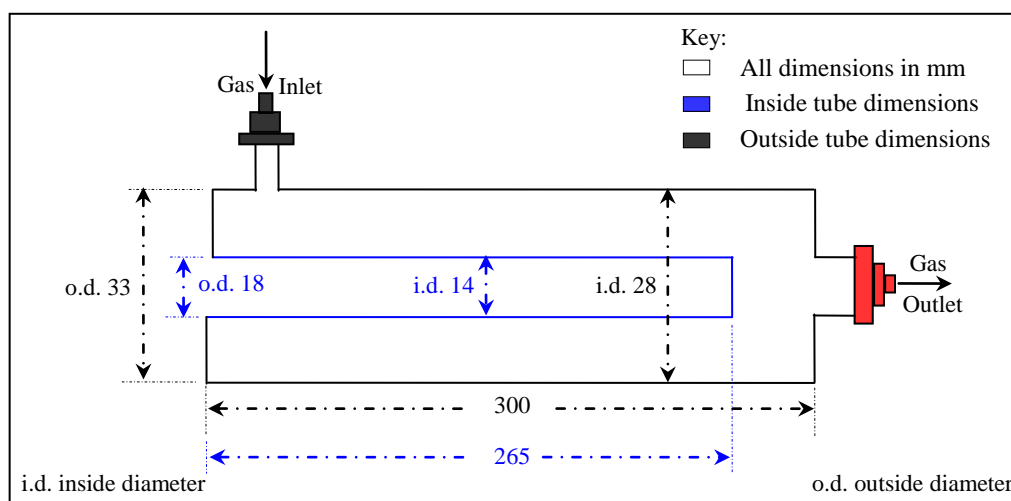
Figure (3.14): A schematic illustration of the plasma reactor dimensions and gas flow scheme

Figure (3.15): The pictorial representation of the plasma reactor.

3.5.2.2. Experimental Procedure

Experiments were performed in the following manner; refer to Figure (3.13), before the actual start of each experiment, all device and pipes were leak tested. Prior to using the fresh crude oil (model tar) in the experiments, the crude in its metal container was warmed in a $30 - 40$ °C water bath to attain well mixing of the contents of the container. Then, 8 litres of fresh crude oil from its metal supplier container was carefully loaded (avoid spillage) into the crude oil vessel (02), where the oil was heated. Once the temperature of the crude oil was raised to 80 ± 1 °C and monitored using a thermocouple (TC-1). Pure CO_2 from a pressurised gas bottle (01) at a controlled flow rate of 1litre/min was bubbled through fresh crude oil vessel (02) at

$80 \pm 1^{\circ}C$ for 3 hours. Resulting model tar/syngas mixture was then fed into the plasma reactor (03). The concentration of the model tar/syngas mixture before and after entering into the plasma reactor (03) was analysed by using the standard tar analysis method where tars are deposited through a series of traps (Jordan and Akay, 2012) using glass beads, silica gel and glass wool. Weight increase in these traps was recorded as condensable tar. The compositions of the model tar/syngas mixture before and after the plasma reactor were monitored at about ½ hour intervals by means of an off-line Agilent 6890N Gas Chromatograph (05). In order to carry out the small scale experiments, there were three set of reactor configuration mode followed:

1. Primary model tar removal by a packed bed of different types of porous PHPs particles, see Figure 3.16.
2. Primary model tar removal by catalytic plasma at different power intensities, see Figure 3.17, and
3. Primary model tar removal by catalytic plasma at different power intensities with a packed bed of s-PHP particles, see Figure 3.18.

3.5.2.2.1. Primary model tar removal by a packed bed of different types of porous PHPs

In this case, the plasma reactor (03) was connected to the model syngas generator (02) as presented in Figure (3.16) below; both the reactor inlet and outlet contained glass wool (04) to prevent glass beads and/or different types of PHPs particles escape. In the diagram, the space between the quartz tubes was packed with 20 g crushed (approximately 2-3 mm in size) of s-PHP or PHP-B30 or PHP-S30 or PHP-S30B10 particles (05). The PHPs particles were trapped in this region by using glass balls (06) at the remaining region of the reactor at the inlet and outlet to facilitate a better heat transfer to the model tar/syngas mixture. Pure carbon dioxide (model syngas) from a pressurised gas bottle (01) at a controlled flow rate of 1 litre/min was bubbled through fresh crude oil vessel (02) at $80 \pm 1^{\circ}C$. The experiments were carried out for 3 hours. Resulting model tar/syngas mixture was then fed into the reactor (03). The concentration of the model tar/syngas mixture before and after entering into the reactor (03) was analysed by using the standard tar analysis method where tars are deposited through a series of traps (Jordan and Akay, 2012) using glass beads, silica gel and glass wool. Weight increase in these traps was recorded as

condensable tar. Temperature of the reactor inlet model tar/syngas mixture was kept at $43 \pm 3\ ^{0}$C. The PHPs particles treated model tar/syngas mixture was subjected to the tar evaluation procedure from which amount of tar present in the model syngas was determined. Small amount of tar/syngas mixture samples were withdrawn at the inlet (SP-1) and outlet (SP-2) of the reactor (03) and analysed by means of an off-line Agilent 6890N Gas Chromatograph.
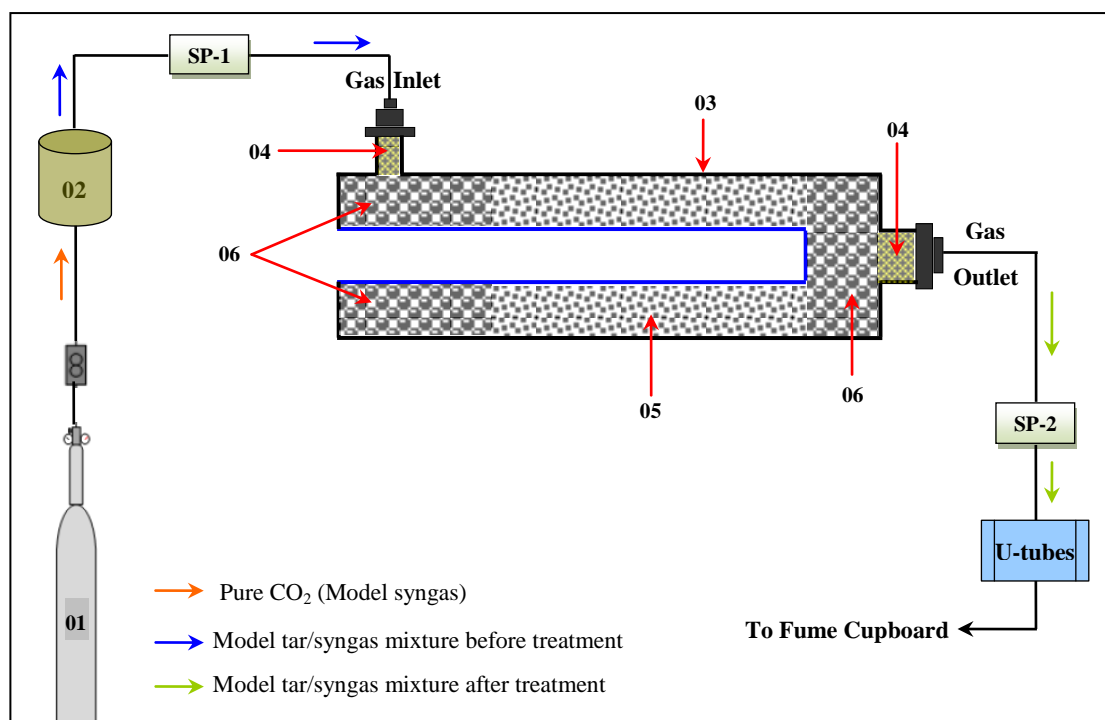
Figure (3.16): Process flow diagram of primary model tar removal by a packed bed of different PolyHIPE Polymers (PHPs) particles

3.5.2.2.2. Primary model tar removal by catalytic plasma at different power intensities

The experimental set-up used for the primary model tar reduction or/and removal by catalytic plasma at different power intensities (40 and 50 W) is shown in Figure (3.17). The cross-sectional view of the plasma reactor is shown in the inset of Figure (3.17). In this case, the plasma reactor (03) was connected to the model syngas generator (02) both the reactor inlet and outlet contained glass wool (04) to prevent glass beads particles escape. In the diagram, the ground electrode (05) in the form of wire mesh is wrapped round the outer cylinder while the high voltage electrode (06) is in the form of a stainless steel bar occupying the space in the inner cylinder. Both electrodes are connected to a high voltage source (07). The length of the ground

electrode (05) was 130 mm and it started from 20 mm from the model tar/syngas mixture inlet region. Therefore the plasma was generated in the first 130 mm of the reactor (03). The plasma region was packed with 3 mm glass balls (08) as plasma catalysis promoter. The next 130 mm region of the reactor (03) (where no plasma was generated) was packed with additional glass balls (08) at the remaining region of the reactor at the inlet and outlet.
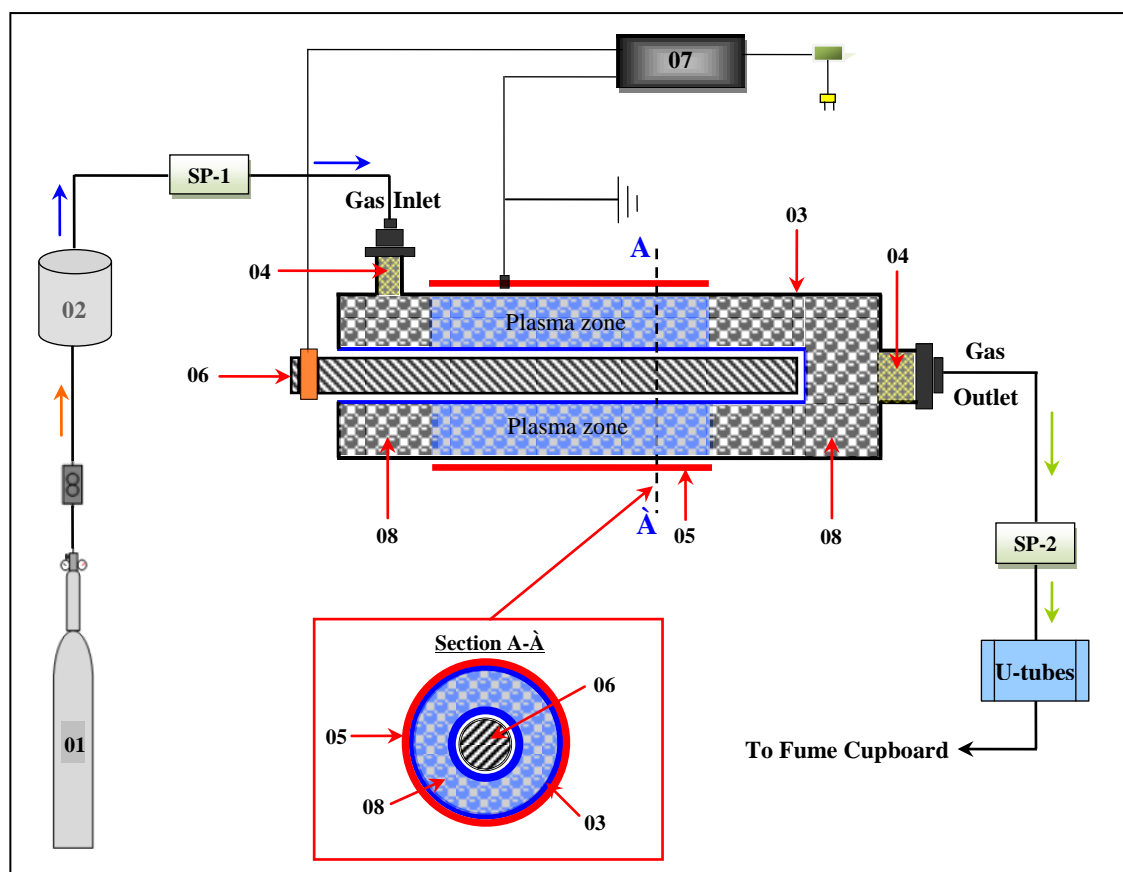
Figure (3.17): Process flow diagram of primary model tar removal by catalytic plasma at different power intensities

Pure carbon dioxide (model syngas) from a pressurised gas bottle (01) at a controlled flow rate of 1 litre/min was bubbled through fresh crude oil vessel (02) at $80 \pm 1^\circ$C. The experiments were carried out for 3 hours. Resulting model tar/syngas mixture was then fed into the reactor (03). The concentration of the model tar/syngas mixture before and after entering into the reactor (03) was analysed by using the standard tar analysis method where tars were deposited through a series of traps (Jordan and Akay, 2012) using glass beads, silica gel and glass wool. Weight increase in these traps was recorded as condensable tar. Temperature of the reactor inlet model

tar/syngas mixture was kept at 43 ± 3 °C. Plasma power intensities were 40 and 50W. Plasma treated syngas was subjected to the tar evaluation procedure from which amount of tar present in the model syngas was determined. Small amount of tar/syngas mixture samples were withdrawn at the inlet (SP-1) and outlet (SP-2) of the reactor (03) and analysed by means of an off-line Agilent 6890N Gas Chromatograph.

3.5.2.2.3. Primary model tar removal by catalytic plasma at different power intensities with a packed bed of porous s-PHP particles

Schematic of the set-up used in tar reduction through catalytic plasma at different power intensities with a packed bed of porous s-PHP particles technique is presented in Figure (3.18) below. The cross-sectional view of the plasma reactor is shown in the inset of Figure (3.18). In this case, the plasma reactor (03) was connected to the model syngas generator (02) both the reactor inlet and outlet contained glass wool (04) to prevent glass beads and/or PHPs particles escape. In the diagram, the ground electrode (05) in the form of wire mesh is wrapped round the outer cylinder while the high voltage electrode (06) is in the form of a stainless steel bar occupying the space in the inner cylinder. Both electrodes are connected to a high voltage source (07). The length of the ground electrode (5) was 130 mm and it started from 20 mm from the model syngas inlet region. Therefore the plasma was generated in the first 130 mm of the reactor (03). The plasma region was packed with 3 mm glass balls (08) as plasma catalysis promoter. The next 130 mm region of the reactor (03) (where no plasma was generated) was packed with 20 g crushed (approximately 2-3 mm in size) PHPs particles (09). These particles were trapped in this region by using additional glass balls (08) at the remaining region of the reactor at the inlet and outlet. Pure carbon dioxide (model syngas) from a pressurised gas bottle (01) at a controlled flow rate of 1 litre/min was bubbled through fresh crude oil vessel (02) at 80 ± 1 °C. The experiments were carried out for 3 hours. Resulting model tar/syngas mixture was then fed into the reactor (03). The concentration of the model tar/syngas mixture before and after entering into the reactor (03) was analysed by using the standard tar analysis method where tars were deposited through a series of traps (Jordan and Akay, 2012) using glass beads, silica gel and glass wool. Weight increase in these traps was recorded as condensable tar. Temperature of the reactor inlet model tar/syngas mixture was kept at 43 ± 3 °C and plasma power intensities was 40 and 50W. Plasma

treated syngas was subjected to the tar evaluation procedure from which amount of tar present in the model syngas was determined. Small amount of tar/syngas mixture samples were withdrawn at the inlet (SP-1) and outlet (SP-2) of the reactor (03) and analysed by means of an off-line Agilent 6890N Gas Chromatograph. In the next section the performance of the pilot scale intensified syngas cleaning system as a different application as a secondary measure to remove model tars from model syngas is discussed.

Figure (3.18): Process flow diagram of primary model tar removal by catalytic plasma at different power intensities with a packed bed of porous sulphonated PolyHIPE Polymer (s-PHP)

3.5.3. Pilot Scale Intensified Syngas Cleaning System Experiments

Having completed experiments on small scale (plasma reactor) intensified syngas cleaning system; other experiments using a pilot (electric field enhanced tar removal equipment) scale intensified syngas cleaning system were also performed to investigate what effect the electric field enhanced tar removal equipment may have on

tar reduction or/and removal efficiency. Initially, the experimental set-up used for pilot scale intensified syngas cleaning system is illustrated schematically in Figure (3.19).

Figure (3.19): Process flow diagram of the pilot (electric field enhanced tar removal equipment) scale intensified syngas cleaning system.

[**Key:** FI = Flow Indicator; V = Valve; SP = Sample Point; TI = Temperature Indicator]

The used system essentially consisted of pressurised pure carbon dioxide (CO_2) cylinder (101), crude oil stainless steel vessel (102); the internal dimensions of this vessel are as follow: height and internal diameter are 335 mm and 204 mm, respectively. Schematic and picture of this unit (crude oil vessel) is given in Appendix G. The vessel (102) is insulated with ceramic fibre insulation to minimise heat loss during heating up. For the purpose of heating the oil (model tar), the vessel is equipped with an electrical coil controlled using a digital temperature controller and K-type thermocouple TC-1 and TC-2 to measure and monitor the crude oil and model tar/syngas mixture temperatures respectively. During the experiments, it was always necessary to ensure that crude oil level is always above the electrical coil to avoid the

heating system damage. In this work, cleaning of the model syngas was achieved through the electric field enhanced tar removal equipment (103) (designed and constructed in Morecroft Engineers Ltd, UK) which is further illustrated in next section 3.5.2.1., high voltage source (INC series 30 kV power intensities supplier supplied by Glassman), a 20 litre PTFE rectangular water tank (104) with a lid, water pump (Lowara, CE), two volume flow meters supplied by Platon, flow bits, UK used in water scrubbing experiments. Set of U-tubes (105) placed in sequence in an ice water container, for trapping tar and moisture at ambient temperature. The first U-tube contained glass beads, to provide a large surface area for gas condensation, which are retained in the tube by glass wool, tar and particulate deposition, occurred on these beads. The second U-tube contained silica gel to absorb the condensate in the produced gas and the third U-tube enclosed glass wool for the final filtration of the gas. The outlet from these U-tubes was fume cupboarded. The gas (model syngas) flow was controlled using a volume flow meter (MFC-1) supplied by Platon, flow bits, UK, and the inlet and outlet model tar/syngas mixture composition were monitored using an off-line Agilent 6890N Gas Chromatography (106). All metal elements in the system were grounded. Pictorial representation of the assembled experimental rig of pilot scale intensified syngas cleaning system is given in Appendix I.

In the pilot scale intensified syngas cleaning system, experiments were carried out in different profiled high voltage electrode arrangement was either completely (totally) insulated electrode (CIE) configuration when it was used with water spray, or it was partially isolated electrode (PIE) configuration when no conductive material was present in the gas stream or in the fixed bed. Using the CIE mode, the equipment was tested under the following processing conditions: creating a planar water spray either at the bottom or top or indeed both sprays could be used, combined water scrubbing and electric field at different intensities, and an electric field at different intensities in the absence and presence of a packed bed of s-PHP particles. While with the PIE manner the equipment was performed under an electric field at different intensities in the absence and presence of a packed bed of s-PHP particles.

3.5.3.1. Reactor Design

The diagrammatic representation of this equipment (reactor) is shown in Figure (3.20). It consists of 3 concentric regions. The central region contains the high voltage electrode in the form of truncated double cones (201a) and (201b) resting on an electrically isolated platform (202). There are two water sprays both producing a water plane though which the gases pass through. The bottom spray nozzle (203) is located just above the gas entrance (204) and the top spray nozzle (205) is located just below the gas outlet (206). Water is supplied to the bottom and top spray nozzles at locations (207) and (208) respectively. Gas inlet and outlet are concentrically located with the water supply to the bottom and top spray nozzles respectively. The exit ports (209) and (210) are used as access to provide facilities for the equipment. The exit port (209) is used for the insulated high voltage cable (not shown on the diagram). This central region is separated from the outer region by a cylindrical porous nickel ground electrode (211) with ground electrode connection at (212) forming the 2nd concentric region. The porous catalytic electrode is caged between two wire mesh screens (213) and (214) respectively on either side of the ground electrode. This assembly is mechanically secured by 3 tie-rods (215) located at $120°$ to each others. The function of this electrode is to capture and retain the tars when they are repelled radically outwards under the combined influence of electric and flow fields. The shape of the electrode is to promote radial component of the gas/tar velocity field. Once captured by the 'collector electrode', tars are either degraded or they form a viscous material which is gradually drained from the outer-concentric region (216) via the outlet (217). These 3 concentric regions are enclosed using two electrically isolated bottoms (218) and top (219) plates to make the reactor gas tight.

When operating under fixed bed mode, catalyst or tar cracking/absorbing material (i.e. s-PHP particles) in the fixed bed is placed between two perforated plates placed on the tray where the central electrode (201) is secured and another perforated plate just under the top cover plate (219) of the reactor. These facilities are not shown in Figure (3.20). Pictorial representation of the detail of the equipment used for the catalytic model syngas cleaning is given in Appendix J.
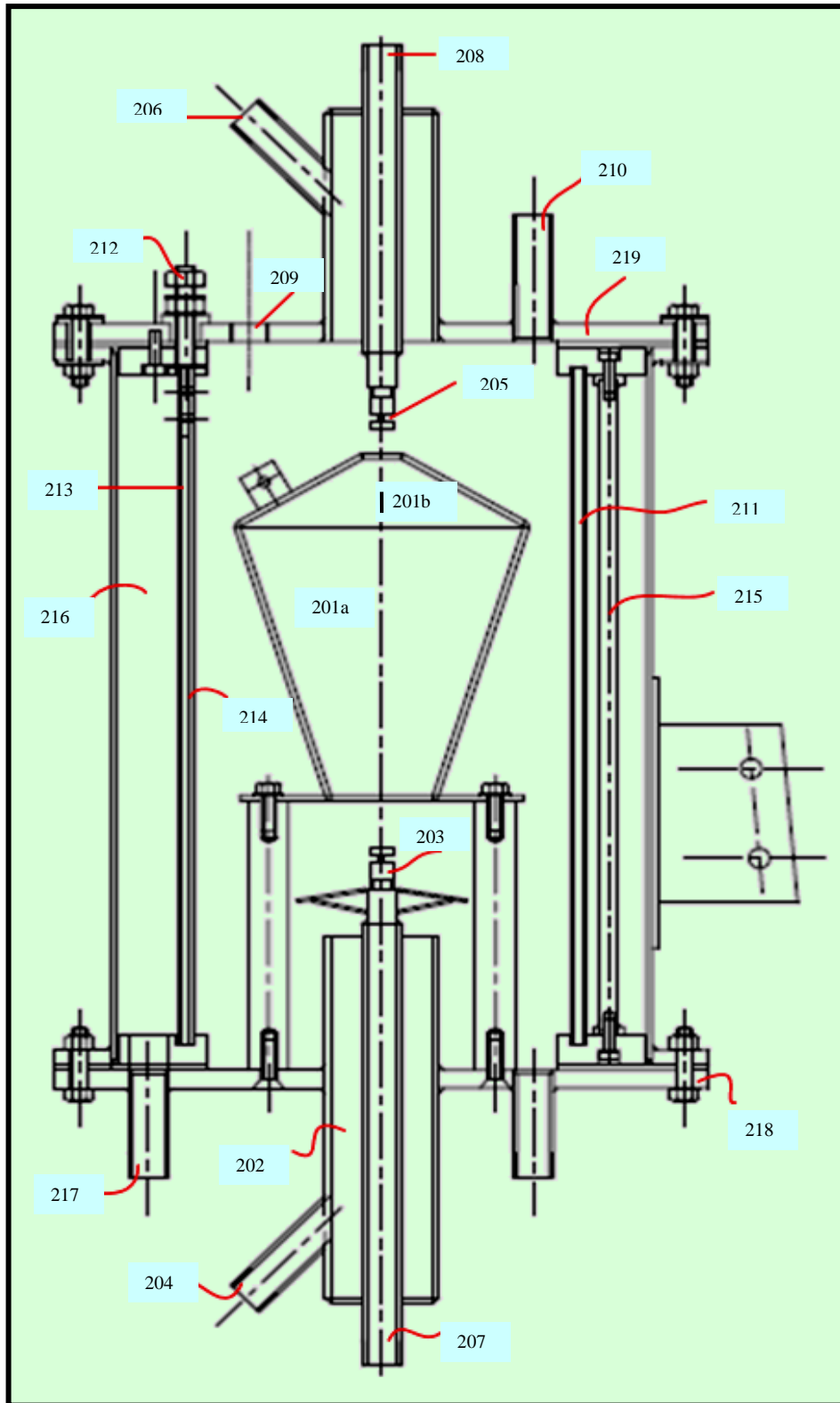
Figure (3.20): Detail of the equipment used for the catalytic model syngas cleaning

The central high voltage electrode is either totally insulated when it is used with water spray, or it is partially isolated when no conductive material is present in the gas stream or in the fixed bed. In the partial electrode isolation of the high voltage electrode, only large conical part (201a) is exposed and the remaining parts are still electrically isolated using high density polyethylene sintered on the stainless steel electrode. The porous collector electrode is again used as the ground electrode. The concentric annular gap between the electrodes is kept constant at 10 mm. Although water could be used when electric field is applied between the electrodes in which the high voltage electrode is isolated.

3.5.3.2. Experimental Procedure

Experiments were performed in the following manner; refer to Figure (3.19). Again before the actual start of each experiment, all device and pipes were leak tested. Prior to using the fresh crude oil (model tar) in the experiments, the crude in its metal container was warmed in a $30 - 40$ $^{\circ}$C water bath to attain well mixing of the contents of the container. Then, 8 litres of fresh crude oil from its metal supplier container was poured into the crude oil vessel (102) where the oil was heated. Once the temperature of the crude oil was raised to 80 ± 1 $^{\circ}$C and monitored using a thermocouple (TC-1), pure CO_2 from a pressurised gas bottle (101) at a controlled flow rate of 1 litre/min was bubbled through fresh crude oil vessel (102) at $80 \pm 1$$^{\circ}$C for 3 hours. Resulting model tar/syngas mixture was then fed into the gas cleaning equipment (electric field enhanced tar removal equipment). The concentration of the model tar before and after entering into the gas cleaning equipment (electric field enhanced tar removal equipment) was analysed by using the standard tar analysis method where tars are deposited through a series of traps (Jordan and Akay, 2012) using glass beads, silica gel and glass wool. Weight increase in these traps was recorded as condensable tar. The inlet and outlet model tar/syngas mixture composition was monitored at about ½ hour intervals by means of an off-line Agilent 6890N Gas Chromatograph (105).

In scrubbing water (tap water) experiments, water scrubbing was done by creating a planar water spray either at the bottom or top or indeed both sprays could be used. Due to the total electrical insulation of the high voltage electrode, it was possible to apply electric field at $10 - 25$ kV. In the case of top scrubbing water (tap water) experiments, valve V-12, as indicated on Figure (3.19) was completely closed

while valve V-11 was completely open. In bottom scrubbing water experiments, theses valves were vice versa. In the case of both sprays (bottom and top) scrubbing water experiments, both valves (V-11 and V-12) open. In all these experiments, the required water flow rate fed to the syngas cleaning equipment was regulated by manipulating valves V-9 and V-10. The following processing conditions were used:

Model syngas flow rate = 1 litre/min;

C_{in} = 22.0 $\pm$ 2.1 g/Nm^3; Gas inlet temperature = 43 $\pm$ 3 $^{\circ}$C;

Gas outlet temperature = 20 $\pm$ 2 $^{\circ}$C;

Scrubbing water (tap water) flow rate = 1.66 litre/min;

Scrubbing water inlet temperature = 20 $\pm$ 2 $^{\circ}$C;

Temperature of the equipment = 20 $\pm$ 2 $^{\circ}$C;

Total surface area of the insulated high voltage electrode = 810 cm^2;

Applied high voltage = 10-25 kV; and Duration of experiments = 3 hours

When operating under fixed bed mode, sulphonated PHP (s-PHP) was placed between two perforated plates placed on the tray where the central electrode was secured and another perforated plate just under the top cover plate of the reactor. Packing materials were only used in the absence of water scrubbing. The following processing conditions were used:

Model syngas flow rate = 1 litre/min;

C_{in} = 22.0 $\pm$ 2.1 g/Nm^3; Gas inlet temperature = 43 $\pm$ 3 $^{\circ}$C;

Gas outlet temperature = 20 $\pm$ 2 $^{\circ}$C;

Temperature of the equipment = 20 $\pm$ 2 $^{\circ}$C;

Total surface area of the exposed part of the partially insulated electrode = 290 cm^2;

Applied high voltage = 10-25 kV; and Duration of experiments = 3 hours

3.5.3.3. Safety Measures

Prior to the operation, it was essential to ensure that the system is assembled such that it complies with the safety procedures of power supplier designed for use up to 30 kV. In accordance to that, the following connection/ disconnection of the HV supplier procedures are given in Appendix K.

3.6. Analytical Methods

3.6.1. Ultimate Analysis

The Ultimate Analysis is used for the determination of the elemental composition (C, H, N and O by difference) of substances and it is an important parameter for the design and control of power plants fuelled by biomass. It was used to determine the C, H, N composition of biomass/biomass waste as well as ash and tar residues from the gasification process. The ultimate analysis results are important for the gasification processes. The ultimate analyses reported in this study were performed in the Department of Chemistry in Newcastle University.

3.6.2. Proximate Analysis

Proximate analysis involves the determination of the moisture, ash, volatile matter and fixed carbon content (by difference). The term fixed carbon is hypothetical and does not imply the existence of chemically bound carbon in the substance, nor does it bear any resemblance to the total carbon as determined in the ultimate analysis (Harker and Backhurst, 1981). This quantity (as percentage) was not determined experimentally but it is calculated as the sum of the percentages of moisture, volatile matter and ash subtracted from 100.

Moisture Content

The moisture content was determined from the percentage loss of mass of an accurately weighed sample of not less than 1 g which was oven dried for four h to constant weight at 105 ^{o}C. The sample was then reheated and reweighed until no further loss of mass occurred. The moisture content was calculated using equation 3.1.

$$M_{ad} = \frac{(m_2 - m_3)}{(m_2 - m_1)} \times 100 \qquad (3.1)$$

Where:

M_{ad} = Moisture content of sample as percentage by mass on a dry basis

m_1 = Mass of empty crucible and lid (g)

m_2 = Mass of crucible, lid and sample before heating (g), and

m_3 = Mass of crucible, lid and sample after heating (g)

Volatile Matter

The volatile matter in a sample of a fuel is defined as the percentage loss in mass, less than that due to moisture when the solid material is heated in its own atmosphere at 900 $^{\circ}$C for 7 min (CEN/TS 15148:2005). To determine the volatile matter in a fuel, approximately 1g of fuel was placed in a crucible of known weight, the crucible lid was replaced and the sample heated out of contact with air in a muffle furnace at 900 $^{\circ}$C for 7 min. The sample was then removed, allowed to cool at room temperature and reweighed. The volatile matter was calculated using equation 3.2.

$$V_d = [\frac{100(m_2 - m_3)}{m_2 - m_1} - M_{ad}] \times (\frac{100}{100 - M_{ad}})$$ (3.2)

Where:

V_d = Volatile matter on a dry basis

m_1 = Mass of empty crucible and lid (g)

m_2 = Mass of crucible, lid and sample before heating (g)

m_3 = Mass of crucible, lid and sample after heating (g), and

M_{ad} = Moisture content of sample as a percentage by mass

Ash Content

The ash content of a fuel is the mass of inorganic residue which remains after heating in air at 550 $^{\circ}$C in a furnace for 2 h (CEN/TS 14775:2004 (E)). The ash content of the fuel was determined from the reduction in mass of accurately weighed samples of not less than 1g. These samples were placed in previously weighed crucibles and then heated in a muffle furnace, the ash content was then determined using equation 3.3.

$$A_d = \frac{(m_3 - m_1)}{(m_2 - m_1)} \times 100 \times \frac{100}{100 - M_{ad}}$$ (3.3)

Where:

A_d = Ash content of fuel on a dry basis

m_1 = Mass of empty crucible and lid (g)

m_2 = Mass of crucible, lid and sample before heating (g)

m_3 = Mass of crucible, lid and sample after heating (g), and

M_{ad} = Moisture content of sample as a percentage by mass

As discussed earlier fixed carbon is a theoretical term and can be calculated by:

Fixed Carbon = 100 - (% Ash + % Moisture + % Volatile Matter)   (3.4)

3.6.3. Energy Content

The bomb calorimeter is the classic device used to determine the Heating Value (HV) of solid and liquid fuel samples at constant volume. Basically, this device burns a fuel sample and transfers the heat into a known mass of water. From the weight of fuel and temperature rise of the water, the heating value can be calculated. The bomb calorimeter is an isolated cylinder which contained the known amount of water and the bomb. The schematic diagram of a bomb calorimeter setup with its components can be seen in Figure (3.21).

Figure (3.21): The schematic diagram of a bomb calorimeter setup with its components.

The water was continuously stirred by a motorized stirrer to homogenize the temperature profile in the whole volume of the container. In the bomb, there is a cup which holds the fuel and it was connected to the electrical source via a cradle of wire or ignition coil, the cross section of a bomb can be seen in Figure (3.22).

Figure (3.22): Cross section of the bomb.

First, the bomb was prepared by placing the known amount of fuel in the ignition cup and connecting the fuse wire. Then, it was pressurized with oxygen and submerged in known amount of water in a stainless steel bucket. This bucket was placed down inside the bomb calorimeter and made contact with pegs on the floor of the bomb calorimeter. The calorimeter cover has a hole that allows a precision thermometer to be lowered down into the water to measure its temperature and also the ignition coils were connected to the electrical source through the hole in the cover. When the cover was closed, the motorized stirrer was switched on to homogenize the temperature of the water. Before igniting the system, the temperature of the system should be monitored for a certain amount of time to make sure that it is in steady state. When the temperature of the system is in steady state, the fuel may be ignited to conduct the analysis.

Ideally, in a calorimeter, a carefully weighed solid fuel sample would be completely burned. All of the heat released would be conducted into a known mass of water. From the resulting rise in water temperature due to the amount of energy released, the heating value, HV, can be determined by the following equation:

$$HV = \frac{\Delta U_{Water}}{m_{Fuel}} = \frac{(mC_v\Delta T)_{Water}}{m_{Fuel}} \tag{3.5}$$

Where

ΔU = Change in internal energy

m = Mass (g)

C_v = Specific heat capacity, and

100

ΔT = Change in temperate

In practice; however, there are complications like the amount of wire used in the analysis, the amount of work added by the stirrer and heat loss to the environment. The complications added by the presence of wire in the bomb can be accounted by:

$$HV = \frac{(mC_v\Delta T)_{Water} - (\Delta mHV)_{Wire}}{m_{Fuel}}$$ (3.6)

Where

Δm = Change in mass (g)

The calorimeter is surrounded by water flowing through a jacket keeping the whole setup in constant temperature close to that of water in the container. But still there can be little heat loss from the test water to the jacket water and to the surrounding. The amount of work added by the stirrer is assumed to be negligible just like the amount of heat loss to the environment. Most of the other parts that get heated are steel and; therefore, good conductors; they should stay at a temperature close to that of the water. The bomb calorimeter used in this study was Gallenkamp with Gallenkamp precision thermometer, which displays three digits after the decimal point in high resolution mode. The actual set up for bomb calorimeter analysis can be seen in Figure (3.23).

Figure (3.23): Actual bomb calorimeter set up used to perform the analysis

3.6.4. Gas Chromatography (GC)

The discovery of gas chromatography (GC) began since mid-19th century (Fifield and Kealey, 1983). GC is the principal analytical method used for hydrocarbon gas analysis. The basic principle of GC is simple. By passing a vaporized sample, contained in a gas stream, through a heated column filled with a stationary phase (packed into a tubular column). The sample to be analyzed is placed at the head of the column and then passed down the column under the influence of the moving phase or the carrier gas. The carrier gas must be chemically inert. Commonly used gases include nitrogen, helium, argon or air. The carrier gas system may also contain a molecular sieve to remove water and other impurities. The components of the sample can be separated at different rates due to differences in boiling point, solubility or adsorption (depending on the stationary phase type) (Fifield and Kealey, 1983). At the end of the column, there is a detector to analyze the presence of the analyte as it elutes from the column. The signal from this detector is amplified and the resulting signal is displayed as a chromatogram. The schematic diagram of a typical GC system can be seen in Figure (3.24). Primary components of a GC include a sample injection port, columns and detectors. These are briefly discussed below.
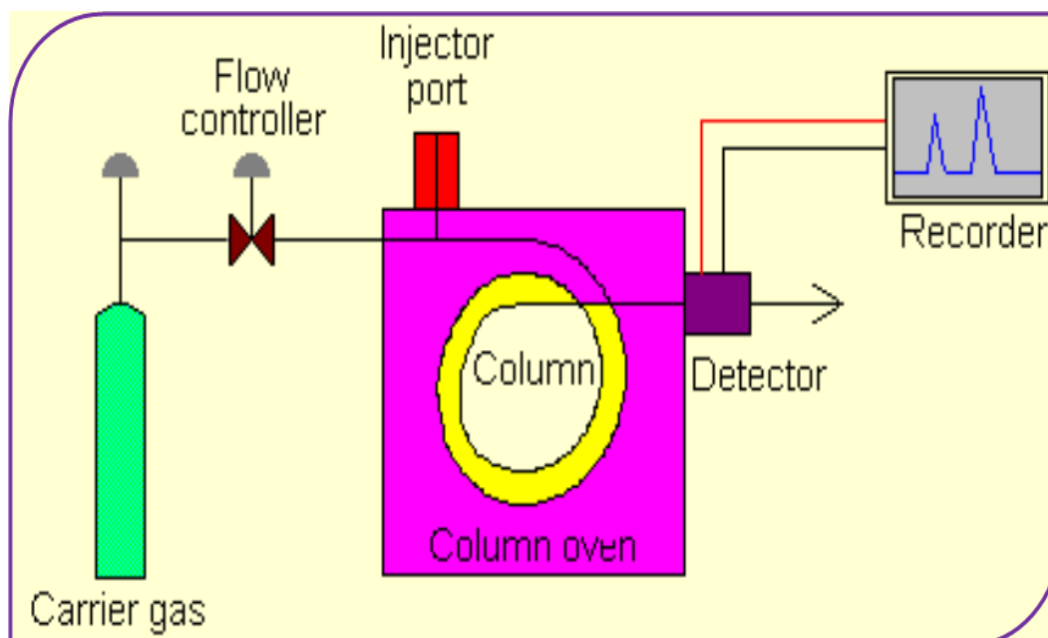
Figure (3.24): Schematic diagram of a typical gas chromatography system.

Sample Injection Port

For optimum column efficiency, the sample should not be too large, and should be introduced onto the column as a "plug" of vapour. Slow injection of large samples causes band broadening and loss of resolution. The most common injection method is where a microsyringe is used to inject a sample through a rubber septum into a flash vaporizer port at the head of the column. The temperature of the sample port is usually about $50^{\circ}C$ higher than the boiling point of the least volatile component of the sample (Gallacher, 1993).

Columns

The column is the essential element in any gas chromatographic setup. There are two general types of columns, packed and capillary (also known as open tubular). Packed columns contain a finely divided, inert and solid support material (commonly based on diatomaceous earth) coated with liquid stationary phase. Most packed columns are 1.5-10 m in length and have an internal diameter of 2-4 mm. Schematic cross sections diagrams of packed and capillary column are shown in Figure (3.25).
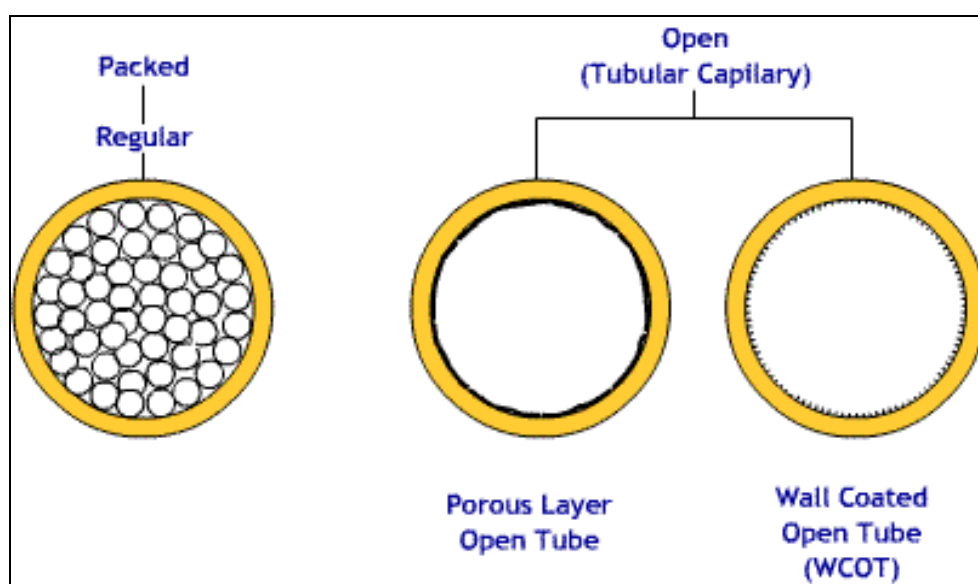
Figure (3.25): Packed and capillary column cross sections.

Capillary columns have an internal diameter of a few tenths of a millimetre. They can be one of two types; wall-coated open tubular (WCOT) or support-coated open tubular (SCOT). Wall-coated columns consist of a capillary tube whose walls are coated with a liquid stationary phase. In support-coated columns, the inner wall of the capillary is lined with a thin layer of support material such as diatomaceous earth,

onto which the stationary phase has been adsorbed. For precise work, column temperature must be controlled to within tenths of a degree. The optimum column temperature is dependant upon the sample to be analyzed. Lower temperatures give good resolution, but increase elution times. If a sample has a wide boiling range, then temperature programming can be useful. The column temperature may be increased (either continuously or in steps) as separation proceeds.

Detectors

The purpose of a detector in a GC is to monitor the composition of the carrier gas as it emerges from the end of the column and to respond in a measurable manner to the presence of sample components (Cowper, 1995). A variety of detectors for GC are available. In general, each detector takes advantage of a unique characteristic of a molecule and uses that characteristic to generate a measurable electrical signal. The requirements of a GC detector depend on the separation application. For example, one analysis might require a detector that is selective for chlorine-containing molecules; another analysis might require a detector that is non-destructive so that the analyte can be recovered for further spectroscopic analysis. There are many types of detectors namely, thermal conductivity detector (TCD), flame ionization detector (FID), electron capture detector (ECD), flame photometric detector (FPD), photo ionization detector (PID), nitrogen-phosphorous detector (NPD). The most common ones are the thermal conductivity detector (TCD) and flame ionization detector (FID). The TCD and FID are the two most commonly used detectors for hydrocarbon gases.

Thermal Conductivity Detector (TCD)

A thermal conductivity detector (TCD) consists of tiny coiled wires arranged in a wheat stone bridge configuration. Electric current flows through the filaments making them glow hot, while carrier gas exiting the column flows past the other two filaments. The gas flow carries away excess heat, and the filaments equilibrate. When a sample compound exits the column, the thermal conductivity of the gas flowing around the filaments is changed. Therefore, the filaments get hotter and the balance of the wheat stone bridge is altered. The TCD is used to detect gaseous compounds, such as nitrogen, oxygen and other non-hydrocarbon compounds (for example, landfill gases). The TCD is not as sensitive as other detectors, but it is non-specific and non-destructive (Cowper, 1995).

Flame Ionization Detector (FID)

A flame ionization detector (FID) consists of a stainless steel jet constructed so that carrier gas exiting the column flows through the jet mixes with hydrogen and burns at the tip of the jet Figure (3.26).
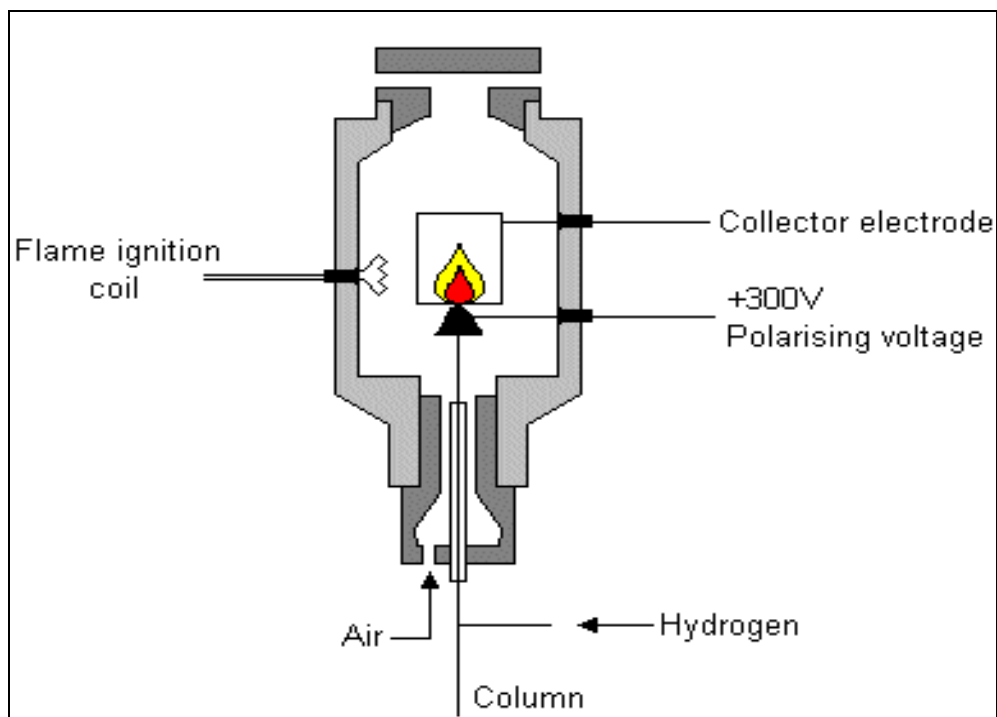
Figure (3.26): Schematic of a Flame Ionization Detector (FID) (Basiaga, 2006).

Organic compounds burning in the flame produce ions and electrons which can conduct electricity through the flame. A large electrical potential is applied at the burner tip, and a collector electrode is located above the flame. The current resulting from the pyrolysis of any organic compounds is measured. FIDs are mass sensitive rather than concentration sensitive; this gives them the advantage that changes in mobile phase flow rate do not affect the detector's response. The FID is a useful general detector for the analysis of organic compounds; it has high sensitivity (low part per billion to high part per trillion ranges), a large linear response range, low noise and it is also robust and easy to use. The FID is a destructive detector that can be used in series only after non-destructive detectors.

Gas Chromatography Analysis

In this work, the gas chromatography used in the gasification experiments work was an Agilent 6890 with two columns; Hayesep Q (1st column) and Molecular Sieve 5a (2nd column), both supplied by Supelco, two valves; one gas sampling and one switching, and a TCD detector. Two gas cylinders were used, Helium being the carrier gas and Nitrogen to operate the valves. The actual setup can be seen in Figure (3.27).

Figure (3.27): Actual gas chromatography setup.

The GC was equipped with a six port gas sampling valve, a six port column isolation valve with an adjustable restrictor and a TCD Figure (3.10). The GC sampling and analysis parameters were controlled by ChemStation B.03.01. Before each gasification run, the GC was calibrated using a standard gas mix (15 mol% H_2, 10 mol% CO_2, 3mol% C_2H_4, 3 mol% C_2H_6, 2 mol% O_2, 49 mol% N_2, 3 mol% CH_4 and 15 mol% CO).

The gas sampling valve system was connected to two columns, an 8 ft x 1/8 in 80/100 mesh Haysep Q and 6 ft x 1/8 in 60/100 mesh Molecular sieve 5A which were used to determine the composition of the syngas. In this column configuration, syngas from the sampling line was trapped in the gas sampling valve and injected into the Haysep Q column. Since O_2, CH_4 and CO was not retained by this column, they immediately flowed with the carrier gas into the Molecular sieve 5A column where they were isolated by the restrictor valve. H_2, CO_2, C_2H_4 and C_2H_6 then eluted from the Haysep Q column and flowed to the detector. Using a timed sequence,

106

immediately after these gases eluted from the column, the gas switching valve then removed the isolation from the Molecular sieve 5A column and the remaining gases then eluted from this column and flowed to the detector.

Another GC used in this work for syngas cleaning experiments was a Varian 450-GC which is a robust and powerful gas chromatograph. It offers single, dual or triple channel configuration flexibility and automation for maximum productivity. It has full digital pneumatic control of all pneumatic parameters; all inlets can be operated up to 10 bar. The GC was equipped with 2 ovens, 5 columns and 2 detectors (TCD and FID). One oven houses 3 columns (hayesep T 0.5m x1/8" ultimetal, hayesep Q 0.5m x1/8" ultimetal and molsieve 13x1.5m x1/8" ultimetal) to detect permanent gases. The second larger oven houses a CP-SIL 5CB FS 25X.25 column for hydrocarbons.

The GC was calibrated using a standards obtained from UK Analytical division of Sigma Aldrich. Calibration mixes included the paraffin mix in 4 different ampoules; each containing 3 to 4 alkanes at different concentrations dissolved in n-octane. The purity of the alkanes ranged from 99.5 to 99.9%. The mix included all straight chain alkanes from C_5 to C_8. From C_{10} to C_{18} the mix included only alkanes with even carbon numbers. The Olefin mix was obtained in 1 ampoule containing all straight chain alkenes from C_5 to C_8 and all the even carbon numbers from C_{10} to C_{20}. The concentration of alkenes was 2% w/w dissolved in 82% w/w octane with purity range between 99.5 and 99.9%.

3.6.5. Environmental Scanning Electron Microscopy-Energy Dispersive X-ray (ESEM-EDX)

The first scanning electron microscopes (SEM) were constructed back in 1930's, but these attempts seemed of a little practical value. The resolution was little better than an optical microscope; however, recording times were long. It was in 1960's when commercial instruments were introduced to the market. After four decades, it has become one of the most widely used instruments in many research laboratories. A picture of a SEM can be seen in Figure (3.28).

Figure (3.28): Picture of a Scanning Electron Microscopy (SEM).

Today, SEM's are utilized in diverse fields to examine solid specimens through a high visual imaging such as medical science, biology, materials development, metallic materials, ceramics and semiconductors. Figure (3.29) shows a schematic diagram of an interaction between electrons and specimen in a SEM setup. The electron column is on the left, in the centre and on the right are display circuits and the scanning mechanism. The electron column consists of an electron gun, de-magnifying lenses, beam-defining apertures and scanning coil. A detector is sensitive to the chosen output signal from the specimen. It is connected through a video amplifier to the grid of cathode-ray tube that is scanned in synchronism with the beam on the specimen. The strength of the signal from a corresponding point on the specimen influences the brightness at any point in the screen. From this point, an image of the specimen surface is built up on the cathode-ray-tube screen point by point (Wells, 1974).
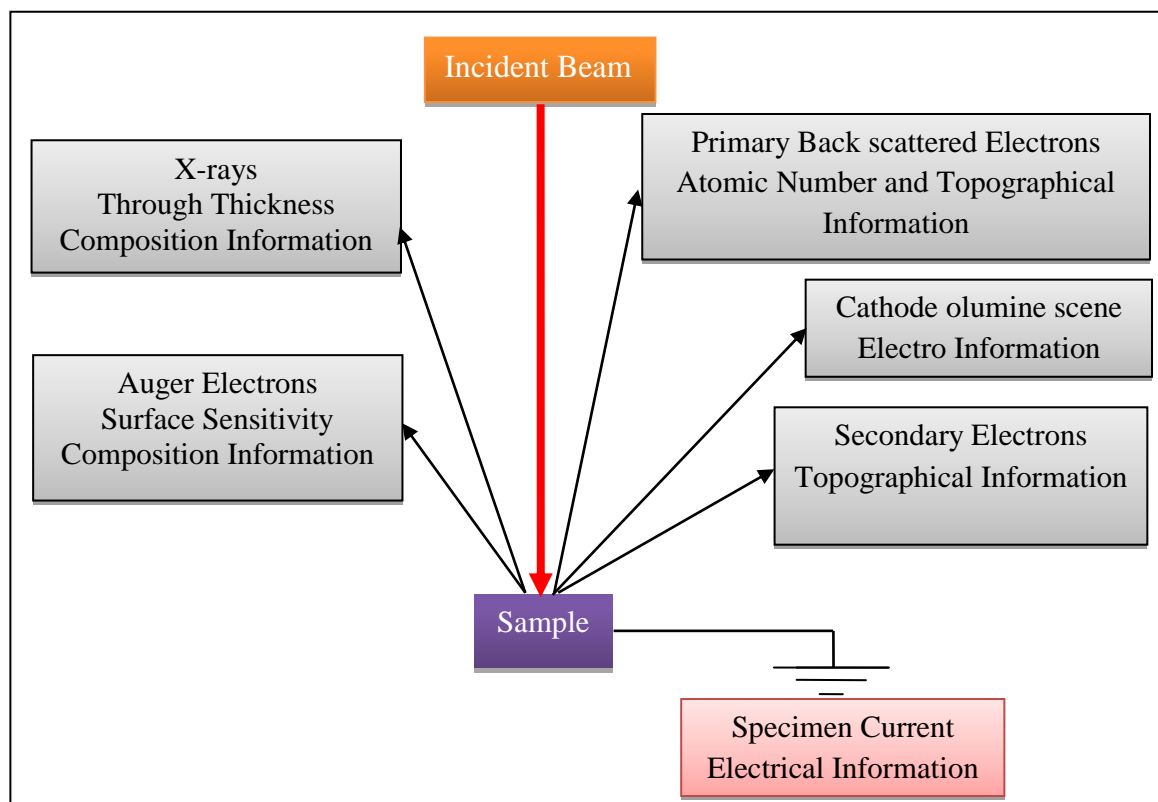
Figure (3.29): Interaction between electrons and specimen in a Scanning Electron Microscopy (SEM) setup.

As can be seen in Figure (3.29), an interaction between electrons and the specimen in a SEM setup is demonstrated. Generally, in surface SEM, the image is formed by collection of a secondary electron. The secondary electron image is very similar in appearance to an optical light microscope but with no colour with improved resolution and depth of focus. Characteristic x-rays are collected in the micro-analyzer. This can be related to the specimen composition. The magnification of a SEM has a wide range, typically from 15 to 100,000 or higher. To identify an area and obtain electron patterns from single crystals, low magnification micrographs are useful. It also can be taken with the optical or transmission electron microscope (TEM) (Wells, 1974).

The model of SEM used to analyze the surface morphology, elemental composition and distribution of samples of PHP and PHP with model tar in this study was the Environmental Scanning Electron Microscopy (ESEM) Hitachi XL30 as shown in Figure (3.30).

Figure (3.30): Scanning Electron Microscopy-Energy Dispersive X-ray (SEM-EDX) Analysis (Electron Microscopy Services at the Advanced Chemical and Materials Analysis (ACMA) Centre in Herschel building, Newcastle University).

Unlike conventional SEM, ESEM is based on the use of a multiple aperture graduated vacuum system which facilitates the imaging of samples in their natural state. ESEM was selected as these samples were non-conductive and readily susceptible to damage. This technique; therefore, permits examination of samples in their natural state without the use of a conductive coating. In our work, each sample was split into two pieces to expose the fractured surfaces. One of the pieces was then mounted 'fractured surface up' on carbon adhesive discs positioned on specimen stubs.

In addition to observation of surface morphology, the XL30 ESEM was equipped with an EDAX SiLi energy dispersive x-ray detector (EDX) which was used to investigate the composition and distribution of elements in the samples being studied. In this analytical technique, the ESEM's primary electron beam is accelerated with enough current to excite electrons from the inner orbitals of atoms in the sample. The vacancies created by these electrons are filled by high energy electrons from outer orbitals; the energy emitted during this process can result in the production of X-rays. The energy of any X-ray produced is characteristic of the atomic structure of a given element; the energy and intensity of the X-rays are measured by the EDX. It is

from this information that an EDX spectrum is generated and the composition and distribution of elements are determined.

3.6.6. Surface Area Analysis (SAA)

Surface area is one of the main physical features of a PHP. Based on the value of its surface area, more information can be drawn about a particular PHP material such as physical structure and water/solvent (depending on the polarity of the polymer) uptake capacity. Although it is not always the case, a PHP material with high surface area usually has high water/solvent uptake capacity to match. Since the PHP efficiency to absorb tar is important in the syngas cleaning experiments, surface area of the PHP materials utilized in the experiments needs to be evaluated. The measurement of surface area may be performed in several different ways but gas sorption by far is the most widely used and accurate method for total surface area measurements. Furthermore, this method can also be applied to measure pore size distributions within the approximate range of 0.4 to 200 nm. This method provides very high resolution data and has a vast applicability. In this study, the instrument used to measure the surface area of the PHP material was Coulter SA 3100 analyzer Figure (3.31), which is manufactured by the Beckman-Coulter company.

Figure (3.31): Surface area analyzer, SA 3100.

This instrument uses gas sorption technique to obtain the surface area and pore size distributions. This technique may be defined as the physical characterization of material structures using a process where gas molecules of known volume, at fairly

low temperatures (cryogenic conditions), are condensed and the resultant sample pressures are recorded and used for subsequent calculation. Within low temperature environment, molecular attractive forces are weak; hence, gas molecules will find it easy to attach to the solid surface. This data, when measured at a constant temperature, allows an isotherm to be constructed.

Materials such as powders and solid pieces of inorganic and organic compounds or mixtures are capable of retaining amounts of gases and vapours within their structure which may occur through either of two processes; absorption or adsorption. Absorption is a process where a material such as gas, vapour or liquid is retained within the body of a material. On the other hand, adsorption occurs when material(s) attach to the surface of another material. During the adsorption process, the adsorbate molecules (the molecules that attached themselves to the surface of the other material) are retained by either physisorption or chemisorption forces. Different adsorbates are used depending on the application including: argon, krypton or nitrogen. Differences in these two mechanisms are summarized in Table (3.5).

Table (3.5): Differences between physisoprtion and chemisorption

Physisorption	Chemisorption
Readily reversible process at adsorption temperature	Irreversible process at adsorption temperature
Bonding is a result of physical attraction	Bonding is formed chemically
Involves lower energy due to process condensation	Involves much higher energy of adsorption due to covalent bonding

The adsorption of nitrogen and other gases such as argon and krypton used in the SA 3100 analyzer may be characterized as physisorption processes. It assumes that all adsorption detected is due to the physically adsorbed gas. No calculation models are provided to account for adsorption caused by chemisorption processes. The surface area and pore size distribution of a sample are calculated from all or part of the adsorption and desorption isotherms. The adsorption isotherms are an incremental set of data which describe the amount of adsorbate gas (in volume) which condense on to a material at a given pressure and at a fixed temperature specifically at STP condition (Standard Temperature and Pressure). The volume is reported by the SA 3100 analyzer in units of cm^3/g. Desorption on the other hand, is the exact reverse

process and is a decremental set of data reported in the same unit. In order to form accurate isotherms, the saturation vapour pressure of the adsorbate gas during analysis needs to be known precisely. The saturation vapour pressure may be considered to be the boiling pressure of the liquid gas which is temperature-dependent. Typical analysis setup usually requires liquid nitrogen as the sample coolant bath. However, the bath temperature will change with atmospheric pressure and the purity of the nitrogen used. Since the liquid nitrogen is usually put in an open container throughout the duration of the analysis, the liquid tends to be contaminated by the atmospheric gases. In order to obtain accurate results, the saturation vapour pressure is measured during the whole length of sample analysis.

The adsorption process is measured volumetrically with a static fully equilibrated procedure. The adsorption and desorption isotherms can be formed from a few to more than a hundred individual data points. The isotherm volume data (Y-axis) is calculated by subtracting the free space of the sample tube (volume of the tube that is not occupied by sample) which is measured using helium gas, from the total volume of gas closed to the sample. Each data point processed is calculated by calculating the volume adsorbed and measuring the sample pressure which is then divided by the saturation vapour pressure. This is known as the relative pressure and is recorded as the X-axis. Since the absorption process is reported at STP, the Ideal Gas Law can be applied for the calculation of both free space and the volume of adsorptive dosed. Then, the volume of the adsorbed gas by the sample can be determined by the following equation:

$$P_M V_M = nRT_M \qquad\qquad (3.7)$$

Where:

P_M = Pressure of the dose manifold

V_M = Volume of the dose manifold

T_M = Temperature of the dose manifold, and

R = Gas Constant

Helium gas is used to measure the free space of the sample tube. Since free space is the volume in the sample tube, it tends to vary with the volume occupied by the sample itself. The volume of helium dosed to the sample tube, i.e. the free space is calculated after opening and closing the sample valve. The free space may be found

from the resultant pressure drop. The temperature or the volume of the intermediate space above the level of the liquid nitrogen or below the manifold volume is not accounted for. This intermediate volume varies with the sample tube, room temperature and also with the level of the liquid nitrogen; therefore, the free space value will change over the course of a long measurement as the liquid nitrogen level drops due to evaporation. However, this effect is minimized by the instrument during a long analysis.

Volume dosed Vd_n, is calculated from the equation below:

$$Vd_n = \frac{(P_{M1} - P_{M2}) \times V_M}{T_M} \times \frac{273.15}{760} + Vd_{n-1} \qquad (3.8)$$

Where:

P_{M1} = Initial manifold pressure

P_{M2} = Final manifold pressure

V_M = Volume of the dose manifold

T_M = Manifold temperature

Vd_{n-1} = Volume dosed from previous data point, and

273.15/760 = Standard temperature and pressure conversion

The helium data points are measured at incremental pressure to ensure accuracy. The helium free space correction is obtained from the linear plot of volume dosed vs. sample pressure. The slope of this line is equivalent to the volume of the sample tube per unit of sample tube pressure. After the helium measurement has been completed, the adsorption isotherm is measured. The volume of adsorptive dosed to the sample is calculated the same way as for the helium free space dose. The volume of gas adsorbed by the sample $Vads_n$, is calculated for each measured data point using the following equation:

$$Vads_n = Vd_n - (P_{Sn} \text{ x slope} + \text{intercept}) \qquad (3.9)$$

Where:

$Vads_n$ = Volume adsorbed

Vd_n = Volume dosed

P_{Sn} = Sample pressure

Slope = Free space measurement slope, and

Intercept = Free space measurement intercept

114

A complete isotherm data can now be plotted. Isotherm data is then subjected to a variety of mathematical models to obtain surface area and pore size distribution results, respectively. There are several other mathematical models that may be used to calculate the surface area from the isotherm data but BET (Brunaeur, Emmet and Teller) is the most commonly used technique since it was first introduced in 1938. However, Barret, Joyner and Halenda (BJH) are the only calculation model that is used by this instrument to determine the pores size distributions. The BET surface area which includes all internal structure is calculated from a multilayer adsorption theory which is based upon the assumption that the first layer of molecules adsorbed on the surface involves adsorbate-adsorbent energies, and subsequent layers of molecules adsorbed involve the energies of vaporization of the adsorbate-adsorbate interaction. At relative pressures from 0.05 to 0.2, the BET adsorption isotherm normally produces straight line plot (in linear form) which usually represented as the following relation:

$$\frac{P_s}{V_A(P_0 - P_S)} = \frac{1}{V_M C} + \left[\frac{C-1}{V_M C}\right] \times \frac{P_S}{P_0} \qquad (3.10)$$

Where:

V_m = Volume of monolayer

$Vads_n$ = Volume adsorbed

P_S = Sample pressure

P_0 = Saturation pressure, and

C = Constant related to the enthalpy of adsorption

The BET surface area, S_{BET} in m^2/g is then evaluated from the following expression:

$$S_{BET} = \frac{V_m \times N_A \times A_M}{M_V} \qquad (3.11)$$

Where:

N_A = Avogadro's number

A_M = Cross-sectional area occupied by each adsorbate molecule (A_M = 0.162 m^2 for nitrogen), and

M_V = Gram molecular volume (22414 ml)

In this study, the surface area analysis of the PHP samples was conducted by placing the sample in the sample tube, which comes in three different sizes namely 3 cm^3, 9 cm^3 and 12 cm^3 (depending on the amount of sample required where a minimum of weight of 1.00g per analysis is ideal in order to obtain an accurate result), after being pre-heated in the oven at 60^oC for a few hours. Then the sample (in the tube) was out-gassed for another five hours at a particular temperature (for PHP samples, out-gassed temperature of 40 to 60^oC was normally used). Nitrogen was used as an adsorbate in this analysis. This was immediately followed by the analysis which was done by connecting the out-gassed sample in the tube to the analytical port and immersing the tube in the liquid nitrogen while the BET surface area was calculated by the equipment. Depending on the nature of the sample and the type of analysis performed (BET or BET and BJH), the analysis would usually take from half an hour up to two hours. After the analysis was completed the results were displayed on the screen of the equipment.

Chapter Four

Results and Observations

Chapter Four

Results and Observations

4.1. Introduction

As explained earlier in chapter three, several batches of wood chips as a reference were gasified. Wood chips were used as a reference due to the ease in handling, relative consistency and availability. Part of this work/research was to use PIM to utilize briquetted refinery sludge-sawdust mixture to produce and clean syngas throughout gasification for power generation via an ICE. To achieve this goal, a small scale gasification system, which employs a novel fixed bed throated downdraft intensive 50 kWe air-blown auto-thermal reactor and gas clean-up trains consisting of cyclone, water scrubber and filter box, has been used. Out of the results obtained from these experiments, comparisons were made between wood chips and oil sludge-sawdust mixture in terms of their syngas composition, heating value and tar level.

The work/research has also focused on developing an intensified syngas cleaning techniques for different applications as a secondary measure to remove model tars from model syngas. Although the syngas cleaning methods developed in this thesis was generic, we have been using a model syngas with a model tar in order to rapid screen the efficiencies of these different methods. Due to the highly toxic and explosive nature of real syngas, we had to use non-toxic and non-explosive model syngas so that the intensification levels of the processes could be evaluated under laboratory conditions without having restrictions on the cost, scope and detail of the experimentation.

Results obtained from these experiments are represented and discussed in this chapter in the following sections. Each experiment was repeated twice and the average reported.

4.2. Results of Gasification Experiments

Gasification experiments were carried out in the pilot plant gasifier using wood chips and oil sludge-sawdust mixture in Newcastle University laboratories. Results of these experiments are reported in this section. The performance of this gasifier was previously evaluated in detail for different biomass feedstocks such as

hazelnut shells, sugar cane bagasse, Municipal Solid Waste (MSW) and Wood chips (Dogru, 2000; Midilli *et al.*, 2001a; Midilli *et al.*, 2001b; Olgun *et al.*, 2001; Akram, 2002; Dogru *et al.*, 2002; Jordan, 2002; Midilli *et al.*, 2002; Dogru *et al.*, 2002a; Dogru *et al.*, 2004; Midilli *et al.*, 2004). The actual setup which was used to conduct the experiments can be seen in Figure (3.11).

4.2.1. Gasification of Wood Chips

Wood chips reference trials were carried out in an intensified 50 kWe air-blown downdraft gasifier. Wood chips were used as a reference feedstock due to the ease in handling, relative consistency and availability. In addition, wood chips were well proven to be a suitable material for gasification. Results of proximate and ultimate analysis of wood chips are given in Table (4.1) and Table (4.2), respectively.

Table (4.1): Proximate analysis of wood chips

	wt %
Moisture	8.65 ± 0.7
Volatile matter	53.74 ± 4
Fixed carbon	15.43 ± 2
Ash	22.18 ± 3
Gross calorific value (GCV) MJ kg $^{-1}$	15.7 ± 0.3

Table (4.2): Ultimate analysis of wood chips

	%
Carbone	42.70 ± 0.03
Hydrogen	6.58 ± 0.3
Nitrogen	0.45 ± 0.08
Sulphur	0.37 ± 0.05
Oxygen*	49.53 ± 0.5

* By difference

4.2.1.1. Results and Observations

Gasification of wood chips in the pilot plant gasifier was carried out in a 2 h trial. The flow rate of the feed was determined as 20 kg/h the day after the trial. The average gas flow rate during the gasification was 35 Nm^3/h. Tar and particulate matter

content of the product gas was 950 ± 10 mg/m^3 after cleaning. Throughout the trial, no operational problems were observed. Within approximately 10 minutes after the start up, the producer gas burned in the flare with the help of the pilot burner. When the system reached a steady state within 30 minutes although the pilot burner was switched off the producer gas burned in the flare till the end of the trial. Ash was constantly removed from the system by the help of the screw at the bottom of the gasifier. The screw was rotated 3 rounds in every 10 minutes to continuously remove the ash from the system.

4.2.1.2. Syngas Composition

The composition of the producer gas collected during gasification of wood chips was analyzed using an online Agilent 6000N GC fitted with a TCD detector. The gas composition of the producer gas from wood chips gasification in pilot plant gasifier can be seen in Table (4.3). According to the data in Table (4.3), the Gross Caloric Value (GCV) of the gas was calculated to be 5.11 ± 0.6 MJ/Nm^3. The downdraft gasification system was found to be generally reliable and easy to operate.

Table (4.3): Gas analysis data from wood chips gasification in pilot plant gasifier.

Components	% v/v
CO	14.3 ± 2.0
N_2	53.4 ± 8.0
H_2	16.6 ± 2.5
CH_4	2.1 ± 0.3
CO_2	13.2 ± 2.0
O_2	0.4 ± 0.1

4.2.2. Gasification of Oil Sludge-Sawdust Mixture

Oil sludge gasification was carried out in an intensified 50 kWe air-blown downdraft gasifier. The oil sludge which was received from Willacy Oil Services Ltd. was already free from any valuable hydrocarbons as it was treated on site to recover oil and also to minimize the amount of waste. The oil sludge was received as non-uniform lumps, so it had to be briquetted prior to gasification. The initial and briquetted appearance of oil sludge can be seen in Figure (4.1). When the oil sludge was fed to the briquetter, it was found that briquettes can not be formed due to the

viscosity of the material. Therefore, before briquetting the oil sludge was mixed with different amounts of sawdust. Mixing sawdust and oil sludge was carried out in a 100 litre capacity cement mixer which is shown in Appendix E. As mentioned in the methodology chapter in section 3.4.2.1., a sample that contained 30 % wt sawdust and 70 % wt oil sludge was densified enough and was with a uniform briquettes shape was then used in large scale briquetting experiments. Other samples; however, were excluded. All the other analyses were conducted by using these briquettes as they were fed to the system.

Figure (4.1): Initial and briquetted appearance of 70 wt% oil sludge and 30 wt% sawdust

Results of proximate and ultimate analyses of oil sludge and sawdust mixture are given in Table (4.4) and Table (4.5), respectively.

Table (4.4): Proximate analysis of oil sludge-sawdust mixture

	wt %
Moisture	7.0 ± 0.6
Volatile matter	43.0 ± 3.3
Fixed carbon	9.0 ± 1.2
Ash	46.0 ± 9.0
Gross calorific value (GCV) MJ kg $^{-1}$	14.5 ± 0.2

Table (4.5): Ultimate analysis of oil sludge-sawdust mixture

Carbone	39.30 ± 0.02
Hydrogen	5.90 ± 0.3
Nitrogen	0.38 ± 0.08
Sulphur	0.42 ± 0.06
Oxygen*	54.0 ± 0.5

* By difference

Chemical composition of oil sludge and sawdust were analysed by energy dispersive x-ray (EDX) using an environmental scanning electron microscopy (ESEM). EDX analysis results for oil sludge can be seen in Figure (4.2) and Table (4.6) and for sawdust in Figure (4.3) and Table (4.7)
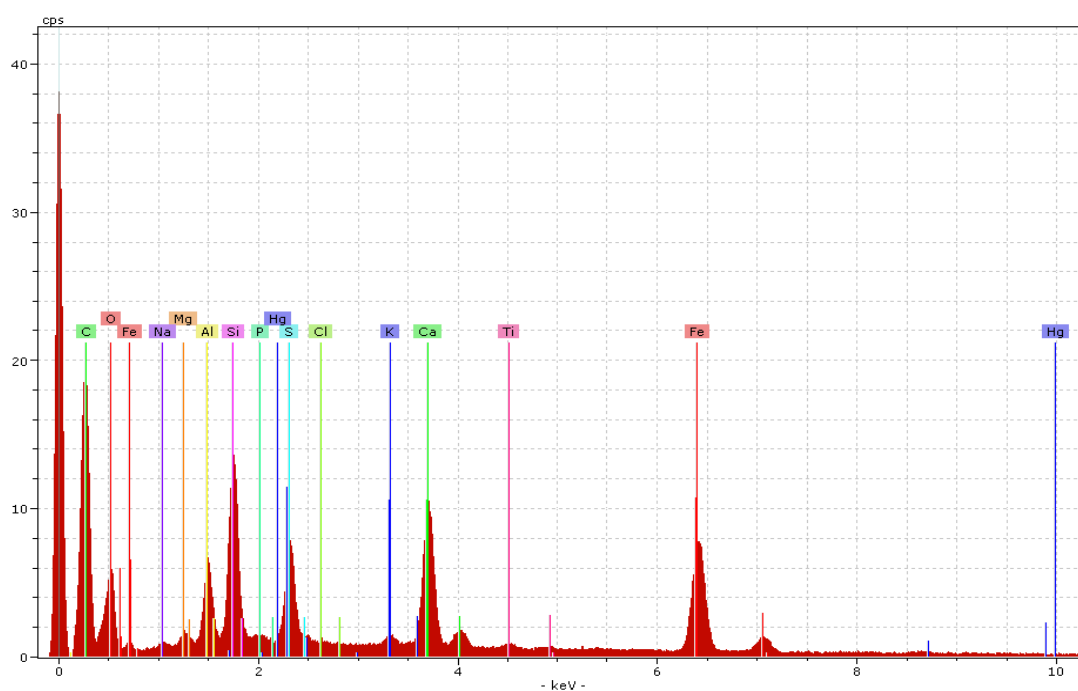
Figure (4.2) Energy Dispersive X-ray (EDX) spectra of oil sludge

Table (4.6) Energy Dispersive X-ray (EDX) analysis results of oil sludge

Element	Normalized C (wt. %)	Atomic (at. %)
C	42.91	54.81
O	40.34	38.68
Fe	6.62	1.82
Ca	4.24	1.62
Si	2.67	1.46
S	1.79	0.86
Al	0.99	0.56
K	0.30	0.12
Cl	0.04	0.02
Na	0.03	0.02
P	0.03	0.01
Mg	0.03	0.02
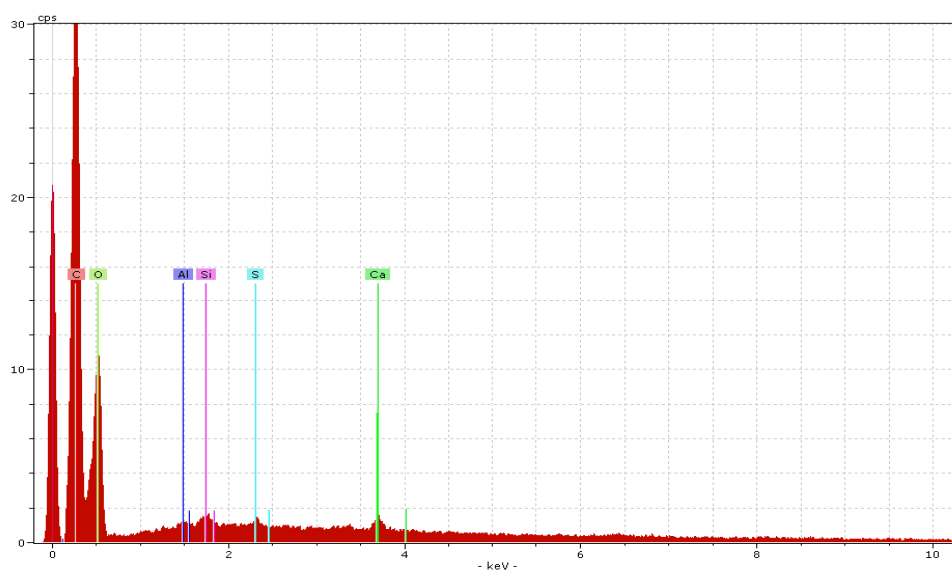
Figure (4.3) Energy Dispersive X-ray (EDX) spectra of sawdust

Table (4.7) Energy Dispersive X-ray (EDX) analysis results of sawdust

Element	Normalized C (wt. %)	Atomic concentration at. %
O	50.73	43.83
C	48.57	55.88
Ca	0.30	0.10
Si	0.21	0.11
S	0.17	0.07

Chemical composition of oil sludge ash was analysed by EDX using an ESEM. EDX analysis results for oil sludge ash can be seen in Figure (4.4) and Table (4.8).
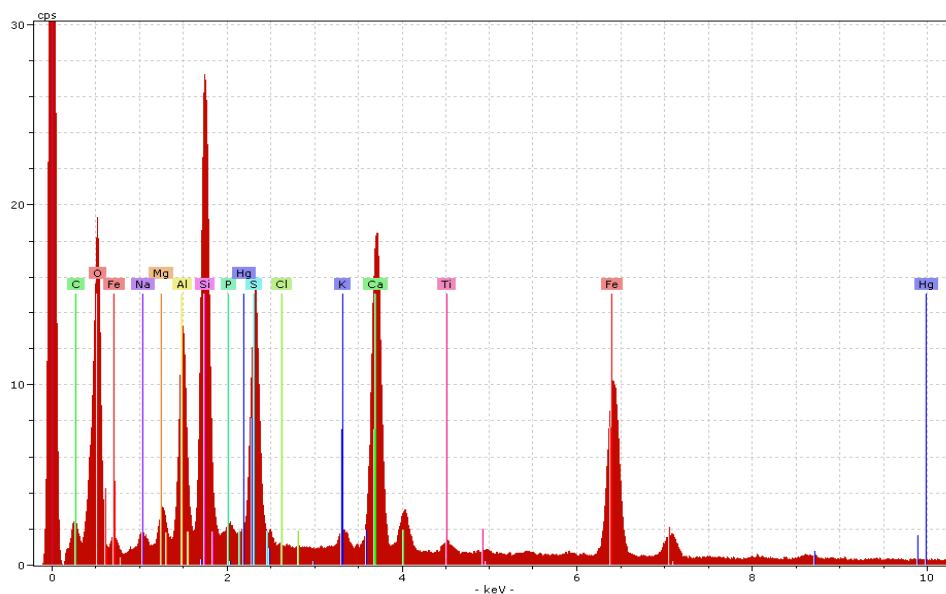
Figure (4.4) Energy Dispersive X-ray (EDX) spectra of oil sludge ash

Table (4.8) Energy Dispersive X-ray (EDX) analysis results of oil sludge ash.

Element	Normalized C (wt. %)	Atomic C (at. %)
O	48.16	67.16
Fe	12.45	4.98
Ca	12.01	6.69
Si	11.41	9.07
S	7.57	5.27
Al	5.23	4.33
Mg	1.02	0.94
P	0.81	0.58
K	0.71	0.40
Na	0.51	0.49
Cl	0.10	0.07
C	0.02	0.03

4.2.2.1. Results and Observation

Oil sludge and sawdust mixture was densified to form briquettes 52 mm long and 29 mm diameter (Figure 4.1), the briquette size used was determined by the type of briquetter which was available for use (Figure 3.5). It must be noted that briquettes of the same size made from several other types of biomass including leather residue, bone meal and sewage sludge (Calkan, 2007) were previously gasified in this gasifier and efficient conversion occurred.

Gasification of oil sludge in pilot plant gasifier was carried out in a 2 h trial. The flow rate of the feed was determined as 20 kg/h the day after the trial. The average amount of gas flow during the gasification was 37 Nm^3/h. The tar and particulate matter content of the gas was less than 90 ± 6.0 mg/m^3. Compared with 950 ± 10.0 mg/m^3 tar and particulate matter obtained for wood chips, the corresponding value of 90 ± 6.0 mg/m^3 is very low. This is due to the presence of several metal impurities in the oil sludge which act as a catalyst for tar cracking. Due to the very high ash content of the oil sludge and sawdust mixture, 46.0 ± 9.0 % dry as shown in Table (4.4), the gasifier was operated very carefully to handle the ash at the bottom of the reactor.

Ash was constantly removed from the system by the help of the screw at the bottom of the gasifier (Figures 3.7-8). The screw was rotated 3 rounds in every 5 minutes to continuously remove the ash from the system. After 45 minutes of operation, a slight drop in the amount of producer gas was observed and ash removal rate was increased from 3 rounds in every 5 minutes to 5 rounds in every 5 minutes. At the end of the two hours trial, the gas flow again dropped and ash removal intervals were shortened to 3 minutes but the volumetric flow of the gas continued to drop slowly. Nevertheless, throughout the trial apart from the start up period, the producer gas burned in the flare with the help of the pilot burner.

4.2.2.2. Syngas Composition

The gas composition of the producer gas from oil sludge-sawdust mixture gasification in pilot plant gasifier can be seen in Table (4.9). According to the data in Table (4.9) the GCV of the gas was calculated to be 3.71 ± 0.4 MJ/Nm^3.

Table (4.9): Gas analysis data from oil sludge and sawdust mixture gasification in pilot plant gasifier

Components	% v/v
CO	12.7 ± 2.0
N_2	61.4 ± 9.0
H_2	10.8 ± 1.6
CH_4	1.8 ± 0.3
CO_2	11.9 ± 1.8
O_2	1.4 ± 0.2

4.2.3. Gasification of Wood Chips vs. Oil Sludge-Sawdust Mixture

The last two sections (4.2.1. and 4.2.2.) have shown the gasification of wood chips and oil sludge-sawdust mixture. Out of the results obtained from these experiments, comparisons were made between wood chips and oil sludge- sawdust mixture in terms of their syngas composition, heating value and tar level. As it was shown in Tables (4.3) and (4.9), wood chips and oil sludge-sawdust mixture gasification generally produced the same components with relatively close compositional percentages of each component, see Figure (4.5).
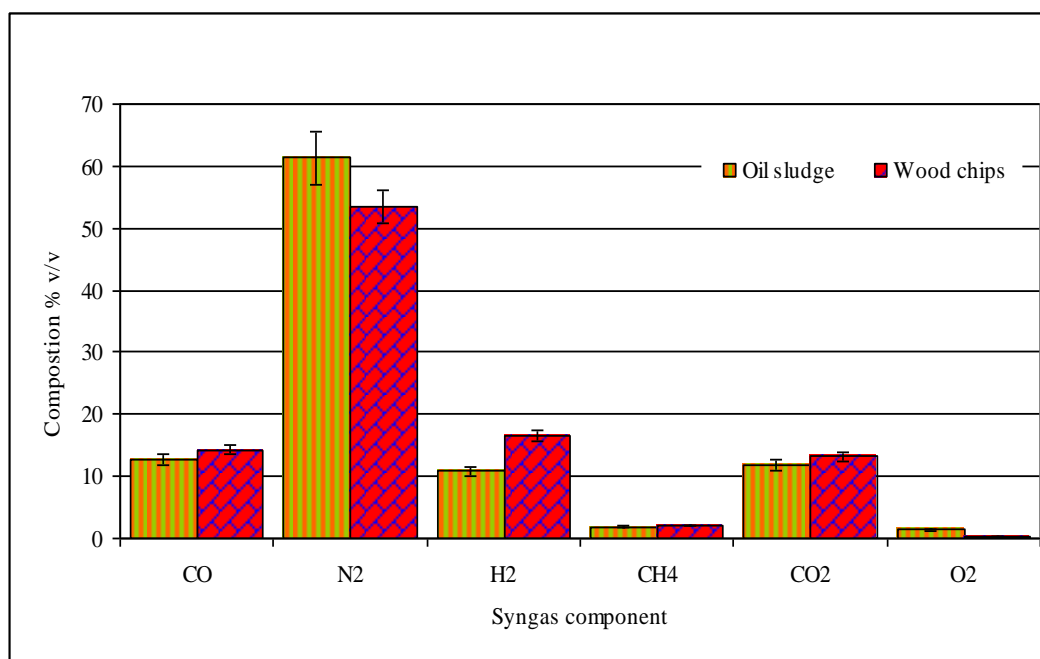
Figure (4.5): Comparison of the mean syngas composition from gasification of wood chips and oil sludge-sawdust mixture

126

According to the obtained results, gasification of wood chips and oil sludge has relatively produced comparable composition of syngas components. Hydrogen obtained via oil sludge gasification is nearly two thirds of that obtained from wood chips gasification. Furthermore, in terms of CO both feedstocks (wood chips and oil sludge-sawdust mixture) are with comparable percentages. These results then suggest that oil sludge could be gasified with low levels of tar as a result of catalytic tar cracking during gasification since refinery sludge initially contained large amounts of catalytic rare earth elements. It contained tar and particulate matter of less than 90 ± 6 mg/Nm^3 and calorific value of 3.71 ± 0.4 MJ/Nm^3 (wet gas), which is sufficient for power generation using an ICE.

4.3. Results of Intensified Syngas Cleaning System Experiments

The results of the experimental work performed on small (plasma reactor) and pilot (electric field enhanced tar removal equipment) scale intensified syngas cleaning systems are represented and discussed in the next sections. In the small scale system, experiments were performed on different types of PolyHIPE Polymers (PHPs) prepared 'in-house', by the methods explained in Chapter 3, section 3.3.1. The effect of plasma tar cleaning at different power intensities in the presence and absence of a packed bed of crushed sulphonated PolyHIPE Polymer (s-PHP) particles was also tested. Whereas, in the pilot scale system, investigation were carried out in different profiled high voltage electrode configuration was either completely (totally) insulated electrode (CIE) when it was used with water spray, or it was partially isolated electrode (PIE) when no conductive material was present in the gas stream or in the fixed bed. Using the equipment with CIE configuration, the following processing conditions were performed: creating a planar water spray either at the bottom or top or indeed both sprays could be used, combined water scrubbing and electric field at different intensities and an electric field at different intensities in the absence and presence of a packed bed of s-PHP. With PIE configuration the equipment was tested under an electric field at different intensities in the absence and presence of a packed bed of s-PHP. In all cases, a model tar and model syngas under laboratory conditions were used. As model tar, fresh crude oil and as model syngas, pure carbon dioxide was employed. Out of the results obtained from these experiments, comparisons were made in terms of tar reduction efficiency and concentration.

4.3.1. Results of Small Scale Intensified Syngas Cleaning System Experiments

The next sections present and discuss the results of the experimental work performed on small scale intensified syngas cleaning system. The effect of several variables on tar reduction or/and removal efficiency and concentration will be discussed and analysed. Each run was carried out in a period of 3 hours. GC sample were obtained approximately every 30 minutes. Each experiment was repeated twice to ensure reproducibility of results.

4.3.1.1. Performance of Different Types of Poly HIPE Polymers (PHPs) in the Model Tar Reduction Efficiency

Different types of crushed PHPs particles namely, s-PHP, PHP-B30, PHP-S30 and PHP-S30B10 as a secondary syngas treatment system were used in syngas cleaning to investigate their impact on model tar reduction efficiency and concentration during the producer of model tar/syngas mixture. The surface area of the PHPs used in this study is presented in Table (4.10). Using PHPs polymers particles could provide a much larger area/volume ratio leading to a much larger residence time for the model tar/syngas mixture and the open pore structure could also play a significant role in controlling model tar reduction efficiency. The concentration of the model tar was measured at the entrance, C_{in}, to the reactor and at the exit C_{out}, after model tar reduction or/and removal. Tar reduction efficiency (X) is calculated from equation (4.1) below.

$$X = [(C_{in} - C_{out})/C_{in}] \times 100 \qquad (4.1)$$

Where, X denotes the model tar reduction efficiency, %, whereas C_{in} and C_{out} are the inlet and outlet model tar concentrations, g/Nm^3, respectively. The experiments were carried out in a period of 3 hours with a model syngas flow rate was 1 litre/min, temperature of the inlet gas was kept at 43 ± 3 ^{0}C and a packed bed of different types of crushed PHPs particles (approximately 2-3 mm in size, total weight 20g). Each run was repeated twice to ensure reproducibility of results. In all cases, the inlet and outlet model syngas composition were monitored using gas chromatography (GC). Out of the results obtained from these experiments, comparisons were made in terms of model tar reduction or/and removal efficiency and concentration. The summary of experimental results is given in Table (4.10).

128

Table (4.10): Performance of different types of PolyHIPE Polymers (PHPs) in the model tar reduction efficiency

Cleaning System → Parameter ↓	s-PHP	PHP-B30	PHP-S30	PHP-S30B10
C_{out}** (g/Nm^3)	9.0 ± 0.5	1.4 ± 0.1	5.6 ± 0.3	3.2 ± 0.16
Efficiency X (%)	59.1 ± 3.0	93.6 ± 4.5	75.5 ± 3.5	85.5 ± 4.0
Surface area* (m^2/g)	9.4 ± 1.0	87.5 ± 7.0	55.4 ± 5.0	66.2 ± 6.0
GC – Figures (4.8-a-d)	Figure (4.8-a)	Figure (4.8-b)	Figure (4.8-c)	Figure (4.8-d)

*Determined by surface area analyzer, SA 3100   ** Model tar concentration after treatment

Therefore, model tar reduction or/and removal efficiency out of a packed bed of crushed s-PHP particles (approximately 2-3 mm in size, total weight 20g) with a model syngas flow rate was 1 litre/min in a period of 3 hours has been calculated from equation (4.1) as follows:

C_{in} = 22.0 g/Nm^3

C_{out} = 9.0 g/Nm^3

Therefore:

X = (22.0–9.0) ÷ 22.0 × 100

   = 0.591 × 100

   = 59.1%

Similarly, the rest of model tar reduction or/and removal efficiency obtained from other types of PHPs crushed particles PHP-B30 or PHP-S30 or PHP-S30B10 have been calculated and are tabulated in the Table (4.10). The results showed that under the influence of a packed bed of crushed PHPs particles (approximately 2-3 mm in size, total weight 20g) used as a secondary model syngas treatment system, the model tar was adsorbed on the active sites of the crushed PHPs particle surface and reducing the concentration. As indicated in Figure (4.6), it clear that the best result is obtained with PHP-B30 particles as a result of high surface area as well as due to the presence of silica (the model tar reduction or/and removal efficiency can be further increased by increasing the surface area of the PHPs particles).

Furthermore, PHP-S30B10 particles and PHP-B30 particles gave the highest model tar reduction efficiency (85.5 and 93.6 %, respectively). PHP-S30 particles gave moderate reduction or/and removal efficiency (75.5 %). Whereas, the s-PHP particles due to its small surface area (9.4 m^2/g) gave a lower model tar reduction or/and removal efficiency (59.1 %). However, the ranking of model tar reduction or/and removal efficiencies obtained are: PHP-B30 > PHP-S30B10 > PHP-S30 > s-PHP.

Also, the model tar reduction or/and removal efficiency results presented above are also clear confirmed by gas chromatography experiments. It can be seen that a large number of components have been reduced; this may be due to tar reaction with PHPs. Nevertheless, there is substantial reduction in the overall model tar content in model tar/syngas mixture following extraction with the use of a packed bed of crushed PHPs particles. Note that the full scales of abundance (μV) are 85000, 34000, 5500, 21000 and 12000 units in Figures (4.7, No treatment), (4.8-a, s-PHP), (4.8-b, PHP-B30), (4.8-c, PHP-S30) and (4.8-, PHP-S30B10), respectively.

Also, the model tar reduction or/and removal efficiency results presented above are also clear confirmed by gas chromatography experiments (hydrocarbon profile of model syngas shifted towards low carbon number after treatment). Figure (4.7) and Figure (4.8-a-d) are the gas chromatograms of model syngas at the entrance to the reactor (Figure 4.7) and at the exit of the reactor after treatment as tabulated in Table (4.10).

It is noted from the experimental results that, the model tar reduction efficiency with the use of a packed bed of crushed PHPs particles (s-PHP, PHP-B30, PHP-S30, and PHP-S30B10) ranging from 59%−93%. A similar reduction in tar was observed by Akay et al., (2013) working on a downdraft gasifier fuelled by fuel cane bagasse as a model biomass who reported that the s-PHP (diameter = 25 mm, thickness = 5 mm) used as a secondary syngas treatment system, was highly effective at adsorbing and reducing the concentration of all class of tars in syngas by 80%−95%. The effect of plasma at different power intensities on the model tar reduction or/and removal efficiency and concentration will discuss in the next section.
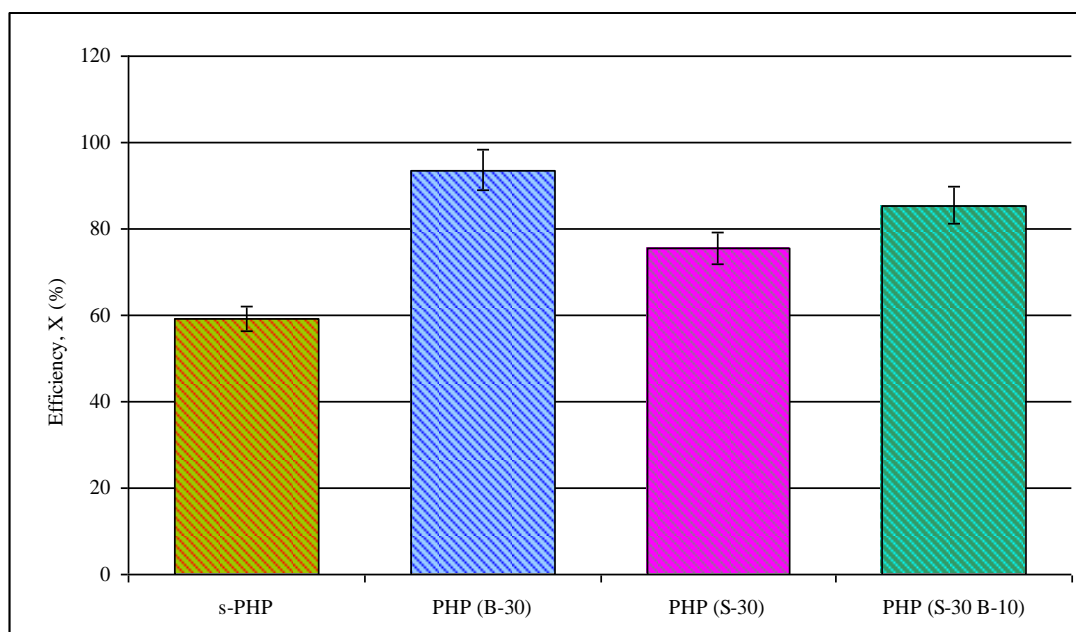
Figure (4.6): Performance of different types of PolyHIPE Polymers (PHPs) in the model tar reduction efficiency
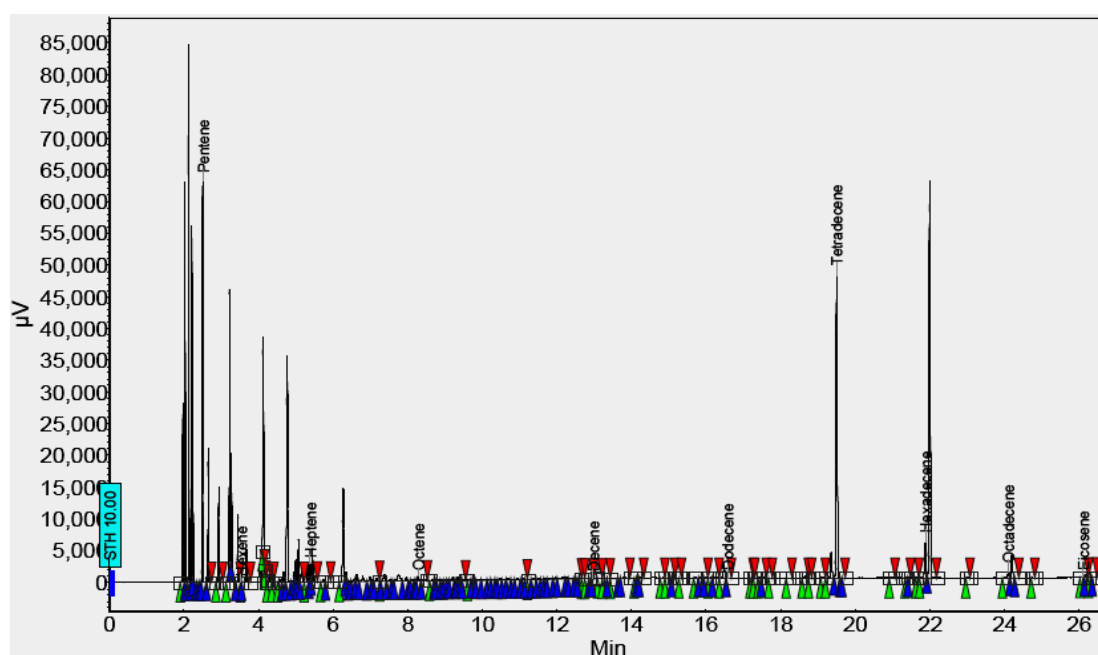
Figure (4.7): Gas chromatogram of the model syngas before treatment (sampling location SP1 before the reactor shown in Figure 3.13). Full scale of the abundance (μV) is 85000 units)

131
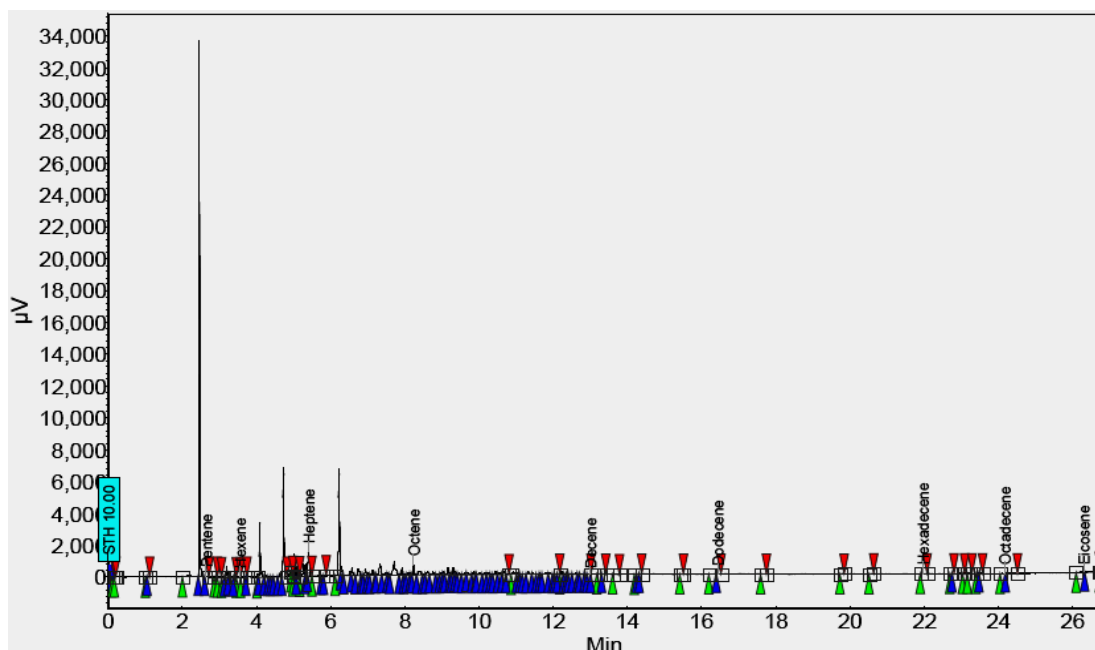
Figure (4.8-a): Gas chromatogram of the model syngas after treatment using sulphonated PolyHIPE Polymer (s-PHP) (sampling location SP2 after the reactor shown in Figure 3.13). Note that the full scale of abundance (μV) is 34000 units
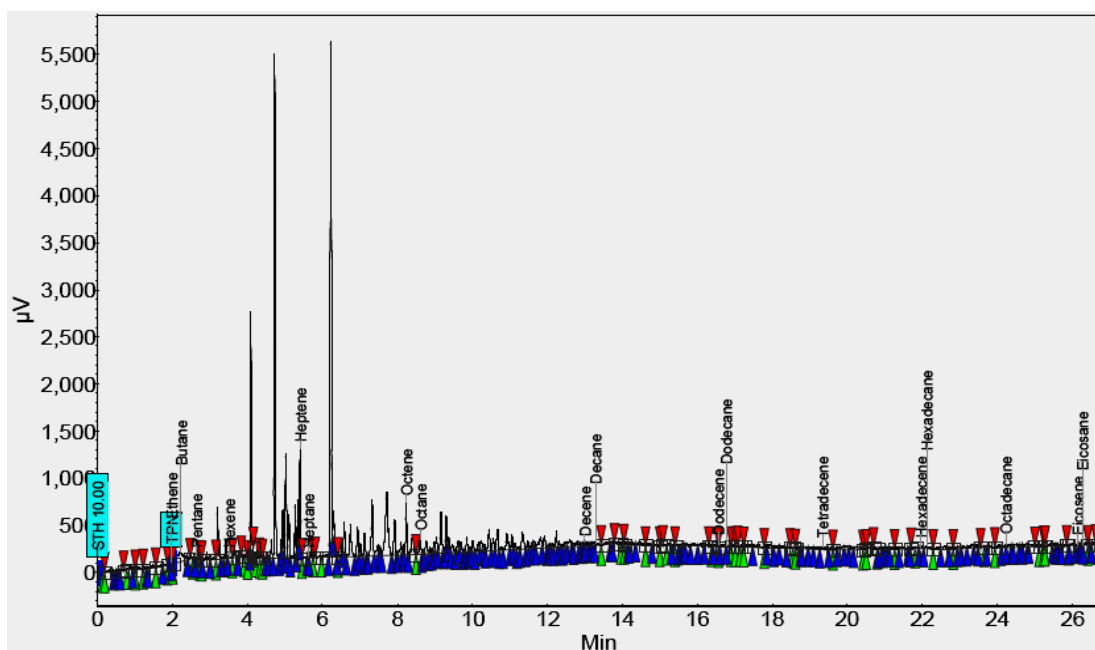
Figure (4.8-b): Gas chromatogram of the model syngas after treatment using PolyHIPE Polymer (PHP-B30) (sampling location SP2 after the reactor shown in Figure 3.13). Note that the full scale of abundance (μV) is 5500 units
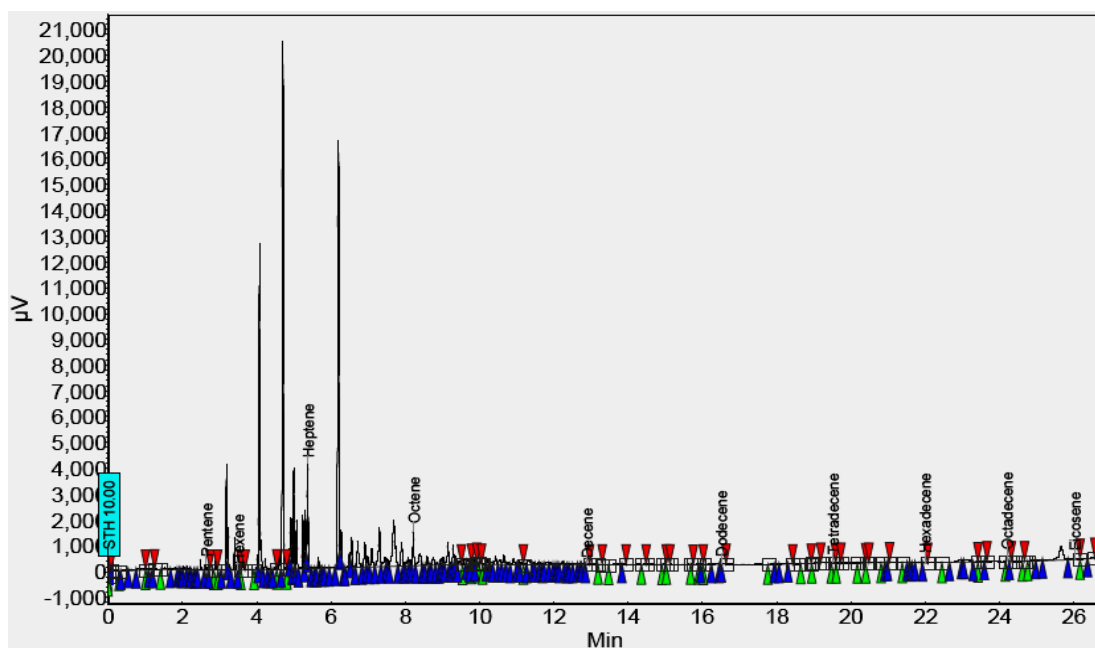
Figure (4.8-c): Gas chromatogram of the model syngas after treatment using PolyHIPE Polymer (PHP-S30) (sampling location SP2 after the reactor shown in Figure 3.13). Note that the full scale of abundance (µV) is 21000 units
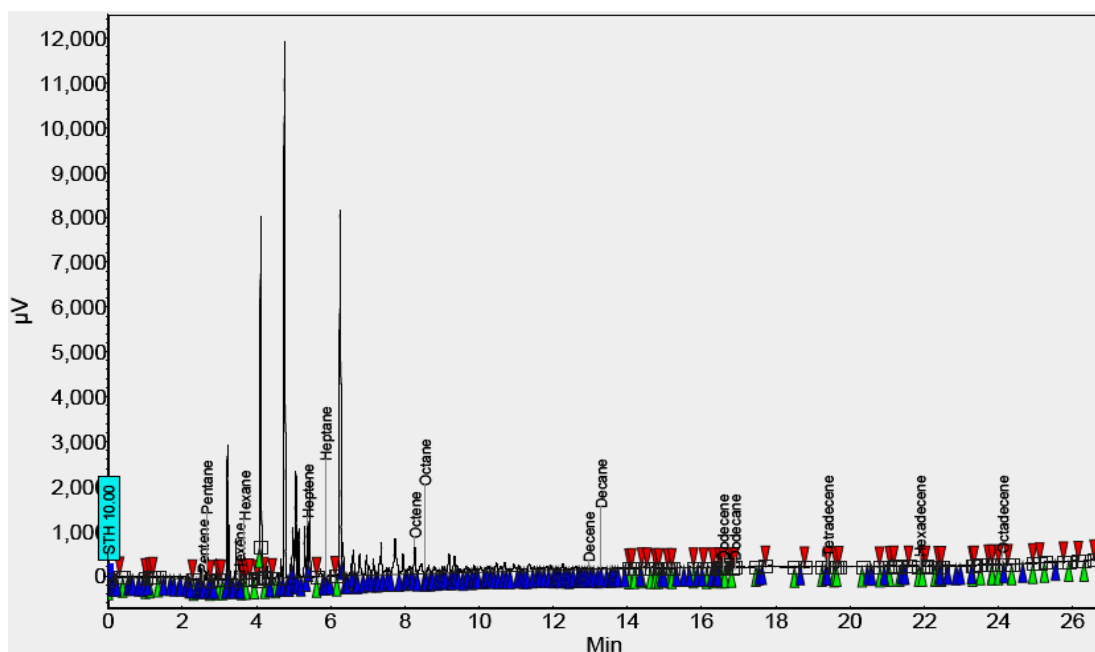
Figure (4.8-d): Gas chromatogram of the model syngas after treatment using PolyHIPE Polymer (PHP-S30B10) (sampling location SP2 after the reactor shown in Figure 3.13). Note that the full scale of abundance (µV) is 12000 units

4.3.1.2. Effect of Plasma on the Model Tar Reduction Efficiency at Different Power Intensities

The previous section presented and discussed the results obtained from the performance of different types of crushed PHPs particles on the model tar reduction efficiency and concentration. In this section, results of model tar reduction efficiency under the influence of DBD will be discussed and analysed. Plasma treated model syngas was subjected to the tar evaluation procedure from which amount of model tar present in the model syngas was determined.

Again, the concentration of the model tar was measured at the entrance, C_{in}, to the reactor and at the exit C_{out}, after model tar reduction or/and removal. Tar reduction efficiency (X) is calculated from equation (4.1). The experiments were carried out in a period of 3 hours with a model syngas flow rate was 1 litre/min, temperature of the inlet gas was kept at 43 ± 3 ^{0}C and plasma power intensities was 40–50W. Each run was repeated twice to ensure reproducibility of results. In all cases, the inlet and outlet model syngas composition were monitored using gas chromatography (GC). Out of the results obtained from these experiments, comparisons were made in terms of model tar reduction or/and removal efficiency and concentration.

The summary of experimental results achieved is given in Table (4.11). The effect of power input on model tar reduction or/and removal efficiency was clear. Model tar reduction efficiency increased as the power increased. As indicated in Figure (4.9) below. A 64.1 % in model tar reduction was achieved with 40W power input and an additional 7 % increase in tar removal was observed when the plasma power increased from 40 to 50W to produce an overall 71.4 % increase in tar removal.

Table (4.11): Influence of plasma at different power intensities on the model tar reduction efficiency

Cleaning System → Parameter ↓	Plasma (40W)	Plasma (50W)
C_{out}** (g/Nm3)	7.9 ± 0.6	6.3 ± 0.44
Efficiency X (%)	64.1 ± 4.5	71.4 ± 5.0
GC – Figures (4.10-a-b)	Figure (4.10-a)	Figure (4.10-b)

**Model tar concentration after treatment
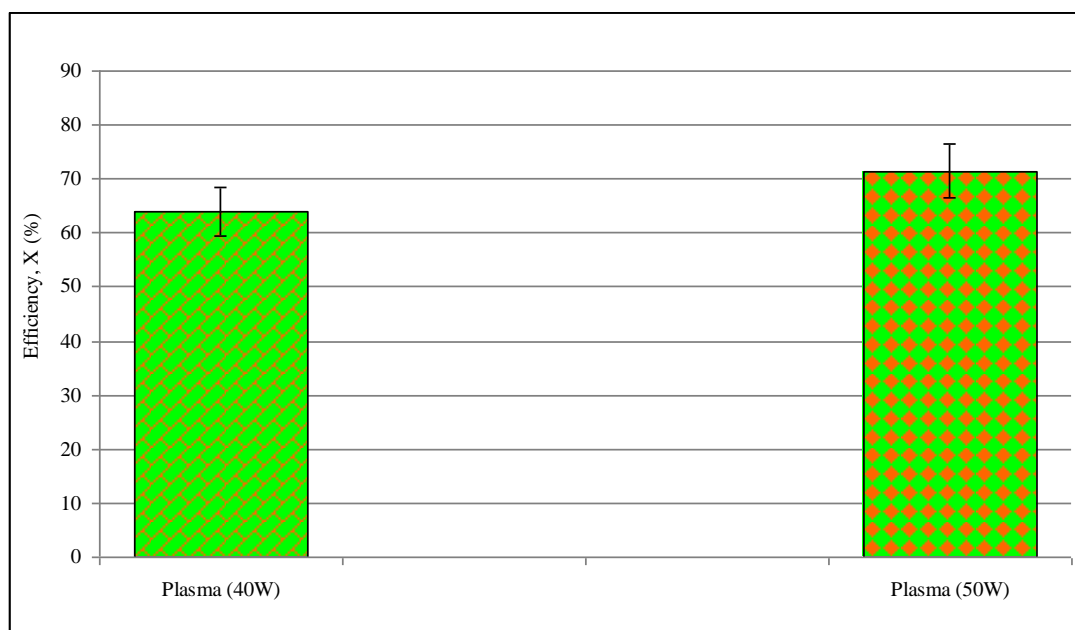
Figure (4.9): Effect of plasma at different power intensities on the model tar reduction efficiency

These results suggest that higher DBD power input have a more significant effect on tar concentration and tar reduction or/and removal efficiency. Non-thermal plasma is a novel molecule activation tool and the plasma formed behaves like a catalyst as the activation energy for destruction of the intermolecular bonds in PAHs is lowered and these compounds are converted to smaller compounds (Nair *et al.*, 2003). Consequently, tar destruction is achieved and syngas yield can be increased. However, in our case, the high energy electrons can attack model tar molecules through electron-impact ionization, dissociation and excitation leading to tar decomposition in the process.

Furthermore, the model tar reduction or/and removal efficiency and concentration results presented above are also confirmed by gas chromatography experiments (hydrocarbon profile of model syngas shifted towards low carbon number after treatment, this could be mean that longer chain of hydrocarbon was broken down by plasma as soon as it was formed. This suggests that the plasma could play a similar role of temperature or/and catalysts in break down the longer chain of hydrocarbons). Figure (4.7) and Figure (4.10-a-b) are the gas chromatograms of model syngas at the entrance to the reactor (Figure 4.7) and at the exit of the reactor after treatment with plasma at different power intensities as tabulated in Table (4.11)

above. In summary, model tar reduction or/and removal increases with increasing DBD power input due to higher reaction energy supplied by the DBD. The effect of the combination of plasma at different power strengths with a packed bed of crushed s-PHP particles (approximately 2-3 mm in size, total weight 20g) as a secondary model syngas treatment system on model tar reduction efficiency and reducing the concentration in producer model syngas will be discussed in the following section.
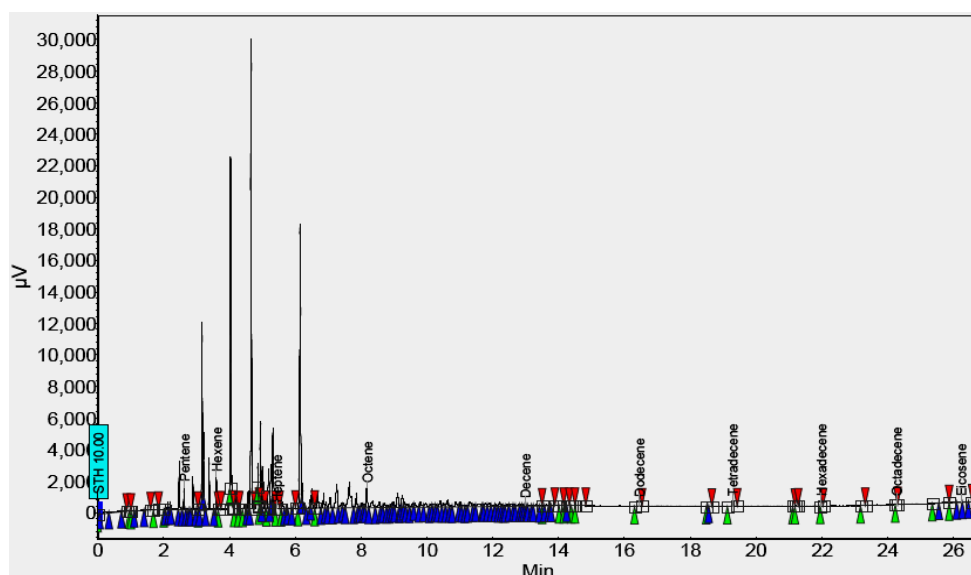
Figure (4.10-a): Gas chromatogram of the model syngas after plasma treatment at 40W without any polymer (sampling location SP2 after the reactor shown in Figure 3.13). Note that the full scale of abundance (µV) is 30000 units

Figure (4.10-b): Gas chromatogram of the model syngas after plasma treatment at 50W without any polymer (sampling location SP2 after the reactor shown in Figure 3.13). Note that the full scale of abundance (µV) is 24000 units

136

4.3.1.3. Effect of the Combination of Plasma at Different Power Intensities with sulphonated Poly HIPE Polymer (s-PHP) on the Model Tar Reduction Efficiency

In this section, the effect of combination of plasma at different power intensities with a packed bed of crushed s-PHP particles on the model tar concentration and tar reduction efficiency as a secondary model syngas treatment system is presented and discussed. No additional runs were carried out with other types of PHPs polymers (PHP-B30, PHP-S30, and PHP-S30B10) due to the unavailability. Similarly, the concentration of the model tar was measured at the entrance, C_{in}, to the reactor and at the exit C_{out}, after model tar reduction or/and removal. Tar reduction efficiency (X) is calculated from equation (4.1).

The experiments were carried out in a period of 3 hours with a model syngas flow rate was 1 litre/min, temperature of the inlet gas was kept at 43 ± 3 ^{0}C and a packed bed of crushed s-PHP particles (approximately 2-3 mm in size, total weight 20g). Each experiment was repeated twice to ensure reproducibility of results. In all cases, the inlet and outlet model syngas composition were monitored using gas chromatography (GC). Out of the results obtained from these experiments, comparisons were made in terms of model tar reduction or/and removal efficiency and concentration. The summary of experimental results is given in Table (4.12) and Figure (4.11). In reference to Figure (4.11), it is clear that increasing the plasma rate from 40 to 50W in the presence of a packed bed of crushed s-PHP particles gave a higher tar reduction or/and removal efficiency up to 91%. However, under this condition, tar drop was doubled.

Table (4.12): Influence of Plasma at different strengths with a Sulphonated PolyHIPE Polymers (s-PHP) on the model tar reduction efficiency

| Cleaning System → Parameter ↓	Plasma with s-PHP (40W)	Plasma with s-PHP (50W)
C_{out}** (g/Nm^3)	4.3 ± 0.17	2.0 ± 0.08
Efficiency X (%)	80.5 ± 3.0	91.0 ± 3.5
GC – Figures (4.12-a-b)	Figure (4.12-a)	Figure (4.12-b)

**Model tar concentration after treatment
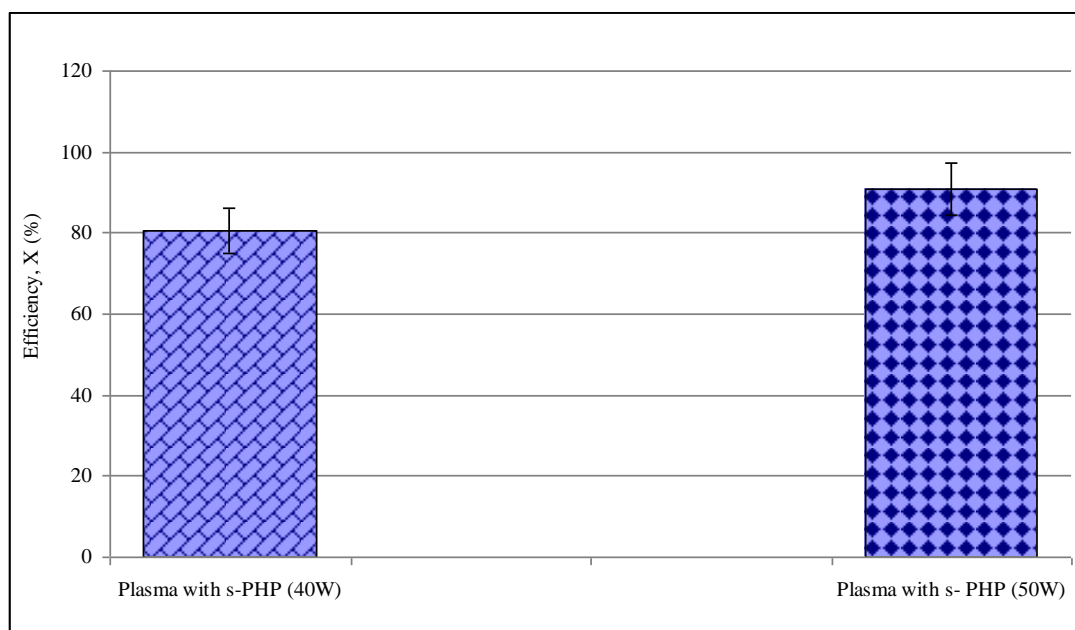
Figure (4.11): Effect of plasma at different power intensities with a Sulphonated PolyHIPE Polymer (s-PHP) on the model tar reduction efficiency

Furthermore, the model tar concentration and tar reduction or/and removal efficiency results presented above, (Table 4.12 and Figure 4.11) are also confirmed by gas chromatography experiments (hydrocarbon profile of model syngas shifted towards low carbon number after treatment). It can be seen that a large number of components have been reduced; this may be due to tar reaction with s-PHP and the high energy electrons can attack model tar molecules through electron-impact ionization, dissociation and excitation leading to tar decomposition in the process. Nevertheless, there is substantial reduction in the overall model tar content in model tar/syngas mixture following extraction with s-PHP disks with or without different rate of high voltage. Note that the full scales of abundance (μV) are 85000, 16000 and 7500 units in Figures (4.7, No treatment), (4.12-a, s-PHP + 40W) and (4.12-b, s-PHP + 50W), respectively. The following section will be summarized the results achieved in sections (4.3.1.1. – 4.3.1.3.).
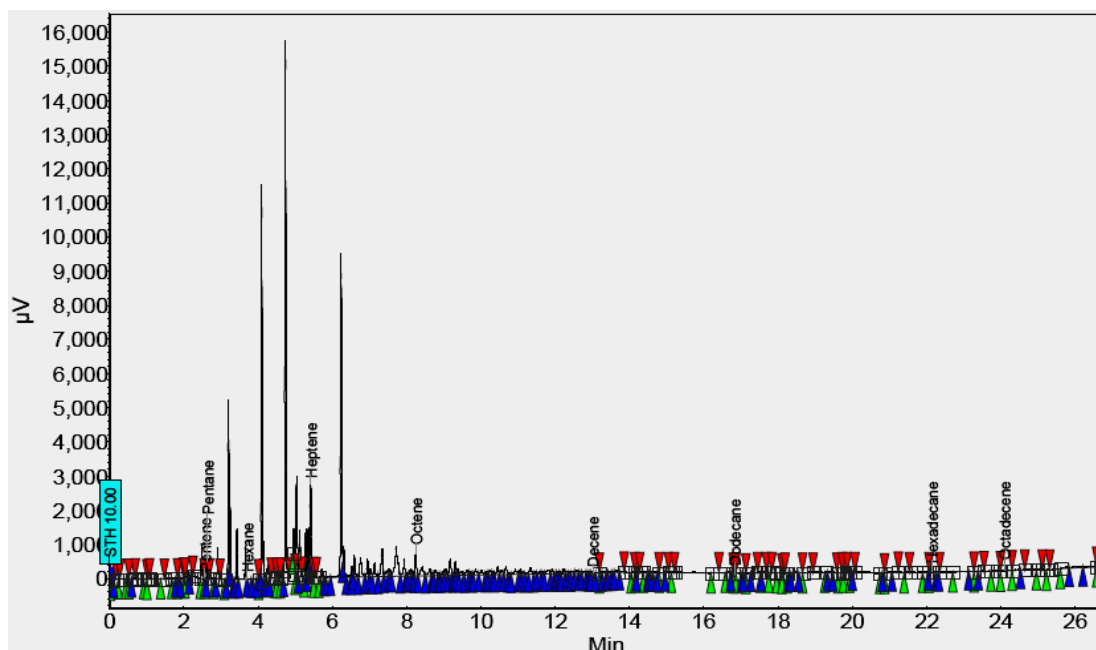
Figure (4.12-a): Gas chromatogram of the model syngas after plasma treatment at 40W with a packed bed of sulphonated PolyHIPE Polymer (s-PHP) (sampling location SP2 after the reactor shown in Figure 3.13). Note that the full scale of abundance (μV) is 16000 units
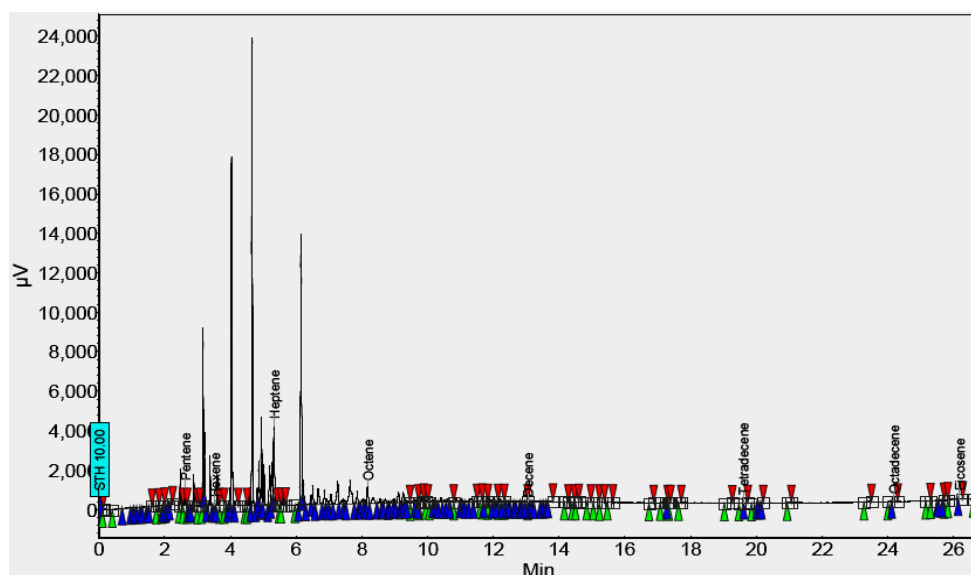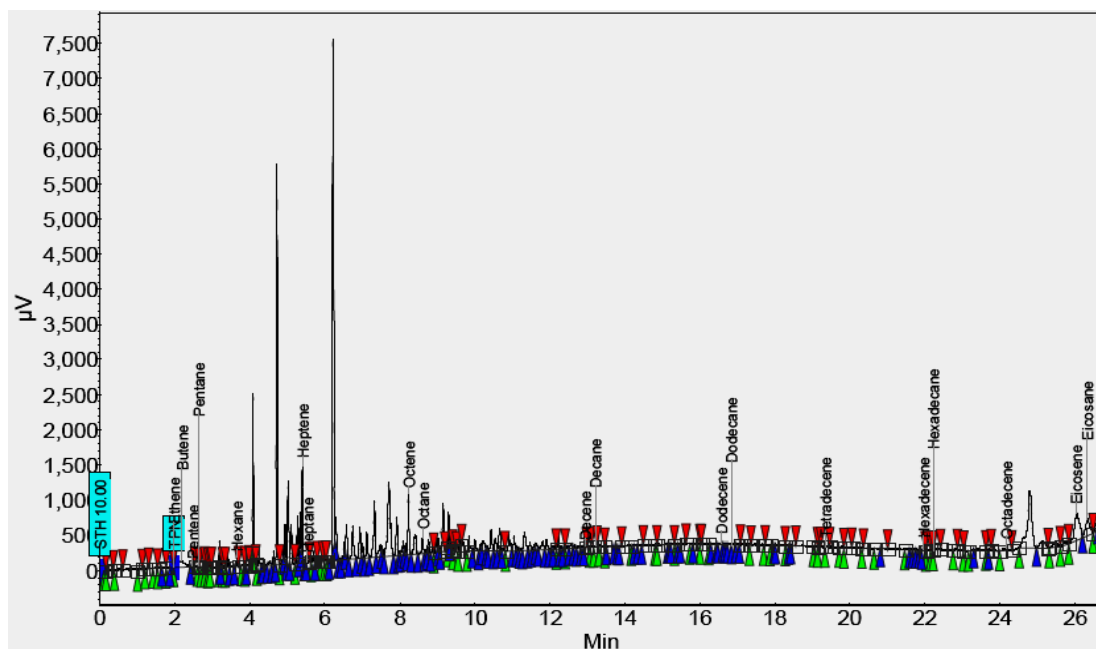

Figure (4.12-b): Gas chromatogram of the model syngas after plasma treatment at 50W with a packed bed of sulphonated PolyHIPE Polymer (s-PHP) (sampling location SP2 after the reactor shown in Figure 3.13). Note that the full scale of abundance (μV) is 7500 units

4.3.1.4. Comparison between the Performance of Different Types of PolyHIPE Polymers (PHPs), Plasma at Different Power Intensities and Their Combination in the Model Tar Reduction Efficiency

The results achieved in sections (4.3.1.1.– 4.3.1.3.) are discussed and summarized here. Table (4.13) below, shows a clear trend of the change in model tar concentration and model tar reduction efficiency. However, in term of model tar concentration, g/Nm^3, see Figure (4.13), in the treated model syngas, in reference to that obtained in the reference experiment, it is to the lowest under the influence of crushed PHP-B30 particles (as a result of high surface area 87.5 m^2/g as well as due to the presence of silica), and with 50W plasma in presence of a packed bed of crushed s-PHP particles (approximately 2-3 mm in size, total weight 20g). It is higher when using PHP-S30B10 particles and via plasma at lower power strength. It is even higher when using plasma by itself at lower power intensities or using a packed bed of s-PHP particles on its own.

Table (4.13): Comparison between the performance of different types of PolyHIPE Polymers (PHPs), plasma at different power intensities and their combination in the model tar reduction efficiency and concentration

Parameter → Cleaning System ↓	C_{in}* (g/Nm^3)	C_{out}** (g/Nm^3)	Efficiency X (%)
Before treatment	22.0 ± 2.1	-	0.0
s-PHP	-	9.0 ± 0.5	59.1 ± 3.0
PHP-B30	-	1.4 ± 0.1	93.6 ± 4.5
PHP-S30	-	5.6 ± 0.3	75.5 ± 3.5
PHP-S30B10	-	3.2 ± 0.16	85.5 ± 4.0
Plasma (40W)	-	7.9 ± 0.6	64.1 ± 4.5
Plasma (50W)	-	6.3 ± 0.44	71.4 ± 5.0
Plasma with s-PHP (40W)	-	4.3 ± 0.17	80.5 ± 3.0
Plasma with s-PHP (50W)	-	2.0 ± 0.08	91.0 ± 3.5

* Model tar concentration before treatment   ** Model tar concentration after treatment

As illustrated in Figure (4.13) below. A 20 g/Nm^3 reduced in tar concentration was found with the use of combination of a packed bed of crushed s-PHP particles and 50W plasma power and a further 0.6 g/Nm^3 reduction occurred with the use a packed bed of PHP-B30 particles alone, as a result of high surface area as well as due to the presence of silica (the model tar concentration can be further reduced by increasing the surface area of the PHPs polymers particles).
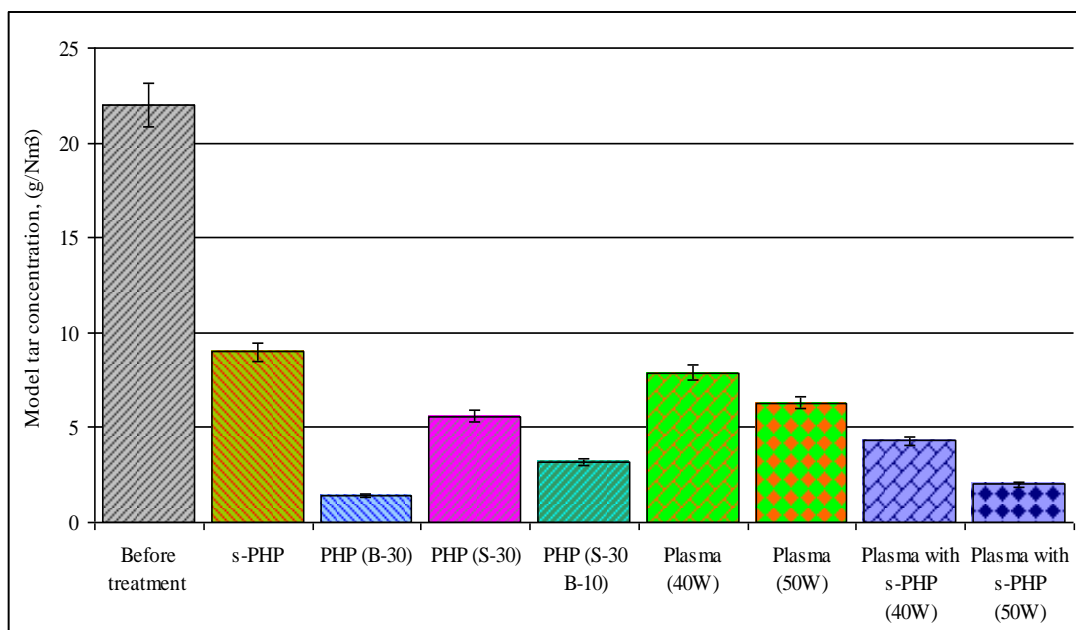
Figure (4.13): Comparison between the performance of different types of PolyHIPE Polymers (PHPs), plasma at different power intensities and their combination vs. the model tar concentration

Also, it can be seen from Figure (4.14) below. A 59 % in model tar reduction was achieved with a packed bed of crushed s-PHP particles alone and an additional 20 % increase in tar removal was observed with the use of a combination of a packed bed of crushed s-PHP particles and 40W power of plasma, and a further increase of 11 % in model tar reduction occurred with the addition of 10W plasma power, however an additional 7 % increase in tar reduction was observed when the plasma alone was increased from 40 to 50W to produce an overall 55 % increase in tar removal.
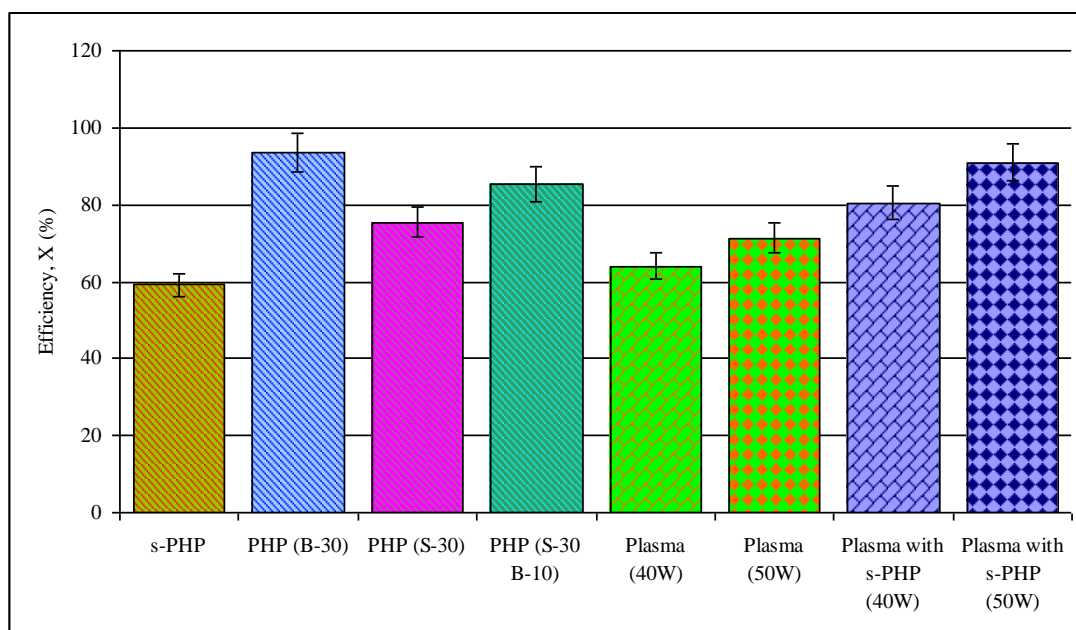
Figure (4.14): Comparison between the performance of different types of PolyHIPE Polymers (PHPs), plasma at different power intensities and their combination vs. the model tar reduction efficiency

In summary, tar reduction efficiency is the highest under the influence of plasma at 40W and via a packed bed of s-PHP particles, PHP-B30 and PHP-S30B10, respectively. Coupling plasma at lower power intensity (40W) with a packed bed of s-PHP particles or using PHP-S30 alone produced a lower tar reduction efficiency. In addition, it is also of interest to observe that model syngas treated with a packed bed of s-PHP particles alone gave the lowest tar reduction efficiency due to its small surface area ($9.4 \ m^2/g$).

Having completed, discussed and analysed the results achieved from the experiments on small (plasma reactor) scale intensified syngas cleaning system; further results from the experimentations using a pilot scale intensified syngas cleaning system will be also presented and discussed in the next sections. In the pilot scale system, investigation was carried out in different profiled high voltage electrode configuration either when it was fully electrically insulated or partially insulated. Out of the results obtained from these experiments, comparisons were made in terms of tar reduction efficiency and concentration.

4.3.2. Results of Pilot Scale Intensified Syngas Cleaning System Experiments

The next sections present and discuss the results of the experimental work performed on pilot scale intensified syngas cleaning system. The effect of several variables on tar reduction or/and removal efficiency and concentration will be discussed and analysed. Each run was carried out in a period of 3 hours. GC sample were obtained approximately every 30 minutes. Each experiment was repeated twice to ensure reproducibility of results. Out of the results obtained from these experiments, comparisons were made in terms of tar reduction efficiency and concentration.

4.3.2.1. Experiments with a Completely Insulated Electrode (CIE)

The results of the experimental work performed with CIE (total surface area of the insulated high voltage electrode = 810 cm^2) configuration are represented and discussed in the following sections. The syngas cleaning equipment with CIE was tested under water scrubbing was done by creating a planar water spray either at the bottom or top or indeed both sprays could be used. Due to the total electrical insulation of the high voltage electrode, it was possible to apply electric field at the range of 10-25 kV. Out of the results obtained from these experiments, comparisons were made in terms of tar reduction efficiency and concentration.

4.3.2.1.1. Effect of Top Water Scrubbing with or without Different Rates of High Voltages on the Model Tar Reduction Efficiency

In this section, the effect of top water scrubbing with or without different rates of high voltages using CIE configuration as a secondary treatment process on model tar reduction or/and removal was presented and discussed. The experiments were carried out in a period of 3 hours and repeated twice to ensure reproducibility of results. The concentration of the model tar was measured at the entrance, C_{in}, to the reactor and at the exit C_{out}, after model tar reduction or/and removal. Tar reduction efficiency (X) is calculated from equation (4.1). The following processing conditions were used:

Model syngas flow rate = 1 litre/min; C_{in} = 22.0 ± 2.1 g/Nm^3;

Gas inlet temperature = 43 ± 3 $^{\circ}$C; Gas outlet temperature = 20 ± 2 $^{\circ}$C;

Scrubbing water (tap water) flow rate = 1.66 litre/min;

Scrubbing water inlet temperature = 20 ± 2 $^{\circ}$C;

Temperature of the equipment = 20 ± 2 $^{\circ}$C;

Total surface area of the insulated high voltage electrode = 810 cm^2; and

Applied high voltage = 0-25 kV

The summary of experimental results is given in Table (4.14), Figure (4.15) and Figures (16-a-e). Overall, in these experiments, effect of high voltage is evident. As the high voltage was increased, tar capture was higher. For instance, tar capture was 41.8 % with no voltage applied and it increased to 57.7 % when the high voltage was 25 kV.

Table (4.14): Influence of top water scrubbing with or without different rates of high voltage on the model tar reduction efficiency

Cleaning System →	Water scrubbing from top with applied voltage (kV)				
Parameter ↓	0	10	15	20	25
C_{out}**(g/Nm^3)	12.8 ± 0.9	11.3 ± 1.0	10.9 ± 0.8	10.7 ± 0.7	9.3 ± 0.65
Efficiency X (%)	41.8 ± 3.0	48.6 ± 3.5	50.5 ± 3.5	51.4 ± 3.5	57.7 ± 4.0
GC – Figures (4.16-a-e)	Figure (4.16-a)	Figure (4.16-b)	Figure (4.16-c)	Figure (4.16-d)	Figure (4.16-e)

**Model tar concentration after treatment

It can be seen from Table (4.14) and Figure (4.15) that a 41.8 % in model tar reduction was achieved with water scrubbing from top without electric field applied, and an additional 8.7 % increase in tar removal was observed with the use of water scrubbing with 15 kV and a further increase of 7.2 % occurred with the addition of 10 kV, however an additional 15.9 % increase in tar reduction was observed when the electric field was increased from 0 to 25 kV to produce an overall 57.7 % increase in tar removal.

Likewise, a 7 g/Nm^3 reduction in tar concentration was found with the use of water scrubbing from top without electric field and a further 2 g/Nm^3 reduction

occurred with the use of water scrubbing with 15 kV. Increasing the electric field to 25 kV produced a 12 g/Nm^3 reduction in tar concentration

Figure (4.15): Effect of top water scrubbing with or without different rates of high voltage on the model tar reduction efficiency

Furthermore, the model tar concentration and tar reduction or/and removal efficiency results presented above (Table 4.14 and Figure 4.15) are also confirmed by gas chromatography experiments (hydrocarbon profile of model syngas shifted towards low carbon number after treatment). Figure (4.7) and Figure (4.16-a-e) are the gas chromatograms of model syngas at the entrance to the reactor (Figure 4.7) and at the exit of the reactor (Figure 4.16-a-e) after treatment with top water scrubbing with or without different rates of high voltages. The effect of bottom water scrubbing with or without different rates of high voltages as a secondary model syngas treatment system on model tar reduction or/and removal in producer model syngas will be discussed in the next section.
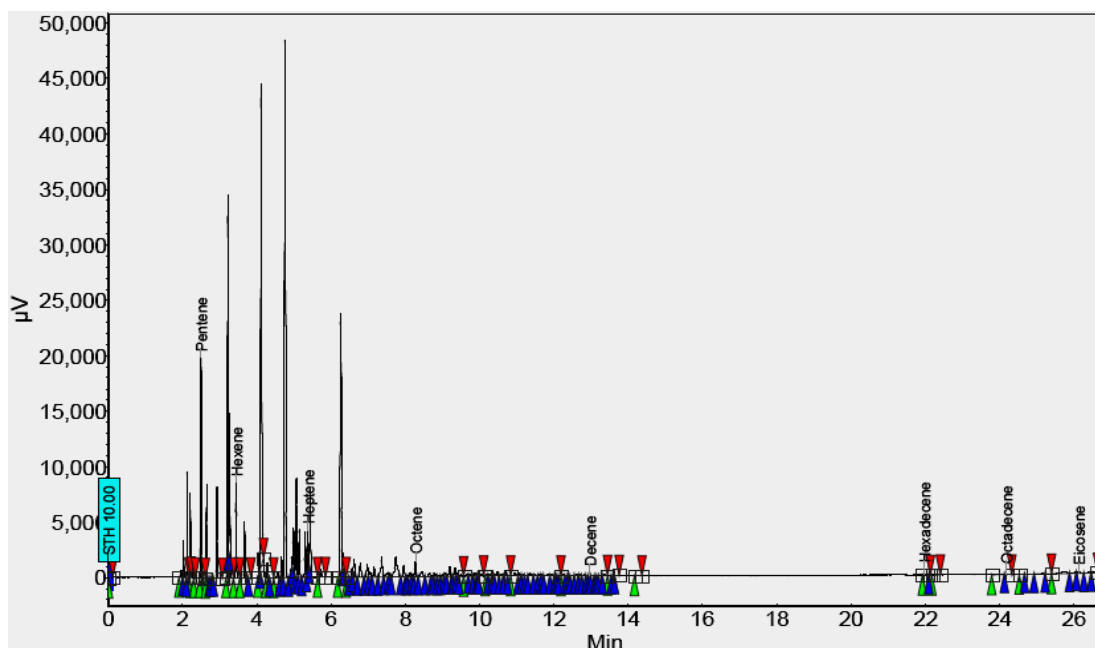
Figure (4.16-a): Gas chromatogram of the model syngas after top water scrubbing treatment without high voltage (sampling location SP2 after the reactor shown in Figure 3.19). Note that the full scale of abundance (µV) is 50000 units
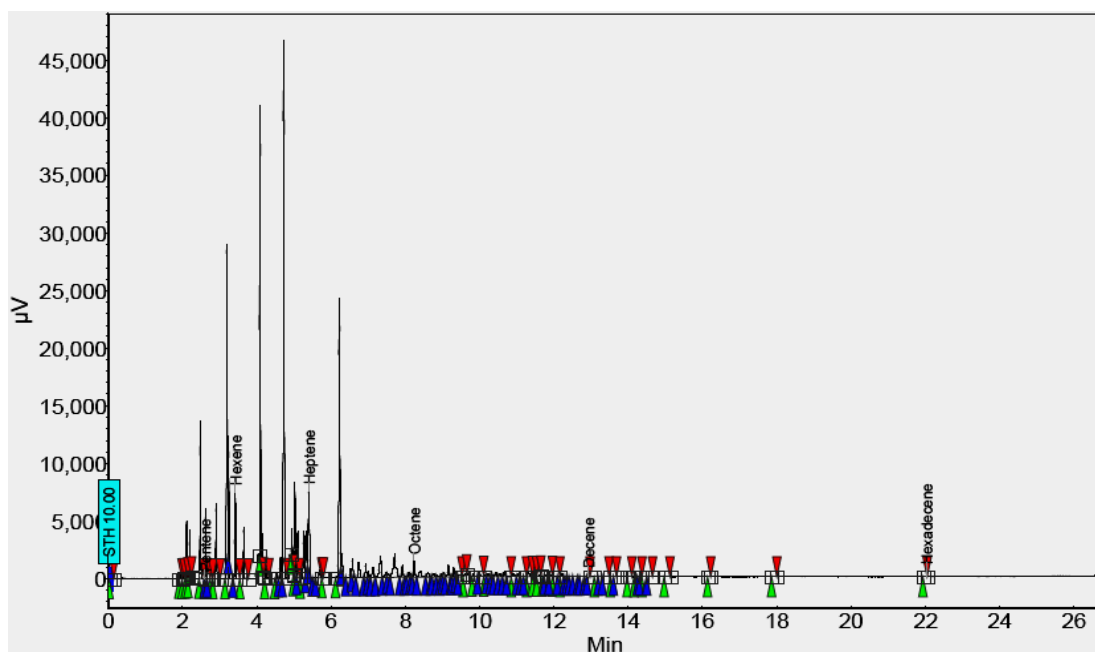
Figure (4.16-b): Gas chromatogram of the model syngas after top water scrubbing treatment with 10kV high voltage (sampling location SP2 after the reactor shown in Figure 3.19). Note that the full scale of abundance (µV) is 45000 units
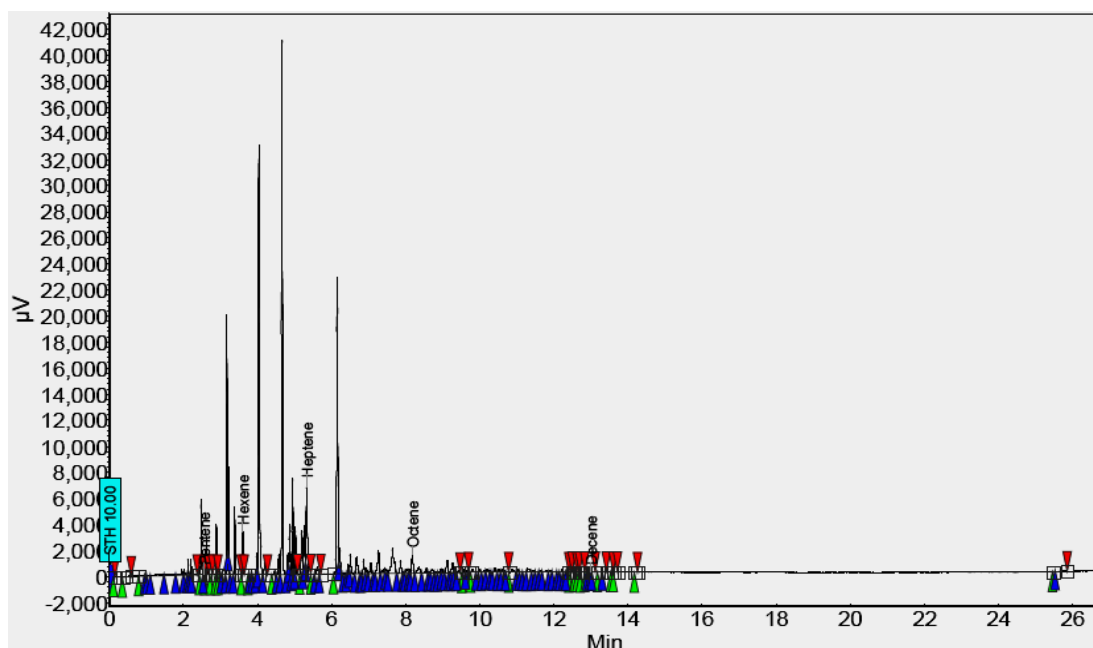
Figure (4.16-c): Gas chromatogram of the model syngas after top water scrubbing treatment with 15kV high voltage (sampling location SP2 after the reactor shown in Figure 3.19). Note that the full scale of abundance (µV) is 42000 units
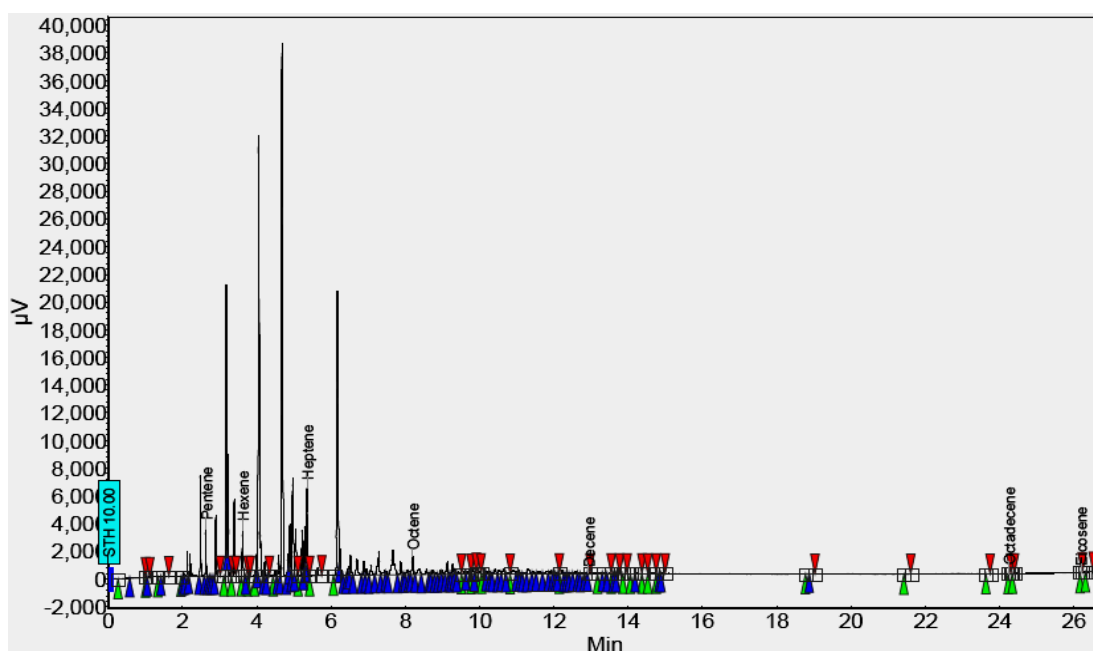
Figure (4.16-d): Gas chromatogram of the model syngas after top water scrubbing treatment with 20kV high voltage (sampling location SP2 after the reactor shown in Figure 3.19). Note that the full scale of abundance (µV) is 40000 units
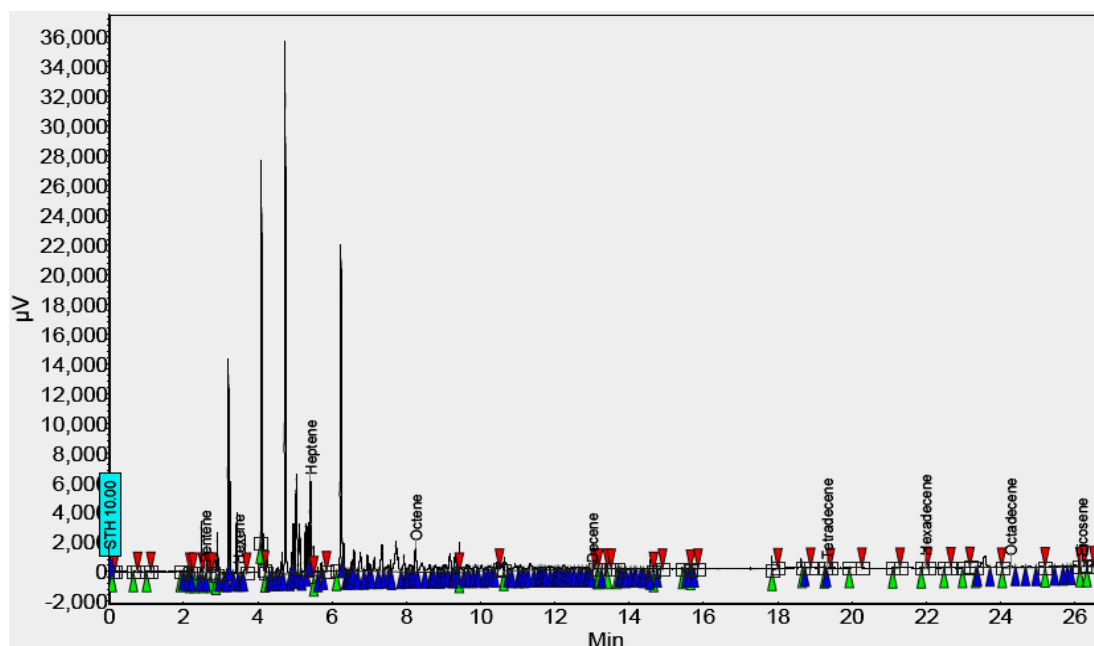
Figure (4.16-e): Gas chromatogram of the model syngas after top water scrubbing treatment with 25kV high voltage (sampling location SP2 after the reactor shown in Figure 3.19). Note that the full scale of abundance (µV) is 36000 units
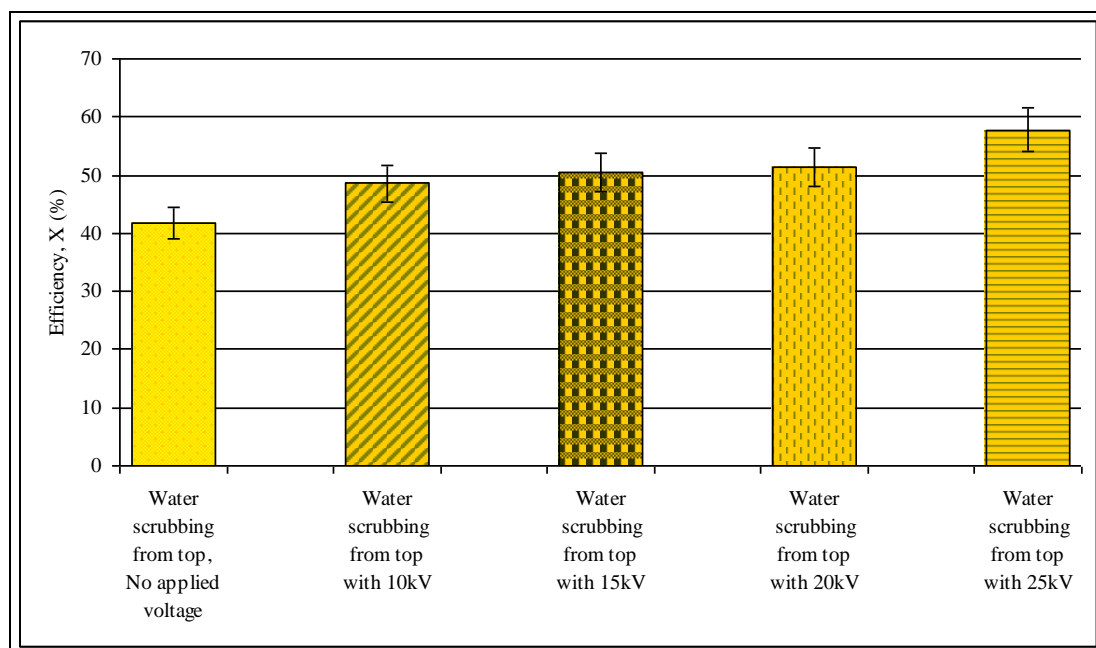
4.3.2.1.2. Effect of Bottom Water Scrubbing with or without Different Rates of High Voltages on the Model Tar Reduction Efficiency

In this section, the effect of bottom water scrubbing with or without different rates of high voltages using CIE configuration as a secondary treatment process on model tar reduction or/and removal was presented and discussed. The experiments were carried out in a period of 3 hours and repeated twice to ensure reproducibility of results. The concentration of the model tar was measured at the entrance, C_{in}, to the reactor and at the exit C_{out}, after model tar reduction or/and removal. Tar reduction efficiency (X) is calculated from equation (4.1). The following processing conditions were used:

Model syngas flow rate = 1 litre/min;

$C_{in} = 22.0 \pm 2.1$ g/Nm^3;

Gas inlet temperature = 43 ± 3 $^\circ$C;

Gas outlet temperature = 20 ± 2 $^\circ$C;

Scrubbing water (tap water) flow rate = 1.66 litre/min;

Scrubbing water inlet temperature = 20 ± 2 $^\circ$C;

Temperature of the equipment = 20 ± 2 $^\circ$C;

Total surface area of the insulated high voltage electrode = 810 cm^2; and

Applied high voltage = 0-25 kV

A comparison of the model tar reduction efficiency with and without different rates of high voltages is illustrated in Table (4.15), Figure (4.17) and Figures (18-a-d). Overall, in these experiments, effect of high voltage is evident. As the high voltage was increased, tar capture was higher. For instance, tar capture was 30.9 % with no voltage applied and it increased to 55.0 % when the high voltage was 25 kV.

Table (4.15): Influence of bottom water scrubbing with or without different rates of high voltage on the model tar reduction efficiency

| Cleaning System → | Water scrubbing from bottom with applied voltage (kV) | | | |
Parameter ↓	0	15	20	25
C_{out}** (g/Nm^3)	15.2 ± 1.5	12.9 ± 1.0	11.2 ± 1.0	9.9 ± 0.9
Efficiency X (%)	30.9 ± 3.0	41.4 ± 4.0	49.1 ± 4.5	55.0 ± 5.0
GC – Figures (4.18a-d)	Figure (4.18a)	Figure (4.18b)	Figure (4.18c)	Figure (4.18d)

**Model tar concentration after treatment

It can be seen from Table (4.15) that decrease in tar concentration and associated increase in tar reduction, it is evident that longer chain of hydrocarbon was broken down by applied electrical field as soon as it was formed. This suggests that the high voltage could play a similar role of temperature or/and catalysts in break down the longer chain of hydrocarbons, resulting in hydrocarbon profile of model syngas shifted towards low carbon number after treatment. The evidence for this was confirmed by gas chromatography experiments (Figures 4.7) and (Figures 4.18-a-d).

Also, a 31 % in model tar reduction was achieved with water scrubbing from bottom without electric field and an additional 10 % increase in tar removal was observed with the use of water scrubbing with 15 kV and a further increase of 8 % in model tar reduction occurred with the addition of 5 kV, however an additional 6 % increase in tar reduction was observed when the electric field was increased from 20 to 25 kV to produce an overall 55 % increase in tar removal

Likewise, a 7 g/Nm^3 reduction in tar concentration was found with the use of water scrubbing from bottom without electric field and a further 2 g/Nm^3 reduction occurred with the use of water scrubbing with 15 kV. Increasing the electric field to 25 kV produced a 12 g/Nm^3 reduction in tar concentration. The effect of simultaneous top and bottom water scrubbing with or without different rates of high voltages as a secondary model syngas treatment system on model tar reduction or/and removal in producer model syngas will be discussed in the next section.
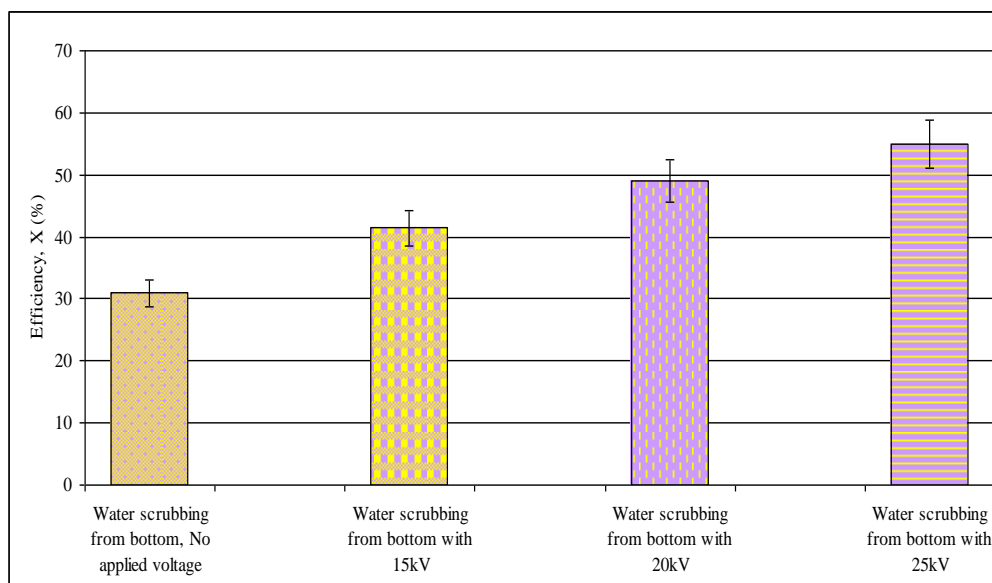
Figure (4.17): Effect of bottom water scrubbing with or without different rates of high voltage on the model tar reduction efficiency
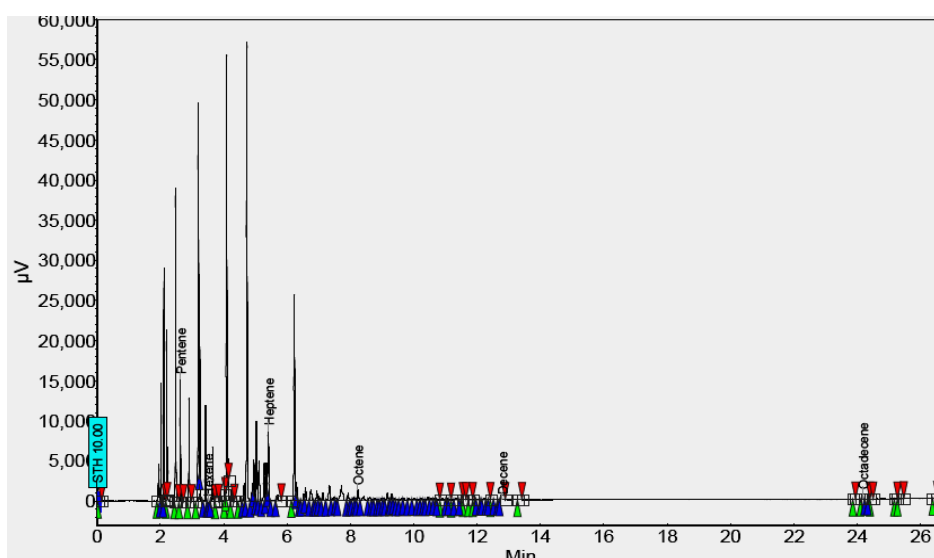
Figure (4.18-a): Gas chromatogram of the model syngas after bottom water scrubbing treatment without high voltage (sampling location SP2 after the reactor shown in Figure 3.19). Note that the full scale of abundance (µV) is 60000 units

150
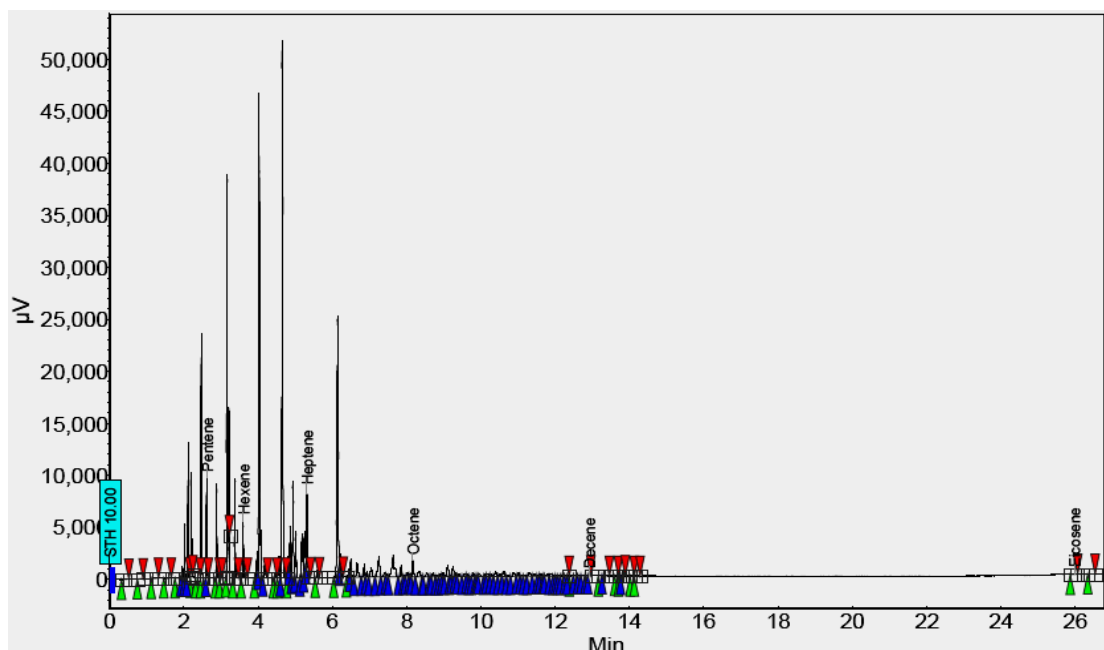
Figure (4.18-b): Gas chromatogram of the model syngas after bottom water scrubbing treatment with 15kV high voltage (sampling location SP2 after the reactor shown in Figure 3.19). Note that the full scale of abundance (μV) is 50000 units
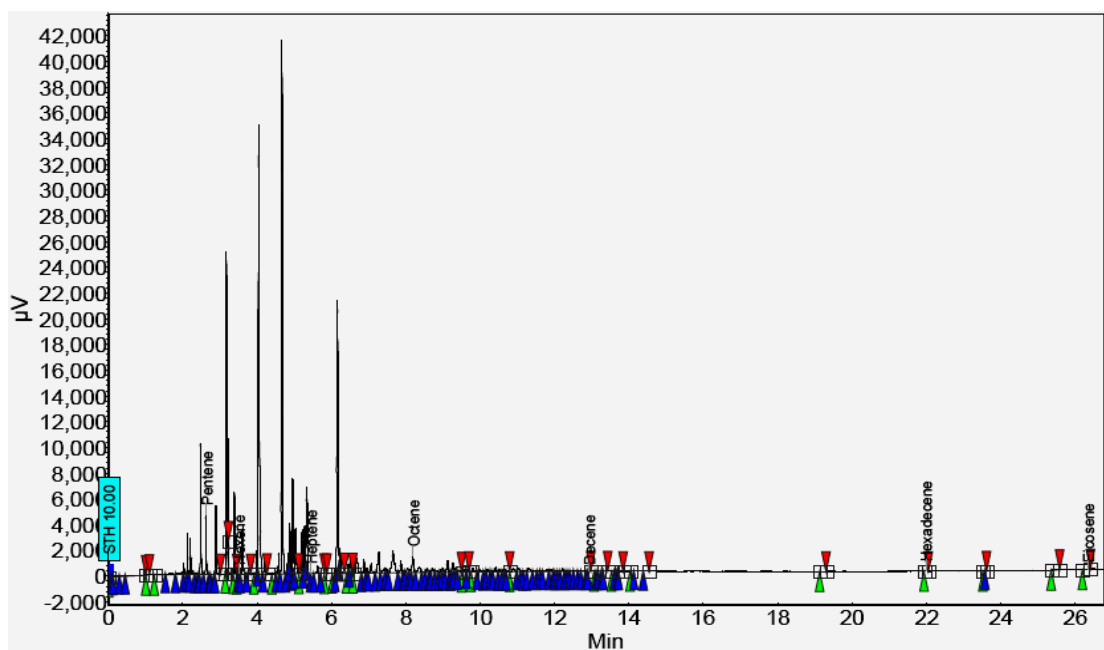
Figure (4.18-c): Gas chromatogram of the model syngas after bottom water scrubbing treatment with 20kV high voltage (sampling location SP2 after the reactor shown in Figure 3.19). Note that the full scale of abundance (μV) is 42000 units
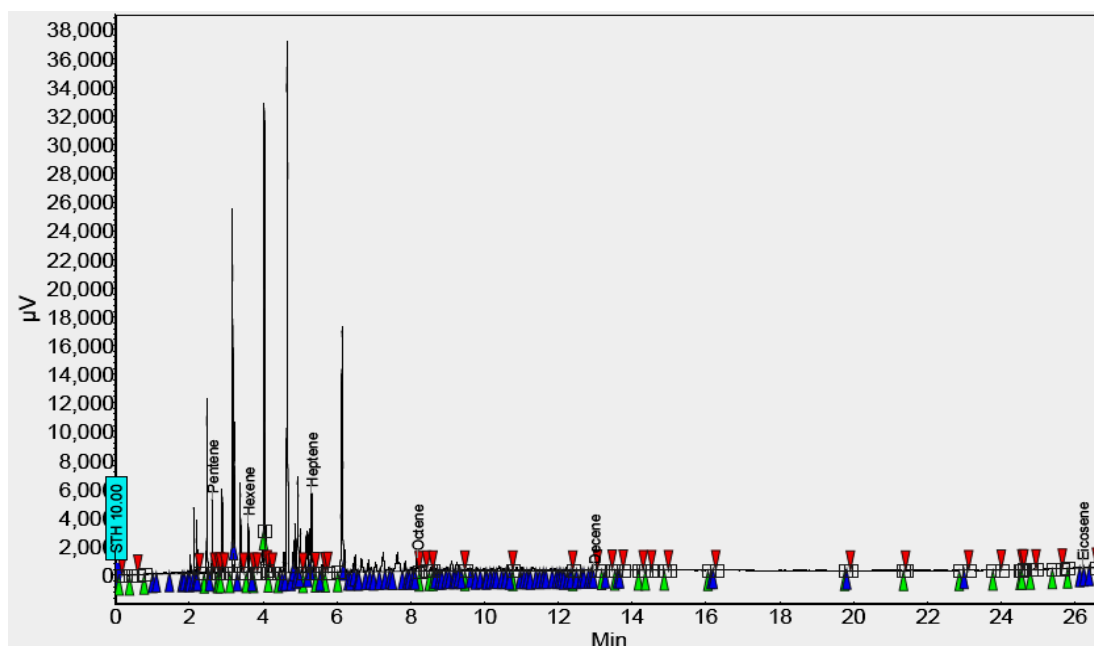
Figure (4.18-d): Gas chromatogram of the model syngas after bottom water scrubbing treatment with 25kV high voltage (sampling location SP2 after the reactor shown in Figure 3.13). Note that the full scale of abundance (μV) is 38000 units

4.3.2.1.3. Effect of Simultaneous Top and Bottom Water Scrubbing with or without Different Rates of High Voltages on the Model Tar Reduction Efficiency

The effect of simultaneous top and bottom water scrubbing with or without different rates of high voltages using CIE configuration as a secondary treatment process on model tar reduction or/and removal was presented and discussed in this section. The experiments were carried out in a period of 3 hours and repeated twice to ensure reproducibility of results. The concentration of the model tar was measured at the entrance, C_{in}, to the reactor and at the exit C_{out}, after model tar reduction or/and removal. Tar reduction efficiency (X) is calculated from equation (4.1). The following processing conditions were used:

Model syngas flow rate = 1 litre/min; C_{in} = 22.0 ± 2.1 g/Nm^3;

Gas inlet temperature = 43 ± 3 $^\circ$C; Gas outlet temperature = 20 ± 2 $^\circ$C;

Scrubbing water (tap water) flow rate = 1.66 litre/min;

Scrubbing water inlet temperature = 20 ± 2 $^\circ$C;

Temperature of the equipment = 20 ± 2 $^\circ$C;

Total surface area of the insulated high voltage electrode = 810 cm^2; and

Applied high voltage = 0-25 kV

152

A comparison of the model tar reduction efficiency with and without different rates of high voltages is illustrated in Table (4.16), Figure (4.19) and Figures (20-a-c). Overall, in these experiments, effect of high voltage is evident. As the high voltage was increased, tar capture was higher. For instance, tar capture was 45.9 % with no voltage applied and it increased to 72.3 % when the high voltage was 25 kV.

Table (4.16): Influence of simultaneous top and bottom water scrubbing with or without different rates of high voltage on the model tar reduction efficiency

| Cleaning System → Parameter ↓	Water scrubbing from top and bottom with applied voltage (kV)		
	0	15	25
C_{out}**(g/Nm^3)	11.9 ± 1.0	9.6 ± 0.95	6.1 ± 0.65
Efficiency X (%)	45.9 ± 4.5	56.4 ± 5.5	72.3 ± 7.0
GC – Figures (4.20-a-c)	Figure (4.20-a)	Figure (4.20-b)	Figure (4.20-c)

**Model tar concentration after treatment

Figure (4.19): Effect of simultaneous top and bottom water scrubbing with or without different rates of high voltage on the model tar reduction efficiency

It can be seen from Table (4.16) and Figure (4.19) that decrease in tar concentration and associated increase in tar reduction, it is evident that longer chain of hydrocarbon was broken down by applied electrical field as soon as it was formed. This suggests that the high voltage could play a similar role of temperature or/and

catalysts in break down the longer chain of hydrocarbons, resulting in hydrocarbon profile of model syngas shifted towards low carbon number after treatment. The evidence for this was confirmed by gas chromatography experiments (Figures 4.7) and (Figures 4.20-a-c).

Likewise, a 45.9 % in model tar reduction was achieved with water scrubbing from top and bottom without electric field and an additional 10.5 % increase in tar removal was observed with the use of simultaneous top and bottom water scrubbing with 15 kV and a further increase of 15.9 % in model tar reduction occurred with the addition of 10 kV to produce an overall 72.3 % increase in tar removal

Also, a 10.1 g/Nm^3 reduction in tar concentration was found with the use of water scrubbing from top and bottom without electric field and a further 2.3 g/Nm^3 reduction occurred with 15 kV. Increasing the electric field to 25 kV produced a 15.9 g/Nm^3 reduction in tar concentration. Summarized the finding achieved in sections (4.3.2.1.1. − 4.3.2.1.3.) will be presented and analyzed in the following section.
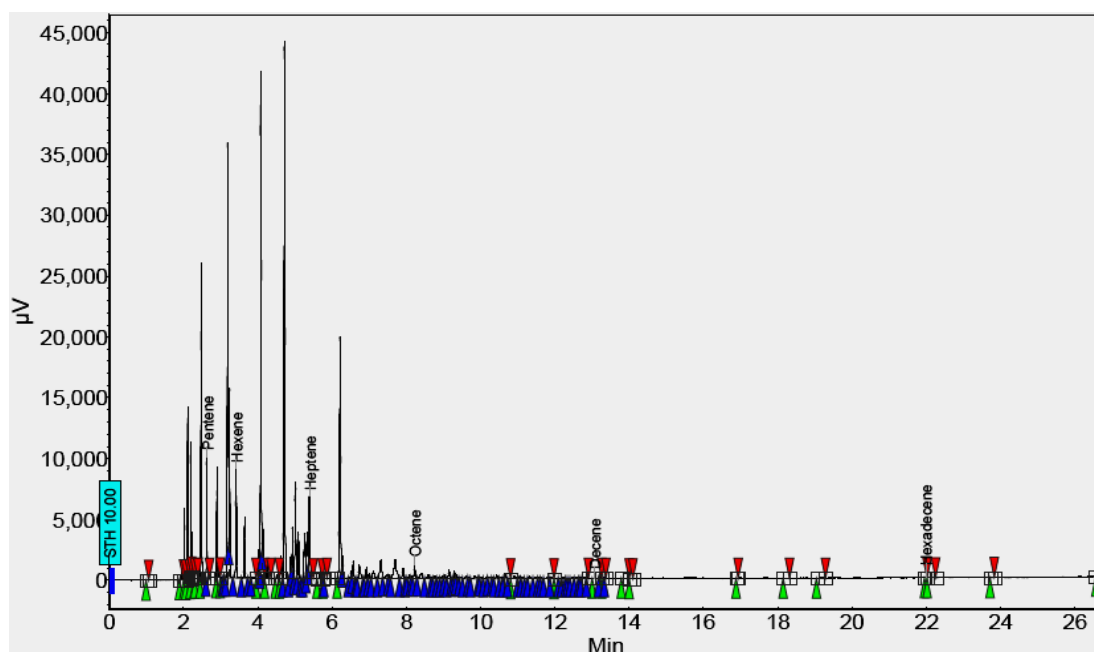
Figure (4.20-a): Gas chromatogram of the model syngas after top and bottom water scrubbing treatment without high voltage (sampling location SP2 after the reactor shown in Figure 3.13). Note that the full scale of abundance (µV) is 45000 units
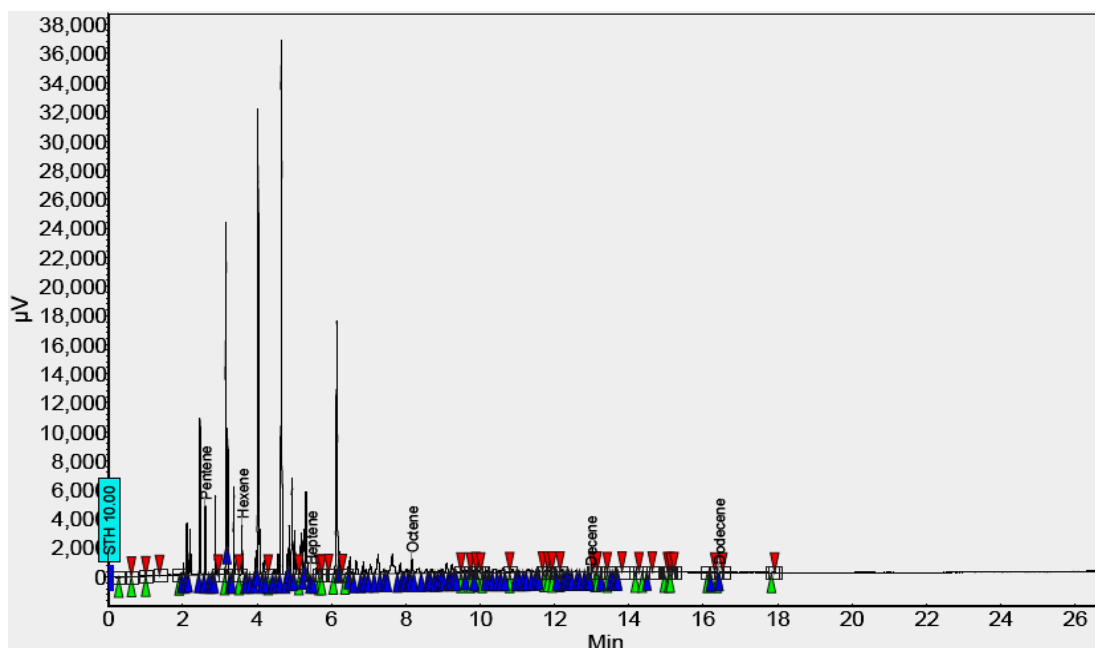
Figure (4.20-b): Gas chromatogram of the model syngas after top and bottom water scrubbing treatment with 15kV high voltage (sampling location SP2 after the reactor shown in Figure 3.13). Note that the full scale of abundance (μV) is 38000 units
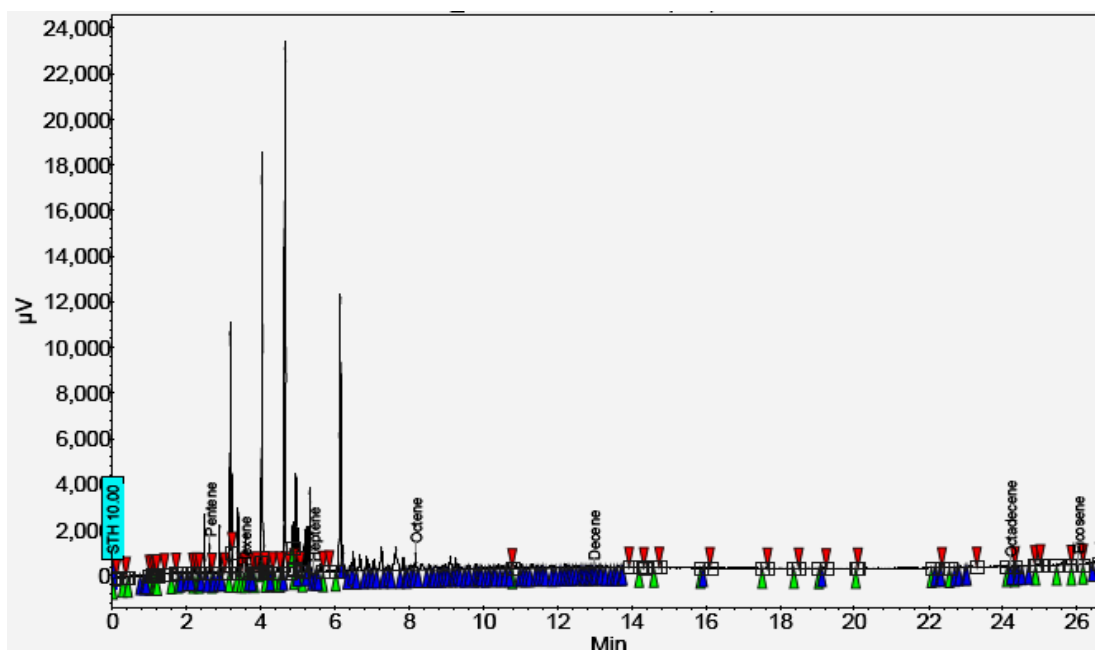
Figure (4.20-c): Gas chromatogram of the model syngas after top and bottom water scrubbing treatment with 25kV high voltage (sampling location SP2 after the reactor shown in Figure 3.13). Note that the full scale of abundance (μV) is 24000 units

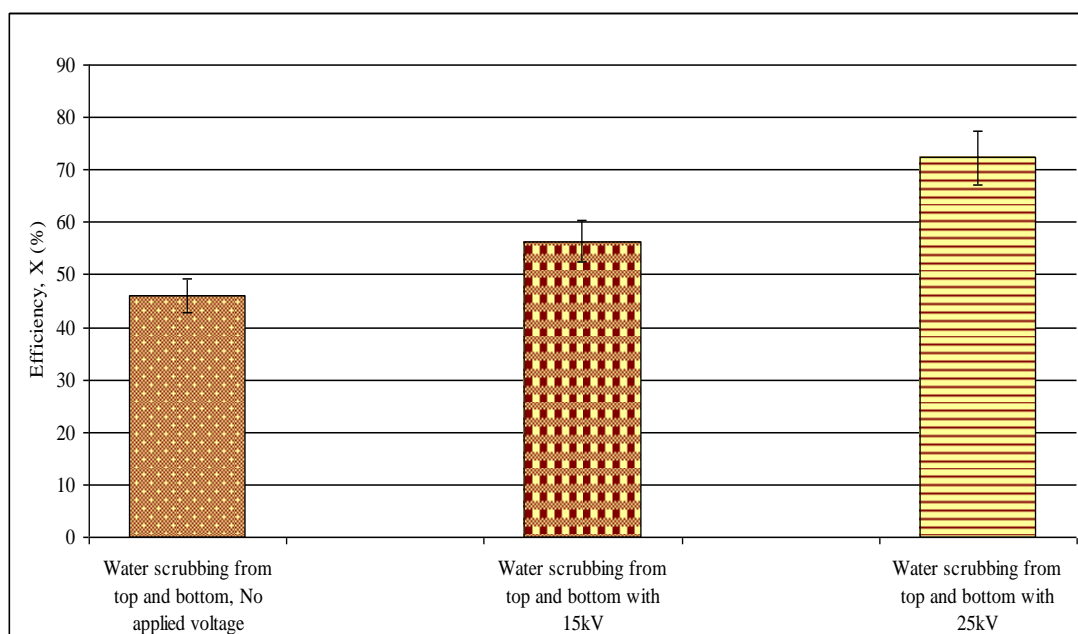### 4.3.2.1.4. Comparison between the Effect of Top, Bottom and Simultaneous Top and Bottom Water Scrubbing with or without Different Rates of High Voltages on the Model Tar Reduction Efficiency

Throughout this work, several techniques have been applied. Effects of: top, bottom and simultaneous top and bottom water scrubbing with or without different rates of high voltages on model tar reduction efficiency have been thoroughly studied and analyzed. The results achieved in sections (4.3.2.1.1. − 4.3.2.1.3.) are discussed and summarized here. Overall, in these experiments, effect of water scrubbing from top, bottom and simultaneous top and bottom with high voltage is evident, as the high voltage was increased, tar capture was higher.

It can be seen from Table (4.17) that a clear trend of the change in model tar concentration and model tar reduction efficiency. However, in term of model tar concentration, g/Nm^3, see Figure (4.21), in the treated model syngas, in reference to that obtained in the reference experiment, it is to the lowest under the influence of water scrubbing from top and bottom with 25kV high voltage, and with water scrubbing from top with 25kV high voltage. It is higher when using water scrubbing from top and bottom and via water scrubbing from top without high voltage, respectively. It is even higher when water scrubbing from bottom without high voltage or using water scrubbing from bottom with 15kV.

Also, as illustrated in Figure (4.21) below a 12.7 g/Nm^3 reduced in tar concentration was found with the use of combination of water scrubbing from top and 25kV high voltage and a further 3.2 g/Nm^3 reduction occurred with the use water scrubbing from top and bottom with a 25kV high voltage applied.

Table (4.17): Comparison between the effect of top, bottom and simultaneous top and bottom water scrubbing with or without different rates of high voltage on the model tar reduction efficiency and concentration

Effect of Parameter → Cleaning System ↓	(g/Nm^3)		Efficiency X (%)
	C_{in} *	C_{out} **	
Before treatment	22.0 ± 2.1	-	0.0
Water scrubbing from top, 0kV	-	12.8 ± 0.9	41.8 ± 3.0
Water scrubbing from bottom, 0kV	-	15.2 ± 1.5	30.9 ± 3.0
Water scrubbing from top and Bottom, 0kV	-	11.9 ± 1.0	45.9 ± 4.5
Water scrubbing from top, 15kV	-	10.9 ± 0.8	50.5 ± 3.5
Water scrubbing from bottom, 15kV	-	12.9 ± 1.0	41.4 ± 4.0
Water scrubbing from top and Bottom, 15kV	-	9.6 ± 0.95	56.4 ± 5.5
Water scrubbing from top, 25kV	-	9.3 ± 0.65	57.7 ± 4.0
Water scrubbing from bottom, 25kV	-	9.9 ± 0.9	55.0 ± 5.0
Water scrubbing from top and Bottom, 25kV	-	6.1 ± 0.65	72.3 ± 7.0

* Model tar concentration before treatment   ** Model tar concentration after treatment
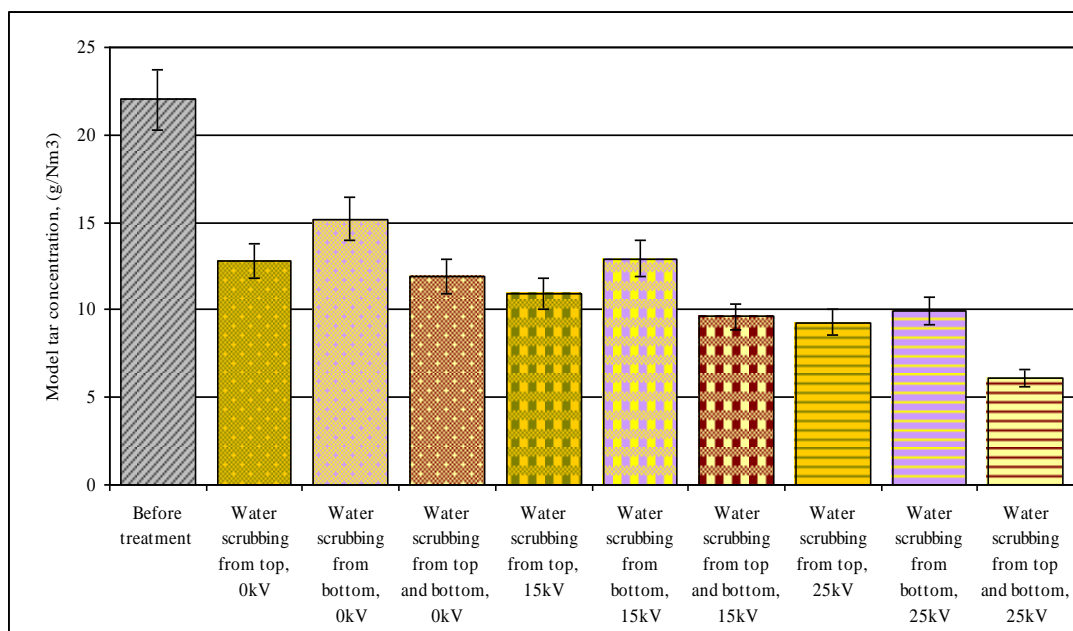
Figure (4.21): Comparison between top, bottom and simultaneous top and bottom water scrubbing with or without different rates of high voltage vs. the model tar concentration
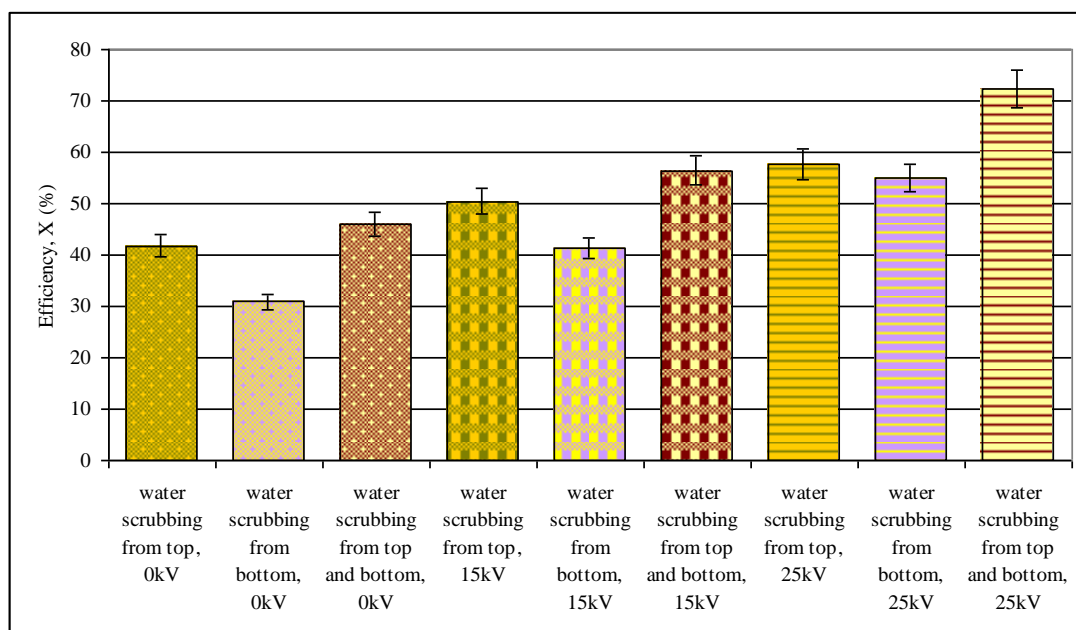
Figure (4.22): Comparison between top, bottom and simultaneous top and bottom water scrubbing with or without different rates of high voltage vs. the model tar reduction efficiency

4.3.2.1.5. Effect of High Voltage at Different Rates on the Model Tar Reduction Efficiency

The previous section presented and discussed the finding obtained from the comparison between the effect of top, bottom and simultaneous top and bottom water scrubbing with or without different rates of high voltages using CIE configuration as a secondary treatment process on the model tar reduction efficiency and concentration. In this section, results of model tar reduction efficiency under the influence of high voltage (CEI) at different rate was tested and discussed. The experiments were carried out in a period of 3 hours and repeated twice to ensure reproducibility of results. The concentration of the model tar was measured at the entrance, C_{in}, to the reactor and at the exit C_{out}, after model tar reduction or/and removal. Tar reduction efficiency (X) is calculated from equation (4.1). The following processing conditions were used:

Model syngas flow rate = 1 litre/min; Cin = 22.0 ± 2.1 g/Nm^3;

Gas inlet temperature = 43 ± 3 $^\circ$C; Gas outlet temperature = 20 ± 2 $^\circ$C;

Total surface area of the insulated high voltage electrode = 810 cm^2; and

Applied high voltage = 0-25 kV

The summary of experimental results is given in Table (4.18), Figure (4.23) and Figures (24-a-c). Overall, the application of an electric field(s) (0–25 kV) resulted in increased model tar reduction efficiency, in comparison to tar reduction or/and removal with no electrical field. For instance, tar reduction was 19.1 % with no voltage applied and it increased to 30.0 % when the high voltage was 25 kV.

Table (4.18): Influence of high voltage at different rates on the model tar reduction efficiency

Cleaning System → Parameter ↓	Applied voltage (kV)		
	0	10	25
C_{out} [**] (g/Nm^3)	17.8 ± 1.06	17.2 ± 1.03	15.4 ± 0.92
Efficiency X (%)	19.1 ± 1.15	21.8 ± 1.3	30.0 ± 1.8
GC – Figures (4.24-a-c)	Figure (4.24-a)	Figure (4.24-b)	Figure (4.24-c)

[**] Model tar concentration after treatment
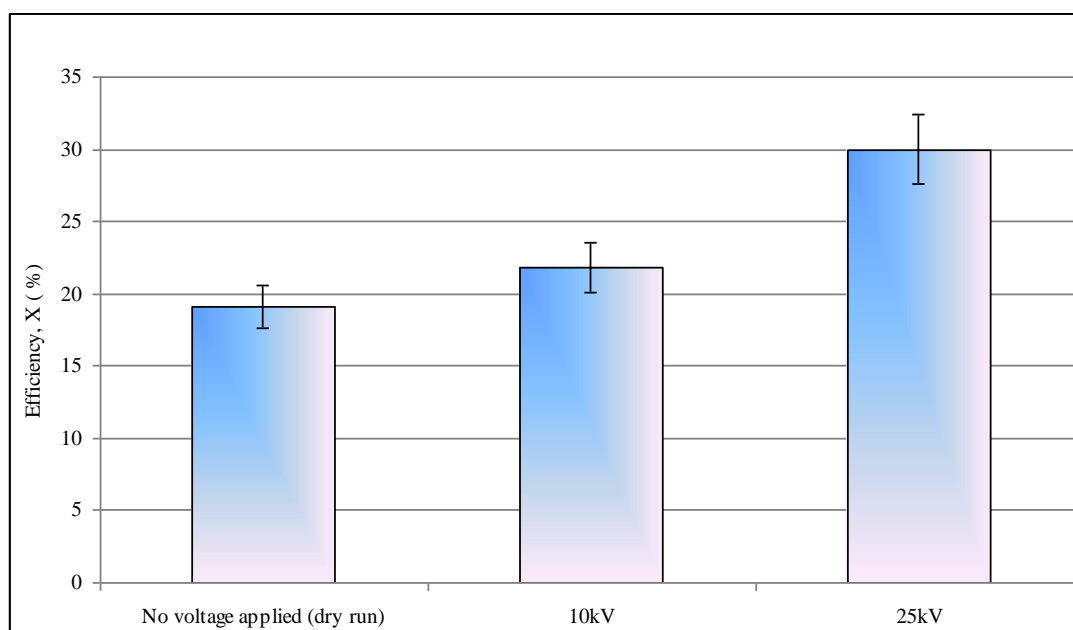
Figure (4.23): Effect of high voltage at different rates on the model tar reduction efficiency

Generally, with reference to Table (4.18) and Figure (4.23), the effect of high voltage input on model tar reduction or/and removal efficiency was clear. Model tar reduction efficiency increased as the high voltage increased. As indicated in Figure (4.23) above. A 21.8 % in model tar reduction was achieved with 10 kV input and an

additional 8.2 % increase in tar removal was observed when the high voltage increased from 10 to 25 kV to produce an overall 30.0 % increase in tar removal.

Also, the model tar reduction or/and removal efficiency results presented above are also clear confirmed by gas chromatography experiments (hydrocarbon profile of model syngas shifted towards low carbon number after treatment). Figure (4.7) and Figure (4.24-a-c) are the gas chromatograms of model syngas at the entrance to the reactor (Figure 4.7) and at the exit of the reactor after treatment with different rate of high voltage as tabulated in Table (4.18). Electric field with a packed bed of sulphonated PHP particles will be discussed in later section of this Chapter.
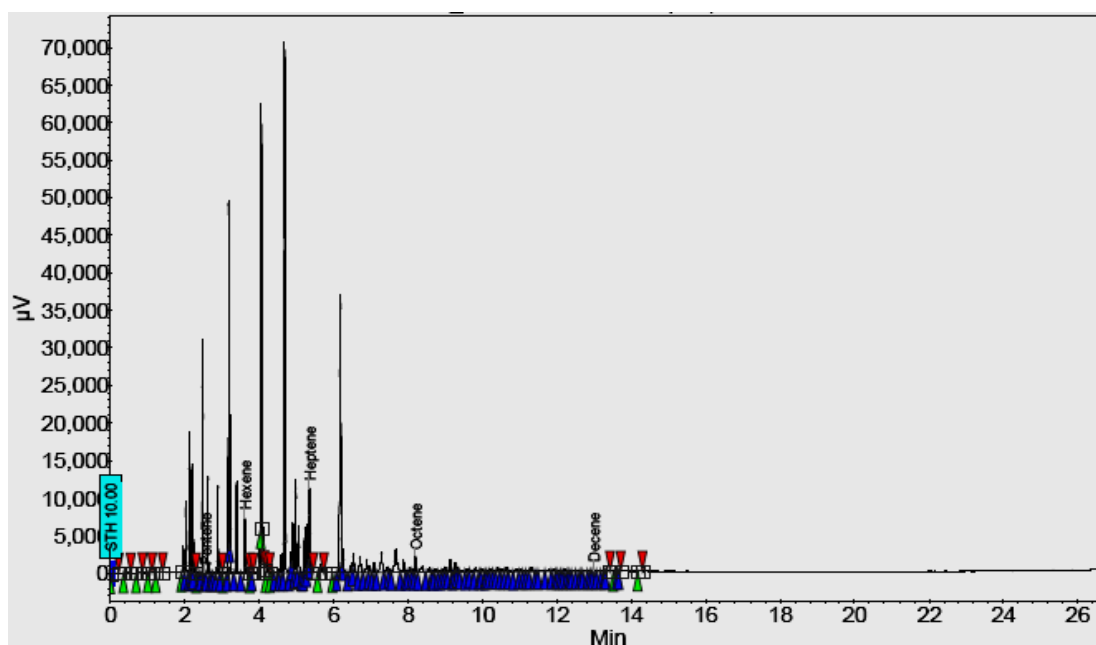
Figure (4.24-a): Gas chromatogram of the model syngas at 0kV and No polymer present (sampling location SP2 after the reactor shown in Figure 3.19). Note that the full scale of abundance (μV) is 70000 units
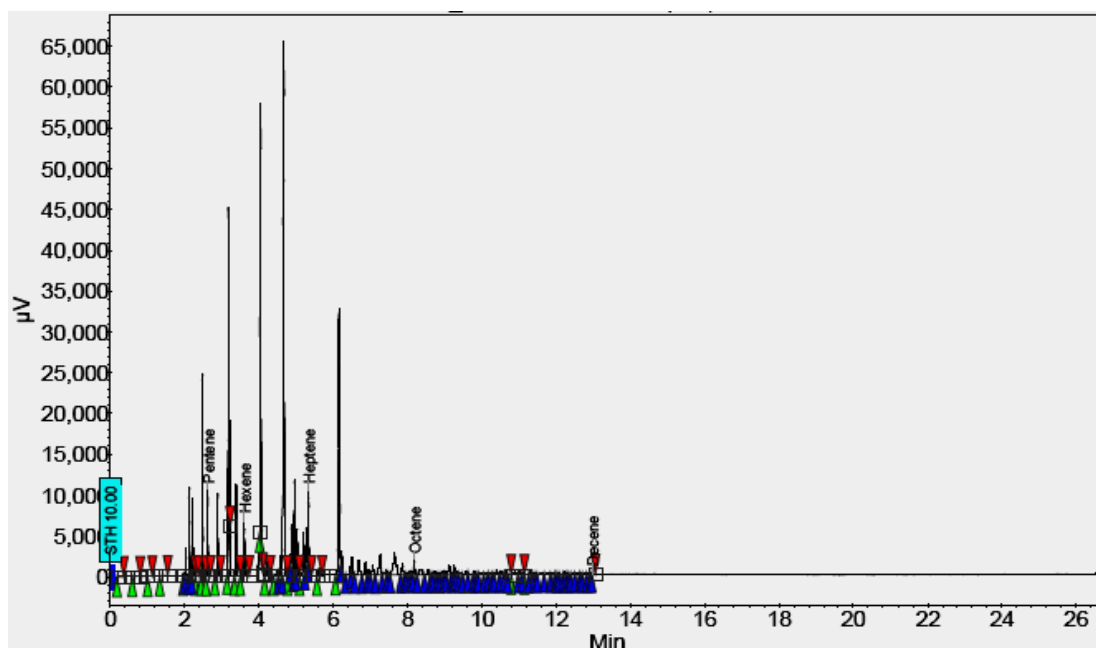
Figure (4.24-b): Gas chromatogram of the model syngas after high voltage treatment at 10kV without any polymer (sampling location SP2 after the reactor shown in Figure 3.19). Note that the full scale of abundance (µV) is 65000 units

Figure (4.24-c): Gas chromatogram of the model syngas after high voltage treatment at 25kV without any polymer (sampling location SP2 after the reactor shown in Figure 3.19). Note that the full scale of abundance (µV) is 60000 units

4.3.2.1.6. Effect of High Voltage at Different Rates with Sulphonated PolyHIPE Polymer (PHP) on the Model Tar Reduction Efficiency

In this section, the performance of packed bed of s-PHP (in the form of ca. 3 cm diameter, 5 mm thick disks) with or without different rate of high voltage in scavenging model tar from model syngas was investigated using a flow-through electric field enhanced tar removal equipment. The packed bed of s-PHP particles were exposed over a period of 3 h to 180 Nm^3 of model tar/syngas mixture. The concentration of the model tar was measured at the entrance, C_{in}, to the reactor and at the exit C_{out}, after model tar reduction or/and removal. Tar reduction efficiency (X) is calculated from equation (4.1). The following processing conditions were used:

Model syngas flow rate = 1 litre/min; Cin = 22.0 ± 2.1 g/Nm^3;

Gas inlet temperature = 43 ± 3 $^°$C; Gas outlet temperature = 20 ± 2 $^°$C;

Total surface area of the insulated high voltage electrode = 810 cm^2;

Applied high voltage = 0-25 kV; and

Amount of sulphonated PolyHIPE Polymer used as packing material (in the form of ca. 3 cm diameter, 5 mm thick disks) = 76g

The results are summarised in Table (4.19) and Figures (4.25) and (4.26-a-c).

Table (4.19): Influence of high voltage at different rates with sulphonated PolyHIPE Polymer (s-PHP) on the model tar reduction efficiency

Cleaning System →	Applied voltage (kV) with a packed bed of s-PHP		
Parameter ↓	0	10	25
C_{out} ** (g/Nm^3)	8.4 ± 0.6	7.2 ± 0.45	4.8 ± 0.42
Efficiency X (%)	61.8 ± 3.8	67.3 ± 4.2	78.2 ± 4.5
GC – Figures (4.26-a-c)	Figure (4.26-a)	Figure (4.26-b)	Figure (4.26-c)

** Model tar concentration after treatment

Tar/syngas mixture collection was carried out at sampling points SP-1 and SP-2 every 30 minutes before and after the packed bed of s-PHP disks (Figure 3.16). GC chromatograms of the tar/syngas mixture collected before and after passing through the packed bed of s-PHP disks at different rate of high voltage are shown in Figures (4.7, before treatment and 4.26-a-c after treatment). It can be seen that a large

number of components have been reduced; this may be due to tar reaction with s-PHP and the function of this electrode is to capture and retain the tars when they are repelled radically outwards under the combined influence of electric and flow fields. Nevertheless, there is substantial reduction in the overall model tar content in model tar/syngas mixture following extraction with s-PHP disks with or without different rate of high voltage. Note that the full scales of abundance (μV) are 85000, 32000, 26000 and 18000 units in Figures (4.7, No treatment), (4.26-a, s-PHP + 0kV), (4.26-b, s-PHP + 10kV) and (4.37-c, s-PHP + 25kV), respectively.

Figure (4.25): Effect of high voltage at different rates with a packed bed of sulphonated PolyHIPE Polymer (s-PHP) on the model tar reduction efficiency
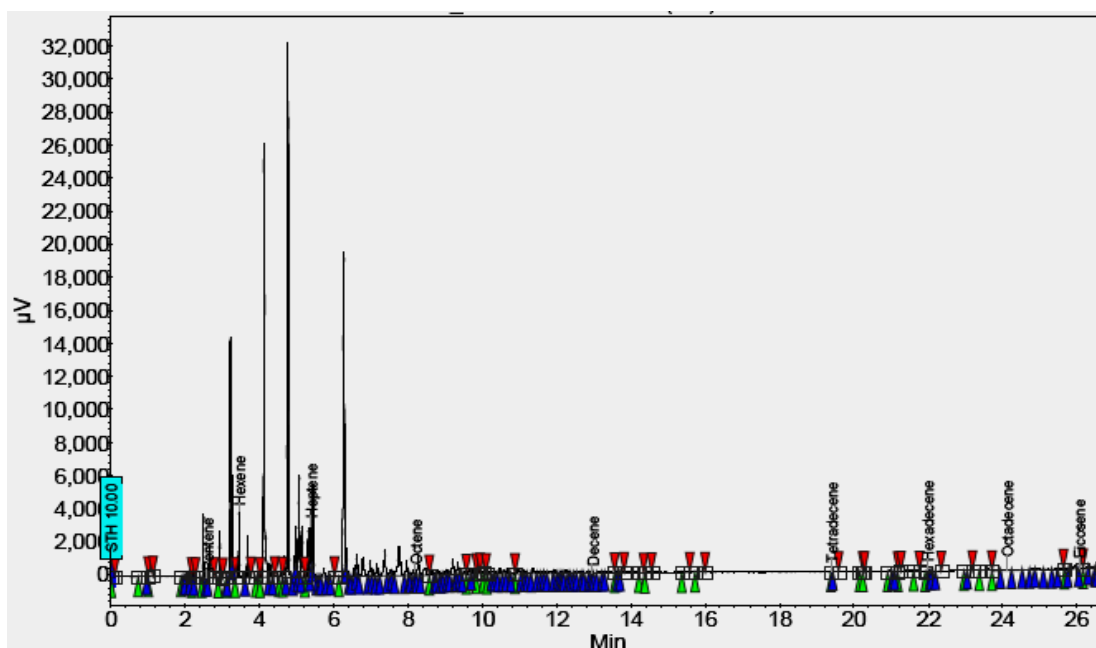
Figure (4.26-a): Gas chromatogram of the model syngas at 0kV with a packed bed of sulphonated PolyHIPE Polymer (s-PHP) (sampling location SP2 after the reactor shown in Figure 3.19). Note that the full scale of abundance (µV) is 32000 units
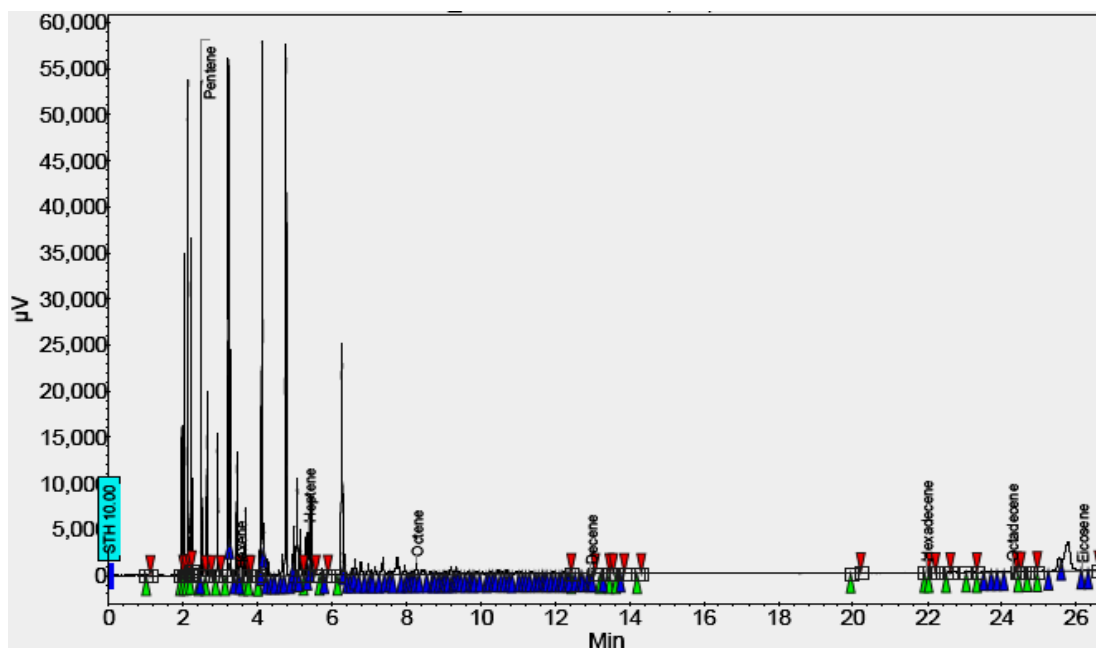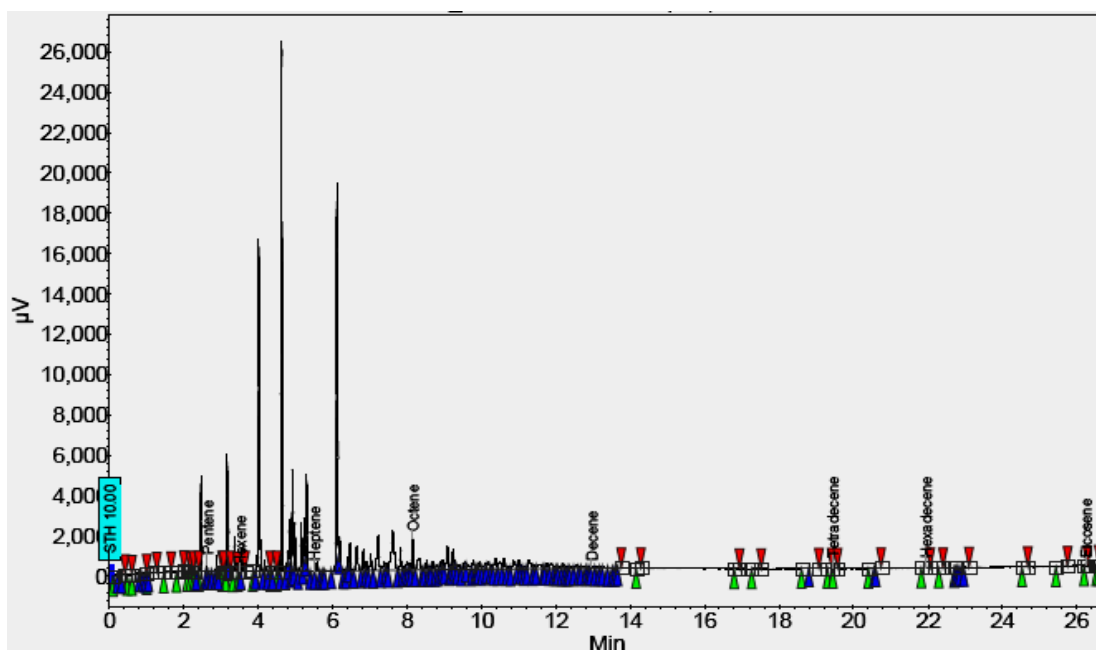

Figure (4.26-b): Gas chromatogram of the model syngas after high voltage treatment at 10kV with a packed bed of sulphonated PolyHIPE Polymer (s-PHP) (sampling location SP2 after the reactor shown in Figure 3.19). Note that the full scale of abundance (µV) is 26000 units

164
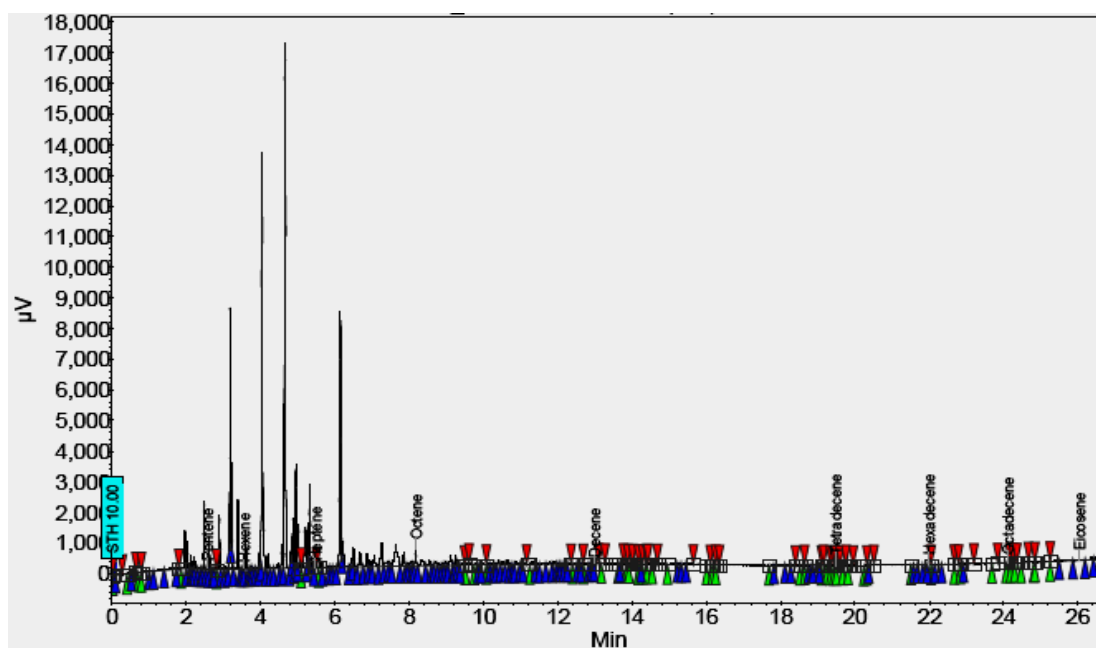
Figure (4.26-c): Gas chromatogram of the model syngas after high voltage treatment at 25kV with a packed bed of sulphonated PolyHIPE Polymer (s-PHP) (sampling location SP2 after the reactor shown in Figure 3.19). Note that the full scale of abundance (μV) is 18000 units

4.3.2.1.7. Comparison between the Effects of High Voltages at Different Rates with or without a Sulphonated PolyHIPE Polymer (s-PHP) on the Model Tar Reduction Efficiency

The objective of this section is to compare the effect of high voltages electrode at different rates with or without a packed bed of s-PHP (in the form of ca. 3 cm diameter, 5 mm thick disks) on the model tar reduction or/and removal performance. The results achieved in sections (4.3.2.1.5. – 4.3.2.1.6.) are discussed and summarized here.

It can be seen from Table (4.20) that a clear trend of the change in model tar concentration and model tar reduction efficiency. However, in term of model tar concentration, g/Nm^3, see Figure (4.27), in the treated model syngas, in reference to that obtained in the reference experiment, it is to the lowest under the influence of a packed bed of s-PHP with 25kV high voltage, and with a packed bed of s-PHP with 10kV high voltage. It is higher when using a packed bed of s-PHP alone and using high voltage at 25kV without s-PHP, respectively. It is even higher with high voltage at 25kV without a packed bed of s-PHP disks.
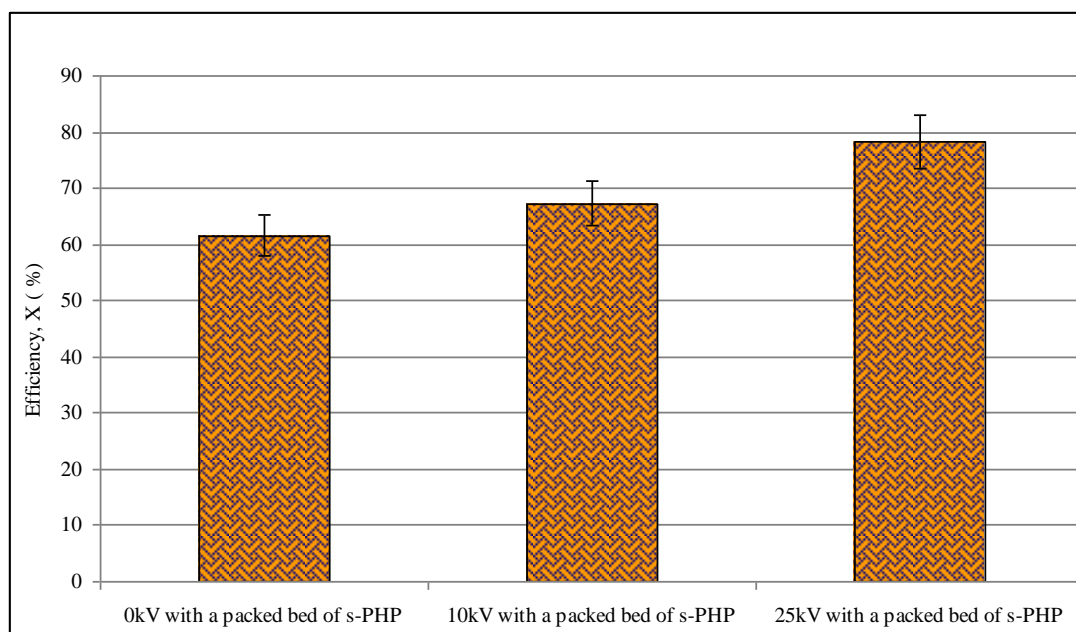
Table (4.20): Comparison between the effect of high voltage at different rates with or without sulphonated PolyHIPE Polymer (s-PHP) on the model tar reduction efficiency and concentration

Effect of Parameter → Cleaning System ↓	(g/Nm^3)		Efficiency X (%)
	C_{in} [*]	C_{out} [**]	
Before treatment	22.0 ± 2.1	-	0.0
0kV, No packed bed present	-	17.8 ± 1.06	19.1 ± 1.15
0kV with a packed bed of s-PHP	-	8.4 ± 0.6	61.8 ± 3.8
10kV, No packed bed present	-	17.2 ± 1.03	21.8 ± 1.3
10kV with a packed bed of s-PHP	-	7.2 ± 0.45	67.3 ± 4.2
25kV, No packed bed present	-	15.4 ± 0.92	30.0 ± 1.8
25kV with a packed bed of s-PHP	-	4.8 ± 0.42	78.2 ± 4.5

[*] Model tar concentration before treatment   [**] Model tar concentration after treatment
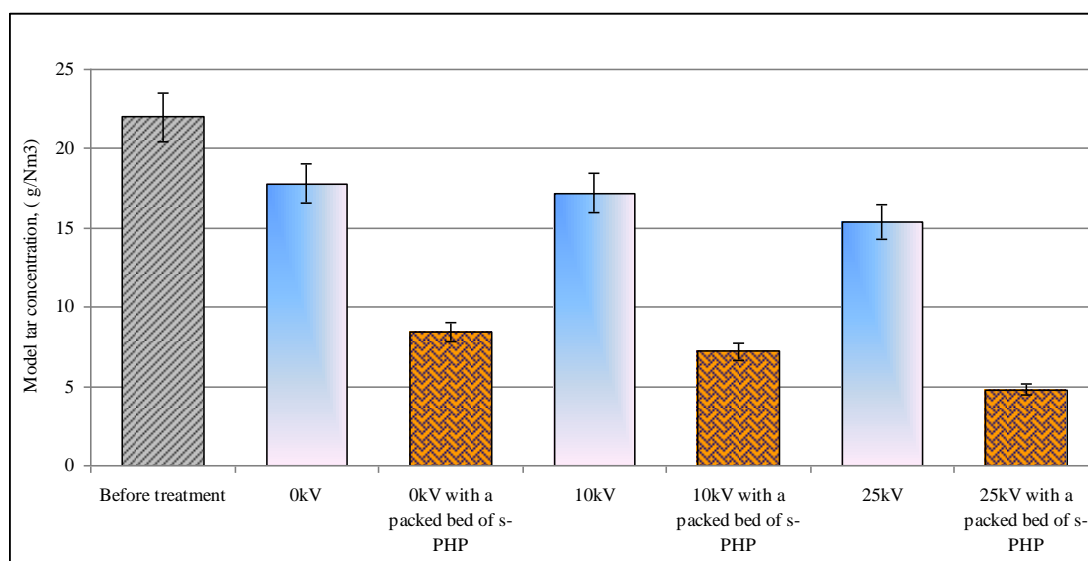
Figure (4.27): Comparison between the effect of high voltage at different rates with or without a packed bed of sulphonated PolyHIPE Polymer (s-PHP) on the model tar concentration
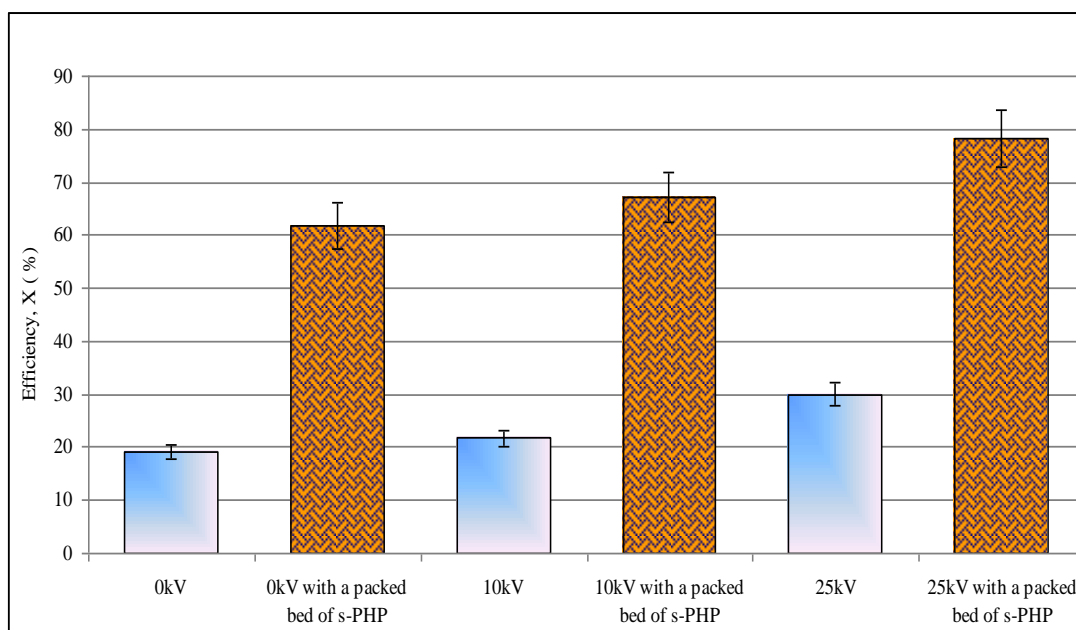
Figure (4.28): Comparison between the effect of high voltage at different rates with or without a packed bed of sulphonated PolyHIPE Polymer (s-PHP) vs. the model tar reduction efficiency

Having completed, discussed and analysed the results achieved from the experiments on the pilot scale system using a completely (totally) insulated electrode (CIE) configuration (total surface area of the insulated high voltage electrode = 810 cm^2); other results using the same equipment but with partially isolated electrode (PIE) configuration (total surfaces area of the exposed part of the partially insulated electrode = 290 cm^2), when no conductive material was present in the gas stream or in the fixed bed, will be presented and discussed in the next sections. Out of the results obtained from these experiments, comparisons were made in terms of tar reduction efficiency and concentration.

4.3.2.2. Experiments with a Partially Insulated Electrode (PIE)

The results of the experimental work performed with PIE (total surfaces area of the exposed part of the partially insulated electrode = 290 cm^2) configuration are represented and discussed in the following sections. The syngas cleaning equipment with PIE was tested under an electric field at different intensities in the absence and presence of a packed bed of s-PHP (in the form of ca. 3 cm diameter, 5 mm thick

disks). Out of the results obtained from these experiments, comparisons were made in terms of tar reduction efficiency and concentration.

4.3.2.2.1. Effect of High Voltage at Different Rates on the Model Tar Reduction Efficiency

The summary of experimental results is given in Table (4.21) and Figure (4.29). In these experiments, effect of high voltage is evident. As the high voltage was increased, tar capture was higher. For instance, tar capture was 80.1 % with 10 kV high voltage was applied and it increased to 97.5 % when the high voltage was 25 kV. These results are also in line with GC results shown in Figures (4.30a-c).

Table (4.21): Influence of high voltage at different rates on the model tar reduction efficiency

Cleaning System → Parameter ↓	Applied voltage (kV)		
	0	10	25
C_{out}** (g/Nm^3)	17.8 ± 1.06	4.3 ± 0.09	0.56 ± 0.01
Efficiency X (%)	19.1 ± 1.15	80.1 ± 1.6	97.5 ± 1.95
GC – Figures (4.30a-c)	Figure (4.30a)	Figure (4.30b)	Figure (4.30c)

** Model tar concentration after treatment
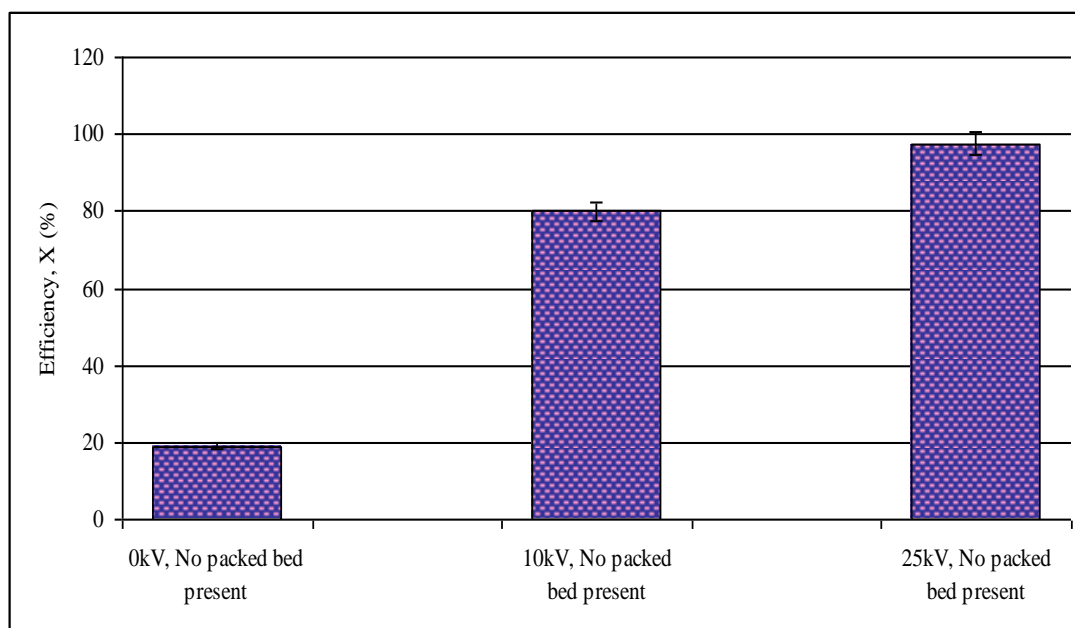
Figure (4.29): Effect of high voltage at different rates on the model tar reduction efficiency

168

The effect of the combination of high voltage at different rate with a packed bed of 20g crushed s-PHP particles (approximately 2-3 mm in size) as a secondary model syngas treatment system on model tar reduction efficiency and reducing the concentration in producer model syngas will be discussed in the following section.
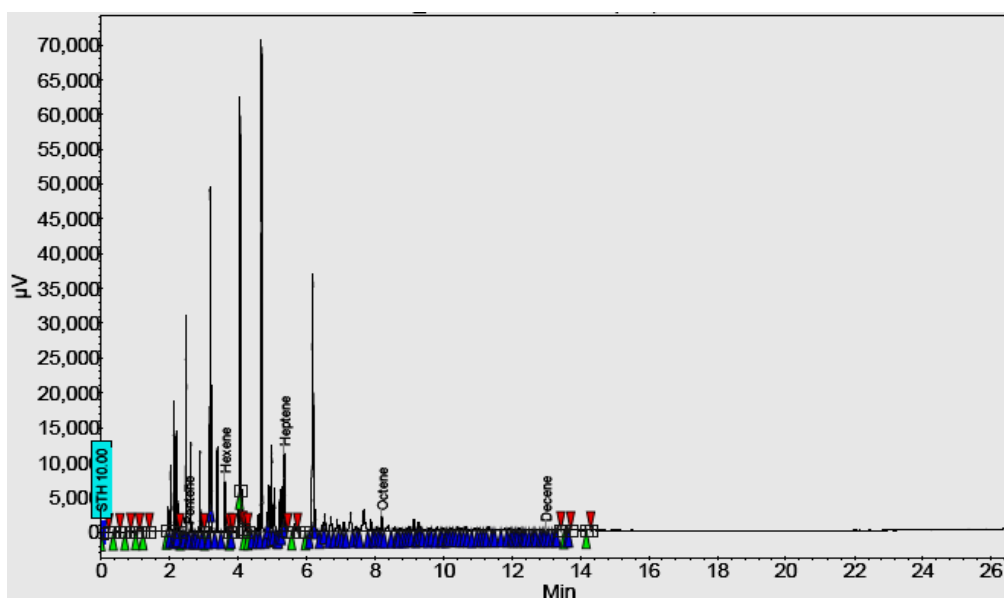
Figure (4.30a): Gas chromatogram of the model syngas at 0kV and No polymer present (sampling location SP2 after the reactor shown in Figure 3.19). Note that the full scale of abundance (μV) is 70000 units
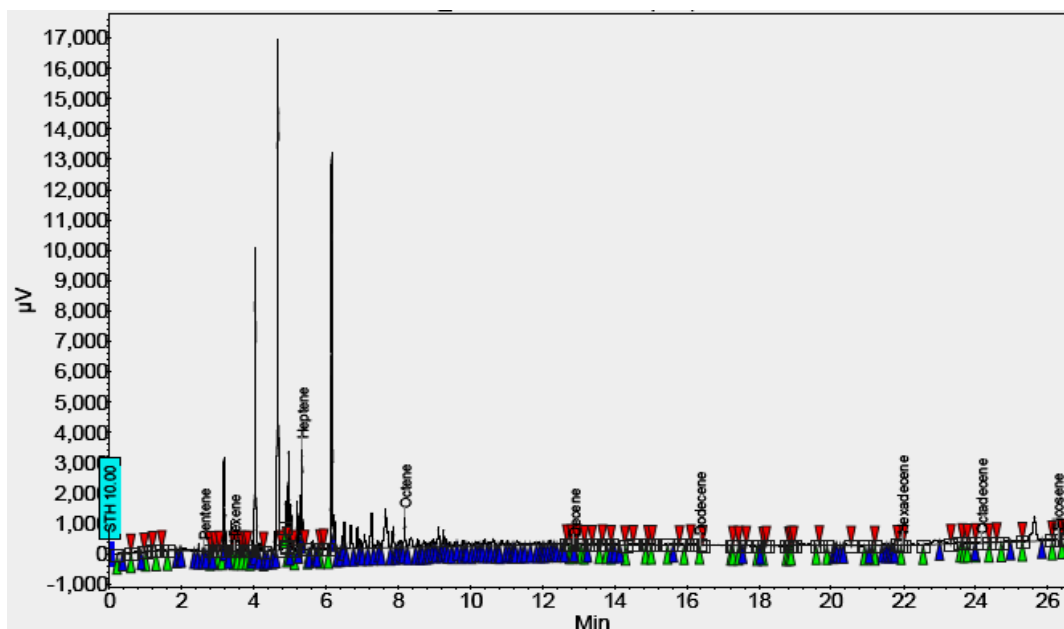
Figure (4.30b): Gas chromatogram of the model syngas after high voltage treatment at 10kV without any polymer (sampling location SP2 after the reactor shown in Figure 3.19). Note that the full scale of abundance (μV) is 17000 units
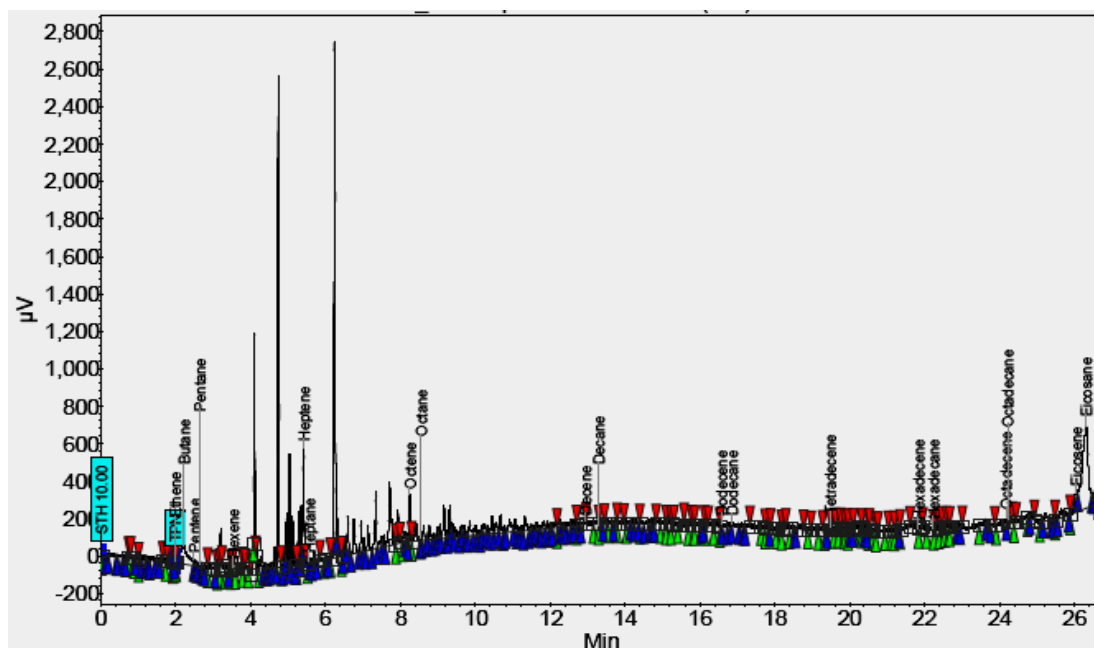
Figure (4.30c): Gas chromatogram of the model syngas after high voltage treatment at 25kV without any polymer (sampling location SP2 after the reactor shown in Figure 3.19). Note that the full scale of abundance (μV) is 2800 units

4.3.2.2.2. Effect of High Voltages at Different Rates with a Sulphonated PolyHIPE Polymer (s-PHP) on the Model Tar Reduction Efficiency

The previous section presented and discussed the results obtained from the effect of high voltage at different rates on the model tar reduction efficiency and concentration. In this section, results of model tar reduction efficiency under the effect of high voltage at different rate with or without the performance of a packed bed of crushed s-PHP particles will be discussed and analysed in this section. The mechanism of tar reduction by PHPs polymer is adsorbed on the active sites of the PHPs particle surface. The surface area of the s-PHP used in this study is presented in Table (4.10). The concentration of the model tar was measured at the entrance, C_{in}, to the reactor and at the exit C_{out}, after model tar reduction or/and removal. Tar reduction efficiency (X) is calculated from equation (4.1).

The experiments were carried out in a period of 3 hours with a model syngas flow rate was 1 litre/min, temperature of the inlet gas was kept at 43 ± 3 ^{0}C and a packed bed of 20g crushed s-PHP particles (approximately 2-3 mm in size). Each experiment was repeated twice to ensure reproducibility of results. In all cases, the

170

inlet and outlet model syngas composition were monitored using gas chromatography (GC). Out of the results obtained from these experiments, comparisons were made in terms of model tar reduction or/and removal efficiency and concentration. The summary of experimental results is given in Table (4.22).

Table (4.22): Influence of high voltage at different rates with sulphonated PolyHIPE Polymer (s-PHP) on the model tar reduction efficiency

Cleaning System → Parameter ↓	Applied voltage (kV) with a packed bed of s-PHP		
	0	10	25
C_{out}** (g/Nm^3)	8.40 ± 0.6	2.94 ± 0.09	0.72 ± 0.02
Efficiency X (%)	61.8 ± 3.8	86.6 ± 2.6	96.7 ± 2.9
GC – Figures (4.32 a-b)	Figure (4.32 a)	Figure (4.32 b)	-

** Model tar concentration after treatment

Therefore, model tar reduction or/and removal efficiency out of a packed bed of 20g crushed s-PHP particles (approximately 2-3 mm in size) with a model syngas flow rate was 1 litre/min in a period of 3 hours has been calculated from equation (4.1) as follows:

C_{in} = 22.0 g/Nm^3

C_{out} = 9.0 g/Nm^3

Therefore:

X = (22.0–9.0) ÷ 22.0 × 100

   = 0.591 × 100

   = 59.1%

The results showed that under the influence of a packed bed of 20g crushed s-PHP particles (approximately 2-3 mm in size) used as a secondary model syngas treatment system, the model tar was adsorbed on the active sites of the crushed s-PHP particle surface and reducing the concentration. As indicated in Figure (4.31), it clear that the best result is obtained with 25 kV with a packed bed of crushed s-PHP particles as a result of PHP particles surface area as well as due to the applied of high voltage.

Also, the model tar reduction or/and removal efficiency results presented above are also clear confirmed by gas chromatography experiments (hydrocarbon profile of model syngas shifted towards low carbon number after treatment). Figure (4.7) and Figure (4.32-a-d) are the gas chromatograms of model syngas at the entrance to the reactor (Figure 4.7) and at the exit of the reactor after treatment with a packed bed of various types of 20g crushed polymers particles (approximately 2-3 mm in size and total weight 20g) as tabulated in Table (4.22).

It is noted from the experimental results that, the model tar reduction efficiency with the use of a packed bed of crushed s-PHPs particles with a high voltage at different rate ranging from 61.8 − 96.7%. A similar reduction in tar was observed by Akay et al., (2013) working on a downdraft gasifier fuelled by fuel cane bagasse as a model biomass who reported that the s-PHP (diameter = 25 mm, thickness = 5 mm) used as a secondary syngas treatment system, was highly effective at adsorbing and reducing the concentration of all class of tars in syngas by 80%-95%.

Figure (4.31): Effect of high voltage at different rates with a packed bed of sulphonated PolyHIPE Polymer (s-PHP) on the model tar reduction efficiency

Out of these experiments, it can be concluded that, the effect of high voltage is evident. As the high voltage was increased, tar capture was higher. For instance, tar capture was 86.6 % with 10kV electric field was applied and it increased to 96.7 % when the electric field was 25 kV. Also, from Table (4.22) above, it can be seen that

172

as the high voltage increased from 0kV to 25kV the model tar reduction increased from 61.8% to 96.7% an increase of 35 %. Also the concentration decreased from 8.4 to 0.72 g/Nm^3 a decrease of 7.7g/Nm^3.
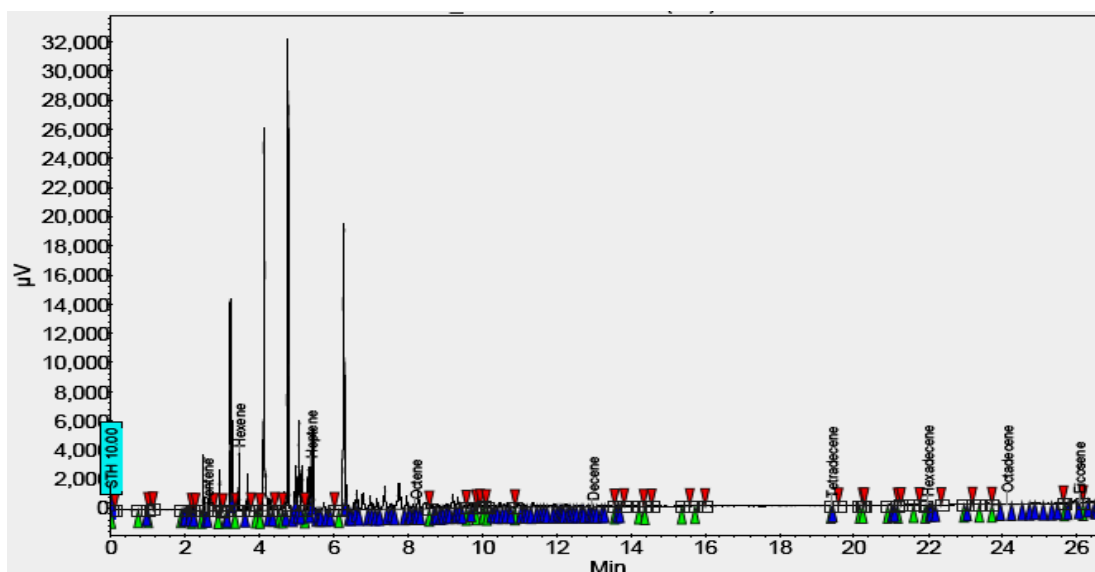
Figure (4.32a): Gas chromatogram of the model syngas at 0kV with a packed bed of sulphonated PolyHIPE Polymer (s-PHP) (sampling location SP2 after the reactor shown in Figure 3.19). Note that the full scale of abundance (μV) is 32000 units
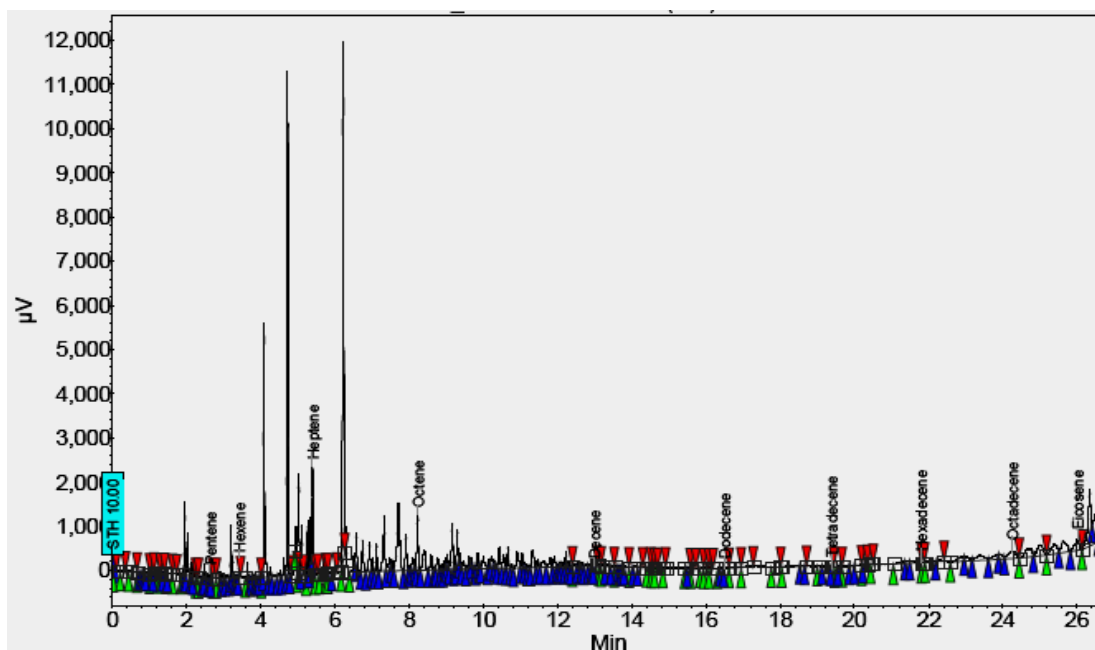
Figure (4.32b): Gas chromatogram of the model syngas after high voltage treatment at 10kV with a packed bed of sulphonated PolyHIPE Polymer (s-PHP) (sampling location SP2 after the reactor shown in Figure 3.19). Note that the full scale of abundance (μV) is 12000 units

4.3.2.2.3. Comparison between the Effects of High Voltages at Different Rates with or without Sulphonated PolyHIPE Polymer (s-PHP) on the Model Tar Reduction Efficiency

The results achieved in sections (4.3.2.2.1.– 4.3.2.2.2.) are discussed and summarized here. Table (4.23) below, shows a clear trend of the change in model tar concentration and model tar reduction efficiency. However, in term of model tar concentration, g/Nm^3, see Figure (4.33), in the treated model syngas, in reference to that obtained in the reference experiment, it is to the lowest under the influence of 25kV, No packed bed present (the function of this electrode is to capture and retain the tars when they are repelled radically outwards under the combined influence of electric and flow fields).
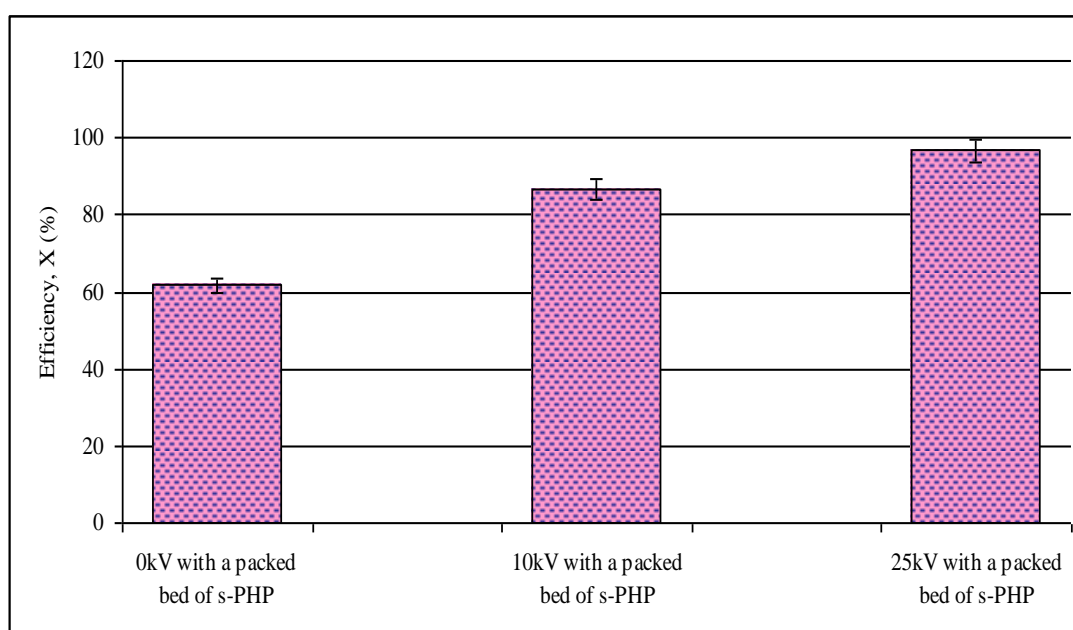
Table (4.23): Comparison between the effects of high voltage at different rates with or without sulphonated PolyHIPE Polymer (s-PHP) on the model tar reduction efficiency and concentration

Effect of Parameter $\rightarrow$	(g/Nm^3)		Efficiency
Cleaning System $\downarrow$	C_{in} *	C_{out} **	X (%)
Before treatment	22.0 ± 2.1	-	0.0
0kV, No packed bed present	-	17.8 ± 1.06	19.1 ± 1.15
0kV with a packed bed of s-PHP	-	8.4 ± 0.6	61.8 ± 3.8
10kV, No packed bed present	-	4.3 ± 0.09	80.1 ± 1.6
10kV with a packed bed of s-PHP	-	2.94 ± 0.09	86.6 ± 2.6
25kV, No packed bed present	-	0.56 ± 0.01	97.5 ± 1.95
25kV with a packed bed of s-PHP	-	0.72 ± 0.02	96.7 ± 2.9

*Model tar concentration after treatment **Model tar concentration after treatment
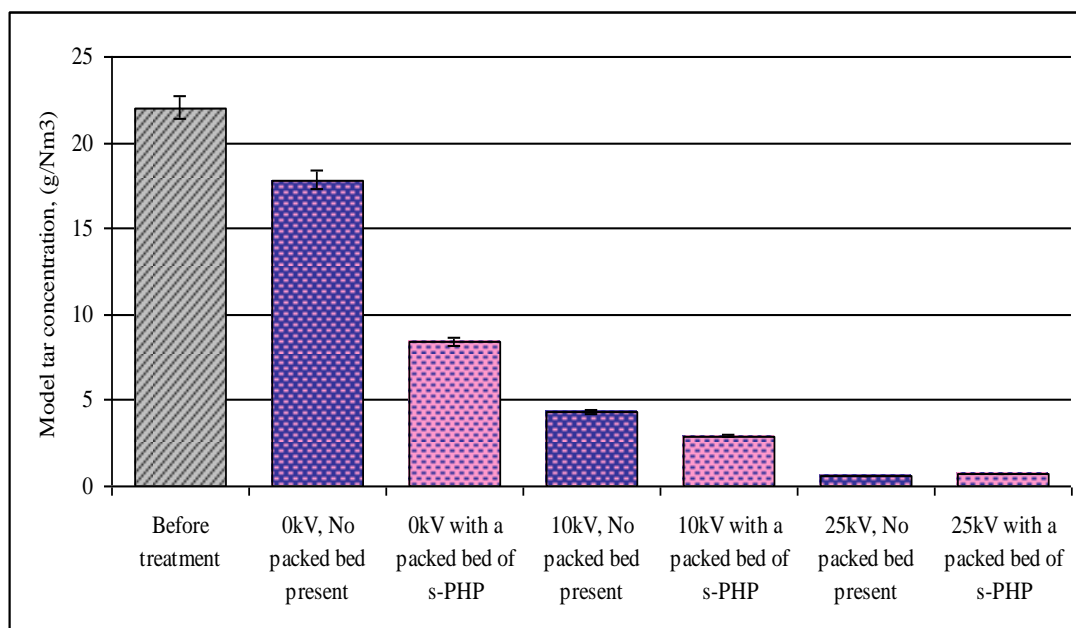
Figure (4.33): Comparison between the effects of high voltage at different rates with or without a packed bed of sulphonated PolyHIPE Polymer (s-PHP) vs. the model tar concentration
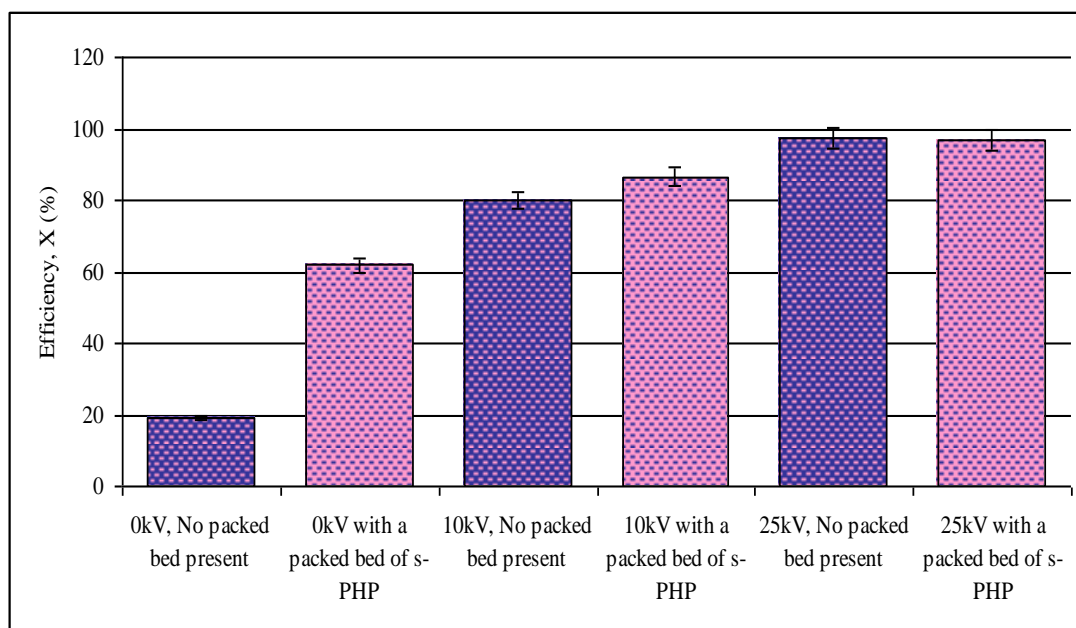
Figure (4.34): Comparison between the effects of high voltage at different rates with or without a packed bed of sulphonated PolyHIPE Polymer (s-PHP) vs. the model tar reduction efficiency

4.3.3. Comparison between the Effects of all Different Intensified Applications Employed on the Model Tar Reduction Efficiency

The aims set at the beginning of this study have been met and this work managed to fill a gap in gas cleanup and treatment technologies. The main characteristics and findings on effects of the variables tested in this work on model tar reduction efficiency and concentrations are summarised in Table (4.24) and Figures (4.35-36). In summary the results of this study show that:

In the small scale intensified syngas cleaning system, experiments on a chemically surface modified PHPs developed in the laboratory and PHPs namely, PHP-B30, PHP-S30 and PHP-S30B10 and plasma at different power intensities with or without sulphonated PHP were performed. It can be concluded that polymer PHP-B30 gave the highest tar removal/conversion of 93.6%, due to its large surface area.

Also, in the small scale intensified syngas cleaning system, when plasma was applied in the presence of the polymer with the poorest performance on its own that's the sulphonated PHP, the highest tar removal/conversion of 91% was obtained. Experiments conducted with plasma only gave much lower tar removal/conversion of no more than 71.4%.

In the pilot scale intensified syngas cleaning system, out of the experiments when a completely insulated electrode (CIE) was used, the highest tar reduction was obtained when applying a high voltage of 25 kV with the aid of a s-PHP and a high voltage of 25 kV with a simultaneous (top and bottom) water scrubbing, respectively.

Furthermore, in the experiments when a partially insulated electrode (PIE) was used, it can be observed that the higher the voltage, the higher the tar reduction was. Out of these experiments, the highest tar reduction was 97.5%. Using a s-PHP while applying a high voltage, generally improves tar reduction up to 96.7%.

Table (4.24): Comparisons between the effects of all different intensified applications employed on the model tar reduction efficiency and concentration

| Effect of Parameter → Cleaning System ↓	C_{out} * (g/Nm^3)	Efficiency X (%)
s-PHP	9.0 ± 0.5	59.1 ± 3.0
PHP-B30	1.4 ± 0.1	93.6 ± 4.5
PHP-S30	5.6 ± 0.3	75.5 ± 3.5
PHP-S30B10	3.2 ± 0.16	85.5 ± 4.0
Plasma only (40W)	7.9 ± 0.6	64.1 ± 4.5
Plasma only (50W)	6.3 ± 0.44	71.4 ± 5.0
Plasma with a packed bed of s-PHP (40W)	4.3 ± 0.17	80.5 ± 3.0
Plasma with a packed bed of s-PHP (50W)	2.0 ± 0.08	91.0 ± 3.5
0kV, No packed bed present, (CIE)	17.8 ± 1.06	19.1 ± 1.1
10kV, No packed bed present, (CIE)	17.2 ± 1.03	21.8 ± 1.3
25kV, No packed bed present, (CIE)	15.4 ± 0.92	30.0 ± 1.8
0kV with a packed bed of s-PHP, (CIE)	8.4 ± 0.6	61.8 ± 3.8
10kV with a packed bed of s-PHP, (CIE)	7.2 ± 0.45	67.3 ± 4.2
25kV with a packed bed of s-PHP, (CIE)	4.8 ± 0.42	78.2 ± 4.5
Water scrubbing from top with 0kV, (CIE)	12.8 ± 0.9	41.8 ± 3.0
Water scrubbing from top with 10kV, (CIE)	11.3 ± 1.0	48.6 ± 3.5
Water scrubbing from top with 15kV, (CIE)	10.9 ± 0.8	50.5 ± 3.5
Water scrubbing from top with 20kV, (CIE)	10.7 ± 0.75	51.4 ± 3.5
Water scrubbing from top with 25kV, (CIE)	9.3 ± 0.65	57.7 ± 4.0
Water scrubbing from bottom with 0kV, (CIE)	15.2 ± 1.5	30.9 ± 3.0
Water scrubbing from bottom with 15kV, (CIE)	12.9 ± 1.0	41.4 ± 4.0
Water scrubbing from bottom with 20kV, (CIE)	11.2 ± 1.0	49.1 ± 4.5
Water scrubbing from bottom with 25kV, (CIE)	9.9 ± 0.9	55.0 ± 5.0
Water scrubbing from top and bottom with 0kV, (CIE)	11.9 ± 1.0	45.9 ± 4.5
Water scrubbing from top and bottom with 15kV, (CIE)	9.6 ± 0.95	56.4 ± 5.5
Water scrubbing from top and bottom with 25kV, (CIE)	6.1 ± 0.65	72.3 ± 7.0
10kV, No packed bed present, (PIE)	4.3 ± 0.09	80.1 ± 1.6
10kV with a packed bed of s-PHP, (PIE)	2.94 ± 0.09	86.6 ± 2.6
25kV, No packed bed present, (PIE)	0.56 ± 0.01	97.5 ± 1.9
25kV with a packed bed of s-PHP, (PIE)	0.72 ± 0.02	96.7 ± 2.9

* Model tar concentration after treatment
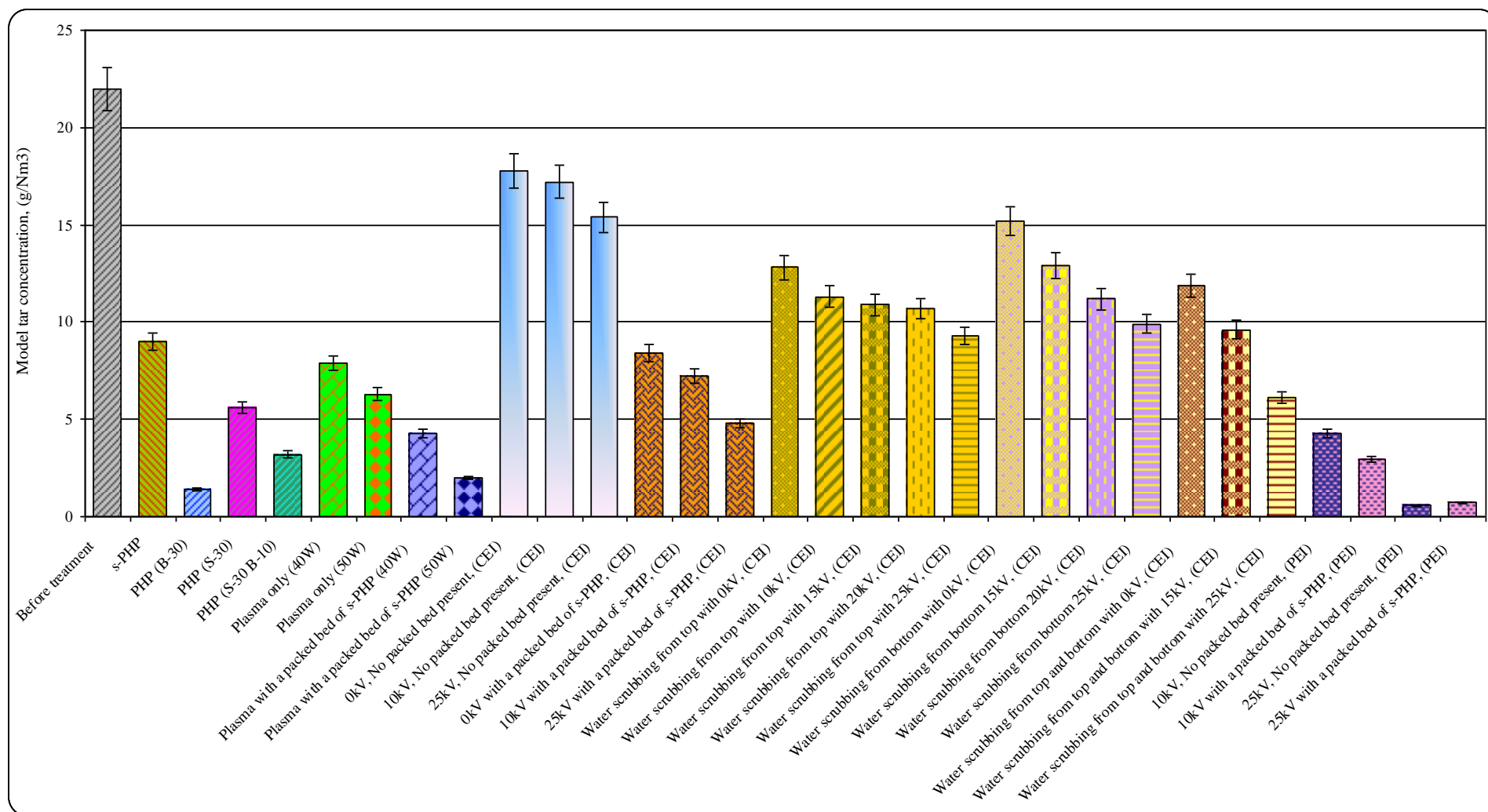
Figure (4.35): Different applications of intensified cleaning systems employed vs. the model tar concentration
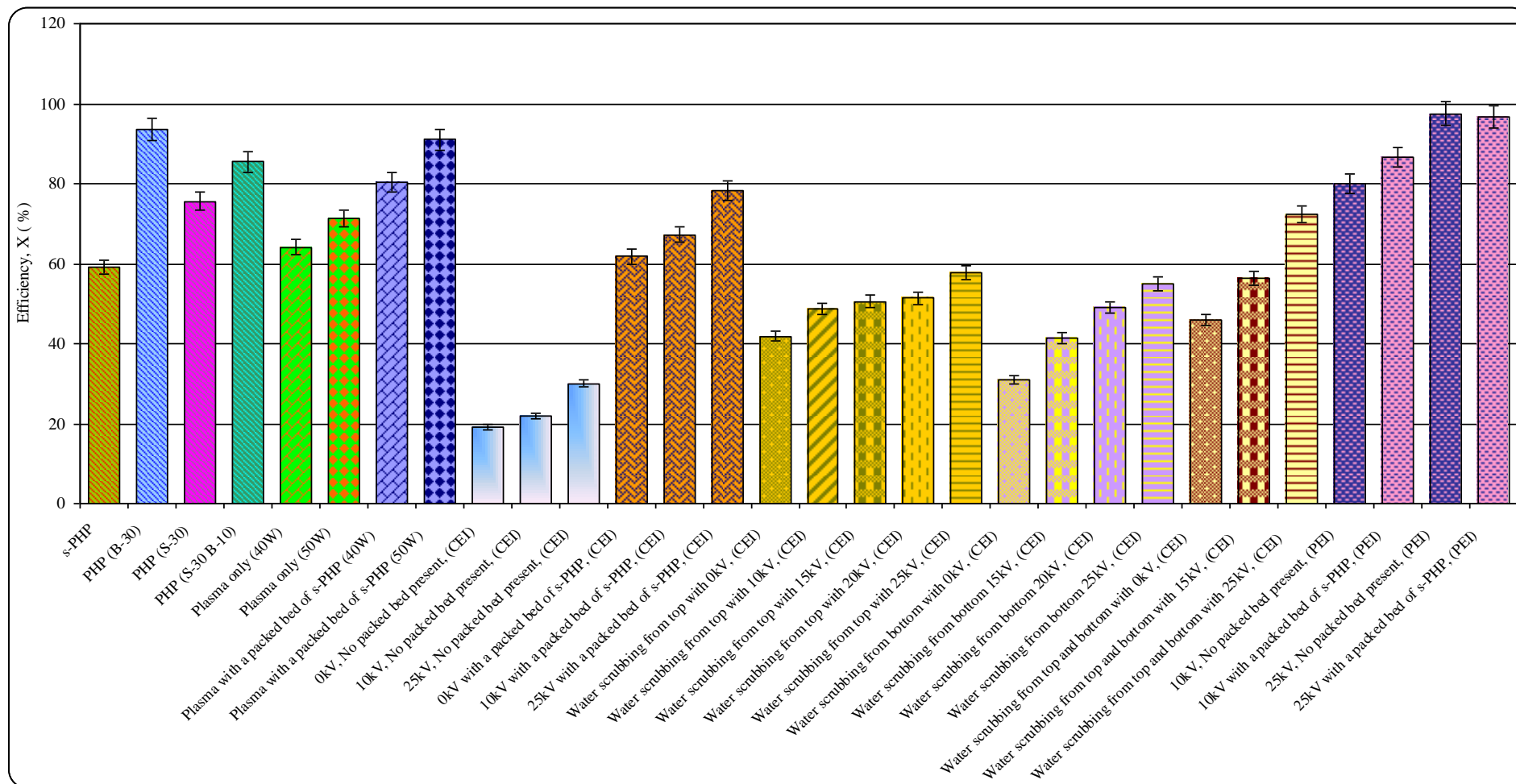
Figure (4.36): Different applications of intensified cleaning systems employed vs. the model tar reduction efficiency

4.3.4. Model Tar (crude oil) Scavenging from Model Syngas (CO_2) using sulphonated PolyHIPE Polymer (s-PHP)

The performance of s-PHP in scavenging model tar (crude oil) from model syngas (CO_2) was investigated using a flow-through two new/novel different setup systems namely, small (glass reactor) and pilot (electric field enhanced tar removal equipment) scale intensified syngas cleaning systems in which model tar/syngas mixture from these different setup flowed through a packed bed of s-PHP. In the case of small scale intensified syngas cleaning system, approximately 2-3 mm in size (Total weight = 20 g) of s-PHP particles were loaded into the space between the quartz tubes and retained by glass wool to prevent PHPs particles escape (Figure 3.16). While, in pilot scale intensified syngas cleaning system (electric field enhanced tar removal equipment), ca. 30 mm diameter, 5 mm thick disks (Total weight = 76 g) of s-PHP particles were placed between two perforated plates loaded on the tray where the central electrode was secured and another perforated plate just under the top cover plate of the reactor (Figure 3.20).

The packed bed of s-PHP particles were exposed over a period of 3 h to 180 Nm^3 of model tar/syngas mixture in both systems. Simultaneous tar/syngas mixture collection was carried out at sampling points SP-1 and SP-2 immediately before and after the packed bed of s-PHP particles (Figure 3.16) and (Figure 3.19), respectively. GC chromatograms of the tar/syngas mixture collected before and after passing through the packed bed of s-PHP disks are shown in Figures (4.37-a), (4.37-b) and (4.37-c), respectively. It can be seen that a large number of components have been reduced; this may be due to tar reaction with s-PHP. Nevertheless, there is substantial reduction in the overall model tar content in model tar/syngas mixture following extraction with s-PHP. Note that the full scale of abundance (μV) are 85000, 34000 and 32000 units in Figures (4.37-a), (4.37-b) and (4.37-c), respectively. The results are summarised in Table (4.25) and Figures (4.38) and (4.39).
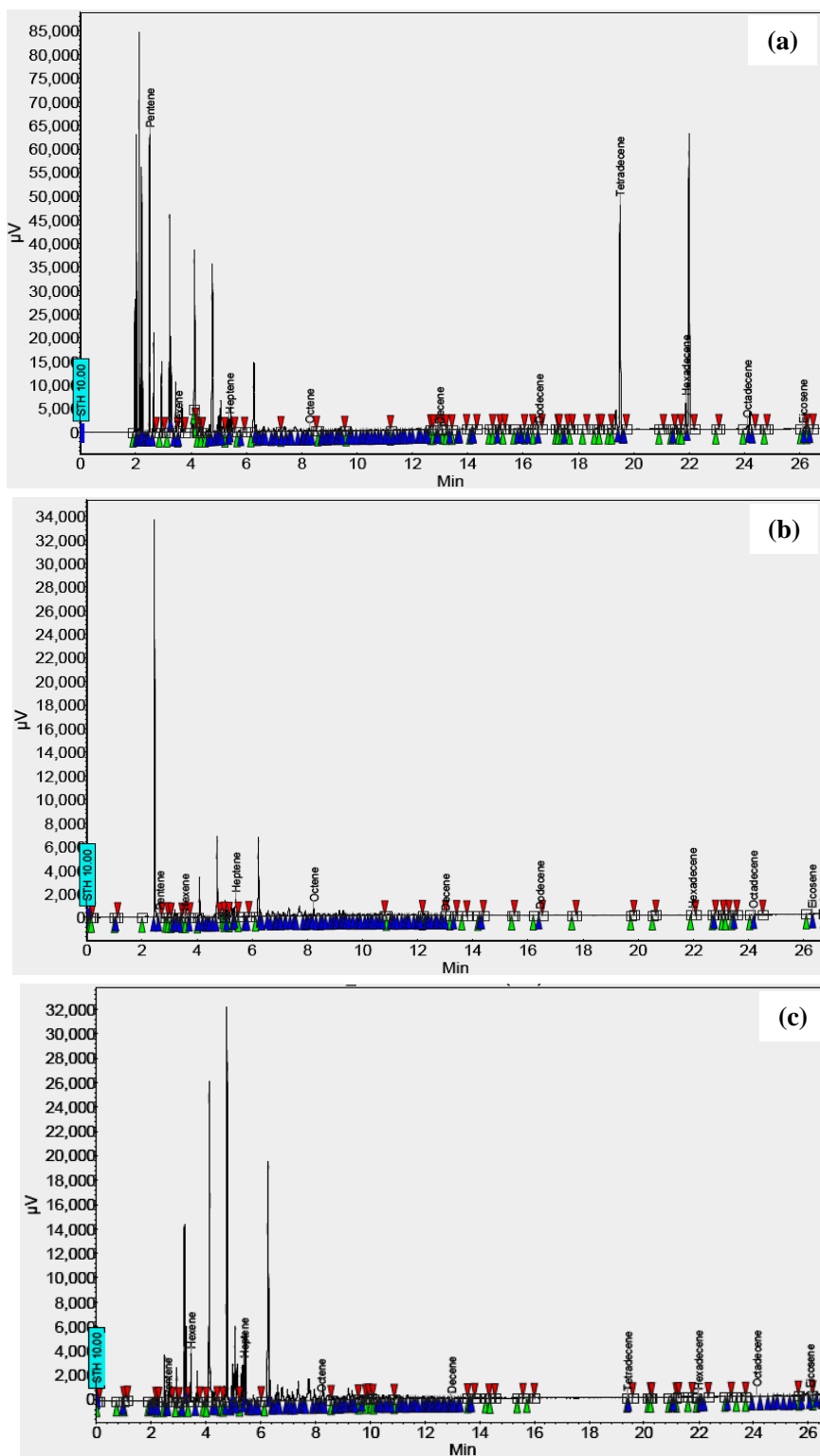
Figure (4.37): (a) Gas chromatogram of the model syngas before treatment, (b and c) Gas chromatogram of the model syngas after treatment using a packed bed of s-PHP, (b) small (glass reactor) and (c) pilot (electric field enhanced tar removal equipment) scale intensified syngas cleaning systems respectively

Table (4.25): Performance of sulphonated PolyHIPE Polymer (s-PHP) in the model tar reduction efficiency (small and pilot scale intensified syngas cleaning process)

Cleaning System $\rightarrow$ Parameter $\downarrow$	Before treatment	s-PHP ♣	s-PHP ⊗
Weight (g)	-	20	76
C_{in}* (g/Nm^3)	22.0 ± 2.1	-	-
C_{out}** (g/Nm^3)	-	9.0 ± 0.5	8.4 ± 0.6
Efficiency X (%)	0.0	59.1 ± 3.0	61.8 ± 3.8
GC – Figure (4.37 a-c)	Figure (4.37-a)	Figure (4.37-b)	Figure (4.37-c)

* Model tar concentration before treatment   ** Model tar concentration after treatment
♣ Packed bed of s-PHP (small scale system)   ⊗ Packed bed of s-PHP (pilot scale system)
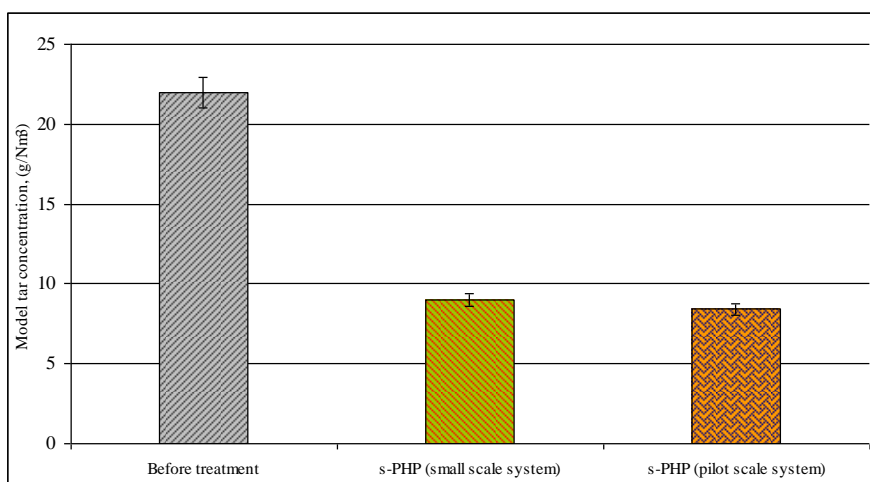
Figure (4.38): Concentration of model tar before and after s-PHP
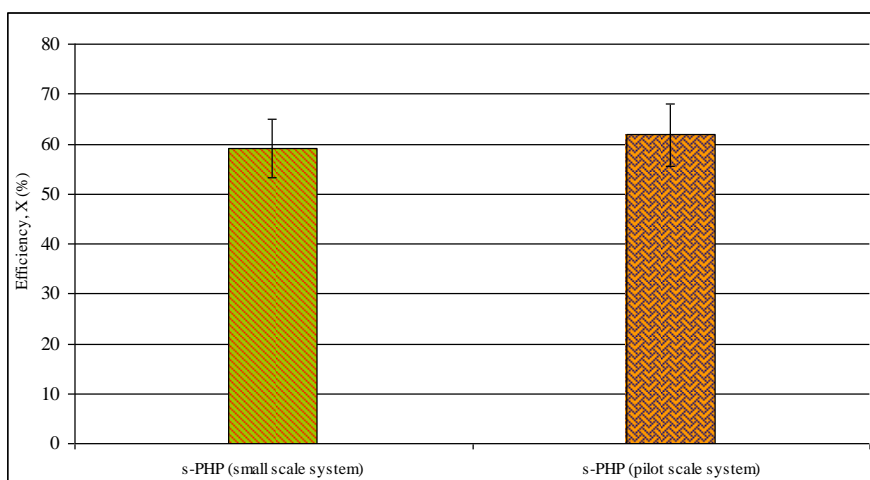
Figure (4.39): Performance of s-PHP in the model tar reduction efficiency (small and pilot scale intensified syngas cleaning process)

This view is further strengthened by the fact that the nano-structured micro-porous ion exchange s-PHP also retained tars from syngas generated by the gasification of fuel cane bagasse as a model biomass (Akay *et al.* 2013). The performance of s-PHP in scavenging tar from syngas was investigated using a flow-through system in which syngas from the gasifier flowed through a packed bed of s-PHP particles (diameter = 25 mm, thickness = 5 mm). The s-PHP particles were loaded into the filter box (Figure 3.8) and retained by a stainless steel mesh to ensure that carryover of s-PHP from the filter box to the induced draft fan did not occur. The s-PHP was exposed over a period of 5 hour to 150 Nm^3 of syngas containing tar. Simultaneous tar collection was carried out at sampling points S2 and S3 immediately before and after the s-PHP packed bed (Figure 3.8). GCMS chromatograms of the tars in syngas collected before and after passing through the s-PHP bed are shown in Figures (4.40) and (4.41), respectively. The identification of various peaks together with mass-to-charge ratio (*m/z*) is shown in Table (K.1) in Appendix L.

It can be seen from Figures (4.40) and (4.41) that a large number of components have been reduced, this may be due to tar reaction with s-PHP. Nevertheless, there is substantial reduction in the overall tar content in syngas following extraction with s-PHP. The tar compounds contained in the syngas after flow through the s-PHP are listed in Table (K.2) in Appendix L. It is evident that many of the Classes 2 and 3 compounds (see Table 2.9) were removed by the s-PHP and no longer present in the syngas.
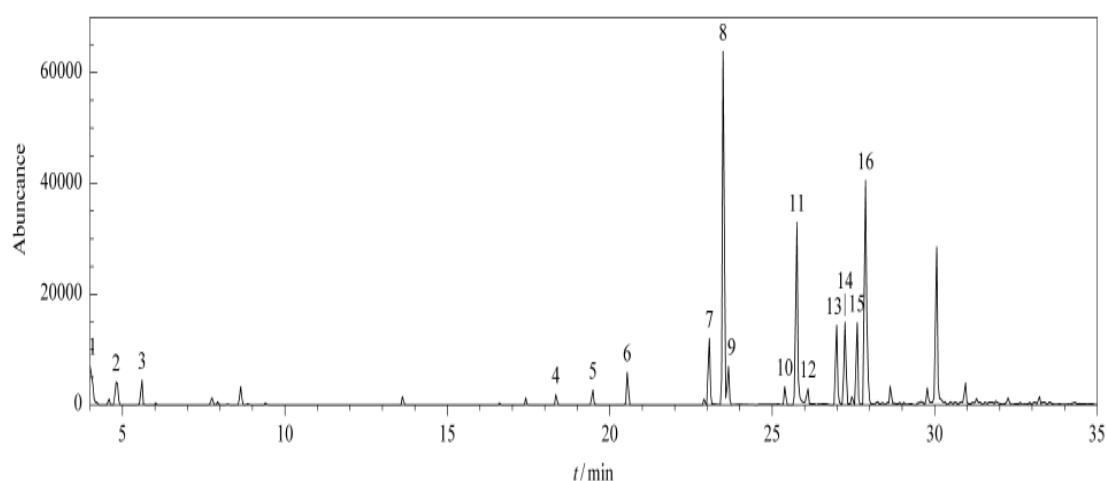
Figure (4.40): GCMS chromatogram of tar in syngas before tar extraction (sampling location S2 before the filter box shown in Figure 3.8). Full scale of the abundance is 62000 units
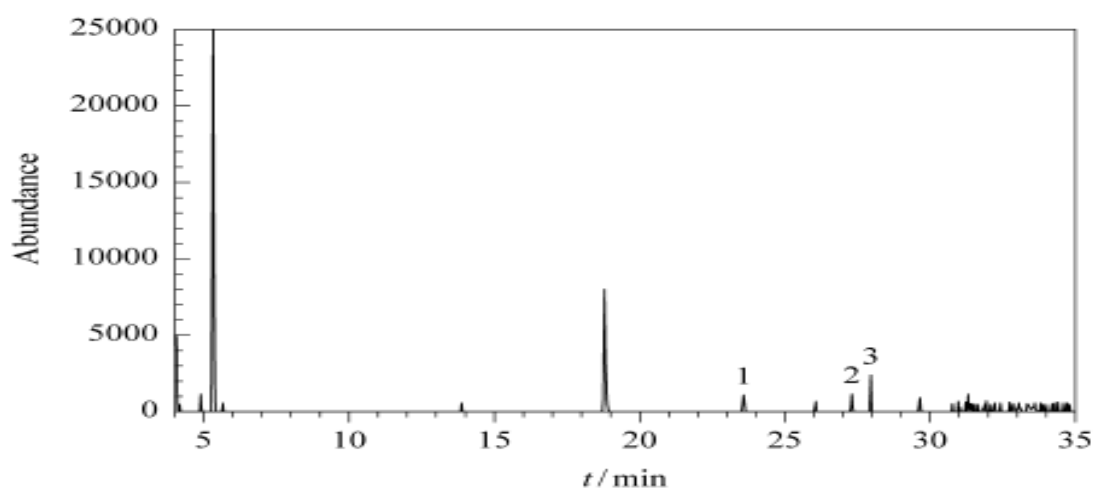
Figure (4.41): GCMS chromatogram of tar in syngas after tar extraction with s-PHP (sampling location S3 after the filter box in Figure 3.8). Note that the full scale of abundance is 25000 units

This tar removal method was also applied to syngas cleaning in a 1 MWe capacity gasifier (scaled up version of the current gasifier) and produced clean gas as indeed observed by the change in the flared syngas as shown in Figure (4.42). Figure (4.42-a) shows the orange colour of the flared syngas before tar extraction with a packed bed of s-PHP while Figure (4.42-b) illustrates the colour of the flared syngas after tar extraction. The description of this 1 MWe gasifier was disclosed previously (Akay *et al.*, 2006; Dogru and Akay, 2011).

Figure (4.42): Visual demonstration of the tar cleaning effectiveness by the method carried out with 1 MWe scaled-up gasifier. Colour of the flare (a) before syngas cleaning, (b) after syngas cleaning

4.3.5. Interaction between the Model Tar and the sulphonated PolyHIPE Polymer (s-PHP)

The interactions between model tar/syngas mixture and sulphonated PHP were investigated by examining s-PHPs used in model tar extraction. Figure (4.43-a) shows the appearance of unexposed s-PHP. Whereas Figure (4.43-b) shows the presence of model tar deposits within the pores of s-PHP after exposure over a period of 3 h to 180 Nm^3 to model tar loaden model tar/syngas mixture. The ESEM images have shown the existence of agglomerates of particulates of the model tar (Figure 4.43-b) which are morphologically different from the polymer structure along (Figure 4.43-a) its whole surface. At ×250 magnifications with scope on these white in colour bits shown through the images, agglomeration of irregular particulates of the model tar bonded to the filter surface can be noticed. Investigation of the s-PHP morphology after exposure to the model tar/syngas mixture using ESEM showed that adsorption of model tar by s-PHP occurred on the surface of the monoliths and also inside the monoliths. Other ESEM images of exposed and unexposed s-PHPs particles at different magnifications are given in Appendix (M). The adsorption of tar on the surface of s-PHP particles also recorded by Calkan and co-workers (Calkan *et al.*, 2006); however, this work was the first to observe the interaction between tar and the nano-structured micro-porous ion exchange network of s-PHP.

The interactions between tar and sulphonated PHP were investigated by examining s-PHPs used in tar extraction (Akay *et al.*, 2013). Figure (4.44-a) shows the presence of tar deposits within the pores of s-PHP after exposure to tar loaden syngas. Through use of SEM-EDX in Figures (4.44-b), (4.44-c) and (4.44-d) droplets of tar associated with fragments of char embedded in the microporous network were identified, providing clear evidence that tar scavenging is not limited to adsorption on the external surfaces of the polymer but that it also occurs across the interconnected pore network. Although tars consist primarily of C, H and O, during gasification of fuel cane bagasse (FCB) ash forming elements and elemental sulphur released to the syngas will also adsorb onto droplets of tar (Jordan and Akay, 2012). The SEM-EDX spectra produced of Points 0, 1 and 2 in Figure (4.44-a) are shown in Figures (4.44-b), (4.44-c) and (4.44-d). Both Figures (4.44-b) and (4.44-c) show the presence of C, H, O and S (which comes from the PHP itself) as well as the main ash forming elements in FCB. In Figure (4.44-d) the SEM-EDX of sulphonated PHP alone is shown.

185
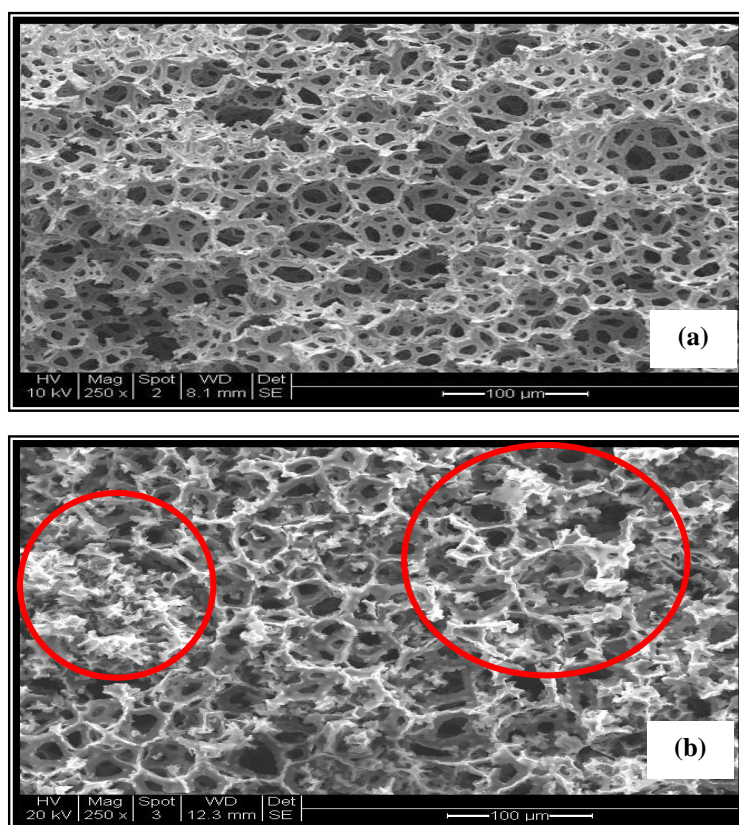
Figure (4.43): (a) ESEM image of unexposed s-PHP (x250). (b) ESEM image showing model tar droplets in s-PHP after exposure over a period of 3 h to 180 Nm^3 to model tar/syngas mixture (x250)

It was noted during the collection of PHP after removal of the tar species from the syngas, that the PHP species no longer had a spongy texture but had become extremely brittle and readily broke into small pieces when compressed. Although mechanical characteristics of s-PHP changed upon reaction with tars, we have not determined their tar absorption capacity as a function of time on-stream. Our on going studies indicate that once s-PHPs become saturated, it is possible to treat them chemically with acid to reverse the elasticity of s-PHPs and to oxidise the tar compounds. Investigation of the sulphonated PHP morphology after exposure to the syngas using ESEM showed that:

(i) adsorption of tar by s-PHP occurred not only on the surface of the particles but also inside the PHP particles as well;

(ii) associations of tar droplets and char particles ranging from 20−80 μm were captured in the microporous network as the syngas flowed through the PHP monoliths.
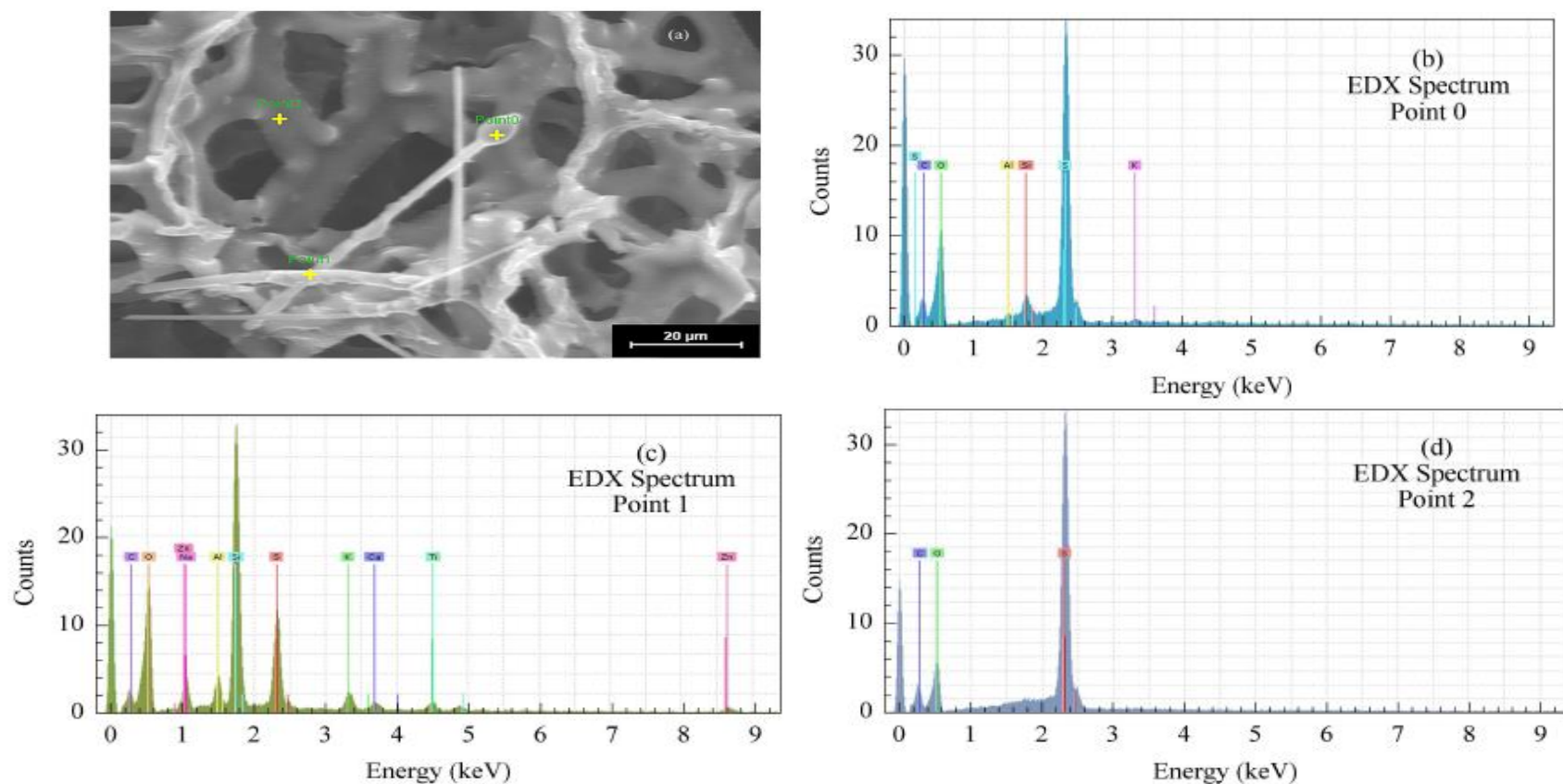
Figure (4.44): ESEM and EDX examinations of PolyHIPE Polymers (PHPs) after tar deposition. (a) ESEM image of tar droplets and char captured in s-PHP (fractured surface) after 3 h exposure to syngas (×1000). Points 0, 1 and 2 indicate the location at which EDX spectra shown below were taken. (b, c and d) EDX spectra of Points 0, 1 and 2 from Figure (4.44-a). The EDX spectrum of Point 2 shows the spectrum of PHP only. Note the difference in elemental composition as compared with the spectra of the char and tar at Points 0 and 1

4.3.6. Mechanism of Tar Removal

The mechanism of tar removal from syngas can be explained by the confinement phenomenon (Akay, 2006; Akay, 2013) which has been utilised in process intensification including bioprocess intensification (Akay *et al*., 2005), tissue engineering (Akay *et al*., 2004), separation processes (Akay and Vickers, 2012; Akay *et al*., 2012), agro-process intensification (Akay and Burke, 2012; Akay and Fleming, 2012) and more recently in chemical catalysis (Akay, 2013). In general terms, according to the confinement phenomenon, the behaviour of matter (including cells/bacteria and reactive chemical species) is dictated by the size and biochemical/chemical structure of the confinement media in which the matter is present. Clearly, the size of the confinement media must be comparable with the size of the matter that is confined. Although the size of the individual molecules are small compared with that of the pores of PHP, nevertheless, surface active or polar molecules can grow as clusters through aggregation within the PolyHIPE Polymers as shown previously (Akay and Wakeman, 1994; Akay and Wakeman, 1994). These structures are highly stable (low entropy) especially in the presence of confinement media and hence, there is a driving force for such molecules to diffuse from the bulk fluid (liquid or gas) into the confinement media where they are stabilised. In liquid systems, this phenomenon was successfully applied to oil-water demulsification (Akay and Vickers, 2012; Akay *et al*., 2012), chemical catalysis (Akay, 2013) and surfactant separations (Akay and Wakeman, 1994; Akay and Wakeman, 1994).

In the case of tar removal from syngas, there is an additional driving force for tar diffusion into s-PHP from syngas due to the chemical reactivity of tars. As shown in section 4.3.4. above tars appeared to undergo chemical changes upon adsorption by s-PHP, therefore tar diffusion enhancement based on chemical potential can be expected.

It is clear that there is a chemical potential driven diffusion of tar molecules from the bulk of the syngas. Once within the pores, some of these molecules undergo chemical reaction which are stabilised. It may be possible to use such tar loaden s-PHPs from gasification of biomass as slow release natural herbicides so that when herbicidal effectiveness disappear, these s-PHPs can then act as soil additives in agro-process intensification (Akay and Burke, 2012; Akay and Fleming, 2012). Although

such applications require further research, the current method of tar removal illustrates the potential of s-PHP in an integrated holistic biorefinery technology.

Tar removal can be further intensified by process intensification fields such as electric and plasma fields with or without PolyHIPE Polymer. We have recently shown that tar removal efficiency can be increased over 98% (Akay *et al*., 2012) using such hybrid methods which also crack tars, thus increasing its calorific value while enabling syngas for catalytic conversion to fuels and chemicals such as ammonia.

Chapter Five

Conclusions, Suggestions and Future Work/Research

Chapter Five

Conclusions, Suggestions and Future Work/Research

5.1. Introduction

Over the past five and half years; initially, some gasification experiments were performed. Then, work has been carried out to implement process intensification and miniaturization (PIM) philosophy in the syngas cleaning. In this work in syngas cleaning experiments, a hydrophobic PHP which was prepared through HIPE polymerization technique and sulphonated along with other PHPs were used. During the course of this work: gasification of wood chips and oil sludge and sawdust mixture and the potential of syngas cleaning have been investigated. In the gasification work, gas composition, tar content and heat content of the produced gas were determined. In the syngas cleaning experiments, tar removal/conversion was examined. We developed and used two systems. These were: small and pilot scale intensified syngas cleaning systems. In the small scale intensified syngas cleaning system, experiments on a chemically surface modified PHP developed in the laboratory and other PHPs namely, PHP-B30, PHP-S30 and PHP-S30B10 and plasma at different power intensities with or without sulphonated PHP were performed. In the pilot scale intensified system; however, experiments were carried out with: only a sulphonated PHP, different high voltages with completely or partially insulated electrodes and their combination and bottom or/and top water scrubbing. Water scrubbing was also coupled with different high voltage intensities. Summary and conclusions drawn from obtained results are given here.

5.2. Conclusions

5.2.1. Gasification

In this work, both wood chips and oil sludge and sawdust mixture have been gasified using a novel downdraft intensive 50kWe air-blown auto-thermal gasifier. Gas composition, tar content and heat content of the produced gas were determined. Although in comparison to the former feedstock the latter one was required to be briquetted to produce pellets with a uniform size. Both feedstocks have produced a syngas with a satisfactory heating value for power generation using an ICE with wood chips which had a higher heating value. Nevertheless, in term of tar level, oil sludge

and sawdust mixture gave a significantly lower tar level than that found in wood chips. This is due to the presence of several metal impurities in the oil sludge which act as a catalyst for tar cracking during gasification since refinery sludge initially contained large amounts of catalytic rare earth elements. It is concluded that, in order to reduce and/or refrain particularly from the environmental pollution, it should be encouraged that oil sludge is converted to syngas by applying appropriate conversion techniques such as downdraft gasification instead of directly combustion or landfill.

5.2.2. PolyHIPE Polymer (PHP)

A number of PHPs have been prepared, modified by means of sulphonation and characterized. Sulphonation of PHPs was carried out in an attempt to improve their hydrophilicity (water absorption). ESEM micrographs for fresh and used PHPs showed a different surface morphology at the PHP surface after the utilization of the sulphonated PHP for the removal of the model tar from the model syngas. The ESEM images have shown the existence of agglomerates of particulates of the model tar which are morphologically different from the PHP wall structure. The use of these PHPs in gas cleaning technologies is promising.

5.2.3. Intensified Syngas Cleaning Systems

5.2.3.1. Small Scale Intensified Syngas Cleaning System

In the small scale intensified syngas cleaning system, experiments on a chemically surface modified PHPs developed in the laboratory and PHPs namely, PHP-B30, PHP-S30 and PHP-S30B10 and plasma at different power intensities with or without sulphonated PHP were performed. It can be concluded that polymer PHP-B30 gave the highest tar removal/conversion of 93.6%, due to its large surface area. The performance of other polymers can be ranked as: PHP-S30B10 > PHPS30 > s-PHP. When plasma was applied in the presence of the polymer with the poorest performance on its own that's the sulphonated PHP, the highest tar removal/conversion of 91% was obtained. Experiments conducted with plasma only gave much lower tar removal/conversion of no more than 71.4%. It is interesting to note that the level of tar removal/conversion observed in this thesis using a model syngas with a model tar is similar to that observed by work carried out on a real syngas (Akay *et al.*, 2013).

5.2.3.2. Pilot Scale Intensified Syngas Cleaning System

In the pilot scale intensified system; however, experiments were carried out with: only a sulphonated PHP, different high voltages with completely or partially insulated electrode and their combination and bottom or top water scrubbing or simultaneously. Water scrubbing was also coupled with different high voltage intensities. The effect of the type of insulation (complete/ partial) is evident since pilot scale intensified system experiments showed that the partially insulated electrode gave a better tar removal/conversion compared to that obtained with the completely insulated one.

Out of the experiments when a completely insulated electrode (CIE) was used, the highest tar removal/conversion was obtained when applying a high voltage of 25 kV with the aid of a sulphonated PHP and a high voltage of 25 kV with a simultaneous (top and bottom) water scrubbing, respectively. In addition, it seems that applying a high voltage in the absence of a sulphonated PHP or water scrubbing either top or bottom is not a good option. In fact, this option gave the lowest tar removal/conversion of no more than 30%. Similarly, water scrubbing either top or bottom or both with/out a high voltage but without a sulphonated PHP, gave a lower, although comparable, tar removal/conversion compared to that obtained when a sulphonated PHP was synergically used.

In the experiments when a partially insulated electrode (PIE) was used, it can be observed that the higher the voltage, the higher the tar removal/conversion was. Out of these experiments, the highest tar removal/conversion was 97.5%. Using a sulphonated PHP while applying a high voltage, generally improves tar removal/conversion up to 96.7%

5.3. Suggestions for Future Work/Research

❖ Although the syngas cleaning methods developed in this work is generic, we have been using a model syngas with a model tar in order to rapid screen the efficiencies of these different methods. Due to the highly toxic and explosive nature of real syngas, we had to use non-toxic and non-explosive model syngas so that the intensification levels of the processes could be evaluated under laboratory

conditions without having restrictions on the cost, scope and detail of the experimentation. Clearly, the next stage of development is to use real syngas which will require substantial modification of the equipment taking into account the toxic and explosive nature of syngas as well as presence of high electrical voltage.

❖ Jordan and Akay (Jordan and Akay, 2012d) have determined tar profiles of real syngas before and after tar removal/conversion after treatment by a sulphonated PHP. These tar profiles should be determined on this real syngas after treatment by electric or plasma fields.

❖ Also, developing of some more PHPs by manipulating some parameters, such as dosing and mixing time, emulsification temperature and composition of the HIPE is recommended. Properties of the produced PHPs, such as pore size distribution and surface area should be further studied. The effect of these parameters on tar removal efficiency should be investigated.

❖ Throughout this work in both small and pilot scale syngas cleaning systems, model tar reduction/removal/conversion was only tested at model syngas flow rate of 1 litre/min while preheating the crude oil (model tar) up to 80°C. Future work should consider other conditions.

References

References

Akay, G. (1998) 'Flow-induced phase inversion in the intensive processing of concentrated emulsions', *Chemical Engineering Science*, 53(2), pp. 203-223.

Akay, G. (2006) 'Renewable resources come together', *The Chemical Engineer*, 784, pp. 27-30.

Akay, G. (2006) In: Lee S ed. Encyclopaedia of Chemical Processing. New York: Marcel Dekker, 183.

Akay, G. (2013) World Patent Application, PCT/GB2013/050122.

Akay, G., Allinson, J.M., Bennett, B., Larter, S.a. and Shakorfow, A.M. (in preparation) 'Process intensification in the demulsification of highly stable water-in-crude oil emulsions. ', *AIChE Journal.*

Akay, G. and Wakeman, R. J. (1994) *J Membr Sci*, 88: 17

Akay, G. and Wakeman, R. J. (1994) *Chem Eng Sci*, 49: 271

Akay, G., Bhumgara, Z. and Wakeman, R.J. (1995) 'Self-supported porous channel filtration modules : preparation, properties and performance : Advanced materials', *Chemical Engineering Research and Design*, 73, pp. 782-797.

Akay, G., Birch, M.A. and Bokhari, M.A. (2004) 'Microcellular polyHIPE polymer supports osteoblast growth and bone formation in vitro', *Biomaterials*, 25(18), pp. 3991-4000.

Akay, G., Bokhari, M.A., Byron, V.J. and Dogru, M. (2005) 'Development of Nano-Structured Micro-Porous Materials and their Application in Bioprocess–Chemical Process Intensification and Tissue Engineering', in *Chemical Engineering*. Trends and Developments, Galan, M. and De Velle, E. (Eds): John Wiley & Sons, Ltd, London, UK, pp. 171-197.

Akay, G., Erhan, E., and Keskinler, B. (2005) *Biotechnol Bioeng*, 90:180

Akay, G., Dogru, M., and Calkan, O F. (2006) *The Chemical Engineer*, 786: 55

Akay, G., Dogru, M. and Calkan, O. (2007) 'Biomass to the rescue', *TCE*, pp. 55-57.

Akay, G. and Burke, D. R. (2012) *Am J Agric Biol Sci*, 7: 150

Akay, G. and Fleming, S. (2012) *Green Process Synth*, 1: 427

Akay, G. and Jordan, A.C. (2012) 'Syngas cleaning using hydrophilic PolyHIPE Polymers.

Akay, G., Pekdemir, T., Shakorfow, A.M. and Vickers, J. (2012) 'Intensified demulsification and separation of thermal oxide reprocessing interfacial crud (THORP-IFC) simulants'', *Green Process Synthesis.*, 1, pp. 109-127.

Akay, G., Vickers, J. (2012) US Patent 8177985; European Patent (2012), 1 307 402.

Akay, G., Al-Harrasi, W. S. S., El-Nagger, A. A., Chiremba, E., Mohamed, A. H., and Zhang, K. (2013) World Patent Application, PCT/GB2013/050125.

Akay, G., Jordan, C.A. and Mohamed, A.H. (2013) 'Syngas cleaning with nano-structured micro-porous ion exchange polymers in biomass gasification using a novel downdraft gasifier', *Journal of Energy Chemistry*, 22, pp. xxx-xxx

Akram, M. (2002) *Gasification of Municipal Solid Waste and Wood Chips using a Throated Downdraft Gasifier*. PhD thesis. University of Newcastle, UK.

Al-Malack, M.H. and Anderson, G.K. (1997) 'Crossflow microfiltration with dynamic membranes', *Water Research*, 31(8), pp. 1969-1979.

Alshammari, J.S., Gad, F.K., Elgibaly, A.A.M. and Khan, A.R. (2008) 'Solid Waste Management in Petroleum Refineries', *American Journal of Environmental Sciences*, 4(4), pp. 353-361.

Anis, S. and Zainal, Z.A. (2011) 'Tar reduction in biomass producer gas via mechanical, catalytic and thermal methods: A review', *Renewable and Sustainable Energy Reviews*, 15(5), pp. 2355-2377.

Aronson, M.P. and Petko, M.F. (1993) 'Highly Concentrated Water-in-Oil Emulsions: Influence of Electrolyte on Their Properties and Stability', *Journal of Colloid and Interface Science*, 159(1), pp. 134-149.

Ayhan, D. (2001) 'Biomass resource facilities and biomass conversion processing for fuels and chemicals', *Energy Conversion and Management*, 42(11), pp. 1357-1378.

Ayhan, D. (2005) 'Potential applications of renewable energy sources, biomass combustion problems in boiler power systems and combustion related environmental issues', *Progress in Energy and Combustion Science*, 31(2), pp. 171-192.

Aznar, M.P., Caballero, M.A., Gil, J., Martín, J.A. and Corella, J. (1998) 'Commercial Steam Reforming Catalysts To Improve Biomass Gasification with Steam−Oxygen Mixtures. 2. Catalytic Tar Removal', *Industrial & Engineering Chemistry Research*, 37(7), pp. 2668-2680.

Bain, R. (2004) 'An Overview of Biomass Gasification', *http://www.nrel.gov/biomass/pdfs/overview_biomass_gasification.pdf*, [Online] (Accessed: November 14, 2010).

Bakr, W.F. (2010) 'Assessment of the radiological impact of oil refining industry', *Journal of Environmental Radioactivity*, 101(3), pp. 237-243.

Barbetta, A., Dentini, M., Zannoni, E.M. and De Stefano, M.E. (2005) 'Tailoring the Porosity and Morphology of Gelatin-Methacrylate PolyHIPE Scaffolds for Tissue Engineering Applications', *Langmuir*, 21(26), pp. 12333-12341.

Belgiorno, V., De Feo, G., Della Rocca, C. and Napoli, R.M.A. (2003) 'Energy from gasification of solid wastes', *Waste Management*, 23(1), pp. 1-15.

Belyaev, A.A., Yampolskii, Y.P., Starannikova, L.E., Polyakov, A.M., Clarizia, G., Drioli, E., Marigliano, G. and Barbieri, G. (2003) 'Membrane air separation for intensification of coal gasification process', *Fuel Processing Technology*, 80(2), pp. 119-141.

Benson, J.R. (2003) Highly porous polymers, American Laboratory, International Scientific Communications and Sunstorm Research Corporation.

Bergman, P.C.A., van Paasen, S.V.B. and Boerrigter, H. (2002) 'The novel OLGA technology for complete tar removal from biomass producer gas', *Pyrolysis and Gasification of Biomass and Waste, Expert Meeting*. Strasbourg, France, 30 September-1 October 2002. Energy research Centre of the Netherlands (ECN).

Bhumgara, Z. (1995) 'Polyhipe foam materials as filtration media', *Filtration & Separation*, 32(3), pp. 245-251.

Bokhari, M.A., Akay, G., Zhang, S. and Birch, M.A. (2005) 'The enhancement of osteoblast growth and differentiation in vitro on a peptide hydrogel polyHIPE polymer hybrid material', *Biomaterials*, 26(25), pp. 5198-5208.

Bridgwater, A.V. (1994) 'Catalysis in thermal biomass conversion', *Applied Catalysis A: General*, 116(1-2), pp. 5-47.

Bridgwater, A.V. (1995) 'The technical and economic feasibility of biomass gasification for power generation', *Fuel*, 74(5), pp. 631-653.

Bridgwater, A.V. (1999) 'Principles and practice of biomass fast pyrolysis processes for liquids', *Journal of Analytical and Applied Pyrolysis*, 51(1–2), pp. 3-22.

Bridgwater, A.V. (2003) 'Renewable fuels and chemicals by thermal processing of biomass', *Chemical Engineering Journal*, 91(2-3), pp. 87-102.

Bridgwater, A.V., Double, J.M. and Earp, D.M. (1986) *Technical and Market Assessment of Biomass Gasification in the UK*. Energy Technology Support Unit, UKAEA, Harwell.

Bridgwater, A.V. and Maniatis, K. (2004) 'The production of biofuels by the thermochemical processing of biomass', in Archer, M.D. and Barber, J. (eds.) *Molecular to Global Photosynthesis*. London, UK: IC Press, pp. 521-612.

Bridgwater, A.V., Meier, D. and Radlein, D. (1999) 'An overview of fast pyrolysis of biomass', *Organic Geochemistry*, 30(12), pp. 1479-1493.

Bridgwater, A.V. and Peacocke, G.V.C. (2000) 'Fast pyrolysis processes for biomass', *Renewable and Sustainable Energy Reviews*, 4(1), pp. 1-73.

Brown, I.J., Clift, D. and Sotiropoulos, S. (1999) 'Preparation of microporous nickel electrodeposits using a polymer matrix', *Materials Research Bulletin*, 34(7), pp. 1055-1064.

Burke, D.R., Akay, G. and Bilsborrow, P.E. (2010) 'Development of novel polymeric materials for agroprocess intensification', *Journal of Applied Polymer Science*, 118(6), pp. 3292-3299.

Busby, W., Cameron, N.R. and Jahoda, C.A.B. (2001) 'Emulsion-derived foams (PolyHIPEs) containing poly(epsilon-caprolactone) as matrixes for tissue engineering', *Biomacromolecules*, 2, pp. 154-164.

Busby, W., Cameron, N.R. and Jahoda, C.A.B. (2002) 'Tissue engineering matrixes by emulsion templating', *Polymer International*, 51(10), pp. 871-881.

Caballero, J.A., Front, R., Marcilla, A. and Conesa, J.A. (1997) 'Characterization of sewage sludges by primary and secondary pyrolysis', *Journal of Analytical and Applied Pyrolysis*, 40–41(0), pp. 433-450.

Caballero, M.A., Corella, J., Aznar, M.-P. and Gil, J. (2000) 'Biomass Gasification with Air in Fluidized Bed. Hot Gas Cleanup with Selected Commercial and Full-Size Nickel-Based Catalysts', *Industrial & Engineering Chemistry Research*, 39(5), pp. 1143-1154.

Calkan, O. (2007) *Intensified, Integrated, Gasification System Development*. PhD thesis. Newcastle University, Newcastle upon Tyne, UK.

Cameron, N.R. (2005) 'High internal phase emulsion templating as a route to well-defined porous polymers', *Polymer*, 46(5), pp. 1439-1449.

Coll, R., Salvadó, J., Farriol, X. and Montané, D. (2001) 'Steam reforming model compounds of biomass gasification tars: conversion at different operating conditions and tendency towards coke formation', *Fuel Processing Technology*, 74(1), pp. 19-31.

Corella, J., Orío, A. and Aznar, P. (1998) 'Biomass Gasification with Air in Fluidized Bed: Reforming of the Gas Composition with Commercial Steam Reforming Catalysts', *Industrial & Engineering Chemistry Research*, 37(12), pp. 4617-4624.

Cowper, C.J. (1995) 'Chromatography in the Petroleum Industry', *Chromatography Library*, 56(Eds. Adlard, E. R.), pp. 1-40.

Deleuze, H., Maillard, B. and Mondain-Monval, O. (2002) 'Development of a new ultraporous polymer as support in organic synthesis', *Bioorganic & Medicinal Chemistry Letters*, 12(14), pp. 1877-1880.

Demirbas, A. (2004) 'Current Technologies for the Thermo-Conversion of Biomass into Fuels and Chemicals', *Energy Sources*, 26(8), pp. 715-730.

Devi, L., Ptasinski, K.J. and Janssen, F.J.J.G. (2003) 'A review of the primary measures for tar elimination in biomass gasification processes', *Biomass and Bioenergy*, 24(2), pp. 125-140.

Devi, L., Ptasinski, K.J. and Janssen, F.J.J.G. (2005) 'Pretreated olivine as tar removal catalyst for biomass gasifiers: investigation using naphthalene as model biomass tar', *Fuel Processing Technology*, 86(6), pp. 707-730.

Dogru, M. (2000) *Fixed Bed Gasification of Biomass*. PhD thesis. Newcastle University, Newcastle upon Tyne, UK

Dogru, M. and Akay, G. (2004) *International Patent Application, PCT/GB2004/004651*.

Dogru, M. and Akay, G. (2006) *Catalytic gasification, EP1687390*.

Dogru, M., and Akay, G. (2011) Japanese Patent, 2006-53894.

Dogru, M., Howarth, C., Keskinler, B. and Malik, A. (2002a) 'Gasification of hazlenut shells in a downdraft gasifier', *Energy*, 27(5), pp. 415-427.

Dogru, M., Midilli, A., Akay, G. and Howarth, C. (2004) 'Gasification of Leather Residues - Part 1: Experimental Study via a Pilot-Scale-Air-Blown Downdraft Gasifier', *Energ Sourc*, 26(1), pp. 35-44.

Dogru, M., Midilli, A. and Howarth, C.R. (2002) 'Gasification of sewage sludge using a throated downdraft gasifier and uncertainty analysis', *Fuel Processing Technology*, 75(1), pp. 55-82.

Dou, B., Zhang, M., Gao, J., Shen, W. and Sha, X. (2002) 'High-Temperature Removal of NH3, Organic Sulfur, HCl, and Tar Component from Coal-Derived Gas', *Industrial & Engineering Chemistry Research*, 41(17), pp. 4195-4200.

Earp, D.M. (1988) *Gasification of Biomass in a Downdraft Reactor*. PhD thesis. Aston University, Birmingham.

Einawawy Amins, S., Ghobrial Fikry, H. and Eliman Abdelghani, A. (1987) *Feasibility Study on Disposal of Oily Sludge in Kuwait, Second International Conference on New Frontiers for Hazardous Waste Management*. Pittsburgh Pennsylvania.

Ergenekon, P., Gürbulak, E. and Keskinler, B. (2011) 'A novel method for sulfonation of microporous polystyrene divinyl benzene copolymer using gaseous SO_2 in the waste air streams', *Chemical Engineering and Processing: Process Intensification*, 50(1), pp. 16-21.

Erhan, E., Yer, E., Akay, G., Keskinler, B. and Keskinler, D. (2004) 'Phenol degradation in a fixed-bed bioreactor using micro-cellular polymer-immobilized Pseudomonas syringae', *Journal of Chemical Technology & Biotechnology*, 79(2), pp. 195-206.

Erlich, C., Björnbom, E., Bolado, D., Giner, M. and Fransson, T.H. (2006) 'Pyrolysis and gasification of pellets from sugar cane bagasse and wood', *Fuel*, 85(10–11), pp. 1535-1540.

Fahmi, R., Bridgwater, A.V., Darvell, L.I., Jones, J.M., Yates, N., Thain, S. and Donnison, I.S. (2007) 'The effect of alkali metals on combustion and pyrolysis of Lolium and Festuca grasses, switchgrass and willow', *Fuel*, 86(10–11), pp. 1560-1569.

Fermeglia, M., De Simon, G. and Donolo, G. (2005) 'Energy production from biomass gasification by molten carbonate fuel cells: process simulation', Palermo, Italy.

Fifield, F.W. and Kealey, D. (1983) *Principles and Practice of Analytical Chemistry*. 2nd edn. International Textbook Company.

Frederick, W.J., Hupa, M. and Uusikartano, T. (1994) 'Volatiles and char carbon yields during black liquor pyrolysis', *Bioresource Technology*, 48(1), pp. 59-64.

Fridman, A., Kennedy, L. A. (2004) *Plasma Physics and Engineering*. New York & London: Taylor & Francis.

Gallacher, J. (1993) *The Elucidaion of the Nature of Naphtheno-aromatic Groups in Heavy Petroleum Fractions by ¹³C NMR and Catalytic Dehydrogenation*. PhD thesis. University of Strathclyde.

Gani, A. and Naruse, I. (2007) 'Effect of cellulose and lignin content on pyrolysis and combustion characteristics for several types of biomass', *Renewable Energy*, 32(4), pp. 649-661.

Gopichandran, R., Patwari, S. I. and Deliwala, J. (2003) 'Options for improving sulphonation. A technical intervention supporting eco industrial development. ', pp. 1-16.

Goswami, D.Y. (1986) *Alternative Energy in Agriculture*. Boca Raton, CRC Press, FL, USA

Graham, B. (2001) 'Technological Plasmas', *Physics World*, 14(3), pp. 31-36.

Haibach, K., Menner, A., Powell, R. and Bismarck, A. (2006) 'Tailoring mechanical properties of highly porous polymer foams: Silica particle reinforced polymer foams via emulsion templating', *Polymer*, 47(13), pp. 4513-4519.

Hainey, P., Huxham, I.M., Rowatt, B., Sherrington, D.C. and Tetley, L. (1991) 'Synthesis and ultrastructural studies of styrene-divinylbenzene Polyhipe polymers', *Macromolecules*, 24(1), pp. 117-121.

Hall, C.W. (1981) *Biomass as as Alternative Fuel*. Maryland: Government Institutes Inc.

Han, J. and Kim, H. (2008) 'The reduction and control technology of tar during biomass gasification/pyrolysis: An overview', *Renewable and Sustainable Energy Reviews*, 12(2), pp. 397-416.

Hanaoka, T., Inoue, S., Uno, S., Ogi, T. and Minowa, T. (2005) 'Effect of woody biomass components on air-steam gasification', *Biomass and Bioenergy*, 28(1), pp. 69-76.

Haq, Z. (1985) 'European Patent', 4,536,521, Merseyside.

Harker, J.H. and Backhurst, J.R. (1981) *Fuel and Energy*. London: Academic Press.

Hasan, H. (2012) *Preparation of Novel PolyHIPE Polymer and Intensified Removal of Tar from Syngas*. PhD thesis. School of Chemical Engineering & Advanced Materials, Newcastle University, UK.

Hasler, P. and Nussbaumer, T. (1999) 'Gas cleaning for IC engine applications from fixed bed biomass gasification', *Biomass and Bioenergy*, 16(6), pp. 385-395.

Hayman, M.W., Smith, K.H., Cameron, N.R. and Przyborski, S.A. (2005) 'Growth of human stem cell-derived neurons on solid three-dimensional polymers', *Journal of Biochemical and Biophysical Methods*, 62(3), pp. 231-240.

Hernández, J.J., Aranda-Almansa, G. and Bula, A. (2010) 'Gasification of biomass wastes in an entrained flow gasifier: Effect of the particle size and the residence time', *Fuel Processing Technology*, 91(6), pp. 681-692.

Higman, C. and van der Burgt, M. (2008) *Chapter 5 - Gasification Processes*. Burlington: Gulf Professional Publishing.

Hoisington, M.A., Duke, J.R. and Apen, P.G. (1997) 'High temperature, polymeric, structural foams from high internal phase emulsion polymerizations', *Polymer*, 38(13), pp. 3347-3357.

Jordan, C.A. (2002) *Gasification of Sugar Cane Bagasse for Power Production Using a Throated Downdraft Gasifier*. MSc thesis. School of Chemical Engineering, University of Newcastle upon Tyne, UK.

Jordan, C.A. (2010) *Intensified gasification of fuel cane bagasse for power production using solid oxide fuel cells*. PhD thesis. School of Chemical Engineering and Advanced Materials, Newcastle University, UK.

Jordan, C.A. and Akay, G. (2012) 'Occurrence, composition and dew points of tars produced during gasification of fuel cane bagasse in a down draft gasifier', *Biomass and Bioenergy*, Vol. 32, pp. 51-58.

Jordan, C.A. and Akay, G. (2012) 'Biomass Bioenerg, 42: 51

Jordan, C.A. and Akay, G. (2012d) 'Effect of CaO on Tar Production and Dew Point Depression during Gasification of Fuel Cane Bagasse in a Novel Downdraft Gasifier', *Fuel Processing Technology*, pp. 1-20.

Kaltschmitt, M. and Dinkelbach, L. (1997) 'Biomass for Energy in Europe - Status and Prospects', in Kaltschmitt, M. and Bridgwater, A.V. (eds.) *Biomass Gasification and Pyrolysis, State of the Art and Future Prospects*. CPL Scientific Ltd. : UK.

Katsoyiannis, I.A. and Zouboulis, A.I. (2002) 'Removal of arsenic from contaminated water sources by sorption onto iron-oxide-coated polymeric materials', *Water Research*, 36(20), pp. 5141-5155.

Katz, D., A. (1998) *Polymers*. Gladwyne.

Kaupp, A. and Goss, J. (1984) *Small Scale Gas Producer-Engine Systems (to 50 kW)*. Federal Republic of Germany.

Keown, D.M., Favas, G., Hayashi, J.-i. and Li, C.-Z. (2005) 'Volatilisation of alkali and alkaline earth metallic species during the pyrolysis of biomass: differences between sugar cane bagasse and cane trash', *Bioresource Technology*, 96(14), pp. 1570-1577.

Kersten, S.R.A., Wang, X., Prins, W. and van Swaaij, W.P.M. (2005) 'Biomass Pyrolysis in a Fluidized Bed Reactor. Part 1: Literature Review and Model Simulations', *Industrial & Engineering Chemistry Research*, 44(23), pp. 8773-8785.

Kinoshita, C.M., Turn, Q.T., Overend, R.P. and Bain, R.L. (1997) 'Power Generation Potential of Biomass Gasification Systems', *Journal of Energy Engineering*, 123(3), pp. 88-99.

Klass, D. (1998) *Biomass for Renewable Energy, Fuels and Chemicals*. London: Academic Press.

Krajnc, P., Leber, N., Štefanec, D., Kontrec, S. and Podgornik, A. (2005) 'Preparation and characterisation of poly(high internal phase emulsion) methacrylate monoliths and their application as separation media', *Journal of Chromatography A*, 1065(1), pp. 69-73.

Kučera, F. and Jančář, J. (1998) 'Homogeneous and heterogeneous sulfonation of polymers: A review', *Polymer Engineering & Science*, 38(5), pp. 783-792.

Küçük, M.M. and Demirbaş, A. (1997) 'Biomass conversion processes', *Energy Conversion and Management*, 38(2), pp. 151-165.

Kuriakose, A.P. and Manjooran, S. (2001) 'Bitumenous paints from refinery sludge', *Surface and Coatings Technology*, 145(1-3), pp. 132-138.

Li, C. and Suzuki, K. (2009) 'Tar property, analysis, reforming mechanism and model for biomass gasification—An overview', *Renewable and Sustainable Energy Reviews*, 13(3), pp. 594-604.

Livshin, S. and Silverstein, M.S. (2008) 'Cross-linker flexibility in porous crystalline polymers synthesized from long side-chain monomers through emulsion templating', *Soft Matter*, 4(8).

Lopamudra, D., Ptasinski, K.J. and Janssen, F.J.J.G. (2003) 'A review of the primary measures for tar elimination in biomass gasification processes', *Biomass and Bioenergy*, 24(2), pp. 125-140.

Lucas, C., Szewczyk, D., Blasiak, W. and Mochida, S. (2004) 'High-temperature air and steam gasification of densified biofuels', *Biomass and Bioenergy*, 27(6), pp. 563-575.

Luo, S., Xiao, B., Hu, Z., Liu, S., Guan, Y. and Cai, L. (2010) 'Influence of particle size on pyrolysis and gasification performance of municipal solid waste in a fixed bed reactor', *Bioresource Technology*, 101(16), pp. 6517-6520.

Maniatis, K. (1986) *Fluidized Bed Gasification of Biomass*. Aston University, UK.

Maniatis, K. and Beenackers, A. (2000) 'Tar Protocols. IEA Bioenergy Gasification Task', *Biomass and Bioenergy*, 18(1), pp. 1-4.

Maschio, G., Koufopanos, C. and Lucchesi, A. (1992) 'Pyrolysis, a promising route for biomass utilization', *Bioresource Technology*, 42(3), pp. 219-231.

McKendry, P. (2002a) 'Energy production from biomass (part 1): overview of biomass', *Bioresource Technology*, 83(1), pp. 37-46.

McKendry, P. (2002b) 'Energy production from biomass (part 2): conversion technologies', *Bioresource Technology*, 83(1), pp. 47-54.

McKendry, P. (2002c) 'Energy production from biomass (part 3): gasification technologies', *Bioresource Technology*, 83(1), pp. 55-63.

Meier, D. and Faix, O. (1999) 'State of the art of applied fast pyrolysis of lignocellulosic materials — a review', *Bioresource Technology*, 68(1), pp. 71-77.

Menner, A., Haibach, K., Powell, R. and Bismarck, A. (2006) 'Tough reinforced open porous polymer foams via concentrated emulsion templating', *Polymer*, 47(22), pp. 7628-7635.

Midilli, A., Dogru, M., Akay, G. and Howarth, C.R. (2002) 'Hydrogen production from sewage sludge via a fixed bed gasifier product gas', *International Journal of Hydrogen Energy*, 27, pp. 1035-1041.

Midilli, A., Dogru, M., Akay, G. and Howarth, C.R. (2004) 'Gasification of Leather Residues - Part 2: Conversion into Combustible Gases and the Effects of Some Operational Parameters', *Energ Sourc*, 26(1), pp. 45-53.

Midilli, A., Dogru, M., Howarth, C.R., Ling, M.J. and Ayhan, T. (2001a) 'Combustible gas production from sewage sludge with a downdraft gasifier', *Energy Conversion and Management*, 42(2), pp. 157-172.

Midilli, A., Dogru, M., R. Howarth, C. and Ayhan, T. (2001b) 'Hydrogen production from hazelnut shell by applying air-blown downdraft gasification technique', *International Journal of Hydrogen Energy*, 26(1), pp. 29-37.

Milne, T.A., Evans, R.J. and Abatzoglou, N. (1998) *Biomass Gasifier "Tars": Their Nature, Formation, and Conversion*. National Renewable Energy Laboratory (NREL).

Morf, P. (2001) *Secondary reactions of tar during thermochemical biomass conversion*. PhD thesis. Swiss Federal Institute of Technology Zurich

Naim, R., Ismail , A.F., Saidi, H. and Saion, E. (2004) *Development of sulfonated polysulfone membranes as a material for Proton Exchange Membrane (PEM), Proceedings of Regional Symposium on Membrane Science and Technology 2004*. Puteri Pan Pacific Hotel, Johor Bharu, Malaysia.

Nair, S.A., Pemen, A.J.M., Yan, K., van Gompel, F.M., van Leuken, H.E.M., van Heesch, E.J.M., Ptasinski, K.J. and Drinkenburg, A.A.H. (2003) 'Tar removal from biomass-derived fuel gas by pulsed corona discharges', *Fuel Processing Technology*, 84(1–3), pp. 161-173.

Ndlovu, T. (2008) *Bioprocess Intensification of Antibiotic Production using Functionalised PolyHIPE Polymers*. PhD thesis. Newcastle University, Newcastle Upon Tyne, UK.

Neeft, J., Knoef, H. and Onaji, P. (1999a) *Behaviour of tars in biomass gasification systems*. Netherlands.

Neeft, J.P. (2002) *12th European Conference for Energy*. Amsterdam, The Netherlands, 17-21 June.

Ni, M., Leung, D.Y.C., Leung, M.K.H. and Sumathy, K. (2006) 'An overview of hydrogen production from biomass', *Fuel Processing Technology*, 87(5), pp. 461-472.

Noor, Z.Z. (2006) *Intensification of separation processes using functionalised polyHIPE polymer*. Ph D thesis. Newcastle University.

Nozaki, T., Muto, N., Kadio, S. and Okazaki, K. (2004b) 'Dissociation of vibrationally excited methane on Ni catalyst: Part 2. Process diagnostics by emission spectroscopy', *Catalysis Today*, 89(1–2), pp. 67-74.

Nozaki, T., Muto, N., Kado, S. and Okazaki, K. (2004a) 'Dissociation of vibrationally excited methane on Ni catalyst: Part 1. Application to methane steam reforming', *Catalysis Today*, 89(1–2), pp. 57-65.

Olgun, H., Dogru, M., Howarth, C.R. and Malik, A.A. (2001) 'Preliminary Studies of Lignocellulosics and Waste Fuels for Fixed Bed Gasification', *International Journal of Global Energy Issues*, 15(3/4), pp. 264-280.

Overend, R. (1979) 'Gasification – An Overview', *Paper presented at the FPRS Conference*. Seattle, USA.

Padban, N. (2001) *Tars in Biomass Thermochemical Conversion Processes, Progress Report SDE Project Primary Measures for Reduction of Tars during Fluidized Bed Gasification of Biomass*.

Patel Naranbhai, K. and Sing, S.S. (1999) 'Hazardous, Toxic and Mixed Chemical Waste's Disposal by Incineration', *Proceedings of the Fifteenth International Conference on Solid Waste Technology and Management*. Phildelphia, USA.

Pemen, G., Devi, L., Yan, K., Van Heesch, B., Kerst, R., Ptasinski, K. and Nair, S. (2007) 'Plasma-Catalytical Removal of Tars from Fuel Gas Obtained by Biomass Gasification', *Journal of Advanced Oxidation Technologies*, 10(1), pp. 116-120.

Pérez, P., Aznar, P.M., Caballero, M.A., Gil, J., Martín, J.A. and Corella, J. (1997) 'Hot Gas Cleaning and Upgrading with a Calcined Dolomite Located Downstream a Biomass Fluidized Bed Gasifier Operating with Steam−Oxygen Mixtures', *Energy & Fuels*, 11(6), pp. 1194-1203.

Perry, R.H., Green, D.W. and Maloney, J.O. (eds.) (1997) *Perry's Chemical Engineers' Handbook*. New York: McGraw-Hill. .

Peter, M. (2002) 'Energy production from biomass (part 1): overview of biomass', *Bioresource Technology*, 83(1), pp. 37-46.

Peterson, B. (2010) 'Victory gasworks - gasifiers and wood gasification.', [Online]. Available at: http://www.wood-gasification.com.

Priyadarsan, S., Annamalai, K., Sweeten, J.M., Holtzapple, M.T. and Mukhtar, S. (2005) 'Co-gasification of blended coal with feedlot and chicken litter biomass', *Proceedings of the Combustion Institute*, 30(2), pp. 2973-2980.

Quaak, P., Knoef, H. and Stassen, H. (1999) *Energy from biomass; a review of combustion and gasification technologies, World Bank Technical Paper no. 422. Energy Series*. Washington, D.C., USA

Rabou, L.P.L.M., Zwart, R.W.R., Vreugdenhil, B.J. and Bos, L. (2009) 'Tar in Biomass Producer Gas, the Energy research Centre of The Netherlands (ECN) Experience: An Enduring Challenge', *Energy & Fuels*, 23(12), pp. 6189-6198.

Raveendran, K. and Ganesh, A. (1996) 'Heating value of biomass and biomass pyrolysis products', *Fuel*, 75(15), pp. 1715-1720.

Reed, T. (2009) *Biomass energy foundation*. URL http://www.woodgas.com.

Reed, T.B. (1981) *Biomass Gasification; Principles and Technology*. Solar Energy, Research Institute (Noyes Data Corporation), Park Ridge, New Jersey, USA.

Reed, T.B. and Das, A. (1998) *Handbook of Biomass Downdraft Gasifier Engine Systems*. 2nd ed Golden edn. Colorado: The Biomass Energy Foundation Press.

Reed, T.B., Levie, B. and Markson, M.L. (1983) *Mathematical model for stratified downdraft gasifiers*.

Rezaiyan, J. and Cheremisinoff, N.P. (2005) *Gasification Technologies, A primer for Engineers and Scientists*. first edn. CRC Press.

Roth, H. (1957) 'Sulfonation of Poly (vinyl Aromatics)', *Industrial & Engineering Chemistry*, 49(11), pp. 1820-1822.

San José Alonso, J., López Sastre, J.A., Romero-Ávila, C. and López Romero, E.J. (2006) 'Combustion of rapeseed oil and diesel oil mixtures for use in the production of heat energy', *Fuel Processing Technology*, 87(2), pp. 97-102.

Schilling, H., Bonn, B. and Krauss. U. (1981) *Coal Gasification, Existing Processes and New Developments*. Graham and Trotman, second edition.

Sergienko, A.Y., Tai, H., Narkis, M. and Silverstein, M.S. (2002) 'Polymerized high internal-phase emulsions: Properties and interaction with water', *Journal of Applied Polymer Science*, 84(11), pp. 2018-2027.

Shafizadeh, F. (1981) *Basic Principles of Direct Combustion in Sofer, S. S. and Zabrsky, O. R.(eds) BIomass Conversion Processes for Energy and Fuels*. New York: Plenum Press.

Shen, L. Q., Xu, Z.-K., Liu, Z.-M. and Xu, Y.-Y. (2003) 'Ultrafiltration hollow fiber membranes of sulfonated polyetherimide/polyetherimide blends: preparation, morphologies and anti-fouling properties', *Journal of Membrane Science*, 218(1–2), pp. 279-293.

Simell, P.A., Hirvensalo, E.K., Smolander, V.T. and Krause, A.O.I. (1999) 'Steam Reforming of Gasification Gas Tar over Dolomite with Benzene as a Model Compound', *Industrial & Engineering Chemistry Research*, 38(4), pp. 1250-1257.

Smith, B. and Shantha, M.S. (2007) 'Membrane reactor based hydrogen separation from biomass gas', *International Journal of Chemical Reactor Engineering*, 5.

Solantausta, Y., Nylund, N. O., Westerholm, M., Koljonen, T. and Oasmaa, A. (1993) 'Wood-pyrolysis oil as fuel in a diesel-power plant', *Bioresource Technology*, 46(1-2), pp. 177-188.

Sonwane, P., Ban, H. and Gale, T.K. (2006) 'Speciation of Chlorine and Alkali Metals in Biomass Combustion and Gasification', *ASME Conference Proceedings*, 2006(47837), pp. 259-265.

Sotiropoulos, S., Brown, I.J., Akay, G. and Lester, E. (1998) 'Nickel incorporation into a hollow fibre microporous polymer: a preparation route for novel high surface area nickel structures', *Materials Letters*, 35(5-6), pp. 383-391.

Souza-Santos, M.L.D. (2004) *Solid Fuels Combustion and Gasification: Modeling, Simulation, and Equipment Operation*. Marcel Dekker, New York, USA.

Stankiewicz, A. and Moulijn, J. (eds.) (2004) *Process Intensification: History, philosophy, principles*. Netherland: Marcel Dekker, Inc.

Suarez, J.A., Luengo, C.A., Felfli, F.F., Bezzon, G. and Beaton, P.A. (2000) 'Thermochemical Properties of Cuban Biomass', *Energy Sources*, 22(10), pp. 851-857.

Sunggyu, L., Speight, J.G. and Loyalka, S.K. (2007) *Handbook of Alternative Fuel Technologies*. CRC Press, first edition.

Tai, H., Sergienko, A. and Silverstein, M.S. (2001) 'Organic-inorganic networks in foams from high internal phase emulsion polymerizations', *Polymer*, 42(10), pp. 4473-4482.

Tchobanoglous, G., Theisen, H. and Vigil, S.A. (1993) *Integrated Solid Waste Management*. Singapore: McGraw-Hill Inc.

Turn, S., Kinoshita, C., Ishimura, D., Zhou, J., Hiraki, T. and Masutani, S. (2000) *Control of Alkali Species in Gasification Systems*.

van Paasen, S.V.B. and Kiel, J.H.A. (2004) *Tar formation in a fluidised-bed gasifier. Impact of fuel properties and operating conditions*. ECN-C-04-013.

van Paasen, V.B., Bergman, P.C.A. and Neeft, J.P.A. (2002) 'Primary Measures for Tar Reduction, Reduce the Problem at the Source', *12th European Conference and Technology Exhibition on Biomass for Energy, Industry and Climate Protection*. Amsterdam, The Netherlands, 17-21 June 2002. p. 47.

Van Veldhuizen, E. (2000) *Electrical Discharges for Environmental Purposes: Fundamentals and Applications*. NOVA Science Publishers Inc.

Wakeman, R.J., Bhumgara, Z.G. and Akay, G. (1998) 'Ion exchange modules formed from polyhipe foam precursors', *Chemical Engineering Journal*, 70(2), pp. 133-141.

Wallman, P.H., Thorsness, C.B. and Winter, J.D. (1998) 'Hydrogen production from wastes', *Energy*, 23(4), pp. 271-278.

Walsh, D.C., Stenhouse, J.I.T., Kingsbury, L.P. and Webster, E.J. (1996) 'PolyHIPE foams: Production, characterisation, and performance as aerosol filtration materials', *Journal of Aerosol Science*, 27, Supplement 1(0), pp. S629-S630.

Wang, J., Liu, C. and Eliassion, B. (2004) 'Density functional theory study of synthesis of oxygenates and higher hydrocarbons from methane and carbon dioxide using cold plasmas', *Energy & Fuels*, 18(1), pp. 148-153.

Wang, W., Padban, N., Ye, Z., Olofsson, G., Andersson, A. and Bjerle, I. (2000) 'Catalytic Hot Gas Cleaning of Fuel Gas from an Air-Blown Pressurized Fluidized-Bed Gasifier', *Industrial & Engineering Chemistry Research*, 39(11), pp. 4075-4081.

Wei, X., Schnell, U. and Hein, K.R.G. (2005) 'Behaviour of gaseous chlorine and alkali metals during biomass thermal utilisation', *Fuel*, 84(7–8), pp. 841-848.

Wells, O. (1974) *Scanning Electron Microscopy*. McGraw-Hill Inc, USA.

Wen, H., et al. (1999) *Advances in biomass gasification power plants, in American Power Conference*. Chicago IIIinois.

Whitehead, J. (2007) *What is Plasma*. Available at: http://people.man.ac.uk/mbdsszjw/Pages/WhatisaPlasma.php (Accessed: 31 Jan 2009).

Williams, A., Pourkashanian, M. and Jones, J.M. (2001) 'Combustion of pulverised coal and biomass', *Progress in Energy and Combustion Science*, 27(6), pp. 587-610.

Williams, J.M., Gray, A.J. and Wilkerson, M.H. (1990) 'Emulsion stability and rigid foams from styrene or divinylbenzene water-in-oil emulsions', *Langmuir*, 6(2), pp. 437-444.

Yaman, S. (2004) 'Pyrolysis of biomass to produce fuels and chemical feedstocks', *Energy Conversion and Management*, 45(5), pp. 651-671.

Yang, H., Yan, R., Chen, H., Lee, D.H. and Zheng, C. (2007) 'Characteristics of hemicellulose, cellulose and lignin pyrolysis', *Fuel*, 86(12–13), pp. 1781-1788.

Zhang, H. and Cooper, A.I. (2005) 'Synthesis and applications of emulsion-templated porous materials', *Soft Matter*, 1(2), pp. 107-113.

Zhao, H., Draelants, D.J. and Baron, G.V. (2000) 'Performance of a Nickel-Activated Candle Filter for Naphthalene Cracking in Synthetic Biomass Gasification Gas', *Industrial & Engineering Chemistry Research*, 39(9), pp. 3195-3201.

Appendixes

Appendix A: Pictures of apparatus used in PolyHIPE Polymers (PHPs) making

(a) Set-up

(b) impeller

Appendix B: Picture of a 4.2 L capacity kitchen mixer, Kenwood chef 800W was used to mix (small scale) different compositions of oil sludge and sawdust samples
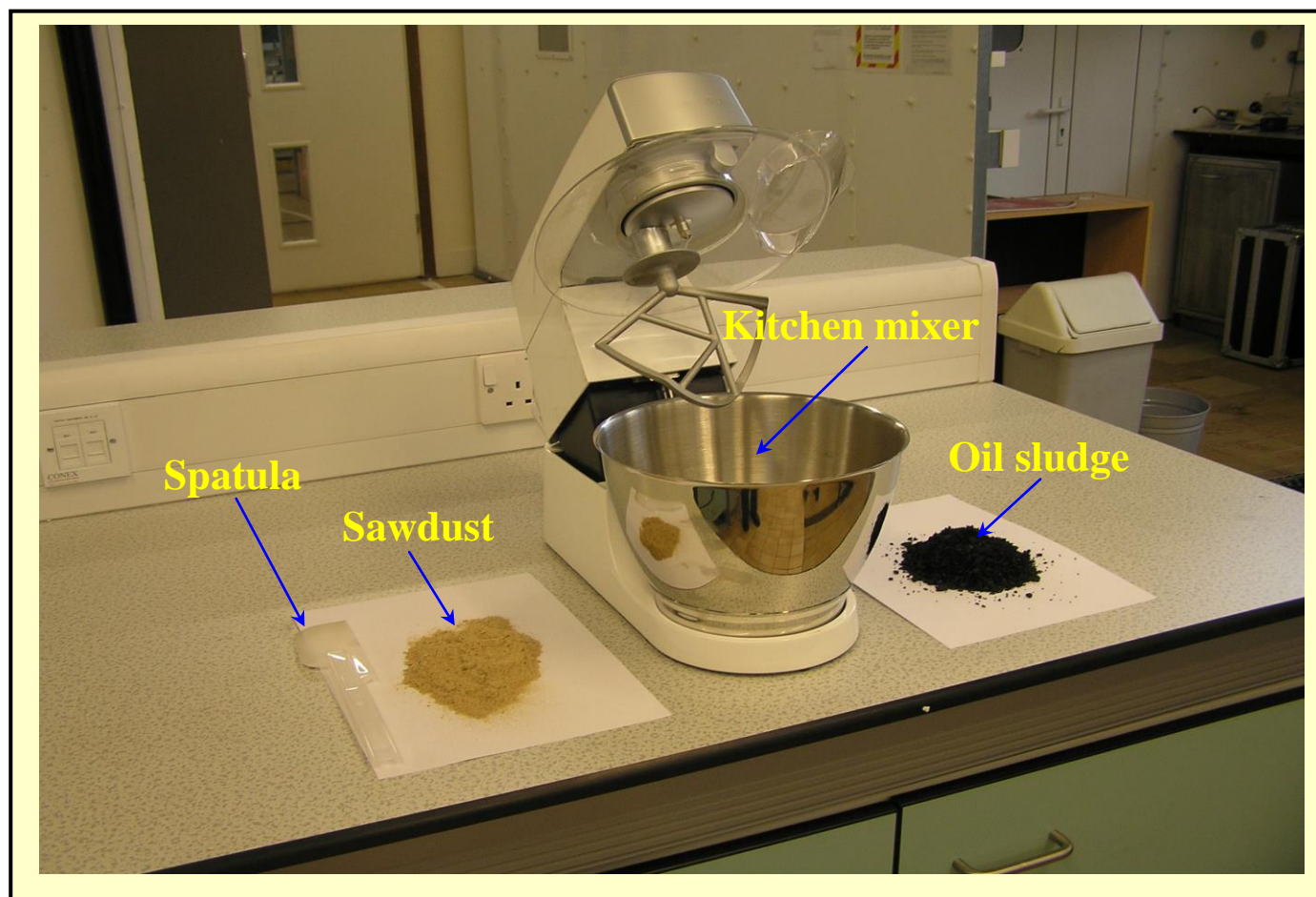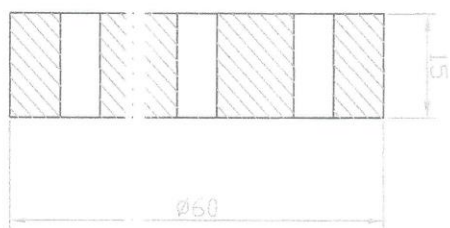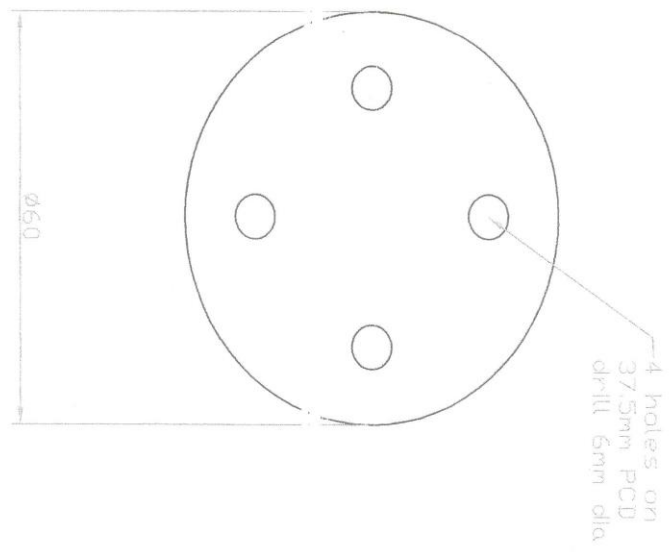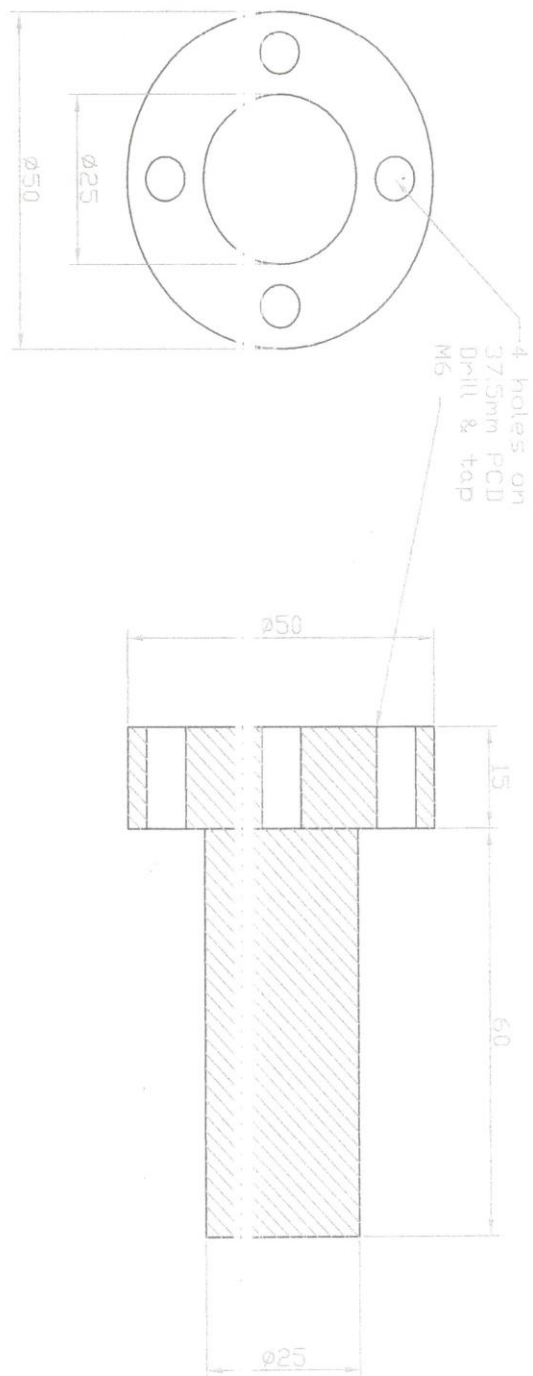
Appendix C:

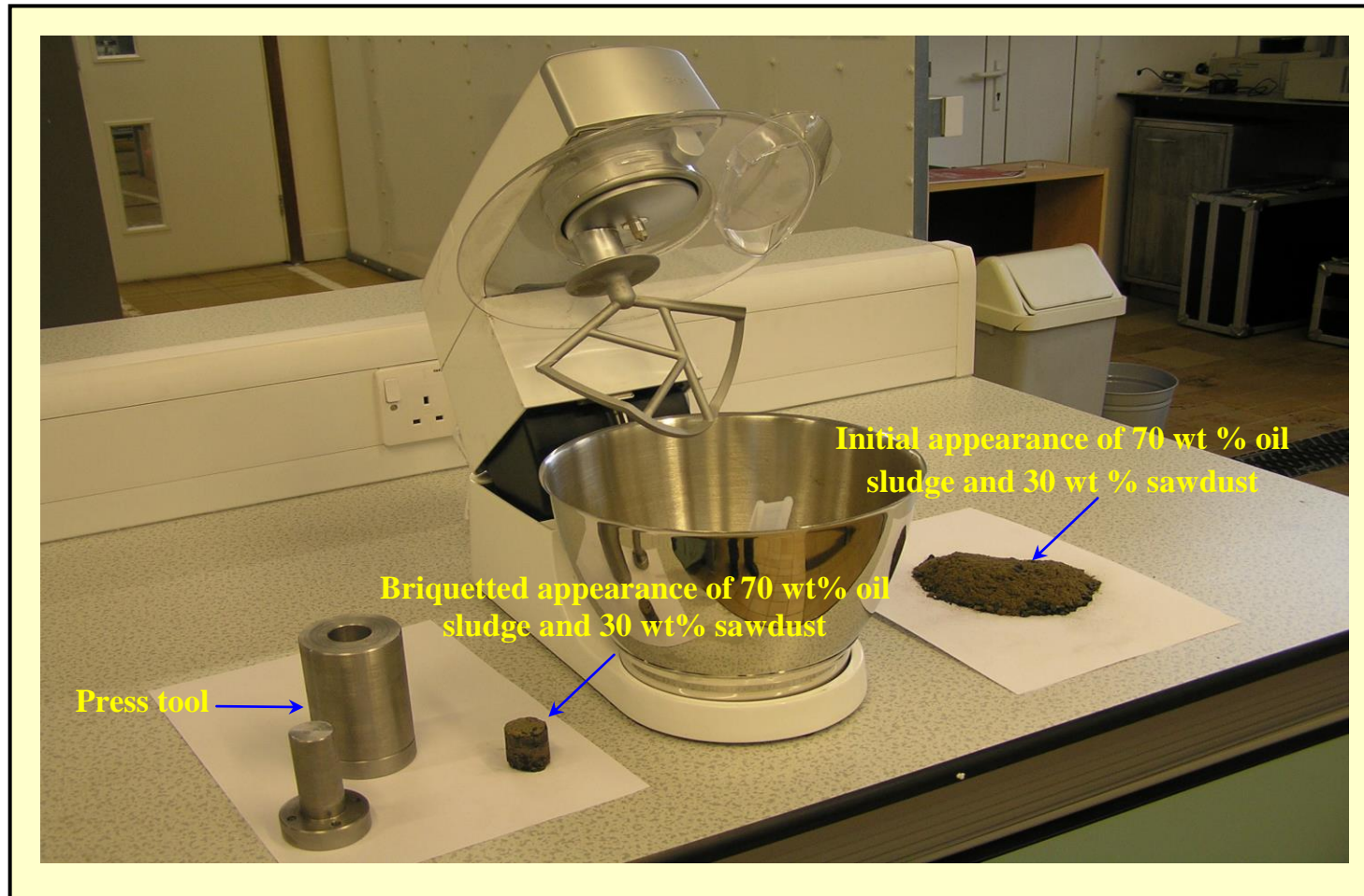**Moulding tube, blank plate and press tool sketches**

Moulding tube

4 holes
on 37.5mm
PCD drill
& tap M6

∅60
∅25

15
85
∅25
∅60

Blank plate

ø60

4 holes on
37.5mm PCD
drill 6mm dia

15

ø60

213

4 holes on
37.5mm PCD
Drill & tap
M6

Ø50

Ø25

Ø50

15

60

Ø25
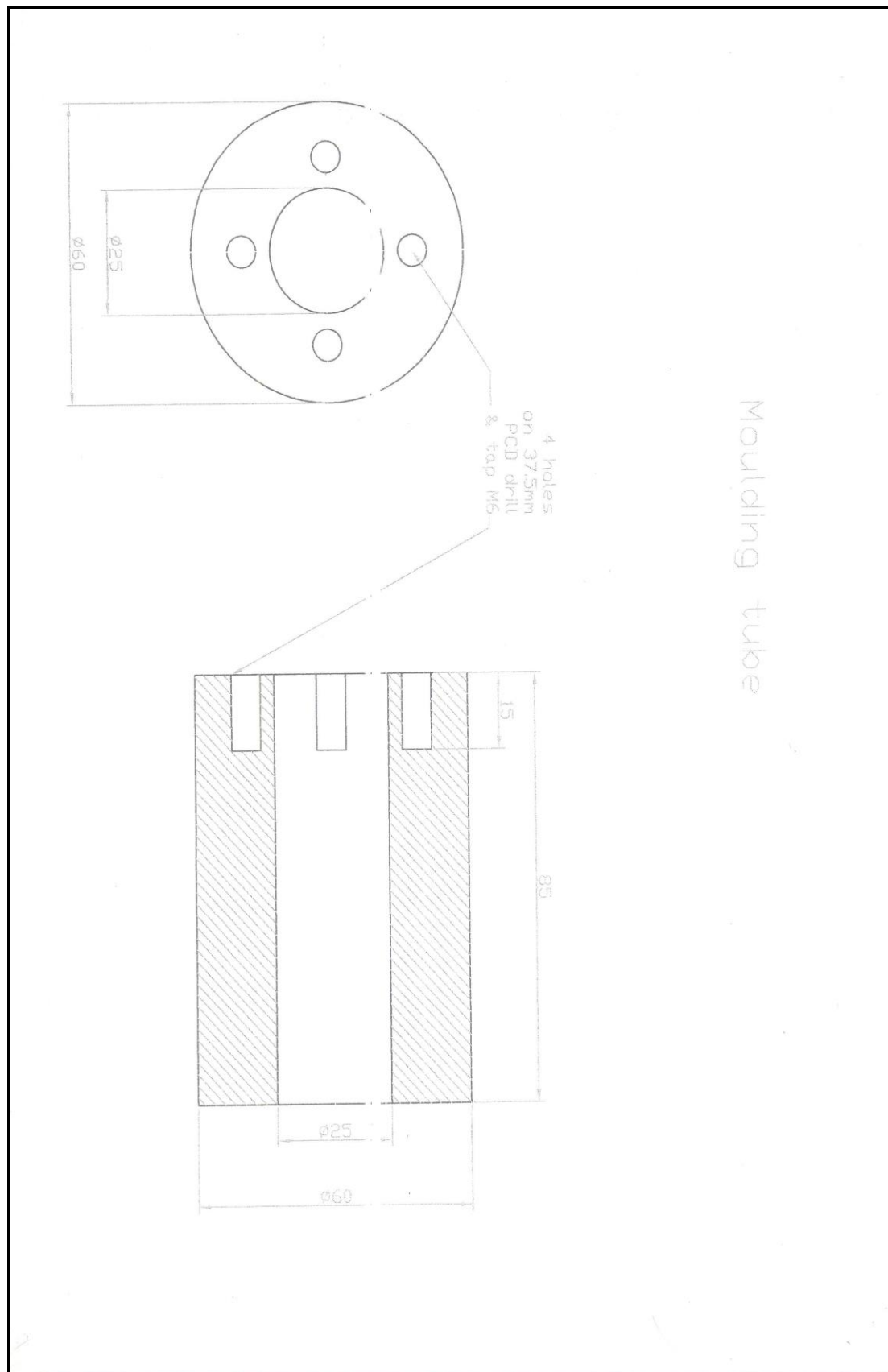
Press tool

Picture of press tool, kitchen mixer and initial briquetted appearance of 70 wt% oil sludge and 30 wt% sawdust (small scale)

Appendix D: Picture of press machine.

Appendix E: Picture of cement mixer (Minimix 130).

Appendix F: Safe Operation of the Gasifier

A number of potential hazards are associated with the operation of a gasifier. The hazards associated with the operation of a gasifier can be considered as either a toxic or an explosion/fire hazard.

Toxic Hazards

The products of a gasifier contain a number of toxic compounds in both the gaseous and liquid products. The product gas contains carbon monoxide (CO), which is colourless, odourless, tasteless and highly toxic. The long-term occupational exposure limit for carbon monoxide is 50 ppm for a weighted average on an eight hour working shift, and in the short term (ten minutes), the exposure limit is 400 ppm, this also being a weighted average. CO is absorbed into the blood to form carboxyhaemoglobin, and the effects of the levels of carboxyhaemoglobin in the blood are detailed in Table (F.1).

Table (F.1): Effects of carboxyhaemoglobin levels in the blood.

% Carboxyhaemoglobin in blood	Symptoms
<20	Nil. Slight breathlessness on exertion.
20-30	Flashing, tightness across forehead, slight headache, some breathlessness on exertion.
30-40	Severe headache, dizziness, nausea, occasional vomiting, weakness of the knees, irritability and impaired judgement.
40-50	As above but more pronounced. Fainting on exertion.
50-60	Loss of consciousness.
>60	Increasing depression of the circulatory and respiratory centres ending in death.

The other gaseous components do not have the serious toxic effects of CO. However, they may represent a potential hazard and their toxic effects are listed in Table (F.2).

Table (F.2): Toxic effects of other gas components (Macrae, 1966).

Component	ppm	First Toxic Effects
Hydrogen (H_2)	-	Asphyxiant
Nitrogen (N_2)	-	Asphyxiant
Methane (CH_4)	-	Narcotic at high concentrations in the absence
Ethane (C_2H_6), Ethene (C_2H_4),Acetylene (C_2H_2), Propene (C_3H_6) and Propane (C_3H_8)	-	Asphyxiant and possible anaesthetic at high concentrations
Hydrogen sulphide (H_2S)	>20*	Paralysis
Ammonia (NH_3)	>100*	Throat irritant
Hydrogen chloride (HCl)	>5*	Throat irritant
Hydrogen cyanide (HCN)	>10*	Headache, paralysis

* Threshold concentration (ppm by volume) as at higher concentrations for continuous 8h exposure with no impairment of health or well-being.

Another potential toxic hazard is represented by the pyrolysis liquids or tars produced in gasification. A large number of different products have been identified in these products, a number of which are toxic and some of which have been reported to be carcinogenic such as methyl napthylene-1-acetate ($C_{13}H_{12}O_2$), toluene (C_7H_8), benzene (C_6H_6) and pyrene ($C_{16}H_{10}$) (Macrae, 1966).

Explosion and Fire Hazards

Gasification is a process by which a solid fuel is converted to a gaseous fuel. It can, therefore, be seen that both the gasifier feed material and gaseous product present a potential fire, and possibly explosion, hazard. The flammable limits of the main components of the product gas in air are presented in Table (F.3), although these limits would not apply for these components in a mixture. They do, however, give an indication of the likely explosive limits for the product gas. It must be noted that the potential fire and explosion hazard is greater at start-up and shut-down, that is when the system is at unsteady state operation. This is due to the possibility of explosive

mixtures of product gas and air occurring in the system (Goss, 1980; Reed and Das, 1998).

Table (F.3): The flammable limits of the main components of the product gas in air.

Component	Flammable limits (%)		Ignition temperature (°C)
	Lower	Upper	
Hydrogen (H_2)	4.0	74.2	585
Carbon monoxide (CO)	12.5	74.2	609
Methane (CH_4)	5.0	15.0	537

Safety Precautions

In order to minimise the dangers inherent with these hazards, safety measures should be taken.

The installation of the gasifier system in a separate room from the main building was one of the main safety precautions. Also the biomass is stored in a container, which is completely detached from the main building.

In order to dispose of the product gas, a pilot gas burner was employed. The produced gas was burnt-off in the chimney. To ensure that the product gas is flaring, the pilot burner light was kept on at all times.

Composition of the CO in the laboratory was monitored by a portable CO detector (Casella TX11). The response of the reactor was less than 1 second and it was able to monitor up to 300 ppm. The alarm was set to be active at 30 ppm. This portable detector was carried by the operator in the laboratory during the experiments. There was also a second CO detector in the laboratory which was mounted on the wall. Both detectors were checked on a weekly basis and each time before the experiments. The air in the laboratory was refreshed continuously with the help of an extractor during the course of gasification experiments.

Laboratory Requirements

A number of measures independent of the gasifier system were taken to ensure the safe operation of the gasifier. These measures include:

- Safety equipment - the laboratory breathing apparatus was used which supplied fresh air through tubing.
- Emergency alarm was installed in the gasifier room to be used in the case of emergency; alarm was connected directly to the department work shop.
- Fire fighting equipment - in addition to the carbon dioxide extinguishers are available in the laboratory at all times. These extinguishers were placed so that, they could be readily reached by the operators when running the gasifier.
- Access - a clear path around the gasifier system was maintained and also from the gasifier to the laboratory exits to ensure evacuation of the laboratory as quick as possible, if required.
- All the experiments and runs were performed in the presence of at least two researchers.

Appendix G: Picture and schematic of the fresh crude oil (model tar) vessel
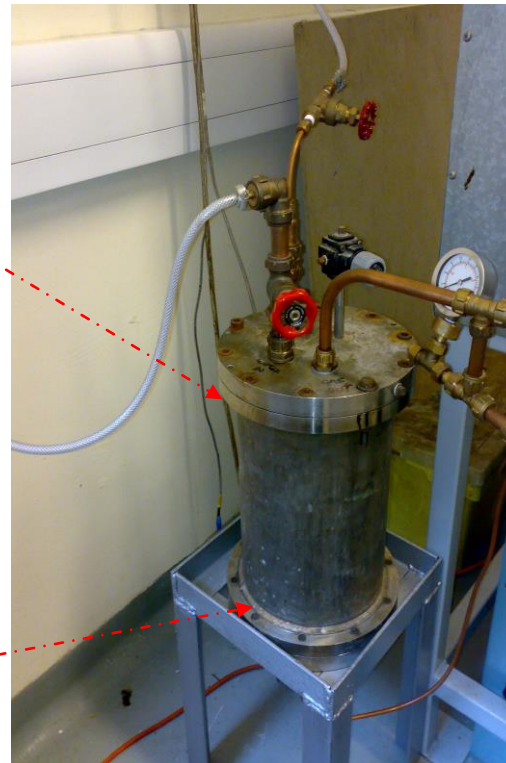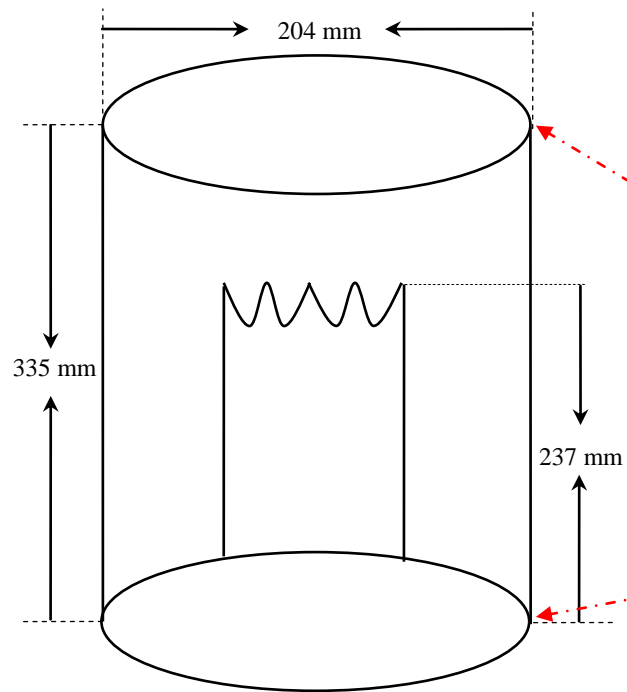
Crude oil (model tar) vessel before insulated

Appendix H: Picture of the assembled experimental setup of small scale intensified syngas cleaning system during one of the experiments

To Fume Cupboard

Key:

01 CO_2 Cylinders (Model syngas)

02 Crude oil vessel (model tar);   03 Glass reactor (syngas cleaner)

04 Cold traps;   05 Gas Chromatography (GC)

06 Digital temperature controller;   07 CO_2 volume regulator

08 CO_2 volume indicator;   09 Thermocouple

10 Gas sample before treatment;   11 Gas sample after treatment
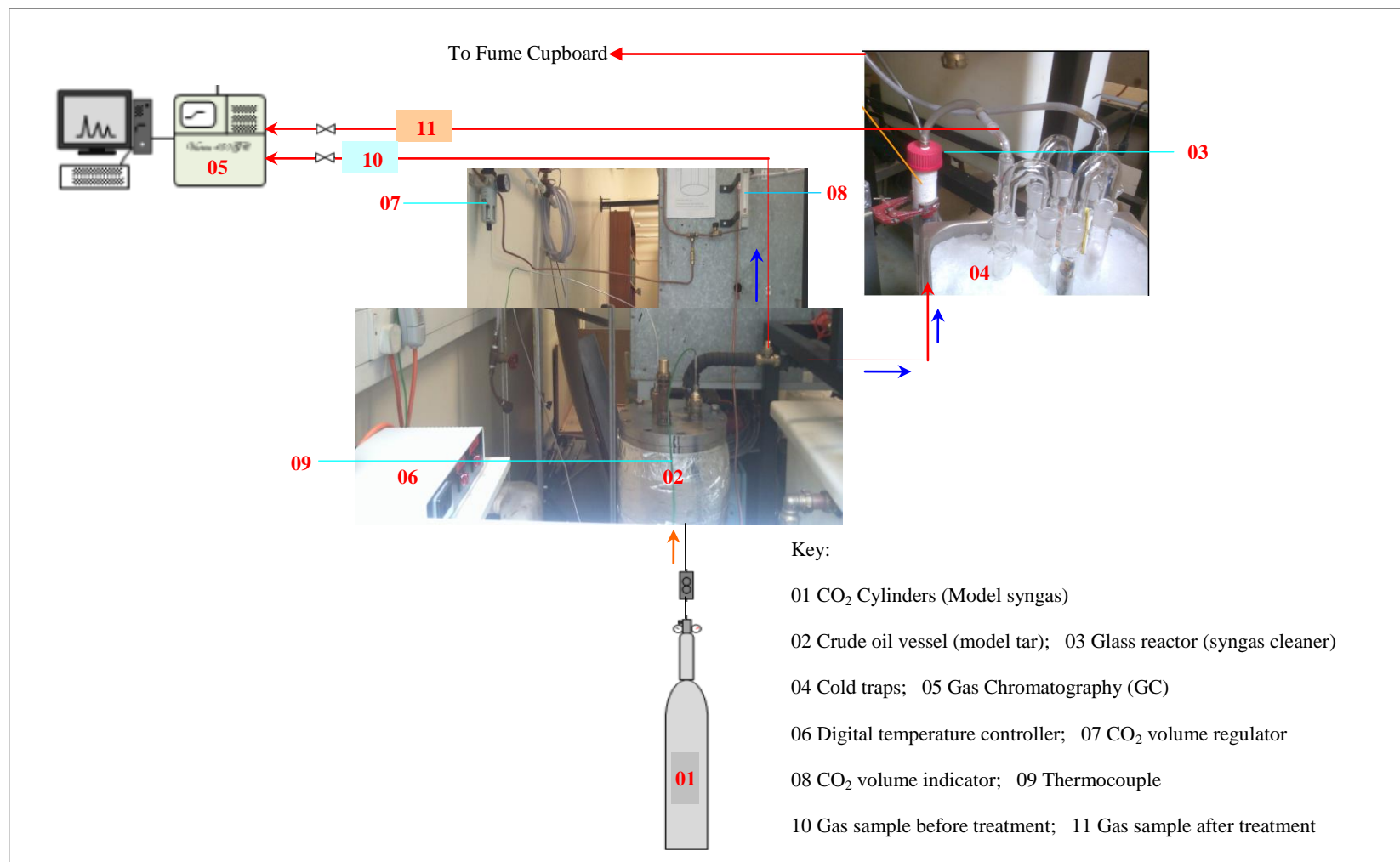
Picture of the assembled experimental setup of pilot scale intensified syngas cleaning system during one of the

experiments

Key:

101 CO$_2$ Cylinders (Model syngas); 102 Crude oil vessel (model tar)

103 Model Syngas cleaner; 104 Water tank; 105 Cold traps

106 Gas Chromatography (GC); 107 Digital temperature controller

108 CO$_2$ volume regulator; 109 CO$_2$ volume indicator

110 Gas sample before treatment; 111 Gas sample after treatment

112 Sight glass; 113 Bottom water flow indicator

114 Top water flow indicator; 115 Thermocouple
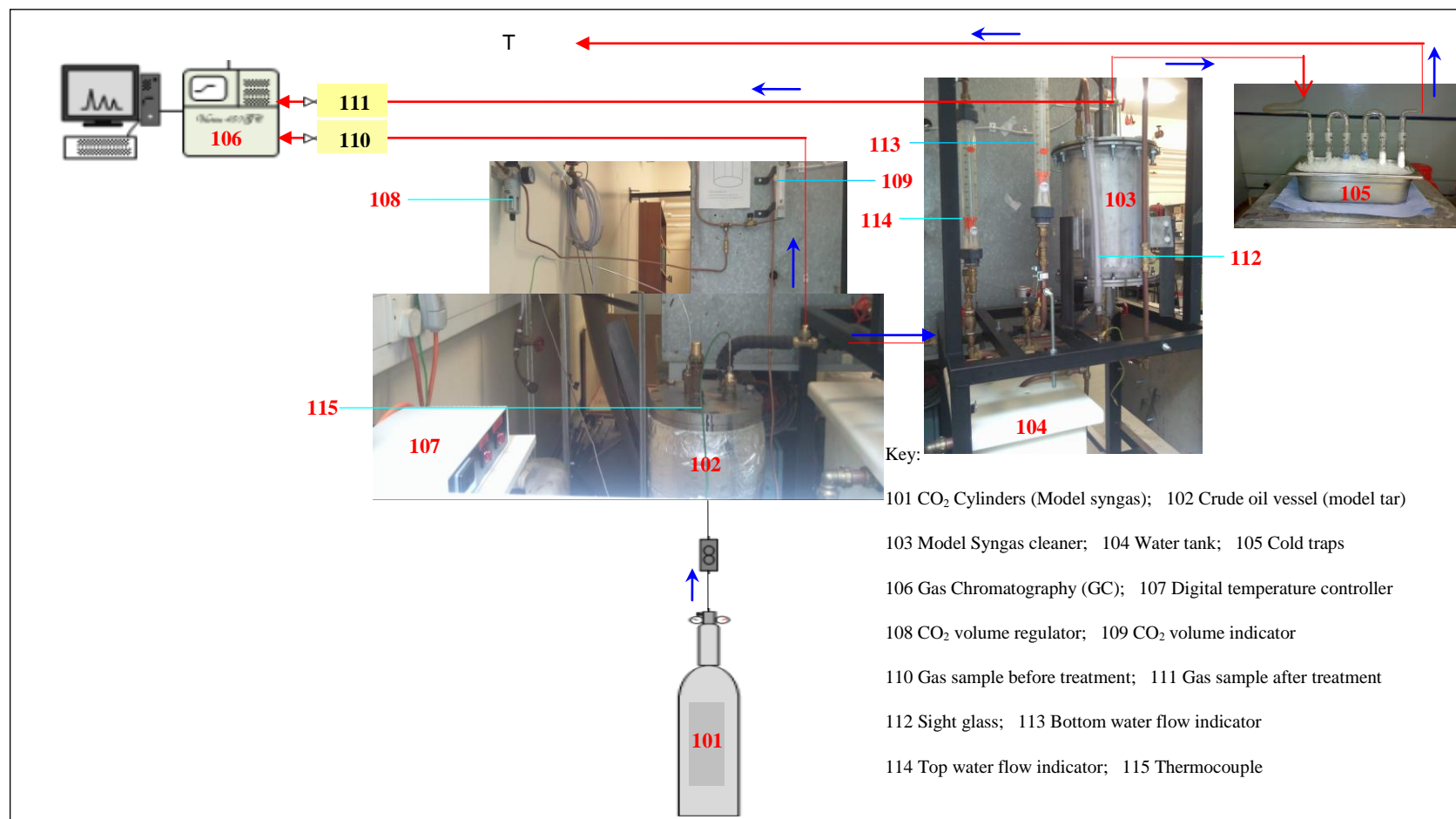
Appendix J: Details of the Electric field enhanced tar removal equipment.

(1) Electrically isolated outer cylinder

(2) Cylindrical porous nickel ground electrode

(3) Cylindrical porous nickel ground electrode in electrically isolated outer cylinder

(4) High voltage electrode (Partial electrode insulation configuration)

(5) The high voltage electrode with sulphonated PolyHIPE Polymer (s-PHP) particles around

(6) Central high voltage electrode in cylindrical porous nickel ground electrode in electrically isolated outer cylinder

(7) Electric field enhanced tar removal equipment assembled.

Appendix K: Safe Operation of the High voltage

Safety Measures

Prior to the operation, it was essential to ensure that the system is assembled such that it complies with the safety procedures of power supplier designed for use up to 30 kV. In accordance to that, the following connection/ disconnection of the HV supplier procedures were followed:

Connection Procedure

1- Ensure all controls are disabled, electrical supplies and HV power supplier are isolated and power turned off.

2- Install the electrode.

3- Install the mesh.

4- Install the lid carefully.

5- Install the electrode enclosure and connect to the HV cable, making sure that interlock switch is correctly located.

6- Connect the mesh earth connection.

7- Connect the lid interlock.

8- The lid is now in position and when secured it is ready for power to be applied to the electrode.

9- Enable the HV relay using the `ENABLE RELAY' button when ready to start the experiment.

10- Turn on the HV power supplier and set the value required for the experiment.

Disconnection Procedure

Once the HV power supplier was switched off at the end of the experiment and before removing the lid of the equipment, the following guidelines were followed:

1- Set HV power supplier to zero. Wait for any potential energy that may still be contained in the electrode to be discharged.

2- Disable HV relay using the `DISABLE RELAY' button.

3- Turn off all other system power.

4- Disconnect the lid interlock.

5- Disconnect mesh earth connection.

6- Remove electrode enclosure enough to disconnect HV cable.

7- Now, remove the equipment lid carefully.

8- Remove the mesh.

9- Remove the electrode.

INSTRUCTION MANUAL
SERIES EL

PS/EL30P01.5-22

MODEL _____

SERIAL # _____

DATE _____10-09-90_____

GLASSMAN HIGH VOLTAGE, INC.

WHITEHOUSE STATION, NJ

Innovations in high voltage power supply technology.

TABLE OF CONTENTS
EL SERIES

C DIGITAL METER OPTION

Units equipped with the digital meter option have the same features as the standard EL with the following modifications:

*   A CURRENT limit control is provided with 10-turn locking vernier dial.

*   3 1/2 digit digital panel meters are provided in place of the standard analog meters.

SECTION II – GENERAL INFORMATION

A. UNPACKING AND INSPECTION

First inspect package exterior(s) for evidence of rough handling in transit. If none, proceed to unpack... carefully. After removing the supply from its shipping container, inspect is thoroughly for damage.

IMPORTANT

In cases of damage due to rough handling in transit, notify the carrier immediately if damage is evident from appearance of package. Do not destroy or remove any of the packing material used in a damaged shipment. Carrier companies will usually not accept claims for damaged material unless they can inspect the damaged item and its associated packing material. Claims must be made promptly- certainly within five days of receipt of shipment.

B. CORRESPONDENCE

1. Each Glassman power supply has an identification label on the chassis that bears its model and serial number.

2. When requesting engineering or applications infor- mation, reference should be made to this model and serial number, as well as to the component symbol number (s) shown on the applicable schematic diagram, if specific components or circuit sections are involved in the inquiry.

GLASSMAN HIGH VOLTAGE, INC.
Route 22 East, Salem Industrial Park
Whitehouse Station, N.J. 08889

TEL. 201-534-9007
TWX. 710-480-2839
FAX. 201-534-5672

C. INSTALLATION AND OPERATION

WARNING!!

NEVER ATTEMPT TO OPERATE THIS UNIT WITHOUT A GOOD EARTH
GROUND CONNECTED TO THE GROUND STUD E1. THE GROUND
WIRE OF THE AC LINE CORD SHALL ALSO BE GROUNDED.

READ AND FULLY UNDERSTAND THE OPERATING INSTRUCTIONS
BEFORE APPLYING POWER TO THIS UNIT.

THIS EQUIPMENT EMPLOYS VOLTAGES THAT ARE DANGEROUS.
EXTREME CAUTION MUST BE EXERCISED WHEN WORKING WITH THIS
EQUIPMENT.

DO NOT HANDLE THE LOAD OR EXPOSED HIGH VOLTAGE
TERMINATIONS OR ATTEMPT TO MAKE OR REMOVE ANY CONNECTIONS
TO THE SUPPLY UNTIL THE LOAD AND/OR SUPPLY HAS BEEN
DISCHARGED (GROUNDED). AN UNLOADED SUPPLY MAY TAKE
UP TO 15 SECONDS TO FULLY DISCHARGE.

ALWAYS MAKE CERTAIN THAT THE RETURN SIDE OF THE LOAD
IS CONNECTED TO COMMON OR GROUND.

The following procedure should be followed to connect and operate the equipment, after it has been placed or mounted in position.

1. Check the input voltage rating on the nameplate of the power supply and make certain that this is the rating of the available power source.

2. Check to see that the power switch is in the OFF (down) position.

3. Connect the high-voltage output cable and ground return lead to the load. Insert the high voltage cable into the receptacle on the rear panel. Spring action should be felt as the probe reaches the bottom of the receptacle. Hold the cable pressed down against the spring as the locking nut is screwed onto the receptacle.

4. Connect the input cable to the power source.

5. Rotate OUTPUT VOLTAGE control to fully counterclock-wise position. (This is optional, but desirable to prevent damage to external equipment caused by in-advertent overvoltage setting. Not required if correct setting has already been determined.)

6. DM OPTION UNITS ONLY: Rotate output CURRENT control clockwise to a level that is greater than the amount that the connected load will require (any setting above zero if no load is connected).

7. Apply input power to the supply by setting POWER SWITCH to ON (up) position.

8. Rotate output VOLTAGE control clockwise until volt-meter indicates desired output voltage.

9. To shut down supply, set POWER SWITCH to OFF (down) position.

WARNING:

DO NOT HANDLE THE LOAD OR EXPOSED HIGH VOLTAGE TERMINATIONS OR ATTEMPT TO MAKE OR REMOVE ANY CONNECTIONS TO THE SUPPLY UNTIL THE LOAD AND/OR SUPPLY HAS BEEN DISCHARGED (GROUNDED). AN UNLOADED SUPPLY MAY TAKE UP TO 15 SECONDS TO FULLY DISCHARGE.

D. POLARITY REVERSAL

For reversible polarity models, the power supply
has been shipped with two high voltage assemblies, one
positive and one negative. Both modules are mounted in
the chassis. The active module is wired into the
chassis harness, and the inactive module is mounted on
the other side of the chassis for shipping/storage.
A label on each high voltage assembly indicates its
polarity. To reverse the polarity of the power
supply, it is necessary to interchange the high
voltage modules.

1. First remove the top cover from the unit.

2. Remove the electrical connectors and the push lug
    which are mounted on the high voltage assembly
    that is presently active.

3. Tip the unit on its side to expose the eight
    counter-sink screws on the bottom that hold in the
    two high voltage modules. Remove these eight
    screws.

4. Swap the positions of the two high voltage
    modules.

5. Visually align the active module circuit board pem
    nuts with the plastic housing and bottom chassis.
    Re-install the four screws and re-connect the
    electrical connectors.

6. Install the inactive module in the shipping/
    storage position with its four screws.

7. Replace the top cover.

Appendix L:

Identification of tar components from the tar collected from syngas and tar compounds in syngas after flow through sulphonated PolyHIPE Polymer.

Table (K.1): Identification of tar components from the tar collected from syngas

Peaks	*m/z*	Compounds
1	94	Phenol
2	106	*m*-xylene, *p*-xylene
3	106	*o*-xylene
4	152	acenaphthylene
5	NA	unknown
6	166	fluorene
7	168	dibenzofuran
8	178	phenanthrene
9	178	anthracene
10	192	methylphenanthrene
11	246	hexadecanoic acid
12	204	9,10-bis(chloromethyl) anthracene
13	NA	unknown
14	202	fluoranthene
15		unknown
16	202	pyrene

Table (K.2): Tar compounds in syngas after flow through sulphonated PolyHIPE Polymer

Tar class	Compounds
1	unknown
2	phenol
	1,2-benzenediol
	3-phenoxy-1,2-propanediol
3	Styrene
	dibenzofuran
4	acenaphthylene
	phenanthrene
5	fluoranthene
	pyrene

Appendix M:

Environmental Scanning Electron Microscopy (ESEM) images of exposed and unexposed sulphonated PolyHIPE Polymer (s-PHP) at different magnifications

1. ESEM images of fresh s-PHP prepared for use in reduction of model tar (crude oil) from model syngas (CO_2) at different magnifications:
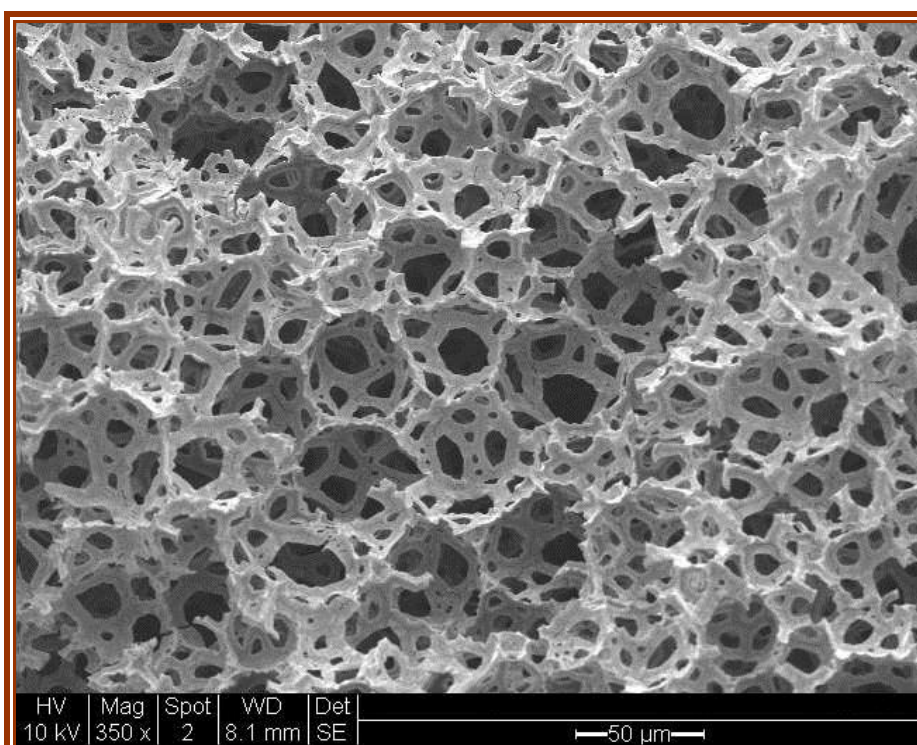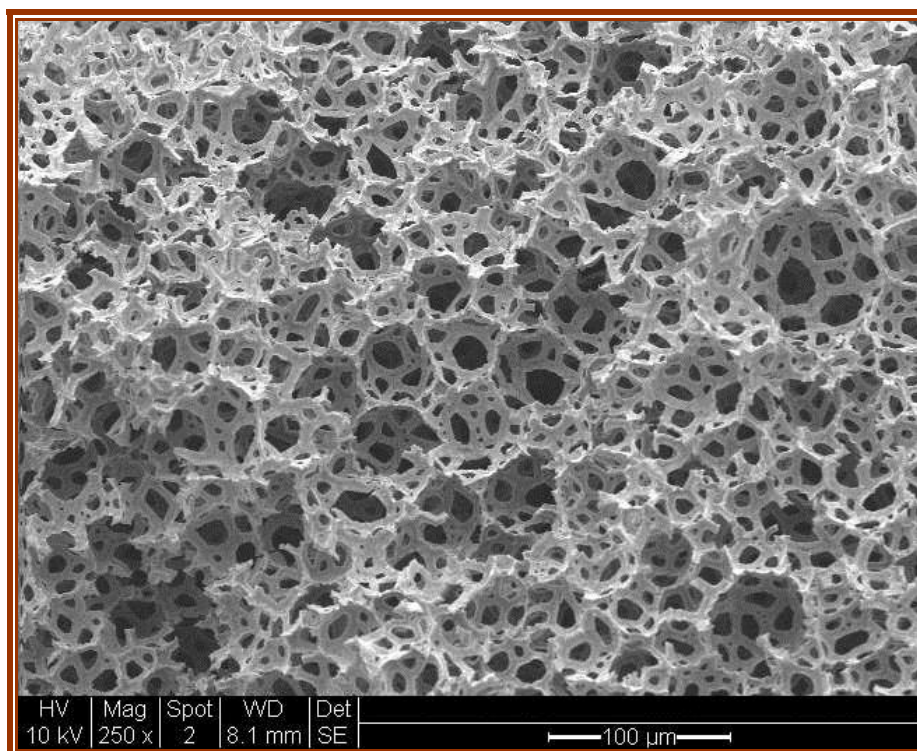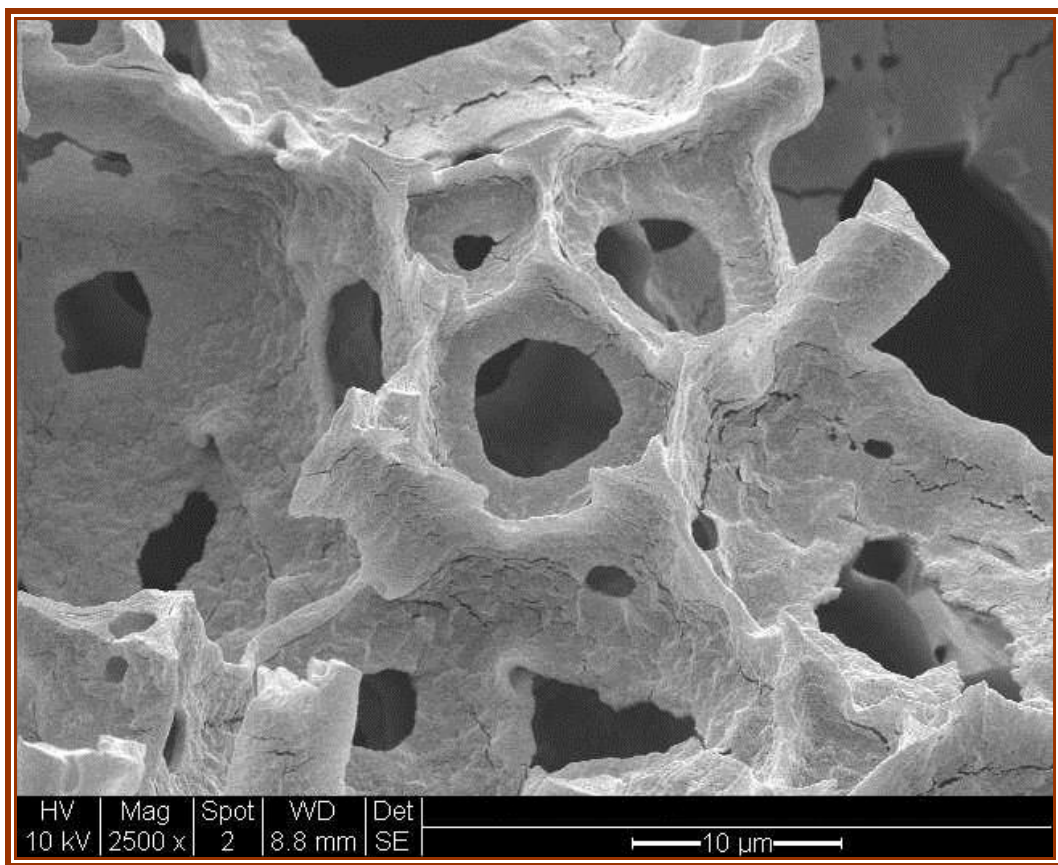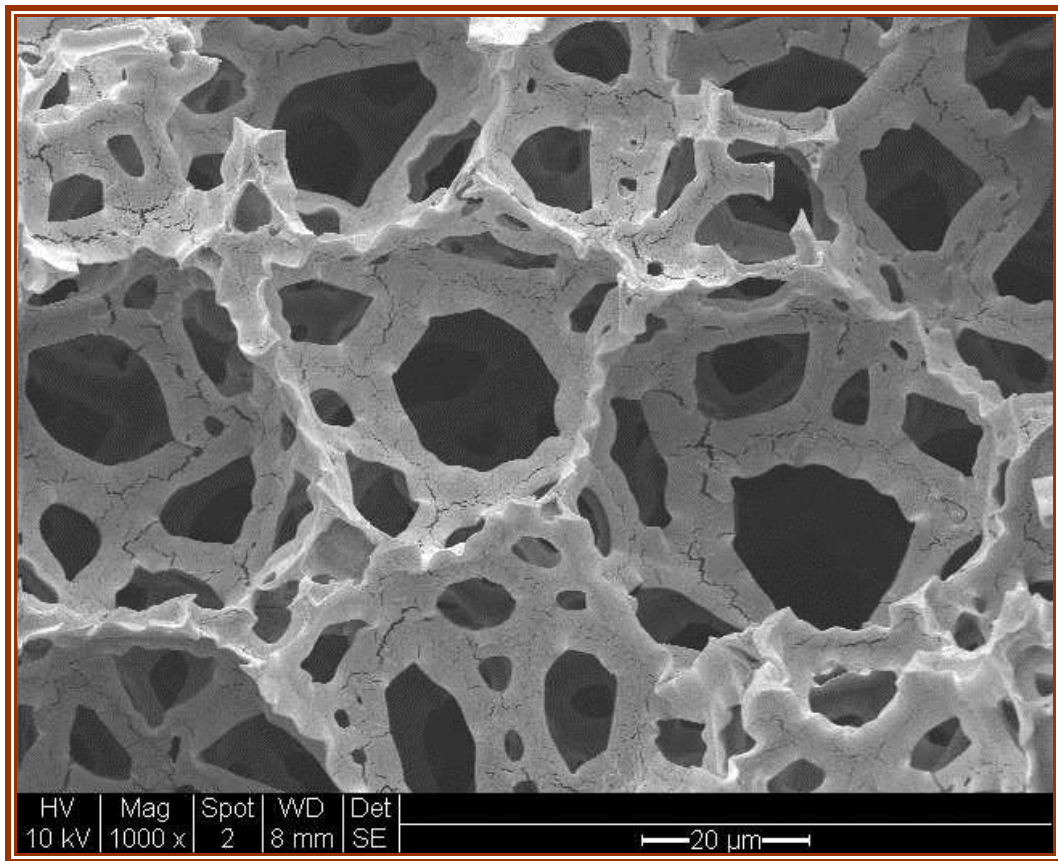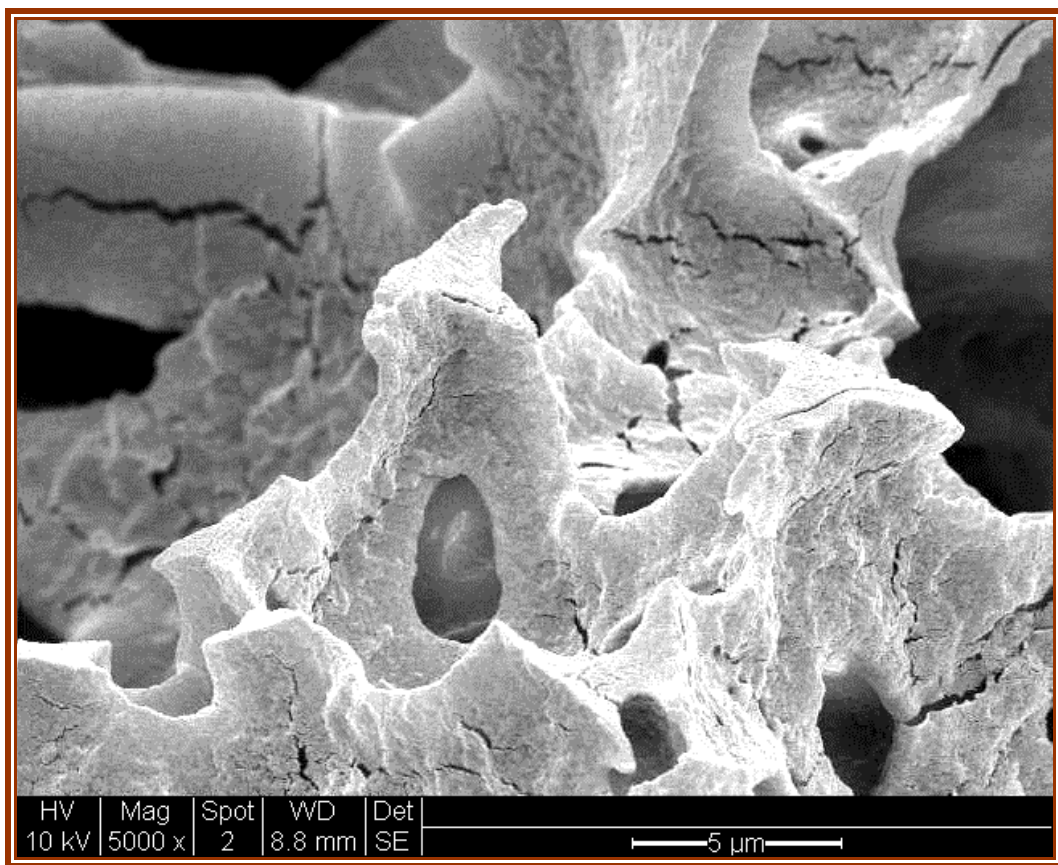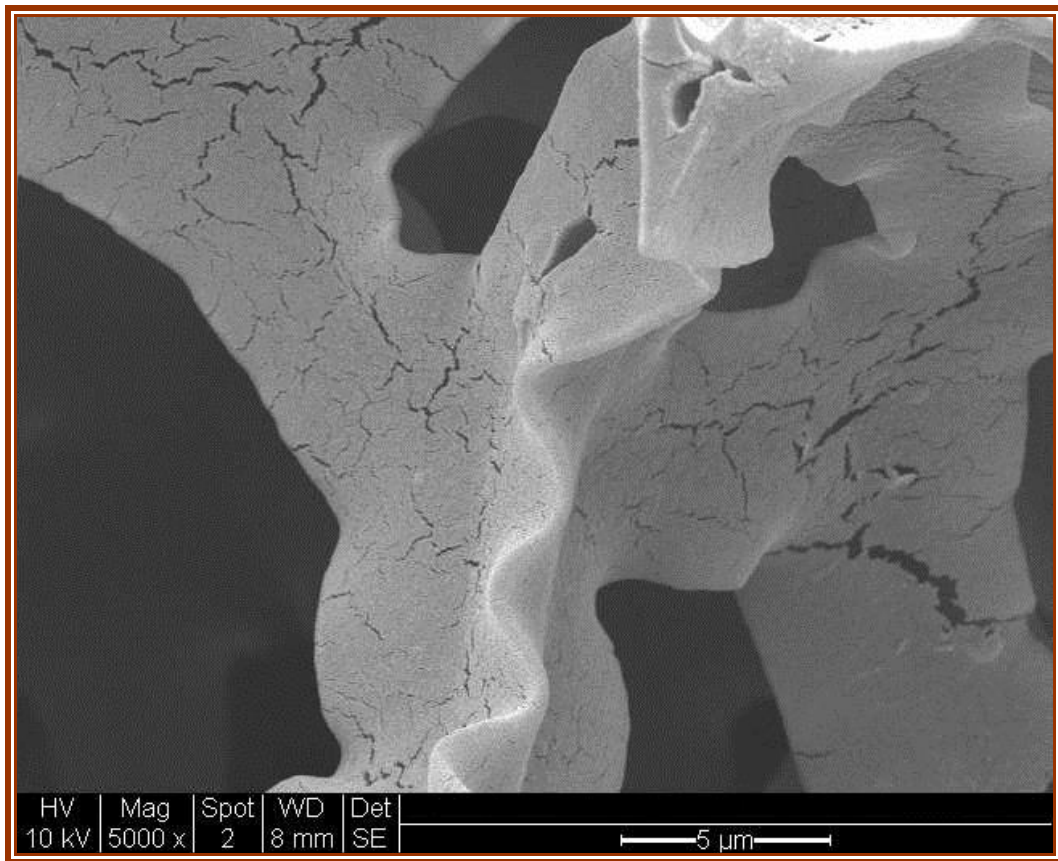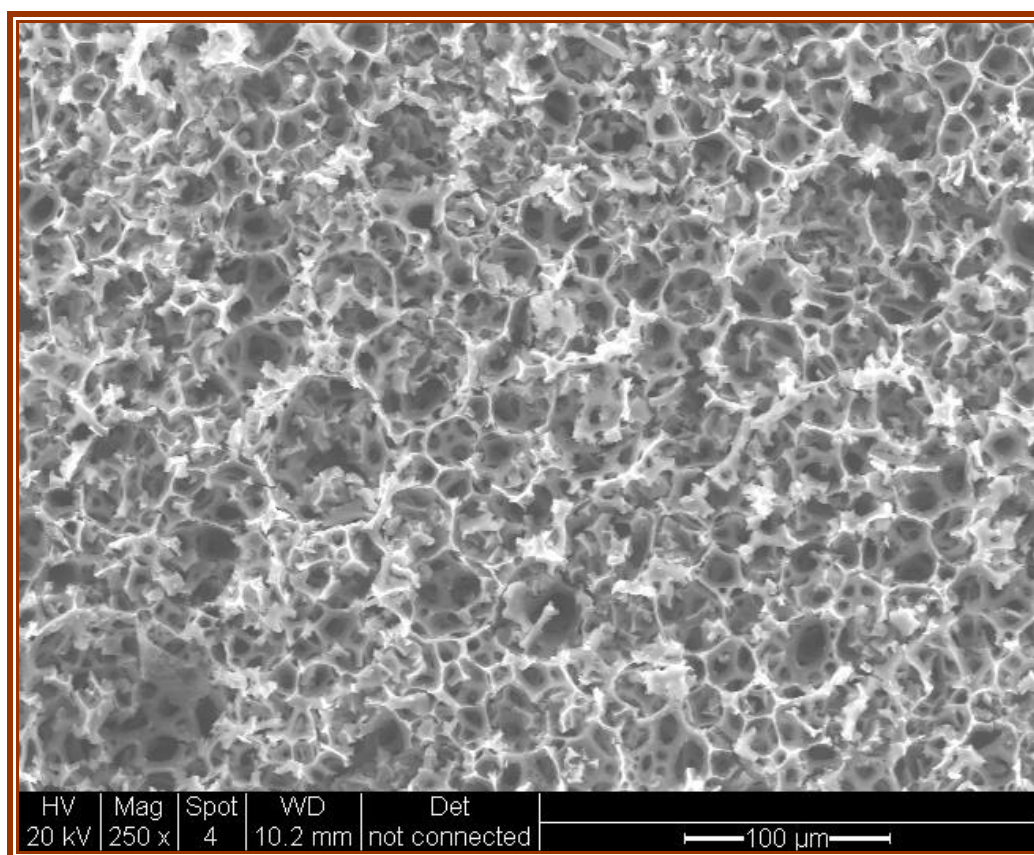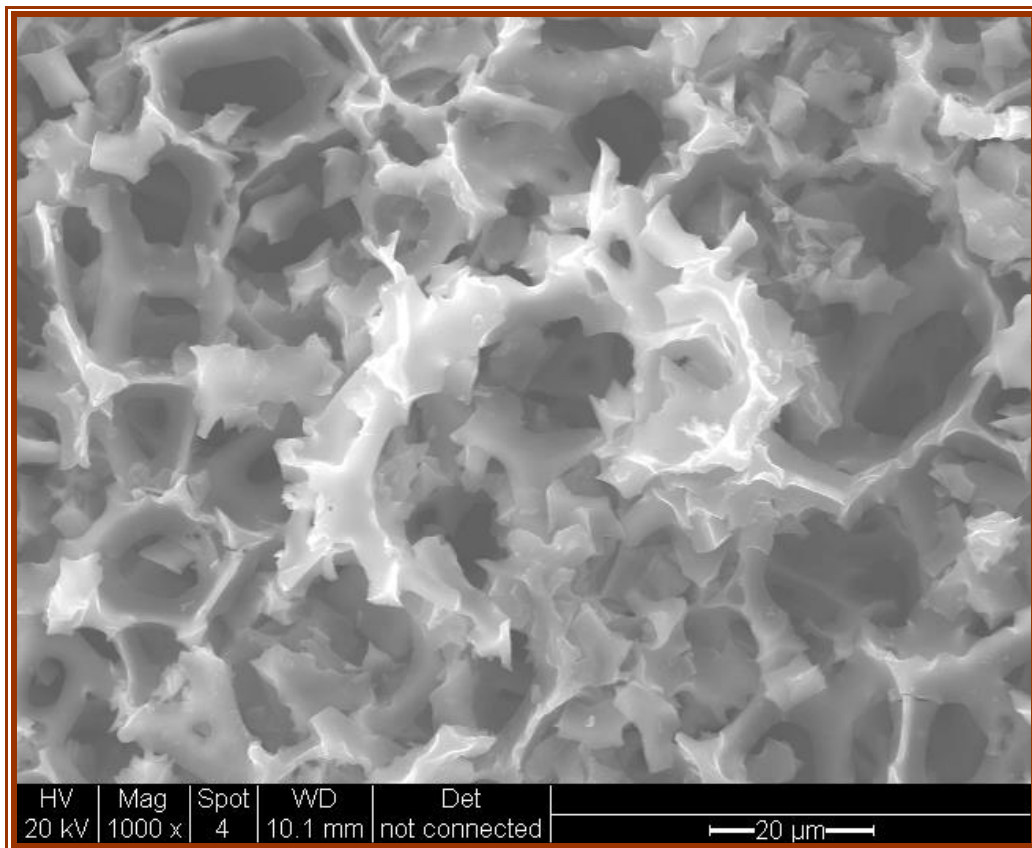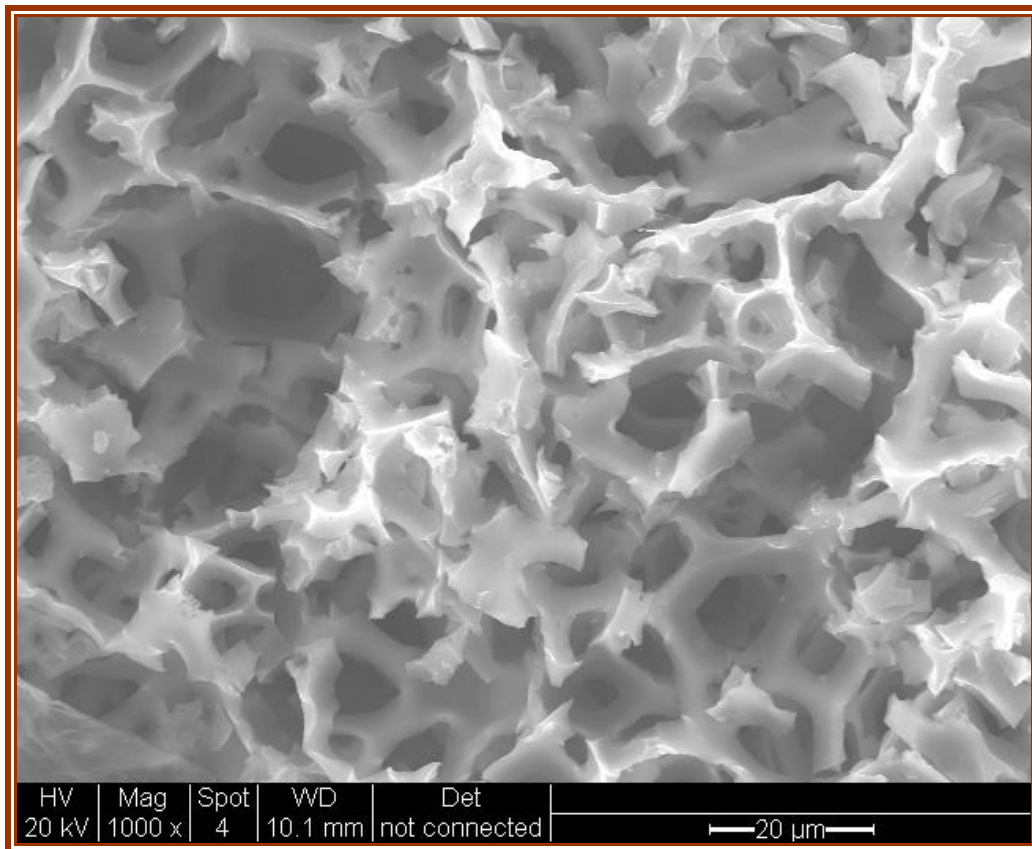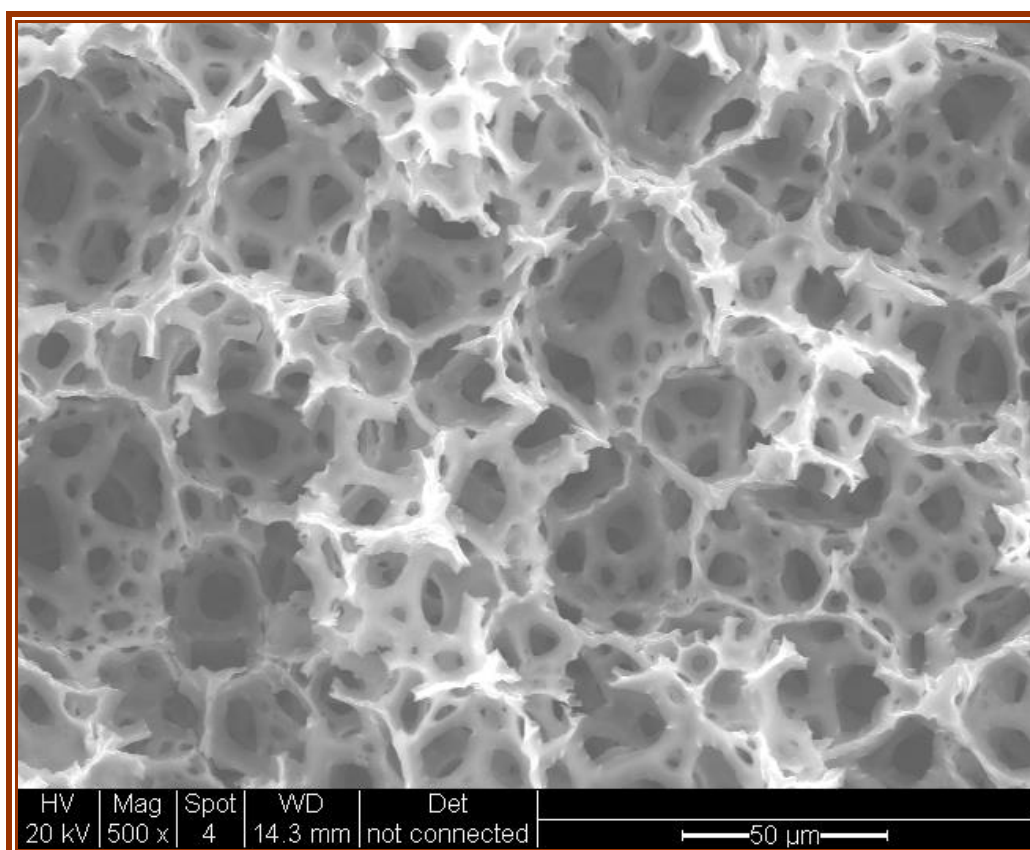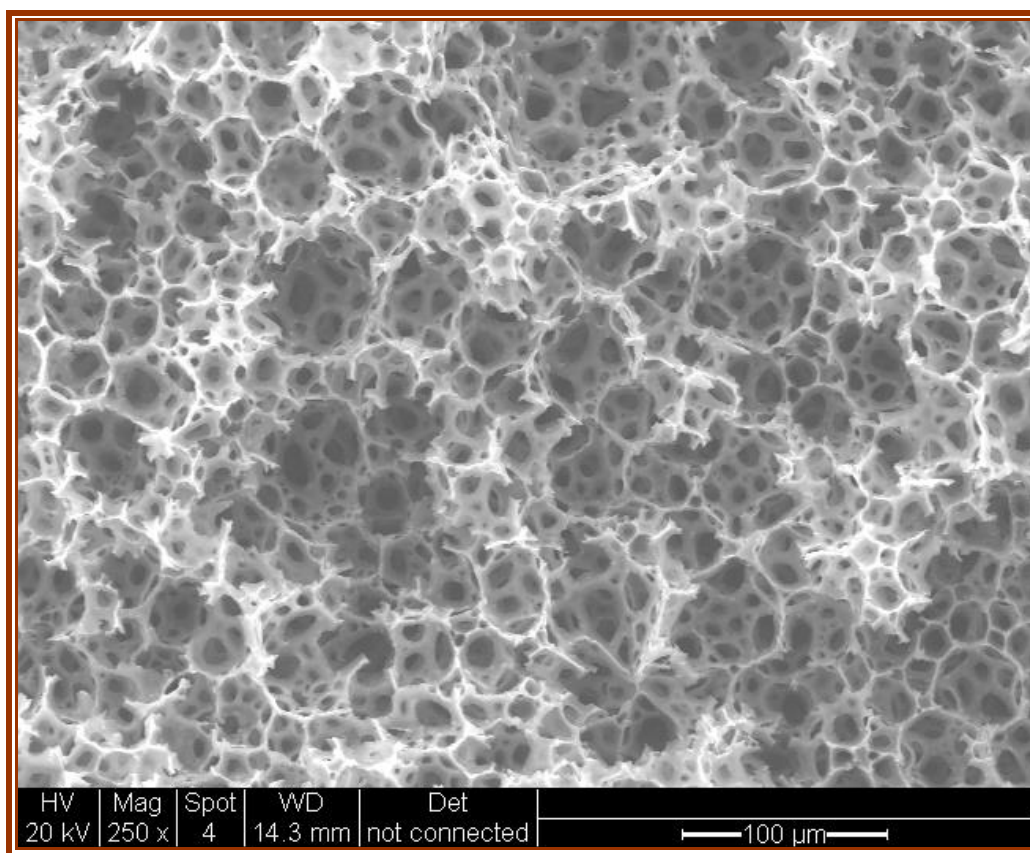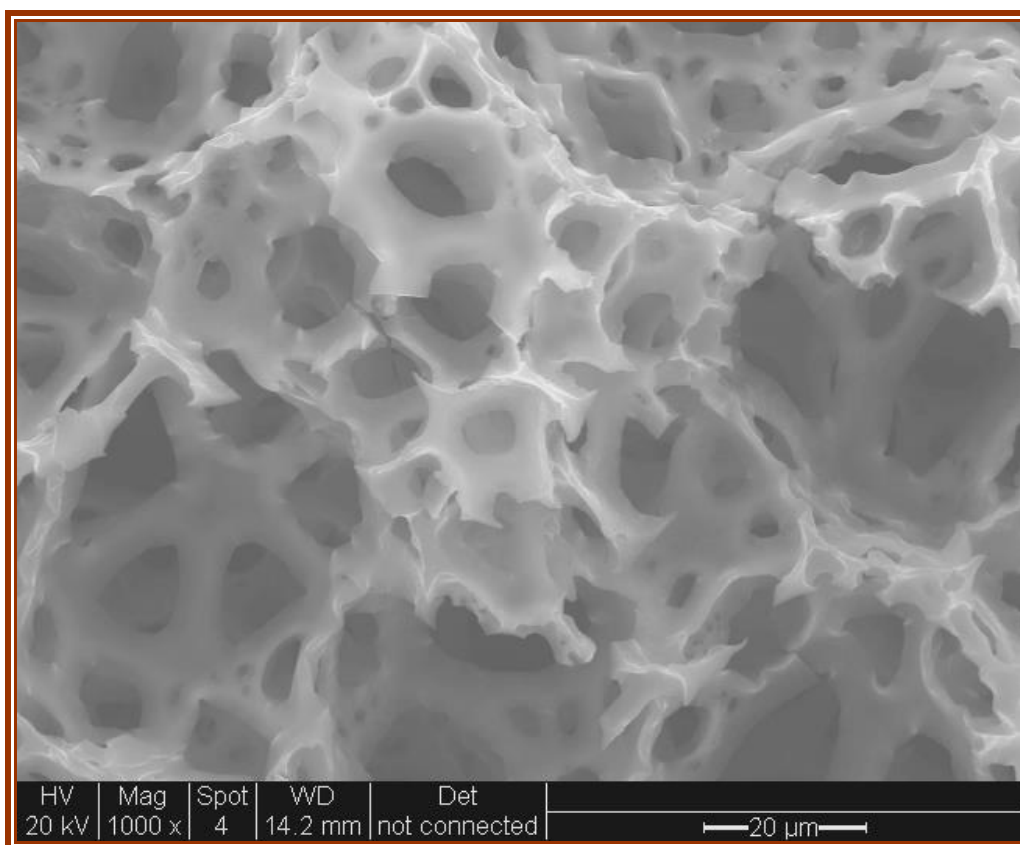
2. ESEM images of s-PHP surface after use in reduction of model tar (crude oil) from model syngas (CO_2) at different magnifications:
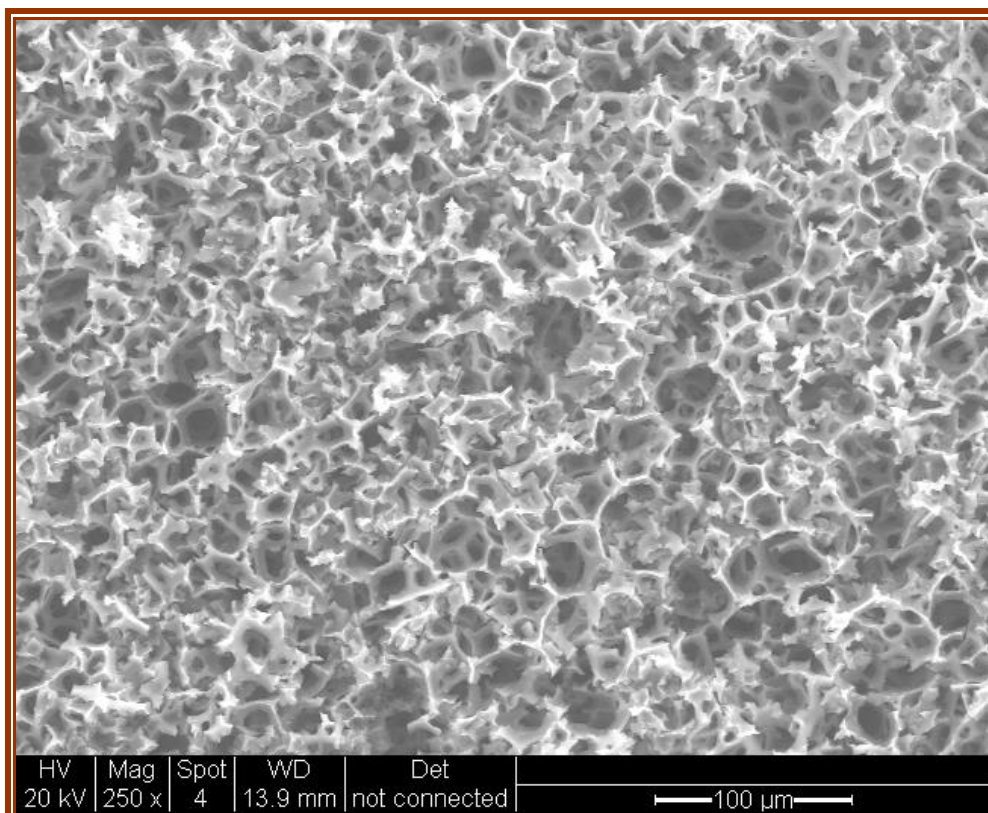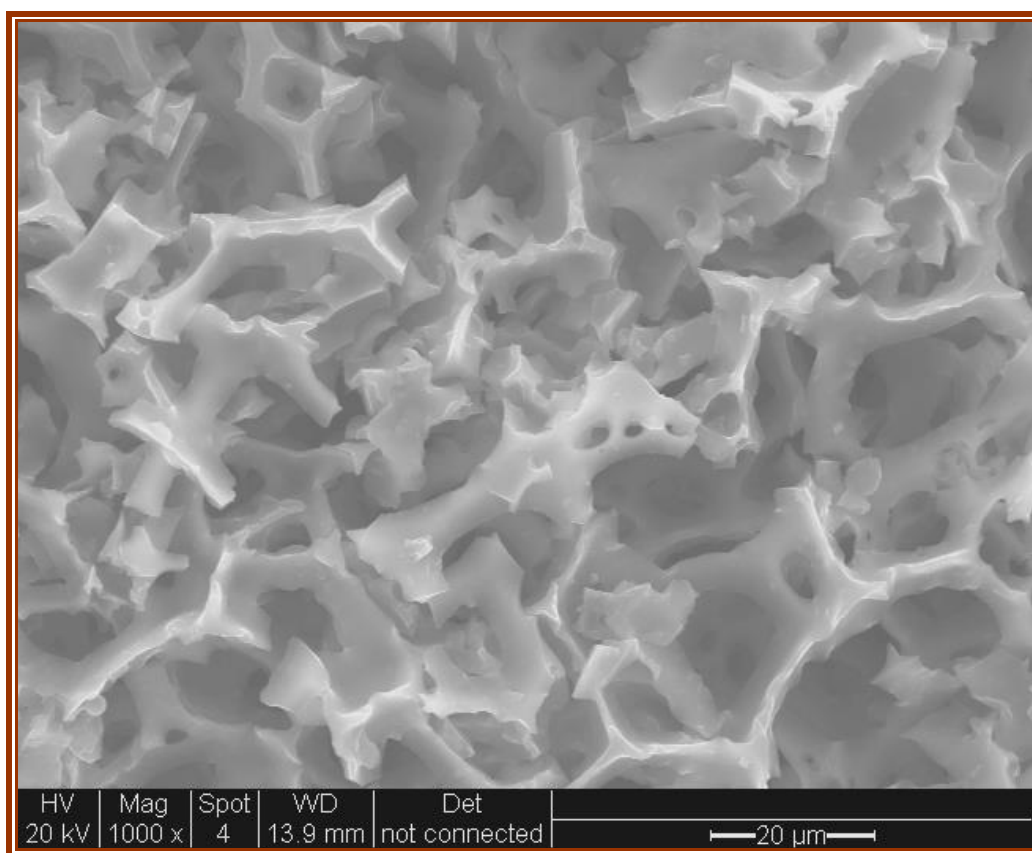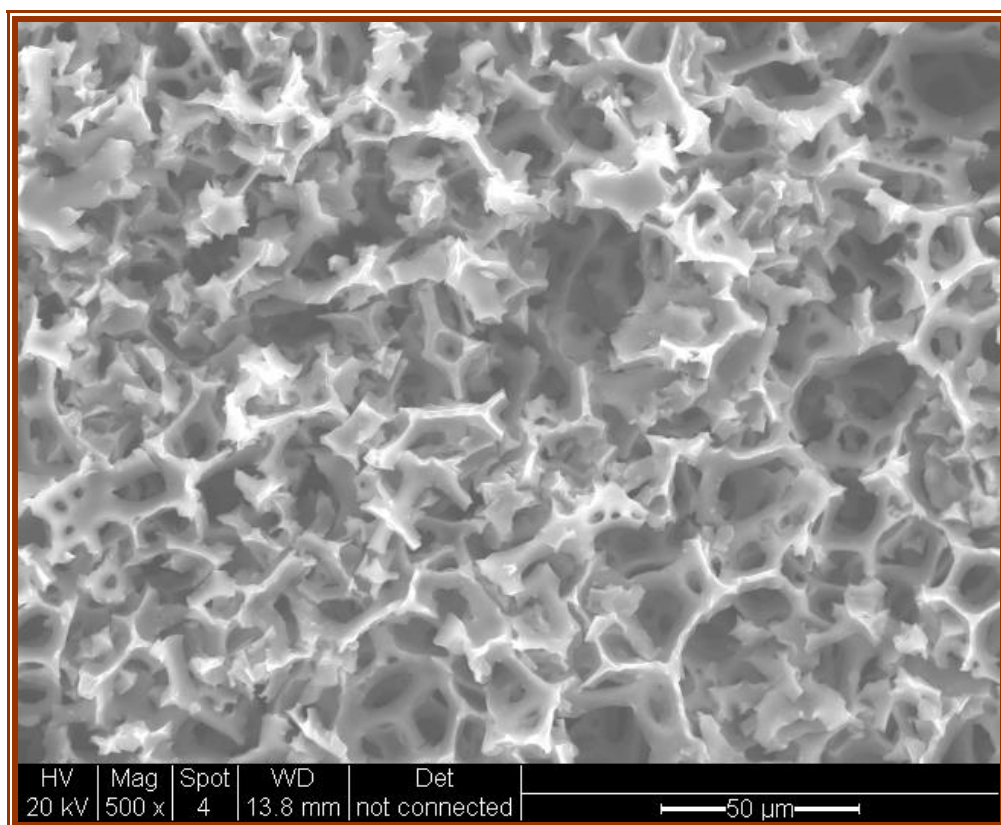
3. ESEM images of s-PHP cross section after used in reduction of model tar (crude oil) from model syngas (CO_2) at different magnifications:

HV: 20 kV | Mag: 50 x | Spot: 3 | WD: 12.6 mm | Det: SE | 500 µm

HV: 20 kV | Mag: 250 x | Spot: 3 | WD: 12.3 mm | Det: SE | 100 µm
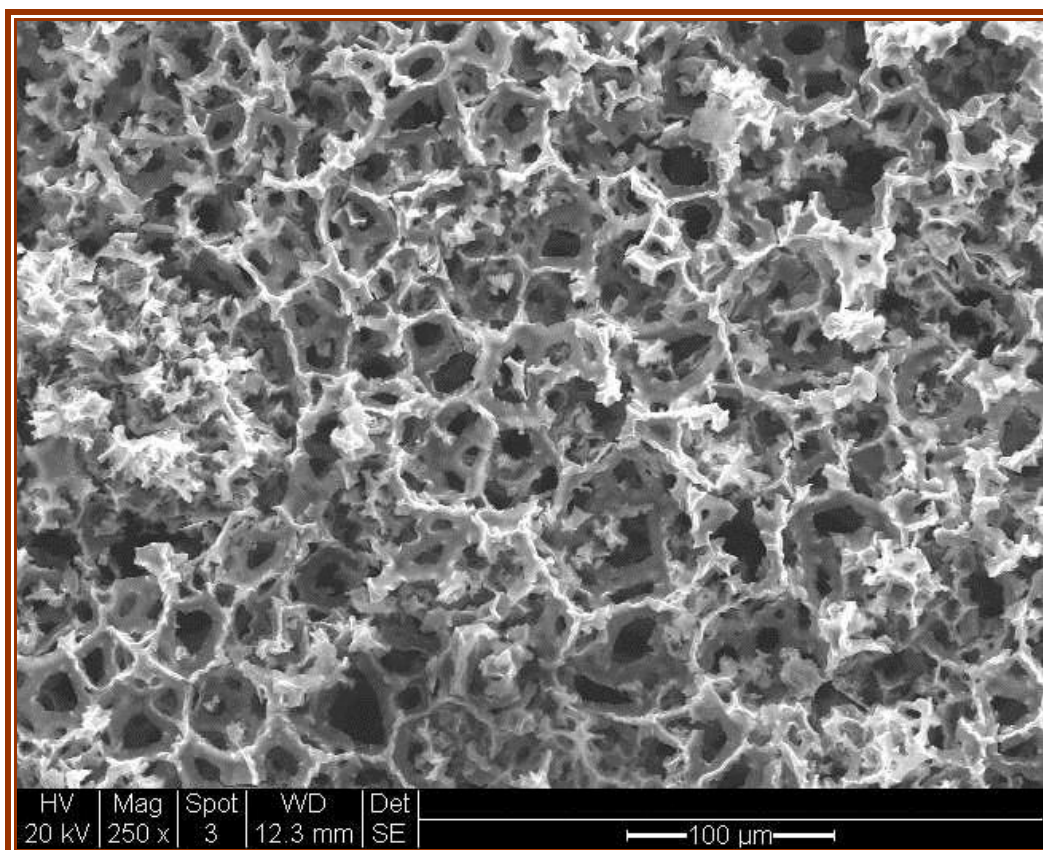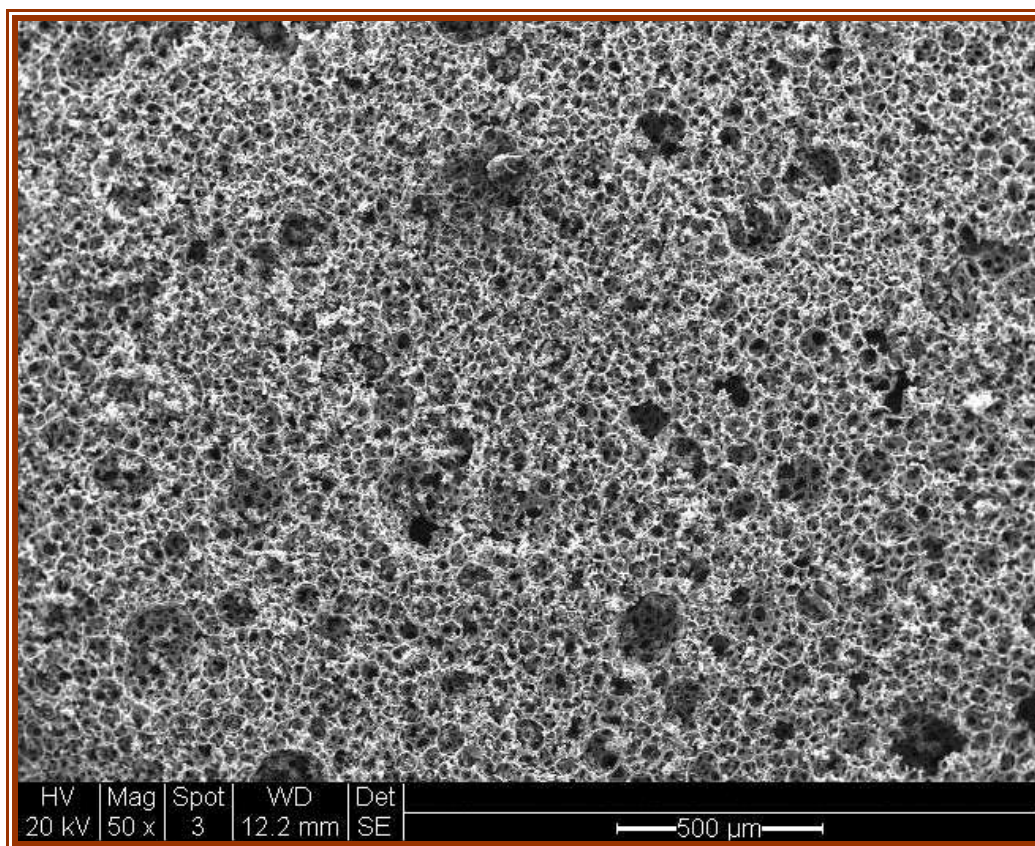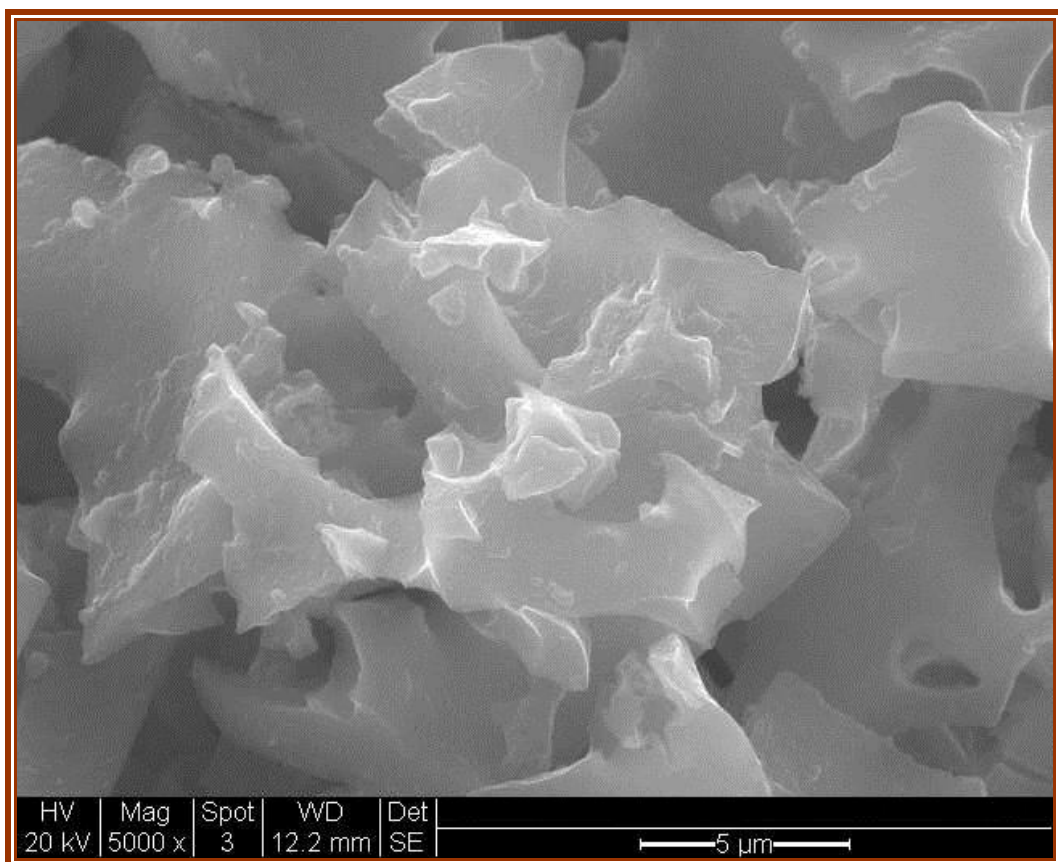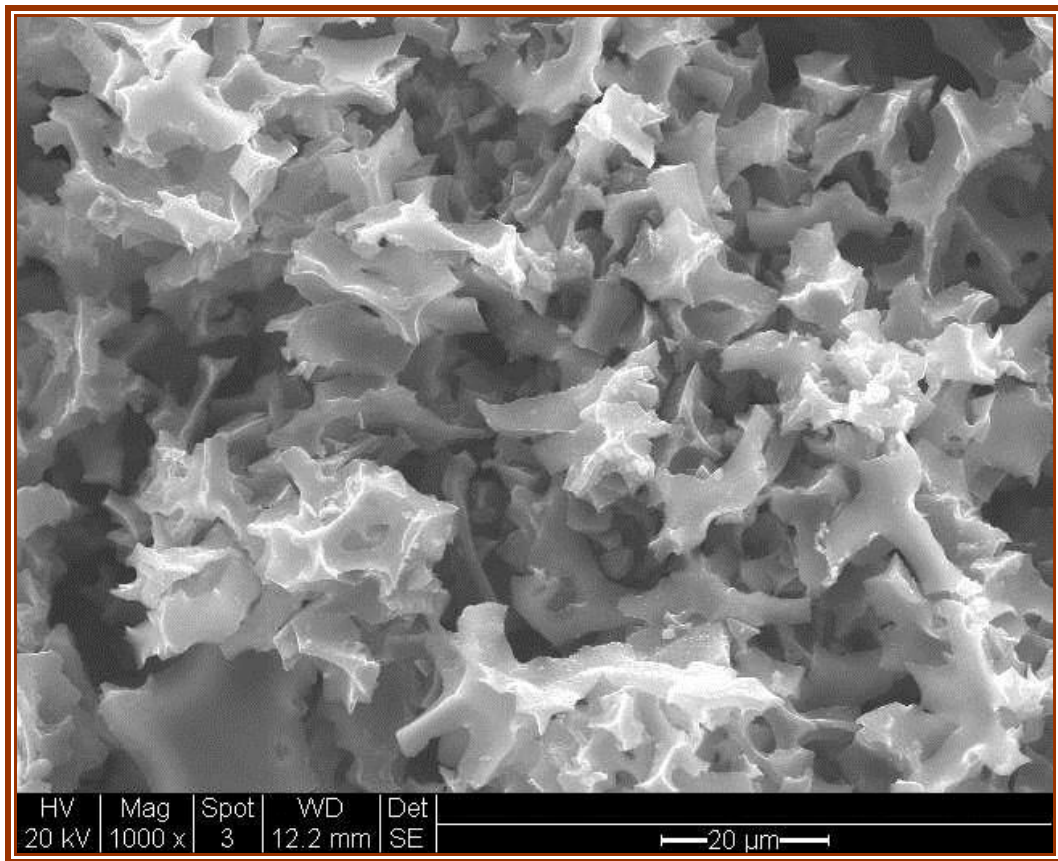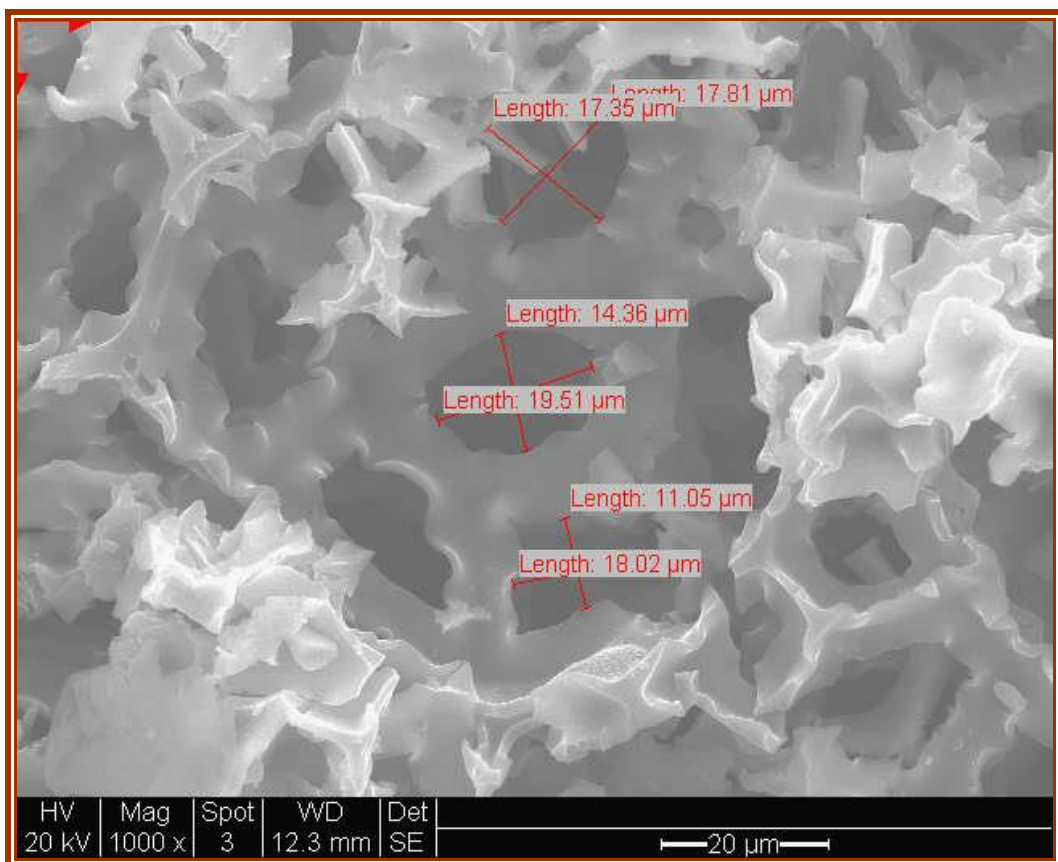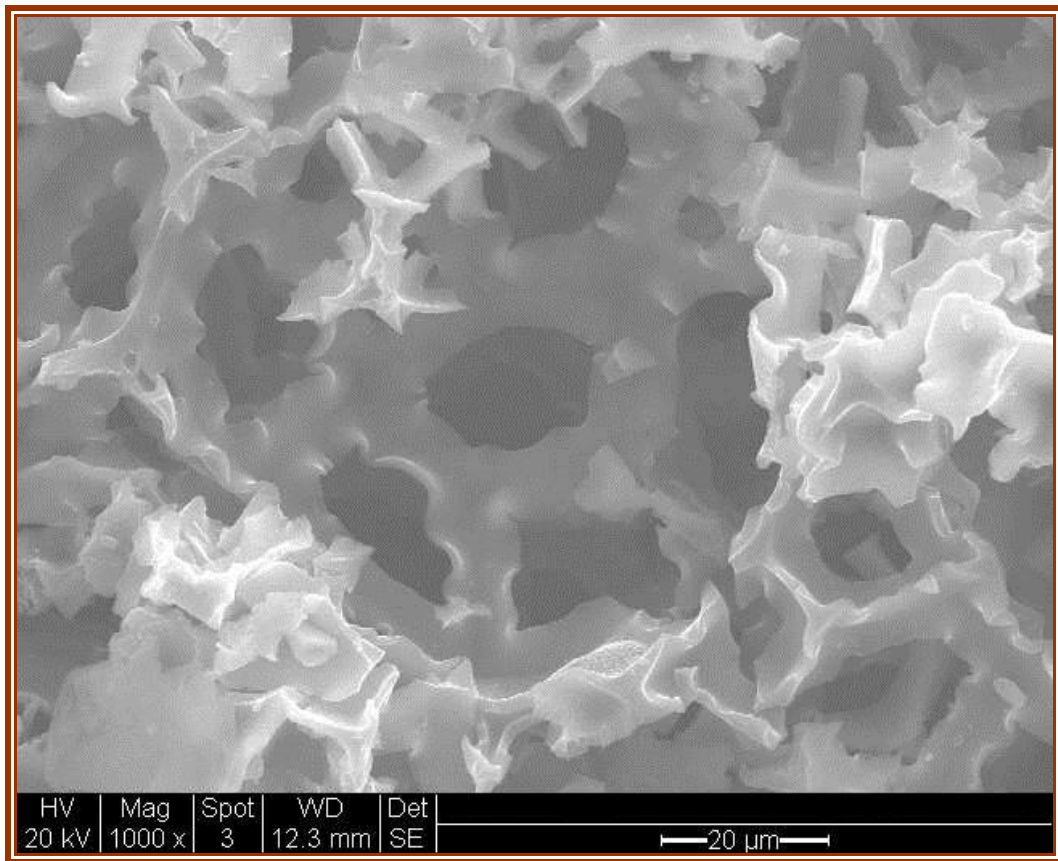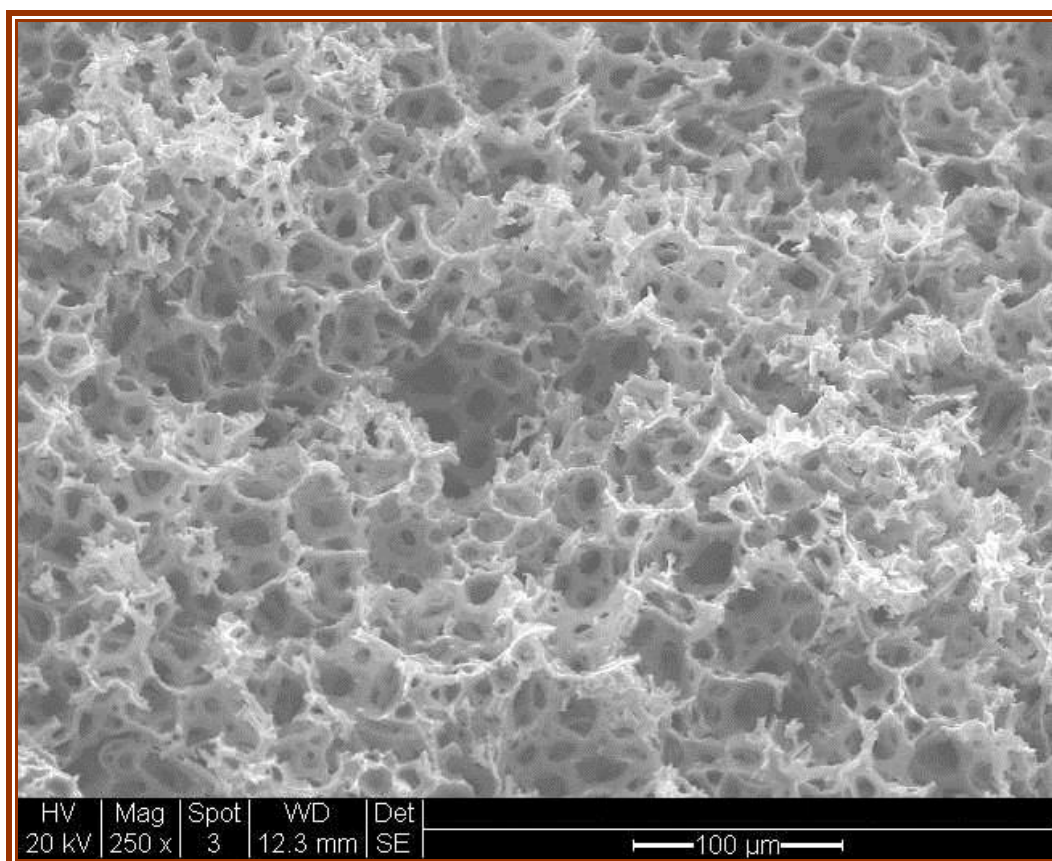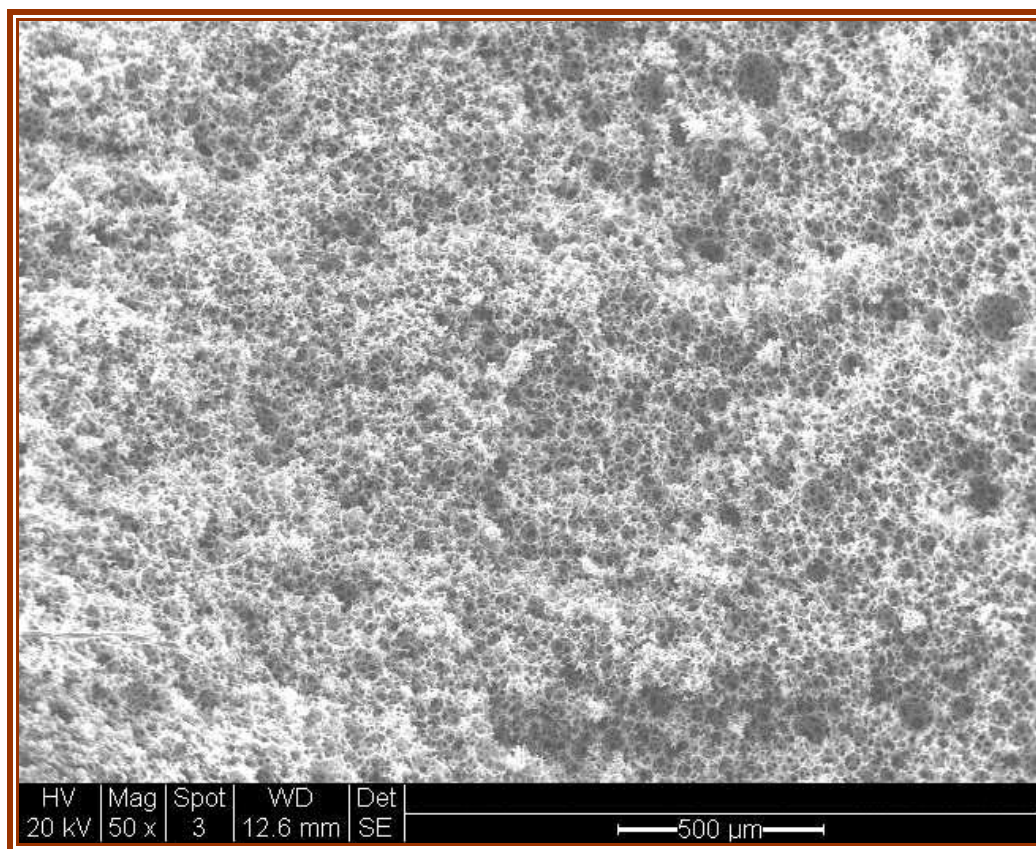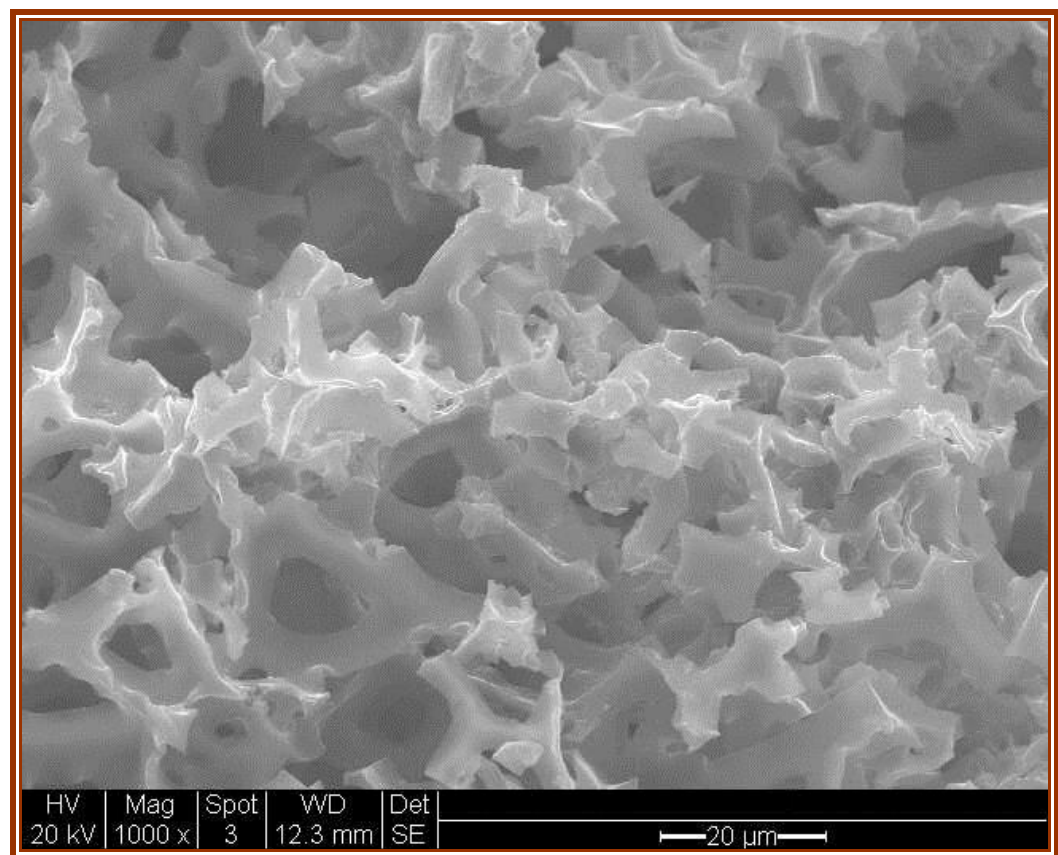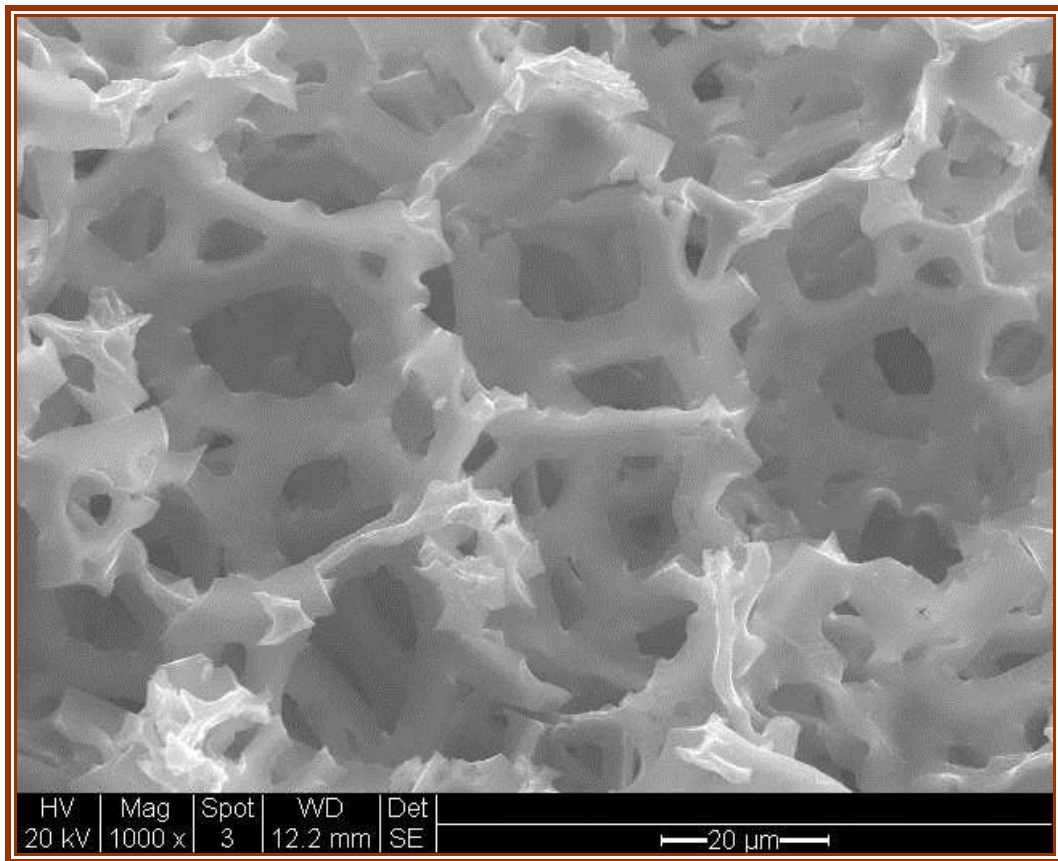
4. ESEM images of s-PHP surface after used in reduction of model tar (crude oil) from model syngas (CO_2) at different magnifications:
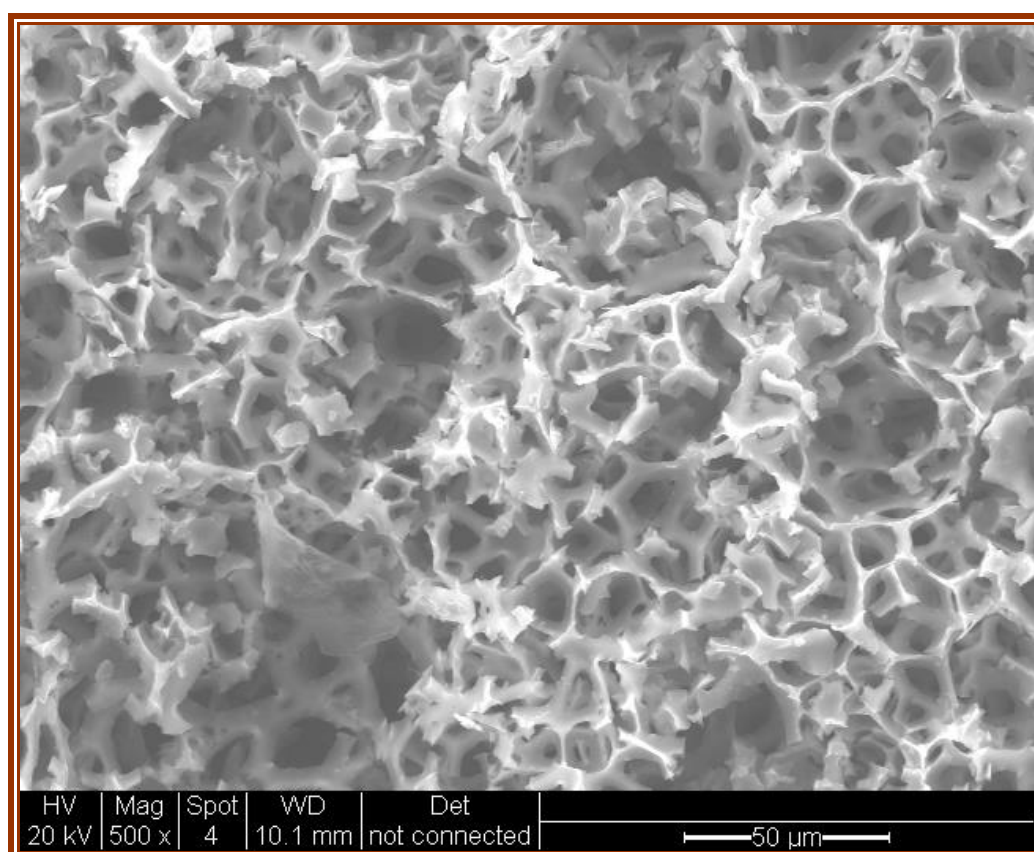
5. ESEM images of s-PHP cross section after used in reduction of model tar (crude oil) from model syngas (CO_2) at different magnifications:
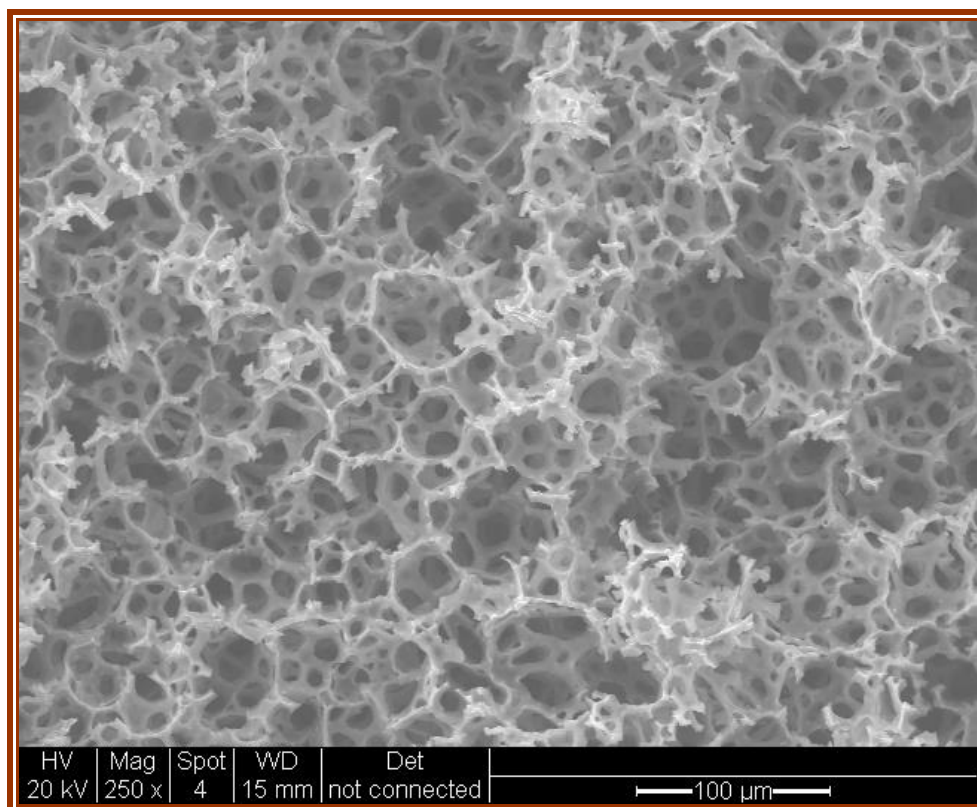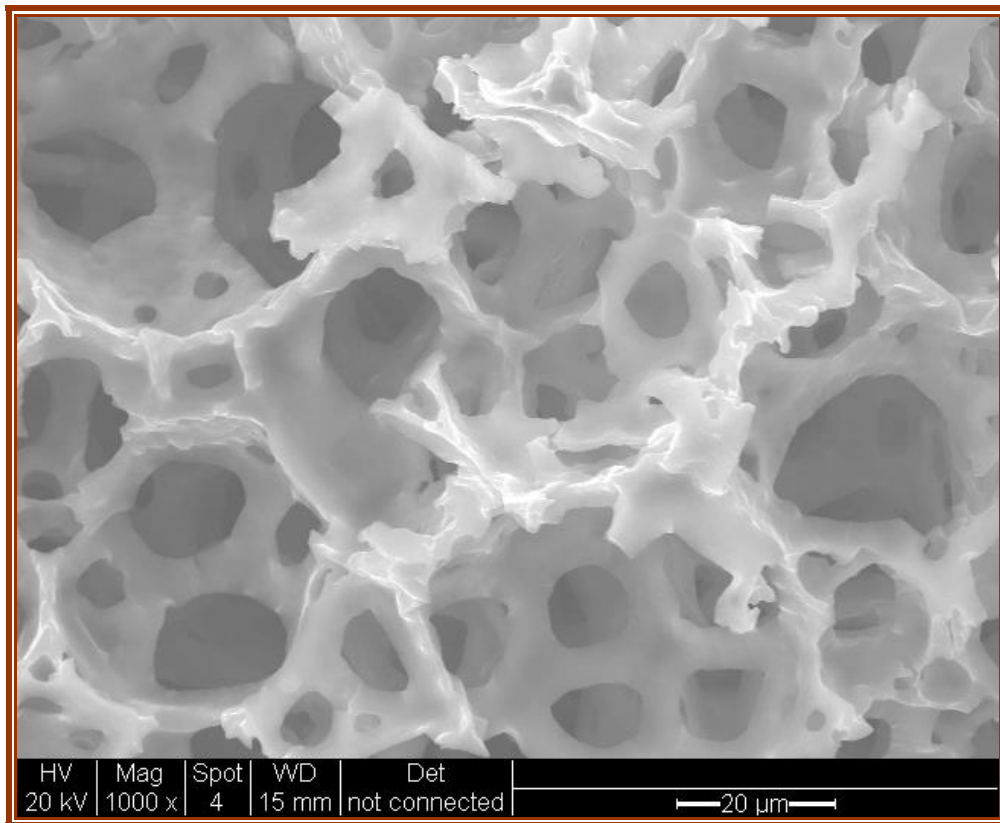
6. ESEM images of s-PHP surface after used in reduction of model tar (crude oil) from model syngas (CO_2) at different magnifications:

247

7. ESEM images of s-PHP cross section after used in reduction of model tar (crude oil) from model syngas (CO_2) at different magnifications:
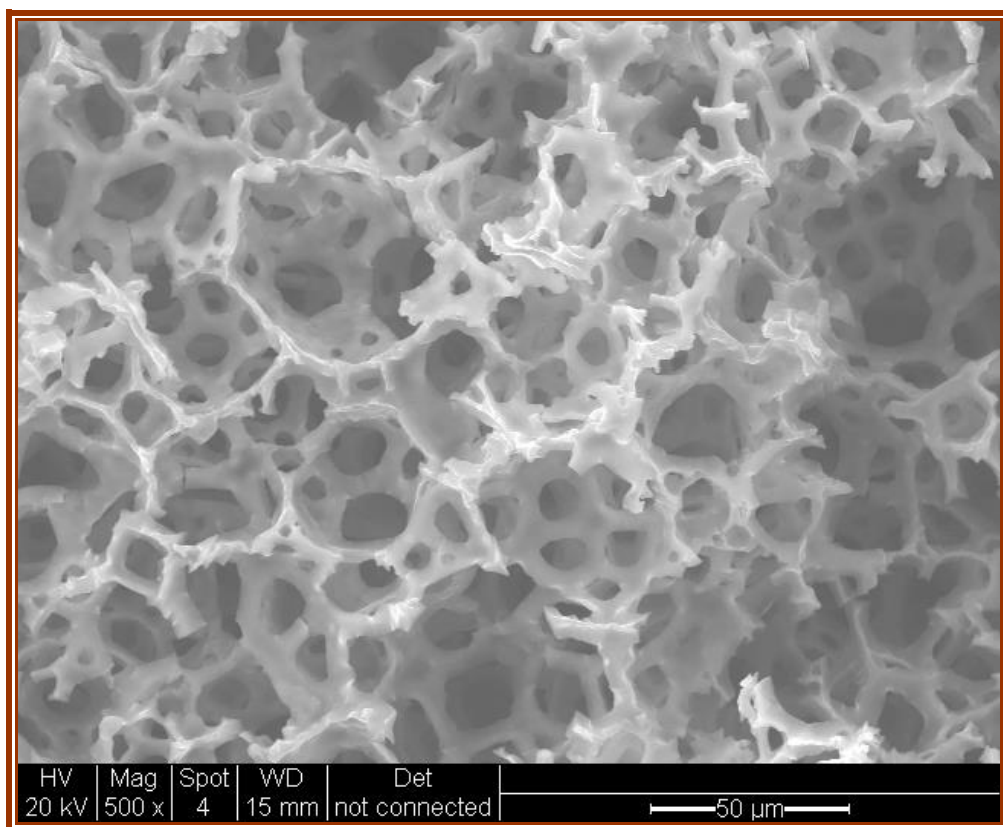
Curriculum Vitae

Abdulaziz (Aziz) Hemmali Mohamed

E-mail: (elgaroshi@yahoo.com) or (dr_aziz201212@yahoo.com)

Aziz was born on June 20, 1962 in Tobruk, Libya. In June 1979, he completed his high school. In March 1985, he finished his B.Sc. degree of Chemical Engineering from Tripoli University, Libya. From October 1985 to April 1994, he worked as a process engineer in Tobruk Oil Refinery, Libya.

In September 1994, he started his Master of Philosophy degree (MPhil) in Strathclyde University, Glasgow, United Kingdom. (Thesis title: Deactivation of FCC Catalysts – Fluidized bed study on coke composition related to stripping). In August 1996, he finished his MPhil. From November 1997 to June 2002, he returned back to work in Tobruk Oil Refinery, Libya as an acting manager in Tobruk Refinery Extension Project (TREP). From July 2002 to July 2006, he moved to the University of Omar Al-Mukhtar, Tobruk, Libya as a coordinator of the Pharmacy Faculty and a lecturer in the Faculty of Engineering.

In January 2007, he started his PhD degree in School of Chemical Engineering and Advanced Materials (CEAM), Newcastle University, UK. (Thesis title: Process intensification in Syngas Production and Cleaning). In June 2013, he finished his PhD.